12-2006

Onset and Persistence of Biogenic Meromixis in a Filling Pit Lake-A Limnological Perspective

Oscar Flite
Clemson University, flite100@sc.rr.com

ONSET AND PERSISTENCE OF BIOGENIC MEROMIXIS IN A FILLING PIT LAKE—A LIMNOLOGICAL PERSPECTIVE

A Dissertation
Presented to
the Graduate School of
Clemson University

In Partial Fulfillment
of the Requirements for the Degree
Doctor of Philosophy
Biological Sciences

---

by
Oscar P. Flite, III
December 2006

Accepted by:
Dr. James E. Schindler, Committee Chair
Dr. Gene W. Eidson
Dr. Timothy J. Shaw
Dr. Alfred P. Wheeler

ABSTRACT

Open pit mining usually results in a void that, over time, fills with water and becomes a pit lake. The goal for pit lakes is to create sustainable systems that positively contribute to local and regional watersheds. However, development of these manmade systems is driven by maximization of safe resource extraction, physical reclamation, and cost minimization, not future pit lake sustainability. As a result, the goal of sustainable pit lakes is not often achieved. One long-standing hypothesis for attaining the goal of sustainability has been to create and maintain meromictic lakes (lakes that do not completely mix on a yearly cycle). It is believed that meromixis minimizes atmospheric oxygen exposure to pit walls and concomitant acid generation and minimizes reentrainment of metals to the upper waters during seasonal mixes. This seems to be a reasonable goal but few lakes achieve and maintain meromixis so it is not clear whether this should be the sustainable goal for pit lakes. The objectives of this study were to: understand the biogeochemical cycling within a filling pit lake, determine the key limnological parameters (physical, chemical, and biological) that may facilitate meromixis within pit lakes, understand the response of pit lakes to perturbations (natural or manmade) and determine how these events affect lake stability, and make informed decisions and recommendations about the stability of this lake, current and future pit lakes, and pit lake sustainability. This study was conducted with the assumption that meromixis was possible in this lake and that meromixis was the desired goal.

This study was conducted at the Kennecott Ridgeway Gold mine in South Carolina from April 2000 through April 2004. For the first time, a holistic limnological approach was applied to a pit lake study. Physical structure parameters were monitored continuously (meteorological parameters and thermistor strings), state variables were monitored weekly with single station, multiparameter sonde (pH, redox, temperature, and

dissolved oxygen) and light profiles, the aquatic chemical environment was monitored quarterly with discrete meter chemistry profiles (metals and nutrients), and the biological assemblage was assessed weekly with integrated photic zone sampling (phytoplankton) and zooplankton tows.

During the course of this study, a persistent meromictic state developed. Observations of the system's response to stochastic perturbations were crucial in determining the mechanisms leading to the persistent meromixis. In the summer of 2000 a significant nutrient laden influent (~25% of the pit lake volume at that time) was introduced to the lake as a result of significant rain events. In the winter of 2000, the lake underwent holomixis and the nutrient load was resuspended within the water column. In the spring of 2001, high nutrient concentrations within the water column stimulated a significant phytoplankton bloom ($8E^{10}$cells/m^3). High rates of photosynthetic activity from the plankton bloom induced formation of precipitates in the upper water. Specific conductance at the strata of highest phytoplankton biomass indicated a loss of 0.13 mS/cm which equated to 0.13 meq/L or $4.93E^3$ equivalents within the entire strata. Upon dieoff, the associated phytoplankton biomass stimulated high rates of benthic bacterial respiration, which was observed as high rates of dissolved oxygen loss in the lower water (31 g O_2/d). Increased rates of bacterial respiration in the lower water poised the redox environment (from 550 mV to 150 mV), which allowed resolubilization of upper water precipitates and potentially induced higher rates of material flux from the sediment. Both of these ancillary events of the large phytoplankton biomass induced a strong enough density difference between mixolimnion (upper water) and monimolimnion (lower water) to overcome the destabilizing force of wind mixing and meromixis was established in the winter of 2001. In 2001, specific conductance at the lowest lake strata increased from 2.5 mS/cm to 3.2 mS/cm, which equated to approximately $7.7E^2$ equivalents. Specific conductance within the lower water continued to increase throughout the study period and meromixis persisted through the end of the study.

Increase in specific conductance within the lowest lake strata from March 2002 to May 2002 resulted from increases in SO_4^{2-} (47%), Ca^{2+} (31%), Mg^{2+} (11%), and Na^{+} (5%). Contributions from potential sources were not elucidated (sediment or precipitates from the mixolimnion) for these elements but they were most likely responsible for the water density difference between the mixolimnion and monimolimnion over the course of the study. Assessment of iron, manganese, and sulfur indicated that cycling of these elements from mixolimnion to monimolimnion and from the sediments to the monimolimnion may have controlled fluxes of other metals which are typical of pit lakes (i.e. Co, Ba, Zn).

Unique physical characteristics of this particular lake (e.g. wind field, lake bathymetry, lake orientation to prevailing winds, and surface water influent) aided in counteracting the destabilizing force of wind and most likely helped to maintain the meromixis over time. Modified Schmidt stability calculations indicated that the lake was completely prone to mixing during the winter. However in the winter of 2001, the wind field was not conducive for mixing the lake from the surface to the bottom (Lake Number) or from the surface to the winter thermocline (Wedderburn Number). Modeled results showed that during winter the surface to thermocline mixing would take place at a daily average wind speed of 1.34 m/s. From 2001 to 2003, this threshold was exceeded 62% of the time. As a result of extended periods of exceedance (~6 months), mixolimnetic deepening was evident but complete holomixis may have been prevented by an unidentified mechanism. Power spectral density analysis of isotherm displacement data indicated that the east end of the lake (shallow section) may have been more energetic than the west end (deep section). This difference may point to the importance of bathymetry in dissipating energy in meromictic systems which is an often overlooked element.

Phytoplankton dynamics throughout the study were similar to a newly filling reservoir. Initially, species numbers were low and biomass was high but over time

species numbers increased and biomass decreased. This trend most likely resulted from the dynamic nutrient trend in this unique system. The nutrient laden influent in 2000 resulted in high phytoplankton biomass but over time nutrients became less available due to the meromictic state as well as the absence of consistent watershed inputs and littoral zone vegetation (as sources of nutrients), and a closed hydrological system, which was dominated by precipitation and evaporation. Initially, the lake was dominated by blue-green algae, which gave way to green algae, leading to the present assemblage of seasonal cycles of diatoms, green algae, and blue-greens. Zooplankton dynamics indicated that the release of water to the lake in 2000 may have introduced an assemblage of calanoid copepods. Initially with low biomass, these copepods flourished during the high phytoplankton period in 2001 but steadily decreased over time, most likely in response to the decreasing phytoplankton biomass trend.

This study elucidated some key factors in understanding how meromictic systems develop and persist. Biogeochemical cycling, in response to a stochastic event, facilitated the onset of meromixis where calcium, sulfate, magnesium, sodium, carbonate, iron, and manganese were controlled by biological processes, which lead to a water column density discontinuity. Persistence of the discontinuity resulted from the interplay between the physical, chemical, and biological domains where biogeochemical cycles, meteorological forcing, and lake bathymetry were found to be significant. This study emphasized the importance of lake bathymetry and that this often disregarded factor may be the key to sustainability within meromictic systems and manmade pit lakes.

DEDICATION

This work is dedicated to my mother, Patricia Scattaglia (1949-2006). I am sorry she did not get to see it.

ACKNOWLEDGEMENTS

Luck, as I have heard defined previously, is the intersection of opportunity and preparation. By this definition, I consider myself to be quite lucky and I would like to thank those who have contributed to both sides of the equation.

I thank my committee, Gene Eidson, Jim Schindler, Tim Shaw, and Hap Wheeler, for their guidance, patience, encouragement, and accommodation. At times, I needed all four. I would like to thank Eidson for the immeasurable opportunity which was offered to me in 2000, for his patience with an obstinate bastard, and for his friendship. None of this would have happened without him. I would like to thank Jim for always pointing me in the right direction, for offering answers to my barrage of questions from his immense breadth and depth of knowledge, and for his friendship. I also thank Kennecott Mineral Corporation, especially Dave Salisbury, Fred Fox, and Roy Duckett, for the immeasurable opportunity, complete accessibility, and patience for allowing the deliberate pace of scientific discovery to proceed.

I would like to thank those mentors/friends who helped me prepare for such an opportunity through prior research opportunities, courses, and wise advice: Rob Shannon at Penn State, Jim Seago, Peter Rosenbaum, and Leland Marsh at SUNY Oswego, and Eric and Susan Ehrhardt in Oswego.

Finally, accomplishments are never achieved or celebrated alone. I share this with all of my family and friends who have encouraged and supported me over the years, especially my wife, Carolyn, to whom I owe everything.

TABLE OF CONTENTS

Page

TITLE PAGE ……. i

ABSTRACT ……... ii

DEDICATION ……... vi

ACKNOWLEDGMENTS …….. vii

LIST OF TABLES ……. x

LIST OF FIGURES…… xi

CHAPTER

I. INTRODUCTION……..…… 1

Physical…….. 3
Chemical……. 5
Biological……... 8
Study Objectives…… 9

II. METHODS AND MATERIALS…….. 11

Study Site…… 11
Site Description…….. 11
Watershed …….. 12
Sampling …… 27

III. RESULTS…….. 27

Overview and Description of Perturbations
to South Pit Lake: 2000-2004…… 27
South Pit Lake Weather Station Data …… 31
Sonde Data Results…… 36
Chemistry Results……... 60
Physical Results…….. 82
Biological Results…….. 100

IV. CONCLUSIONS……... 116

Physical…….. 116
Chemical……. 120

Table of Contents (Continued)

Page

Biological……... 125
The Future of South Pit Lake ……...……. 130
The Biogeochemistry of Pit Lakes……. 133
On the Restoration of Current Pit Lakes
and an Outlook on Future Pit Lakes ……... 136
A [Brief] Treatise on Limnology…… 137

APPENDICES…… 139

A. Bathymetric Maps Of All Meromictic Lakes
in *Limnology and Oceanography* (v. 1-43) ……... 140
B. Lake mixing event simulation using PHREEQC2……. 145

REFERENCES……... 169

LIST OF TABLES

Table		Page
1.	Pit lake literature search results in relation to the three broad categories of limnology	9
2.	Reporting limits for chemical constituents	25
3.	Average concentrations of pit lake water (mg/L)	61
4.	Average concentrations of nutrients in pit lake water (mg/L)	62
5.	Speciation results of the South Pit lake chemistry mixolimnion (7-24-02)	74
6.	Speciation results of the South Pit lake chemistry monimolimnion (7-24-02)	74
7.	Discrete meter PHREEQC results for South Pit Lake (1-15-02)	75
8.	Discrete meter PHREEQC results for South Pit Lake (3-20-02)	75
9.	Discrete meter PHREEQC results for South Pit Lake (5-9-02)	76
10.	Assessment of chemical species responsible for conductivity increase in monimolimnion from 2-20-02 through 5-9-02	77
11.	Discrete meter PHREEQC ion activity product results for South Pit Lake (11-7-02)	81
12.	Visual MINTEQ results of simulated monimolimnetic sulfur and iron species	81

LIST OF FIGURES

Figure		Page
1.	Location of study site, Ridgeway, SC ……	11
2.	Kennecott-Ridgeway mine site and points of interest for watershed…….	13
3.	Bathymetric map of South Pit Lake during the study (~33 m maximum depth)…….	14
4.	Profile view of South Pit Lake during the study (~33 m maximum depth)……	14
5.	Bathymetric map of South Pit Lake (~56 m maximum depth)……...	15
6.	Profile view of South Pit Lake at maximum depth (~56 m)……...	15
7.	South Pit Lake hypsographs shown as area-vs.-depth (left) and as % volume-vs.-depth (right)…….	16
8.	Total daily rainfall for South Pit Lake from April 2000 through March 2003 ……	32
9.	Total monthly rainfall data from April 2000 through June 2004……	33
10.	Wind direction for SPL in 2001……..	33
11.	Wind speed for SPL in 2001……...	33
12.	Wind direction for SPL in 2002……..	34
13.	Wind speed for SPL in 2002……...	34
14.	Wind gusts for SPL in 2002……	34
15.	Wind direction for SPL from April 2001 through December 2001……	35
16.	Wind direction for SPL from January 2002 through December 2002……	35
17.	Wind direction for SPL from January 2003 through December 2003……	35

List of Figures (Continued)

Figure		Page
18.	Wind direction for SPL from January 2004 through June 2004…….	35
19.	South Pit Lake temperature isopleth depth-time diagram from April 2000 through April 2004……	37
20.	Temperature profile of South Pit Lake on July 24, 2003, showing dichothermy……..	38
21.	Temperature of individual strata throughout the study period……...	38
22.	South Pit Lake specific conductance isopleth depth-time diagram from April 2000 through April 2004……	41
23.	Specific conductance trends of individual strata throughout the study period ……...	43
24.	Phytoplankton and conductivity trends from February 2001 through December 2001 ……	44
25.	Correlation between plankton counts and conductivity in the lowest strata…….	45
26.	Phytoplankton and 16 meter conductivity trends from January 2001 through July 2001……	45
27.	South Pit Lake pH isopleth depth-time diagram from April 2000 through April 2004……..	46
28.	Phytoplankton counts versus pH trends of six selected depths in South Pit Lake from 2000 through 2002……	47
29.	South Pit Lake dissolved oxygen isopleth depth-time diagram from April 2000 through April 2004……	48
30.	Theoretical versus measured water column DO content……	50
31.	Stratum saturation throughout the study period with lake bottom as the 0 reference ……...	50
32.	Oxygen content of the lower 12 meters, by stratum, of South Pit Lake from 2000-2004 ……	52
33.	Dissolved oxygen content of 12m and 0m strata from 2-2-01 through 12-12-01 ……..	53

List of Figures (Continued)

Figure Page

34. Correlation between 0m and 12m DO loss trends from 2-2-01 through 3-22-01 ……. 53

35. Dissolved oxygen content of the 0 m and 12 m strata within South Pit Lake from March 2001 through December 2001……. 54

36. South Pit Lake oxidation reduction potential isopleth depth-time diagram from April 2000 through April 2004 …….. 54

37. South Pit Lake oxidation reduction potential isopleth depth-time diagram from April 2000 through April 2004 …….. 56

38. South Pit Lake bathymetry showing possible feature responsible for observed redox profiles ……. 56

39. South Pit Lake turbidity isopleth depth-time diagram from April 2000 through April 2004…….. 57

40. South Pit Lake PAR isopleth depth-time diagram from April 2000 through April 2004…….. 58

41. Rate of light absorption for each profile date for South Pit Lake from April 2000 through April 2004……. 59

42. Rate of light absorption and total rainfall for South Pit Lake from April 2000 through March 2003…….……. 60

43. Rate of light absorption and total phytoplankton counts for South Pit Lake from April 2000 through October 2002 …… 61

44. Depth-time diagram of isopleths of volume weighted sulfate concentration…….…….. 63

45. Depth-time diagram of isopleths of volume weighted calcium concentration……. 64

List of Figures (Continued)

Figure Page

46. Depth-time diagram of isopleths of volume weighted alkalinity (as mg $CaCO_3$/L)……. 65

47. Depth-time diagram of isopleths of volume weighted magnesium concentration……... 66

48. Depth-time diagram of isopleths of volume weighted potassium concentration……. 67

49. Depth-time diagram of isopleths of volume weighted sodium concentration……. 67

50. Depth-time diagram of isopleths of volume weighted silica concentration……. 69

51. Depth-time diagram of isopleths of volume weighted manganese concentration……... 69

52. Depth-time diagram of isopleths of volume weighted dissolved organic carbon concentration……. 70

53. Depth-time diagram of isopleths of volume weighted iron concentration …….. 71

54. Depth-time diagram of isopleths of volume weighted barium concentration…….. 71

55. Depth-time diagram of isopleths of volume weighted cobalt concentration……... 72

56. Correlation between iron and manganese concentrations and conductivity……. 79

57. Correlation between cobalt concentration and conductivity……... 79

58. Thermistor data, wind speed, wind direction for South Pit Lake from August 13, 2001 through August 17, 2001 ……... 82

59. 18° C isotherm displacement, wind direction, and wind speed for South Pit Lake from 9-9-01 through 9-14-01 ……. 83

List of Figures (Continued)

Figure Page

60. Spectral density analysis results of the 18° C isotherm displacement data..... 84

61. Approximate location of 18° C isotherm during September 2001..... 86

62. Bathymetric pressure trend for South Pit Lake from 9-9-01 through 9-15-01 86

63. Percent contribution of each strata to the total water column heat content for South Pit lake from December 2000 through February 2003 88

64. Total heat content for South Pit Lake from December 2000 through February 2003 89

65. Percent heat contribution to the water column by the 0m stratum from December 2000 through February 2003..... 89

66. Rates of heating for 5 selected strata in South Pit Lake from December 2000 through April 2003..... 90

67. Depth-time diagram of revised Schmidt stability for South Pit Lake from April 2000 through March 2003..... 92

68. Total water column stability for South Pit Lake from April 2000 through March 2003..... 93

69. Wedderburn Number, Lake Number, and modified Schmidt stability for South Pit Lake from 5-18-01 through 6-17-02..... 95

70. Impact of wind speed on Wedderburn Number for South Pit Lake..... 97

71. Impact of wind speed on Lake Number for South Pit Lake..... 98

72. Average daily wind speed for each month from April 2001 through May 2003..... 99

73. Specific conductance depth time diagram from July 2002 through April 2004..... 99

List of Figures (Continued)

Figure Page

74. Total phytoplankton counts for South Pit Lake from March 2000 through February 2003…….. 101

75. Trends between phytoplankton classes for South Pit Lake from March 2000 through March 2003……. 102

76. Trends between phytoplankton classes for South Pit Lake from December 2001 through February 2003……... 103

77. Cyanophyceae species for South Pit Lake from March 2000 through March 2003 …….. 103

78. Expanded view of Cyanophyceae species for South Pit Lake from March 2000 through March 2003 …….. 104

79. Bacillariophyceae species for South Pit Lake from March 2000 through March 2003 ……. 105

80. Euglenophyceae species for South Pit Lake from March 2000 through March 2003 ……. 106

81. Chlorophyceae species for South Pit Lake from March 2000 through March 2003 …….. 107

82. Chlorophyceae species for South Pit Lake from March 2000 through March 2003 emphasizing the 2001-2003 dynamics…….. 107

83. *Cryptomonas* spp. for South Pit Lake from March 2000 through October 2002 ……... 109

84. *Chrysophyceae* species for South Pit Lake from March 2000 through March 2003 …….. 109

85. *Nanoplankton* for South Pit Lake from March 2000 through March 2003 …….. 110

86. Phytoplankton species richness for South Pit Lake from March 2000 through March 2003 ……. 110

87. Total calanoid copepod counts (all stages) for South Pit Lake from May 2000 through January 2003 …….. 111

List of Figures (Continued)

Figure Page

88. Naupliar and copepodid stage calanoid counts for South Pit Lake from May 2000 through January 2003……. 112

89. Calanoid copepod counts broken down by life stages for South Pit Lake from February 2001 through January 2003……. 112

90. Cyclopoid copepod counts for South Pit Lake from May 2000 through January 2003……... 113

91. Rotifer counts for South Pit Lake from February 2001 through December 2002 …….. 114

92. *Brachionus* spp. counts for South Pit Lake from January 2000 through December 2002 …….. 114

93. Copepod phytoplankton dynamics for South Pit Lake from May 2000 through October 2002 ……. 115

94. Biotic dynamics for South Pit Lake from May 2000 through October 2002 …….. 115

95. Venn diagram of the holistic, biogeochemical approach to pit lake studies ……... 134

CHAPTER I

INTRODUCTION

Mining voids result from open pit mining activity for varied extractables, some of which are precious metals like gold, silver, and copper. These precious metals are usually associated with much larger quantities of pyrite (FeS). As rock is removed from the ore body and processed, the target metal is extracted and the pyritic waste is transported to another on-site location, leaving a void at the original location of extraction. As a result of improvements in prospecting, removal, and extraction technologies, these voids have extended deep into the earth's crust. Depths at precious metal mining sites vary considerably and have exceeded 600 meters at some locations. Two drawbacks to scouring to such depths are severing of the groundwater flow paths and exposure of the reduced ore to the oxidizing conditions of the atmosphere. Both work together in pyritic ore deposits to produce acid mine drainage.

Severing the groundwater flow path causes the void to act as a groundwater discharge and the void begins to fill with water. During mining the water is pumped from the void and a cone of depression in the groundwater system is established. Upon cessation of mining, backfilling, and pit contouring, the cone of depression steadily recovers toward the historical groundwater level and the pit is allowed to fill, ultimately forming a pit lake.

Oxidation of the pyrite bearing ore body, in the presence of water, produces acidity. En route to the filling pit lake, influent groundwater, precipitation, and runoff slowly dissolve the extensive surface area of newly oxidized rock. Furthermore, sulfur and iron oxidizing bacteria significantly increase acid generating potential. Depending upon the ratio of acid neutralizing rock to acid generating rock in the deposit, the

resultant lake water can range from slightly alkaline to highly acidic. Aside from elevated concentrations of relatively benign elements, circumneutral pit lakes are typically innocuous. Acidic lakes, on the other hand, have been of significant regulatory concern. The issue is not limited to low pH, but extends to concerns of mobilization of metals associated with low pH waters that threaten local and regional ecosystems. As the lake fills and becomes a source of discharge for surrounding surface waters and groundwaters, pit lake water quality becomes an important issue.

Water within the lake itself is thought to minimize acid generation by decreasing contact between atmospheric oxygen and wall rock pyrite. As a result, one approach to pit lake remediation has been to rapidly fill these lakes with either freshwater (see Castro and Moore, 2000) or a combination of seawater and freshwater (see Fischer, 2002). In an effort to minimize the perpetual effects of oxidation and subsequent acidification in pit lakes and to minimize potential toxicity of heavy metals resulting from pit wall dissolution, most often the objective is to facilitate a lake that is meromictic. Meromictic lakes do not completely mix from top to bottom throughout a one-year period. Some lakes may be temporarily or permanently meromictic. An additional benefit that is thought to be achieved through meromictic pit lakes is that the anoxic monimolimnion (isolated bottom water) will provide sufficient conditions for sulfate reducing bacteria to generate alkalinity through the dissimilatory reduction of sulfate to sulfide. Whether this meromictic approach is sensible or even possible is yet to be determined. Kalin and Steinberg (1998) indicated that more research is needed before suggesting that meromixis be the a-priori assumption for pit lakes.

Meromixis is a unique and complex combination of physical, chemical, and/or biological features, so unique in fact that only 43 meromictic lakes have been reported in North America (Walker and Likens, 1975). Most natural meromictic lakes are stabilized by deep-water density, which is stable enough to withstand the destabilizing forces of wind generated and density currents (Kalff, 2002). This increased density is more a

function of salinity than temperature (Cole, 1996). Establishment of such deep water salinity could develop from dilute or highly saline influents (ectogenic meromixis), events as a consequence of epilimnetic and hypolimnetic productivity (biogenic meromixis), freezing conditions (cryogenic meromixis), or deep water saline springs (crenogenic meromixis) (Wetzel, 2001). The "permanence" of meromixis results from continuation of the aforementioned events, a uniquely stabilizing lake morphometry, and decreased impact from destabilizing forces (wind mixing, density currents, direct solar heating of the hypolimnion, etc.). Meromictic lakes have similar morphometry. They are unusually deep compared to their surface area (Cole, 1996; Kalff, 2002). This morphometric feature is quantified in a parameter called relative depth. Relative depth is the ratio of a lake's maximum depth to its mean diameter (see Cole, 1996). Since pit lakes usually have high relative depth ratios, the assumption is that most pit lakes will be meromictic. However, many pit lakes with high relative depths (compared to natural lakes) undergo seasonal mixes (see Miller et al., 1996; Doyle and Runnels, 1997). Clearly relative depth alone does not guarantee meromixis.

Physical

Few pit lake studies have focused on the true physical limnology involved with understanding pit lake mixing. Typically, wind, meteorology (relative humidity, solar radiation, evaporation, and temperature), basin subsurface topography, inflow (due to pumping, groundwater, overland flow, surface water, precipitation), outflow (due to pumping, groundwater, evaporation, surface water outlet), and dissolved substances are the most important parameters when dealing with lake physics. The latter has the ability to adsorb or scatter solar radiation as well as create a density gradient within the water column. Mining specific events, such as density currents due to overland flow over unvegetated soil and backfilling material directly into the pit lake, impact lake physics too. The surrounding topography plays a role as well in that it determines how buffered a

lake is from wind (effective fetch). Wind is the most important factor for lake mixing (Hutchinson, 1957) and to my knowledge only a few studies have considered this parameter (e.g. Stevens and Lawrence, 1998; Hamblin et al., 1999). Wind not only determines the thermocline depth throughout the year but is also the driving force for internal basin scale, stationary oscillations or seiches (Hutchinson, 1957). Seiching can induce deep mixing events where oxygenated water is injected into the anoxic hypolimnion or hypolimnetic water is forced up the edges of a lake onto the surface. In addition, small scale mixing processes at the sediment-water interface (benthic boundary layer) causes perturbations, which increase chemical transfer rates toward the water column. All are unintended consequences if the goal for pit lakes is permanent anoxia in the bottom waters and decreased metals concentrations in the water column.

Relative depth ratio is a general description of lake morphometry and does not account for detailed subaqueous pit topography. To my knowledge no pit lake study has taken into account subaqueous pit topography and how it decreases or increases lake stability. Defining the key physical parameters of lake mixing, lake stability, and lake development is a limitation, not only for pit lake studies, but has been pervasive throughout limnology and oceanography. This has resulted in the broad use of general descriptors, such as relative depth ratio, to define complex physical phenomena. Applying such generalizations falls short of the tools necessary for making informed decisions about pit lake development and sustainability. One reason for the lack of robust physical descriptors may have been the lack of specialized instrumentation for making complex physical measurements in situ. For example, much of the study concerning the bathymetric effects on mixing was initiated in oceanography and began mostly with observational changes in temperatures along slopes (Lee, 1961), theoretical exercises (Wunsch, 1968), and laboratory studies (e.g. Cacchione and Wunsch, 1974). Until recently, few studies in limnology had focused on the effects of specific bathymetric features such as ledges and slopes on mixing processes in lakes (e.g. Thorpe

et al. 1972; Eriksen, 1982; Boegman et. al 2005) and possibly just one example in pit lakes (Boerher and Stevens, 2005). Furthermore, it has only been within the last decade or so that researchers have been applying acoustic technology for direct physical measurements.

Mining voids are usually shaped to maximize safe target mineral retrieval so each pit's shape is quite unique. Furthermore, backfill material replaced during reclamation is added to minimize reclamation costs and without knowledge of future pit lake impacts. How subaqueous topography, pit orientation (in reference to the prevailing wind direction), backfill material placement, and surrounding topography influence pit lake stability is crucial to understanding the long term sustainability of these systems. Unfortunately the tools necessary for making detailed predictions on pit lake development and sustainability may be limited to the developing field of physical limnology.

Chemical

Most pit lake studies have focused on the complex chemistry and geochemistry of these systems. The major reason for this is that pit lakes pose a significant potential chemical impact on local and regional watersheds, as evidenced by extremely poor water quality observed downstream of abandoned mine sites and within most pit lakes. A limnological perspective has been lacking in pit lake research because most limnologists deal with the chemistry of specific biological nutrients and not complex matrices like pit lake waters. This has lead to the isolation and specialization of pit lake research by geoscientists with little input by limnological generalists. Although pit lake chemistry can often be quite different from the typically studied carbonate buffered system, the overarching goal is to facilitate the rehabilitation of these "fringe" systems to something that represents the "typical" limnological system. It should be argued that the tools used by geochemists to make predictions about pit lake chemistry (e.g. geochemical

equilibrium models) are general enough to be used, and indisputably should be used, in the teaching and research of limnology.

Today the focus on chemistry is shifting to the emerging paradigm of sustainable development in the mining industry. In understanding pit lakes, however, one must see pit lake chemistry as a segment of the overall understanding. Mixing mechanisms and biological controls on pit lake chemistry must be incorporated into making predictions about future pit lake chemistry. Miller et al. (1996) suggested that predictions of final pit lake water quality need to be carefully assessed and that several factors be taken into consideration during assessment: oxygen status of the lake, pH, hydrologic flow system, wall rock composition, evapoconcentration (climate), biological activity, and hydrothermal inputs. It is therefore crucial to apply a limnological perspective to pit lake studies.

Many studies have pointed to the importance of hydrologic and geologic controls on pit lake water quality. It is a widely held belief in the geochemical literature that pit lake chemistry is controlled by pit wall minerology, groundwater and surface water input and composition, geochemical equilibrium, and evapoconcentration. Studies such as Newbrough and Gammons (2002) have shown good correlation between pit wall mineralogy and pit lake chemistry while studies such as Shevenell et al. (1999) have shown good correlation between decreased water quality and increased runoff at mine sites, so there is good reason to believe such controls are extremely important. However, many pit lake studies have not been intensive enough for making informed decisions about pit lake chemistry. Conclusions about pit lake chemistry have been drawn from limited sampling dates (from 1 to 4 profiles per year) or from data compiled from previous regulatory samplings, most of which were from the epilimnion only or from one epilimnion and one hypolimnion sample. Under such constraints, conclusions drawn about pit lake chemistry would not have included stochastic impacts such as density currents (runoff), pumping and/or influent regimes, influent water quality, rainfall, and

biological productivity and respiration. These events alter the chemical profile of a lake by affecting chemical constituents within the water column, either by introduction (density currents due to runoff or pump/groundwater inflow, oxygenation due to phytoplankton), removal (pump withdraw or groundwater outflow), or dilution (pump/surface water inflow). Unfortunately the major assumption for pit lake chemistry is that all constituents are approaching equilibrium, but events such as those just described would reset the processes of equilibrium. This would not necessarily affect equilibria which are assumed to be relatively rapid (e.g. acid-base chemistry) but would affect processes which take longer to reach equilibrium (e.g. redox reactions). Recognizing events and processes, which reset geochemical equilibrium controls, is important for understanding and predicting future pit lake water quality.

As mentioned previously, pit wall mineralogy is believed to be a major control on pit lake chemistry. However many mine sites attempt to minimize contact between the atmosphere and the pit wall by covering the walls with fine material. In addition, backfill heaps of low-grade material are also of the same consistency. The consistency and quality of this material may impact water quality to a much larger degree than the bare rock alone. In situ and conceptual models developed by Atkins et al. (1997) and Peterson et al. (1998) showed higher oxygen consumption rates (indicating sulfate generation and concomitant acidification) in small fragment waste piles than in low permeability pit bench material and blasted rock piles. Many times these small fragment waste piles extend from the pit rim to the depths of the pit. As a result of wind lapping, wind induced currents, and rising water levels, these backfill piles may add chemical constituents and impact water quality for much longer periods of time than bare rock walls. Such an impact would also create disequilibrium for most pit lake species.

Biological

Attention to biota within pit lakes has been minimal. Not unlike much of the limnological literature dealing with aquatic biota, most of the literature and attention to pit lake biota has focused on phytoplankton. There is good reason for this, however. Steadily increasing water levels, steep sided walls, minimal and/or unsuitable littoral substrate, disproportionately small watershed, and poor water quality limit much of the pit lake productivity to pelagic organisms such as phytoplankton and bacteria. Focus on phytoplankton and bacteria may also be due to the importance of these organisms in the biogeochemical cycles of pit lake waters. Some species of plankton and bacteria are known to remove metals from waste streams and natural lakes and some biological processes, such as photosynthesis and anaerobic metabolism, oxidize and reduce metals such as iron, manganese, and sulfate in the epilimnia and hypolimnia of lakes and oceans. These processes are important to mining lakes because the aforementioned metals are often the major constituents of pit lake water. Furthermore, biogenic formation of zinc carbonates and manganese oxides have been associated with coprecipitation of heavy metals in mine waters (Podda et al., 2000), Lake Zurich (Sigg et al., 1987), and the Sargasso Sea (Sunda and Huntsman, 1990). Mining water quality with high concentrations of metals undoubtedly benefits from phytoplankton and bacterial communities.

Primary productivity in pit lakes is essentially limited to the pelagic zone. One significant drawback to this fact is that the littoral zone is considered to be the most productive and diverse portion of a lake (Kalff, 2002). Limiting productivity in such a way might limit the in situ biological treatment potential of pit lakes. For instance, lack of suitable substrate for organisms such as *Metallogenium* spp. (manganese oxidizing bacteria) would decrease their remediation potential in the epilimnion. Nutrients generated within a suboptimally sized and degraded littoral zone may also decrease the

remediation potential of anaerobic bacteria in the hypolimnion because pit lakes may rely more heavily on littoral zone nutrients.

Primary productivity may also be limited by the pit lake watershed. Pit lakes often replace habitats that were historically not the location of a terminal water body. After reclamation, a watershed is formed in the landscape, but for the most part, may be considered a closed system because allochthonus imports are limited and may not be of the same quality as natural lake inputs. Pit lakes frequently are surrounded by a watershed that has been severely degraded and may have been denuded of vegetation for long periods of time. Such conditions may render the pit lake watershed sterile for some time. Constant influx of sediment impacts the light quality and displaces the pelagic biota out of the photic zone into the hypolimnion.

Study Objectives

A literature review of three comprehensive databases with the search terms “pit lake” and “mining lake” and “mine lake” revealed 89 peer reviewed articles. Table 1 shows the results when considering the broad categories of biology, chemistry, and physical limnology. Clearly most pit lake studies have focused on chemistry of mining lakes (37%) and none on the interplay of all three limnological domains.

Table 1. Pit lake literature search results in relation to the three broad categories of limnology.

Limnological domain	# of references	% of total
C	33	37
C-B	19	21
P	16	18
B	11	12
P-C	9	10
P-B	1	1
B-C-P	0	0

B=Biological; C=Chemical; P=Physical.

The objectives of this study were:

- To study the biogeochemistry of a filling pit lake
- To determine the key limnological parameters (physical, chemical, and biological) that may facilitate meromixis within pit lakes
- To understand the response of pit lakes to perturbations (natural or manmade) and determine how these events affect lake stability
- To make informed decisions and recommendations about the stability of this lake, current and future pit lakes, and pit lake sustainability.

These objectives were assessed by applying a comprehensive limnological approach to the study of a filling pit lake. This study was conducted with the assumption that meromixis was possible in this lake and that meromixis was the desired goal.

CHAPTER II

METHODS AND MATERIALS

Study Site

The study site was located at the Kennecott Ridgeway Minerals Corporation mine in Fairfield County, Ridgeway, South Carolina (Figure 1). The mine was 8 km east of the town of Ridgeway and approximately 32 km north of Columbia, SC.

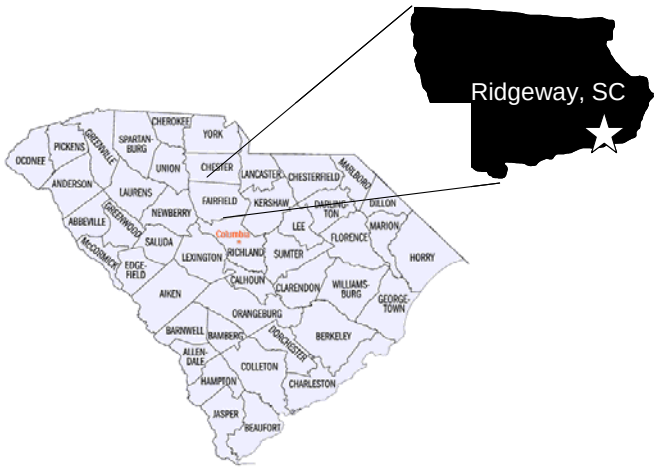

Figure 1. Location of study site, Ridgeway, SC.

Site Description

The mine was situated within the Carolina Slate Belt, which is characterized by metamorphosed volcanic or fine-grained sedimentary rocks (Hanna Murphy, 1995). The primary target metals were gold and silver, which was contained in turbidites (sedimentary deposits settled out of turbid water carrying particles of widely varying grade size) and was also embedded in the many dikes and faults that transected the host rocks (Gillon et al., 1995). South Pit geology consisted of three hydrothermal alterations;

quartz + sericite + 1% pyrite, quartz + sericite + 1-1.5% pyrite, and quartz>>sericite + pyrite (Gillon et al., 1995). Kennecott mined gold and silver beginning in 1988 and ceased operations in 2000. Upon cessation of mining South Pit Lake was allowed to fill with water. Water quality in the early period was typical of acid mine drainage lakes, low pH and high concentrations of trace metals. Reclamation of the site began in 2000 and consisted of partially backfilling the pits, soil capping the tailings impoundment, designing constructed wetlands and sluiceways, revegetating most of the site with grasses, and tree planting and seed dispersal within the wetlands. Figure 2 shows an aerial photograph of the mine site, which was taken in June 2001.

Watershed

In the following description, all numbers in parentheses refer to Figure 2. The watershed for both pit lakes (1, 2) was composed of a 126 ha vegetated tailings impoundment (17), four constructed wetland complexes (3, 4, 5, 6) totaling ~12 ha, nine ponds (one artificial (14) and eight natural (7, 8, 9, 10, 11, 12, 15, 16)), a $3.785E^5$ m^3 lined reservoir (13), and several natural wetlands. Upland portions of the watershed totaled nearly 445 ha and consisted of ~348 ha of pine/scrub oak forest and ~85 ha of newly reclaimed and vegetated area (grasses). Most of the upland watershed, which fed the lakes during the first 1.5 years of this study, was disturbed during mining and had no vegetation. The site was revegetated during the second year of this study.

Pit Lakes

South Pit (SP) was initially mined in 1988 and reclamation began in 1996. It reached maximum depth at -6 m (msl) but was backfilled with low grade material to an elevation of 65 m (msl) (pit floor). Dewatering ceased and South Pit Lake (SPL) began filling in September 1996. North Pit (NP) was initially mined in 1990 and reclamation began in 2000. It reached maximum depth at -18 m (msl) but was backfilled with low-

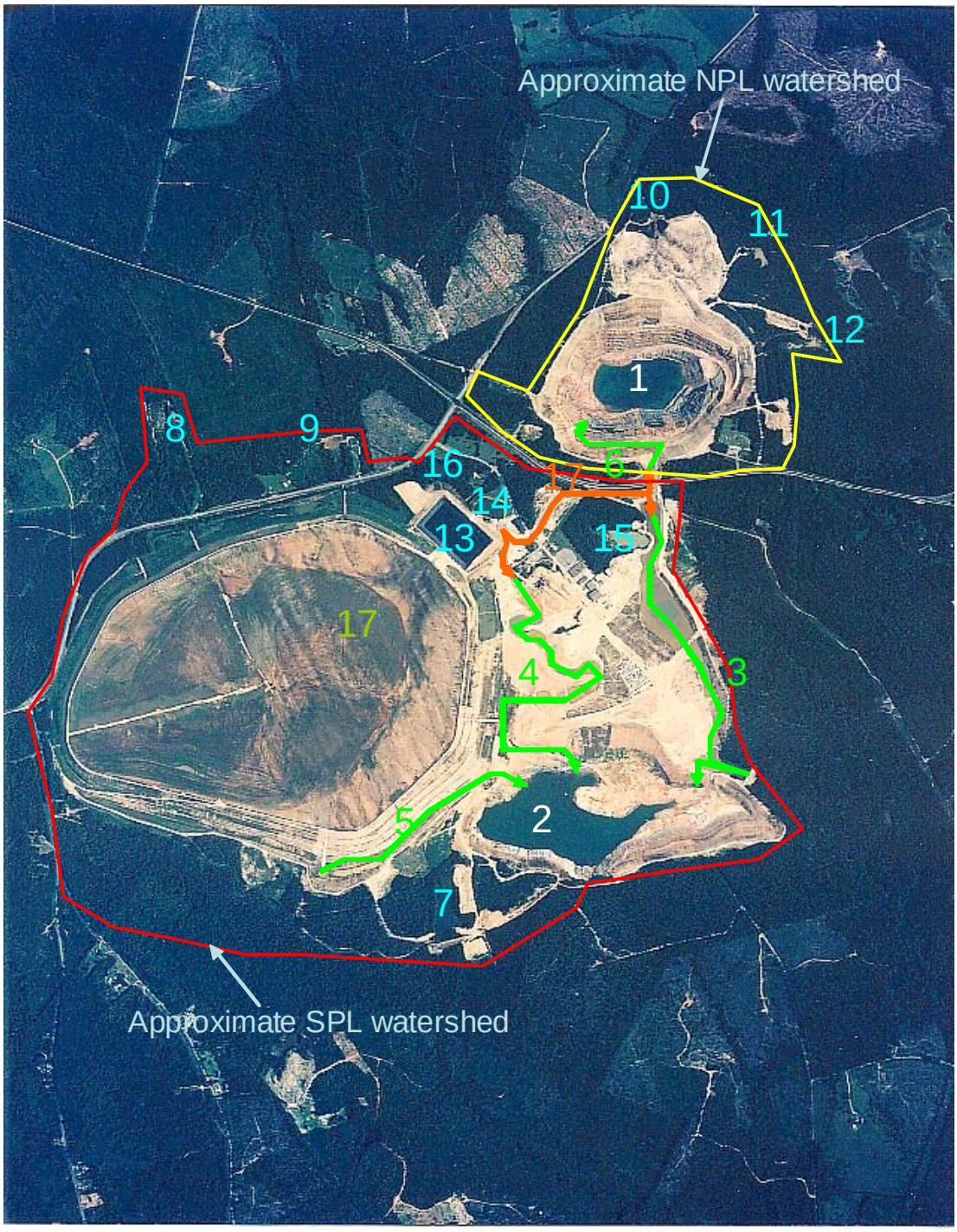

Figure 2. Kennecott-Ridgeway mine site and points of interest for watershed. SPL= South Pit Lake, NPL=North Pit Lake

grade material to an elevation of 12 m (msl) (pit floor). Dewatering ceased and North Pit Lake (NPL) began filling in November 1999. A series of lifts and ramps were constructed in both pits with low grade material upon filling. The pit walls of both pits were partially covered with blasted material in an effort to decrease weathering of the parent material and concomitant release of wall constituents. The pit rims were blasted and contoured to a final slope of 3:1.

South Pit Lake (SPL) bathymetry was determined with over 100 depth soundings (Wetzel and Likens, 2000) and GPS. A bathymetric map of SPL during the study period (33 m maximum depth) is shown in Figure 3 and a profile view is shown in Figure 4.

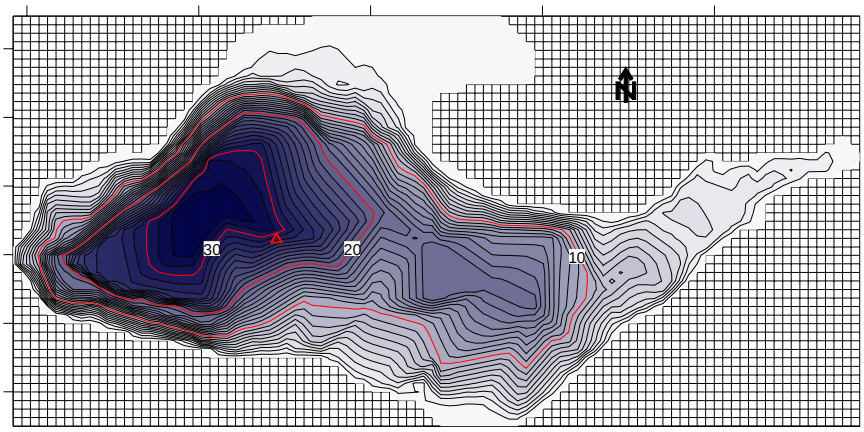

Figure 3. Bathymetric map of South Pit Lake during the study (~33 m maximum depth). Depth contours are shown in meters from surface. Triangle indicates location of center buoy.

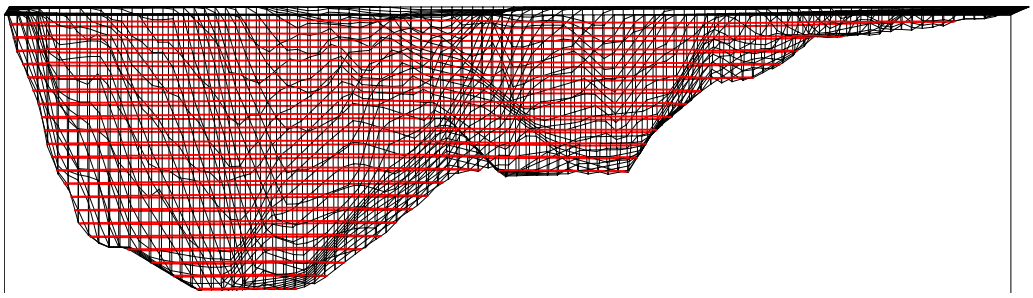

Figure 4. Profile view of South Pit Lake during the study (~33 m maximum depth). View is shown from the south looking north.

A bathymetric map of the lake at future maximum depth (~56 m) is shown in Figure 5 and a profile view is shown in Figure 6.

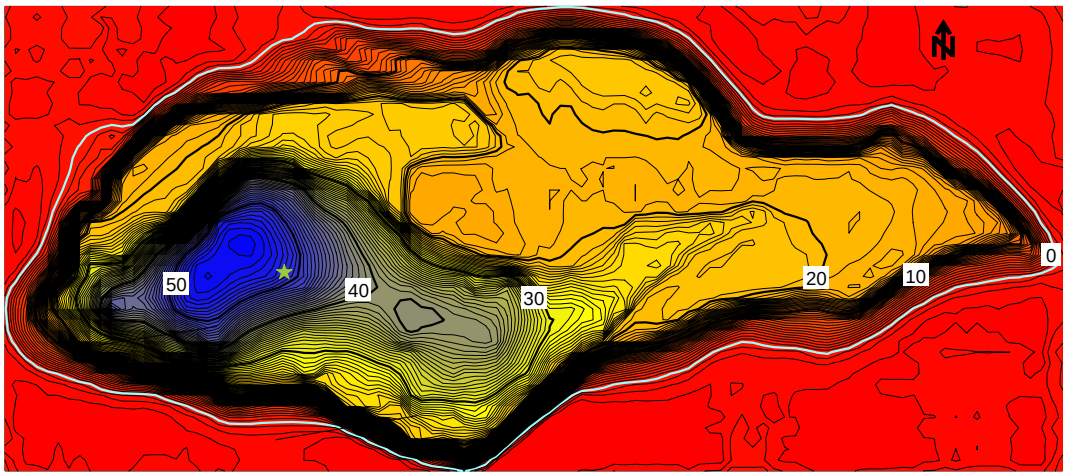

Figure 5. Bathymetric map of South Pit Lake (~56 m maximum depth). Depth contours are shown in meters below surface (blue contour).

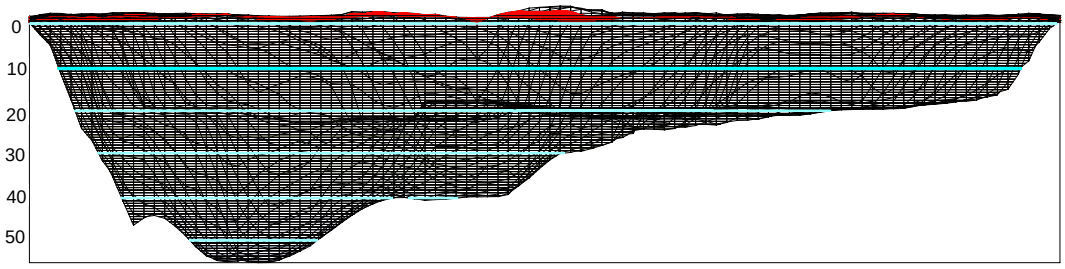

Figure 6. Profile view of South Pit Lake at maximum depth (~56 m). View is shown from the south looking north and depth is shown in meters.

South Pit Lake was oriented with its longest axis in the east-west direction and at the 98 m elevation (surface elevation throughout most of the study) the length was ~734 m. The maximum breadth in the north-south axis at the same elevation was ~335 m. As a result of mining and backfilling, the west end was nearly 25 m deeper than the east end. Figure 7 shows hypsographs as area (m^2) and as % volume of SPL during the study period. The center of volume for SPL was 10.7 meters.

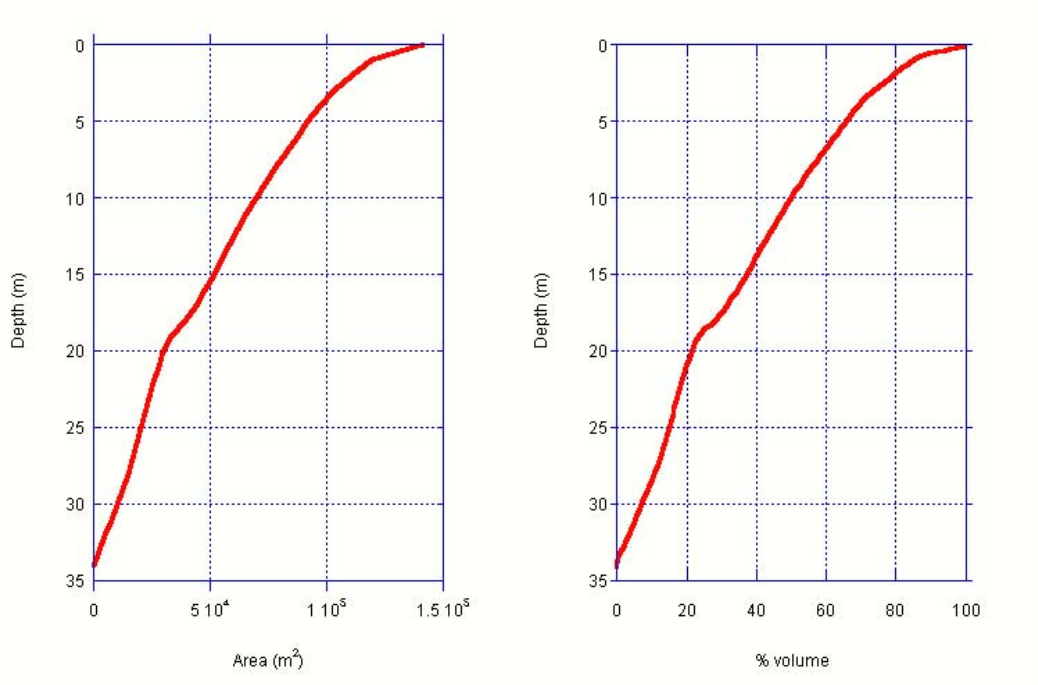

Figure 7. South Pit Lake hypsographs shown as area-vs-depth (left) and as % volume-vs-depth (right).

Pit lakes typically have significantly larger maximum depth:mean diameter ratios than most natural lakes. This morphometric parameter is called the relative depth ratio (Z_r) and is defined as:

$$Z_r(\%) = \frac{50 Z_{max} \sqrt{\Pi}}{\sqrt{A_0}}$$

where:

Z_{max} is maximum depth
A_0 is area at the surface

Certain types of natural lakes (calderas, grabens, fjords, and crater lakes) have a Z_r that exceeds 3%, but most natural lakes are less than 2% (Hutchinson, 1957; Cole, 1996; Wetzel, 2001). Pit lakes typically have a Z_r of 10% or more (Doyle and Runnels, 1997). Lakes with high Z_r are generally highly transparent and nutrient poor and are often meromictic (Kalff, 2002; Walker and Likens, 1975). Meromixis results in a zone of anoxia in the monimolimnion, so this circulation pattern has long been the goal for pit lakes in the mining industry.

Z_r of SPL during the study was 9.18% and the projected value of the filled SPL is 9.59%. Although SPL will get much deeper and the bathymetry will drastically change from its current configuration, surface area and depth will increase proportionally (according to the above formula) so Z_r will remain relatively unchanged. These values fall within the range of lakes known to be meromictic due to biogenic processes (Cole 1994). The most significant change in surface area will occur when the lake level reaches ~25 m depth (in Figure 5). This bathymetric feature, known from here forward as the solar plate, was a large section of graded backfill material placed in the pit from 1999-2000.

Tailings Impoundment

The lined impoundment held approximately $4.5x10^{10}$ kg of tailings and at the surface was about 125 ha. It had a soil cover that was slurried into place in 2000. The cover was designed so runoff would drain to the east and empty into the netted pond. In 2000 the soil cover was hydroseeded with grasses and vegetation began growing in the spring of 2001. Several wetland plant species have become established in the cap as well through natural recruitment. Most of the wetland species were at the east end where water drained to the netted pond.

Netted Pond

The netted pond was a 244 m x 152 m lined reservoir with a total volume of ~$3.8E^5$ m^3. It received direct precipitation and runoff from the vegetated tailings impoundment. Water could be released from the netted pond to either NPL via the granite lined channel/NPL wetland or SPL through the east wetland complex and/or the gravel lined channel/west wetland complex.

Constructed Wetland Complexes/Natural Wetlands

Approximately 12 ha of wetlands were designed for the site. The east wetland system was 6.5 ha and consisted of 5 cells and one pond. Each cell had a marsh-pond-marsh configuration with each section approximating one third of the area. In 2001, 6 ha of this system was planted with a mixture of cattails and bulrushes on 3 m centers. Most of those plants were pulled up by geese in the summer of 2001 but the plants remained in the wetland area. In the fall of 2001 and the spring of 2002, the plants became established along the wetland edges. Each cell has nearly full coverage today. In addition to the emergent vegetation, the first cell had ~200 bald cypress and black gum tupelo planted throughout its 0.6 ha. Almost all trees planted in that cell survived. In addition, nuttall and shumard oaks were planted along the banks of the first cell and along the eastern shore of the east wetland complex. Except for grazing by deer, those trees have had nearly 100% survivability as well.

The east wetland system currently receives water from the netted pond through a granite-lined channel. Once North Pit Lake is filled, overflow water will gravity feed through the east wetland system to the surface of South Pit Lake.

The west wetland system had 3.5 ha and consisted of four constructed wetland cells with the aforementioned configuration, and one natural wetland at the end. The natural wetland has been on site since mining commenced. This system receives water from the netted pond and flows down a vegetated corridor to the South Pit Lake ramp and into the lake. The west system was not planted in 2001, but had cattail seeds disbursed throughout each cell. Full establishment was delayed by approximately 6 months, but coverage was nearly complete in this complex as well.

Natural/Manmade Ponds

Several natural ponds were on site throughout the life of the mine and several ponds were established for water catchments. Of note, the Bear Creek pond was on site

previous to mining and has received much runoff throughout the history of the mine. This pond was decanted and dredged several times directly to South Pit Lake during mining and reclamation. The biotic importance of this pond may have been significant in establishing South Pit Lake biota.

Sampling

Weekly Pit Lake Sampling Regime

When possible, each lake was sampled weekly. Dates were more or less chosen at random and were determined mostly by the weather, but NPL was not sampled for an extended period due to safety concerns. No sampling was attempted during storm events but may have been completed prior to or subsequent to storm events. Each sampling event consisted of vertical water column profiles of several water quality parameters including photosynthetically available radiation (PAR), Secchi depth, and sampling of phytoplankton and zooplankton. The methods for each parameter are described below. Each sampling event was performed at a single fixed location at the center of each lake. Both sites were chosen for their central location and did not necessarily coincide with the deepest part of the lake.

Multiparameter Sonde Profiles

A Hydrolab 4a multiparameter sonde (Hydrolab Corporation, Austin, TX) was used for all in situ water quality analyses. The sonde measured depth, pH, dissolved oxygen (DO), specific conductance (SpCond), turbidity (Turb), oxidation-reduction potential (ORP) (Pt electrode), and temperature (Temp).

According to Hydrolab “Specific conductance readings are conductivity readings that are corrected (compensated) to 25° C, regardless of the current measurement temperature, following the equation:

Specific Conductance = conductivity x f(T)

where, the function f(T) is a nonlinear equation using temperature (T) in °C as an input" (Hydrolab manual, 1997).

The sonde offered several specific conductance temperature compensation functions. The freshwater function was chosen for this research which was derived from a 0.01N KCl solution as follows:

$$f(T) = c1T5 + c2T4 + c3T3 + c4T2 + c5T + c6$$

where c1= 1.4326 x 10-9, c2= -6.0716 x 10-8, c3= -1.0665 x 10-5, c4 = 1.0943 x 10-3, c5 = -5.3091 x 10-2, c6 = 1.8199.

In July 2001, a fluorometer was added to the sonde for in situ chlorophyll *a* measurement. The same instrument was used for all profiles unless that instrument was returned for periodic maintenance. During these instances, a similar sonde with the same parameters with the exception of the fluorometer was used.

The sonde was calibrated in the lab according to the manufacturer using prepared standards before each profile. Post calibration checks were done in the lab either directly after the profile or during the next profile calibration. Almost all calibration data were within 10% error and data outside the 10% cutoff were discarded. Most data were under 5% error. Accuracy of each probe according to the manufacturer was as follows: depth (± 0.3 m), pH (± 0.2 units), D.O. (0.2 mg/L), specific conductance (1% of calibrated range (1.413-8.974 uS/cm^2)), turbidity (5% of calibrated range (0-100 NTU)), ORP (± 20 mV), chlorophyll *a* (0.02 µg/L) and temperature (0.1°C). The fluorometer was initially calibrated with a NPL chlorophyll *a* extraction. Subsequent calibrations were done using a secondary calibration chlorophyll *a* standard, which was standardized to the initial NPL extraction.

Profiles consisted of meter-by-meter sampling from the surface to the bottom. Each reading was taken only when the pH and ORP readings (believed to be slowest to

equilibrate) centered around one number. This equilibration time was ~1-2 minutes and might have taken longer around the redoxycline and below. In November 2001, readings were taken every 0.2 m through the photic zone, which was determined during each profile prior to the sonde profile. Once the sonde was out of the photic zone, meter by meter sampling resumed.

Assessment of the Light Field

Two LI-COR LI-192SA underwater quantum sensors (LI-COR Environmental, Lincoln, NE) attached to a lowering frame were used to measure upwelling and downwelling Photosynthetically Active Radiation (PAR) in the lake. An onboard sensor was not used to correct for cloud cover, but an attempt was made to take readings during homogenous conditions (total cloud cover or clear skies). Readings were taken meter by meter from a few cm under the surface to the depth of <1 μE. Data were collected with a LI-COR LI-1400 data logger and were downloaded and analyzed weekly. Secchi disk readings were taken according to Wetzel and Likens (2000) with a standard disk and were recorded on weekly data sheets.

Thermistor Strings

Two sets of thermistor strings were deployed in order to assess basin scale motions within the lake. One string was deployed at the center buoy location (West string) and one above the prominent ledge to the east (East string) of the center buoy. Each string had seven StowAway TidbiT underwater temperature loggers (Onset Computer Corporation, Bourne, MA) which were deployed at the following depths: surface, 2 m, 4m, 6 m, 10 m, 14 m, and 18 m. The loggers were accurate to within 0.2° C for the temperature range of this study. The thermocline was located ~4 m during the analysis. Isotherm displacements were calculated by linear interpolation of data collected from two adjacent thermistors. The Signal Processing Toolbox (version 6) for MATLAB

7 (www.mathworks.com) was used to perform power spectral density analysis on the isotherm displacement data.

Phytoplankton Sampling And Analysis

Phytoplankton were sampled with a 12 volt self-priming pump attached to a metered and intake end-weighted 40 m Tygon® tube. The tube was wound on a typical garden hose reel and was lowered to the desired depth. Prior to each sample collection, the hose volume was flushed with an equivalent of three times the hose volume. In year 1, 200 mL samples were taken from surface-10m at whole meter increments and an additional 200 mL sample at 15 m. Samples were kept in separate bottles and were not composited. In year 2, 200 mL of sample was taken from surface-15 m at 1-meter increments with a graduated cylinder and composited in the lab. In year 3, the entire photic zone (determined on each sampling date with the LI-COR photometers) was sampled by reeling the hose up from the bottom of the photic zone to the surface at a constant rate. The sample was composited in a 5 L carboy and was subsampled into 2-200 mL samples and 1-1 L sample (for chlorophyll *a* extraction). All samples were preserved in the lab with a 10% povidone iodine solution at a mixing ratio of 1mL:200 mL sample. All sample counts are presented as cells/m^3.

Phytoplankton were identified and enumerated by the Uttermol technique with inverted light microscopy according to Wetzel and Likens (2000). When appropriate, organisms were identified with higher magnification (up to 1000x oil immersion) light microscopy or phase-contrast microscopy. All species were identified with taxonomic keys according to morphology. No DNA identifications were attempted. All unidentifiable organisms, mostly nannoplankton, were placed into general categories.

Chlorophyll *a* extractions were done according to Wetzel and Likens (2000). A 0.45 µm acetate filter and faucet aspirator were used to filter samples. The extractions

were analyzed with an Ocean Optics S2000 fiber optic spectrometer (Ocean Optics, Dunedin, FL).

Zooplankton Sampling and Analysis

Zooplankton samples were collected with a Wildco Fieldmaster Plankton Net (Buffalo, NY) with a mesh size of 80 μm and mouth sample area of 127 cm^2. The plankton net was lowered to depth and was retrieved at a constant rate to the surface. Numbers of zooplankton collected were standardized by multiplying the maximum depth sampled by the area of net mouth. Zooplankton were identified and enumerated using the Uttermol technique with inverted light microscopy according to Wetzel and Likens (2000). All species were identified to the lowest practicable taxon.

Weather Stations

To assess the impact of weather on the chemistry, physics, and biology of both pit lakes, each lake had identical, stand-alone weather stations. Two Davis EZ-Mount GroWeather systems (Hayward, CA) were used. Each was equipped with the following options: data logger, solar kit, barometric pressure, air temperature, anemometer, a 0.254 mm increment rain collector, humidity, leaf wetness sensor, and solar radiation sensor. Stevens and Lawrence (1998) discussed the importance of placing weather stations near the surface of pit lakes instead of the pit rim or even further away to minimize errors due to pit wall effects on local meteorology so each weather station was placed as close as possible to the surface of each lake. The weather stations were installed in backfill material and were moved as necessary due to rising water levels. Each weather station was programmed to collect data every 5 minutes and the data were downloaded to a laptop computer three times per week.

Chemistry Sampling

All chemistry samples were collected with a battery-powered pump connected to a metered and end-weighted Tygon™ tube. Samples were taken after the hose had been flushed with the equivalent of three hose volumes, and were placed in new nitric acid preserved bottles (metals), sulfuric acid preserved bottles (Total Kjeldahl Nitrogen (TKN), ammonia, and total phosphorus), or bottles with no preservative (sulfate, orthophosphorus, chloride, DOC, and nitrate). Samples were immediately placed on ice in the field and held in cold storage until transfer to the analytical lab (usually within 24 hrs).

Alkalinity was analyzed in the laboratory by potentiometric titration to an endpoint pH of 4.5 (EPA 310.1). All other analyses were completed by an independent laboratory located ~50 km from the mine site. Metals and silica (calculated from silicon according to EPA method 200.7) were analyzed according to EPA method 200.8 using a PerkinElmer AAnalyst 600 graphite furnace atomic absorption spectrometer. Sulfate and chloride were analyzed according to EPA method 300.0 using a Dionex ICS-2000 ion chromatograph. Phosphate and orthophosphorus were analyzed by the ascorbic acid method (EPA method 365.2). A Lachat Quick-Chem 8000 was used to measure nitrate (cadmium reduction method -EPA 353.2), ammonia (automated phenate method -EPA 350.1), and TKN (semi-automated block digestion method -EPA 351.2). Reporting limits for each constituent are shown in Table 2.

On two dates, two sets of samples were analyzed, one filtered and one unfiltered. Filtrations were performed in the laboratory with a 0.45um filter under slight vacuum. Results for most analytes showed little to no difference between filtered and unfiltered samples (results not shown). Shevenell et al. (1999) also found little difference between filtered and unfiltered samples when studying pit lakes in Nevada. Therefore, all concentrations in this report are presented as total concentrations.

Table 2. Reporting limits for chemical constituents.

Constituent	Limit (mg/L)
Ag	0.0050
Al	0.20
Ar	0.0050
B	0.050
Ba	0.025
Be	0.0040
Ca	5.0
Cd	0.0020
Cl	1.0
Co	0.025
Cr	0.0050
Cu	0.0050
DOC	1.0
Fe	0.10
K	5.0
Mg	5.0
Mn	0.015
Mo	0.040

Constituent	Limit (mg/L)
Na	5.0
NH_3	0.5
Ni	0.040
NO_3	0.020
Ortho-P	0.0010
Pb	0.0030
P	0.0010
Sb	0.0050
Se	0.0050
Si	0.50
SO_4	50
Ti	0.050
TKN	0.50
Tl	0.010
Tn	0.050
V	0.050
Zn	0.020

Mass calculations were performed using all chemistry data which was usually collected at 5 meter intervals. Throughout the study, pit lake depth fluctuated and ranged from 28 m to 32 m. Instead of using elevation as a benchmark and lake bottom as the zero reference depth, the water surface for that particular sampling day was used as the zero reference depth. As a result, the sampled depths and therefore stratum volume changed over time. In order to correct for this error and still be able to do a mass balance analysis, the lake was divided into upper and lower halves and results for the individual halves were averaged then multiplied by the volume of either the upper or lower half. Results were compared to all other dates in depth-time diagram format.

Two geochemical models were used in this study to calculate saturation indices, define chemical species, model monimolimnetic density dynamics, and to simulate the resulting chemistry of the pit lake in the case of a complete mixing event. The models used were PHREEQC Interactive v. 2.8 (http://wwwbrr.cr.usgs.gov/projects/GWC_coupled/phreeqc/index.html) and Visual MINTEQ v. 2.50 (http://www.lwr.kth.se/English/OurSoftware/vminteq/). Geochemical equilibrium models are used extensively in pit lake studies as a tool for predicting future pit lake water quality because they offer the ability to calculate ion activities and saturation indices in seconds whereas doing the

same calculations by hand would be inefficient. Although several limitations exist regarding geochemical models (see Parkhurst, 1995), they can be fairly accurate for many systems. In assessing the applicability of available geochemical models (BALANCE, MINTEQA2, PHREEQE, WATEQF, and WATEQF4) to pit lakes, Bird (1993) and Bird et al (1994) showed that those programs were capable of predicting pit water geochemistry within acceptable error. Eary (1999) pointed out that PHREEQC is often used in pit lake studies because of its ability to predict the geochemistry of a mixed water scenario and the ease with which one can specify equilibrium controls. Levy et al (1997) used MINTEQA2 to calculate the accuracy of all analytes within their pit water samples based upon solution charge imbalances and also used the model to perform Fe^{2+}/Fe^{3+} activity ratios based upon measured Pt electrode redox potentials. Geochemical model output is a simulation of the theoretical equilibrium situation. However, in open systems influents, effluents, and biota continuously disturb the path toward theoretical equilibrium. Therefore, care should be taken when using any model to ensure that output data makes sense.

CHAPTER III

RESULTS

Overview and Description of Perturbations to South Pit Lake: 2000-2004

Major perturbations to SPL in 2000 included backfilling, blasting and pit rim contouring, runoff due to rainfall, and release of $2.84E^3$ m^3 of water from the netted pond. Each of these perturbations introduced significant amounts of sediment to the water column, which impacted the physical, chemical, and biological parameters of the lake at all depths. Perturbations in the latter half of 2001 through 2004 were more benign. During this time, rainfall events were not associated with massive loads of sediment in runoff because the site was mostly vegetated. Influents to SPL were from mostly vegetated channels and wetlands. Some sloughing of loose backfill piles along the pit walls continued to impact the lake as well as submergence of new low-grade backfill material as the water level increased. SPL to NPL pumping was sporadic throughout the study period and was used mostly to increase pH in NPL with lime amendment.

Year 2000: Dynamics Due to Rain Events and Netted Pond Release

Several rain events took place during spring and summer 2000. During that time most of the site was being reclaimed to the final topography; so much of the watershed for both pit lakes was bare soil. Prior to June 2000, there were no significant rain events; so water column perturbations were associated with backfilling and pit rim contouring. Backfilling from an area above the surface into the lake diminished or overcame the stabilizing forces of stratification. This was done by homogenizing water column density with turbidity currents. Rain events in early, mid, and late June totaled 7.6 cm and increased turbidity throughout the water column; each event was isolated in the turbidity

depth-time diagram. July was similar with three significant events and each event was captured in the depth time diagrams as well. As a result of runoff from the entire SPL watershed, the associated sediment load had a significant oxygen demand and water column DO decreased rapidly during that time. In addition, heated sediments and soils (resulting from solar radiation) transported to the lake via overland flow (netted pond release and rainfall) or backfilled into the lake, penetrated the epilimnion and released heat to the cooler hypolimnetic water. This phenomenon is shown in the hypolimnion for SPL starting in late June 2000. Light penetration was not significantly impacted because the rate of light extinction decreased (i.e. light penetration increased). Conductivity increased slightly and the trend showed little to no stratification due to conductive material.

In June 2000, the top of the tailings impoundment (~121 ha) was hydroseeded with grasses and nutrients. Shortly thereafter, significant rainfall induced runoff from the top of the tailings impoundment into the netted pond. A significant amount of netted pond water was released to SPL in early August 2000. The release valve for the netted pond water was at the base of the reservoir; so the cooler, silt-laden, bottom water comprised most of the flow initially. As the water exited the netted pond, it flowed through a pipe for nearly 500 m then traveled by overland flow for nearly 500 m. The final 500 m overland flow sequence was ~300 m of bare soil, a small perched wetland, a 21 m waterfall, and nearly 60 m of backfill material. Temperature of the overland flow was measured on one date only in the summer of 2000 and was found to be near the temperature of the epilimnion at that time. Since the temperature was nearly the same, the influent water would have been denser due to the suspended load it was carrying and would have descended to its equivalent buoyancy in the lake or lake bottom.

In early August (~8-4-00 on depth-time diagrams) when the first netted pond influent entered the lake, it decreased the temperature of the epilimnion, increased the temperature of the hypolimnion, and increased the turbidity at all depths, although

turbidity increases were larger at the surface, thermocline and at lake bottom. This pattern would suggest deep water penetration due to heavy sedimentation, but portions of the density current peeled off and remained at the surface or slid along the thermocline. After the initial flush of sediment (~8-17-00 on depth-time diagrams), turbidity remained high in the hypolimnion, slightly higher in the epilimnion, and decreased in the metalimnion. Temperature rapidly increased in the epilimnion because suspended materials scattered the incident light and retained that energy in the epilimnion. Temperature decreased in the hypolimnion at that time and may have been due to decreased light penetration in conjunction with rapid filling. Impact due to the influent was isolated to the hypolimnion and somewhat to the epilimnion. This pattern resulted from decreased sediment load due to channelization of the overland flow pathway and may have indicated that most of the sediment to the hypolimnion resulted from subsurface backfill pile slope failures and subsurface scouring of the final backfill pile at the water surface-influent interface (Incidentally, two scour marks can be seen on the SPL bathymetric map). The lowest conductivity during the study period was in the epilimnion during this time. As a result of netted pond influent and solar radiation, a horizontal lake circulation pattern was set in motion. Conductivity and DO in the epilimnion increased, indicating the circulation pattern and nutrients from the netted pond water were stimulating the algal community. Shear forces along the thermocline sealed off oxygen flow and diffusion to the hypolimnion and bacterial respiration commenced hypolimnetic oxygen depletion. ORP started to decline in the hypolimnion during this time, indicating bacteria may have been helping to poise the hypolimnetic redox environment.

Runoff as a result of rain events in September 2000 increased the sediment load to the pit. Conductivity and turbidity increased in the water column and a pulse of oxygen accompanied the density current to lake bottom. This sediment load may have had significant oxygen demanding waste or nutrients because the DO was quickly purged in

the hypolimnion. Thermal stratification was not significantly affected during this time, but onset of winter set the processes of holomixis in action and the lake completely mixed in the winter of 2000.

2001

A significant spring phytoplankton bloom increased the DO at ~5 meters. This bloom most likely resulted from redistributed nutrients from lake bottom during turnover. Conductivity in the epilimnion decreased, indicating significant amounts of calcite, iron, manganese, and possibly gypsum were being precipitated due to phytoplankton photosynthetic processes. pH increased in the epilimnion, which also indicated photosynthetic processes were at work. A concomitant increase in conductivity in the hypolimnion was evident. This may have indicated epilimnetic precipitates were being resolubilized in the hypolimnion and that redox sensitive species were being mobilized from the sediment. ORP during this time indicated a slight shift toward more reducing conditions, but the process may have been interrupted by density currents due to runoff events (rapid influx of chemical elements and possibly low amounts of DO). As the spring bloom died off, the algal cells descended to the lake bottom. This process was captured with the fluorometer (results not shown). The algal cells most likely enriched the benthic bacteria because DO was slowly depleted. ORP in the hypolimnion began decreasing during this time, which indicated a trend toward more reducing conditions.

Onset of winter had a rapid impact on the water column. Mixing and cooling processes decreased the depth of the thermocline from ~12 m to ~25 m within a one month period. Unseasonably warm temperatures, increased density at lake bottom, and decreased wind speeds protected the lake from holomixis and meromixis commenced in early 2002.

2002-2003

Phytoplankton density was not nearly the same as in 2001, which resulted in less photosynthetic oxygen production in the nephloid layer and may have decreased the amount of constituents precipitated from the mixolimnion.

In the winter of 2002-2003, a brief pulse of oxygenated water was injected to the lake bottom. pH in the entire water column decreased briefly, the result of monimolimnetic ferric iron oxygenation and concomitant water column mixing. Mixing was incomplete in 2002 and meromixis was maintained through the rest of the study period.

Significant rainfall in 2003 increased lake depth and submerged the solar plate by about 3 m. Submergence of the solar plate helped to decrease the amount of sediment to the lake and added a significant physical feature to the bathymetry.

South Pit Lake Weather Station Data

Precipitation

The SPL weather station has been in place since April 2001. Its location has been moved three times due to the increase in water level, but has always remained near the lake surface. Figure 8 shows the daily rainfall for SPL from April 2000 through March 2003. Rainfall data prior to April 2001 were recorded from an on site rain gauge located about 1.5 km away from the lake. Of the 1071 days within the study period, 785 (73%) had no precipitation. 65 days (6%) had precipitation between 0.025 cm and 1.27 cm, 149 days (14%) had precipitation between 1.30 cm and 2.54 cm, 44 days (4%) had precipitation between 2.57 cm and 3.81 cm, 22 days (2%) had precipitation between 3.84 cm and 5.08 cm, 4 days (0.4%) had precipitation over 5.08 cm.

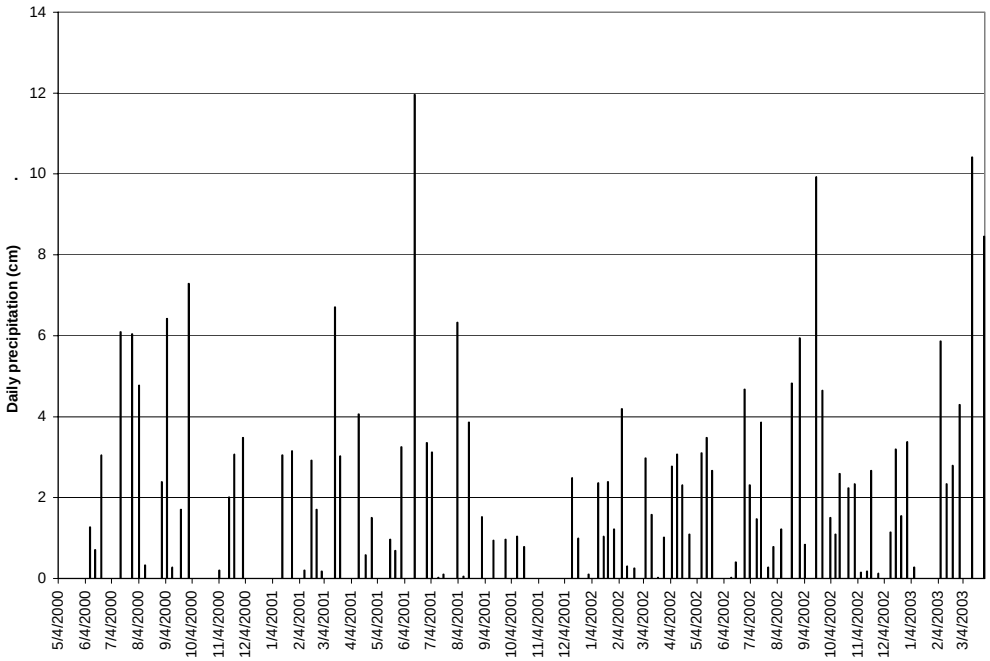

Figure 8. Total daily rainfall for South Pit Lake from April 2000 through March 2003.

about 1.5 km away from the lake. Of the 1071 days within the study period, 785 (73%) had no precipitation. Sixty-five (65) days (6%) had precipitation between 0.025 cm and 1.27 cm, 149 days (14%) had precipitation between 1.30 cm and 2.54 cm, 44 days (4%) had precipitation between 2.57 cm and 3.81 cm, 22 days (2%) had precipitation between 3.84 cm and 5.08 cm, 4 days (0.4%) had precipitation over 5.08 cm.

Figure 9 shows the total monthly rainfall data from April 2000 through June 2004. Of the 51 months, 19 months (37.3%) had 0.0 cm - 4.83 cm of precipitation, 21 months (41.2%) had 5.08 cm - 9.91 cm of precipitation, 6 months (11.8%) had 10.16 cm – 15.24 cm, and 5 months (9.8%) had over 15.24 cm of precipitation.

South Pit Lake Wind Field

Figures 10 and 11 show wind direction and wind speed data for SPL from April 2001 through December 2001 (5-minute interval averaged data). Most of the wind

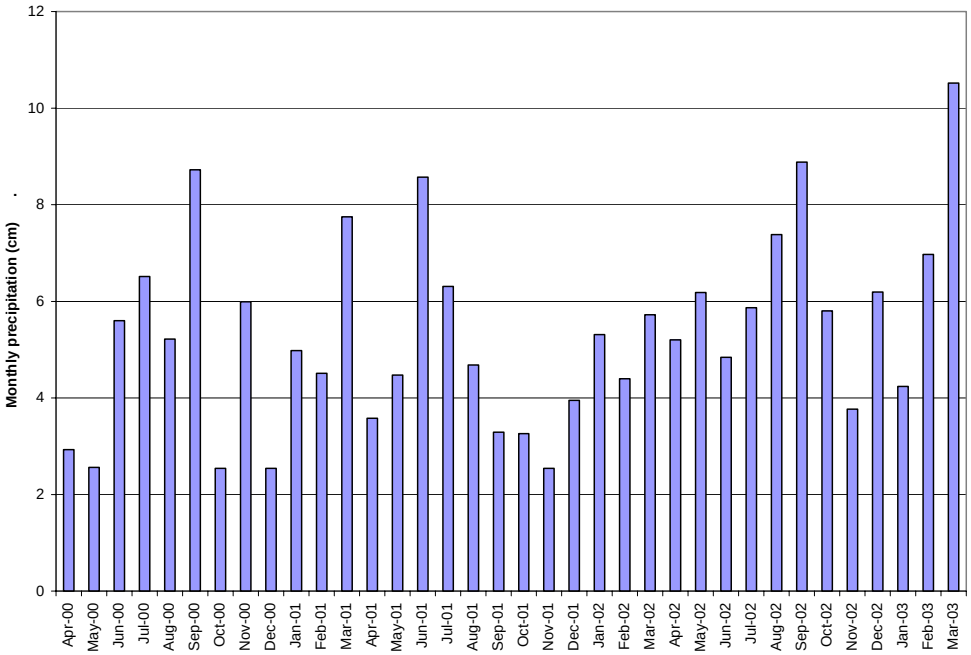

Figure 9. Total monthly rainfall data from April 2000 through June 2004.

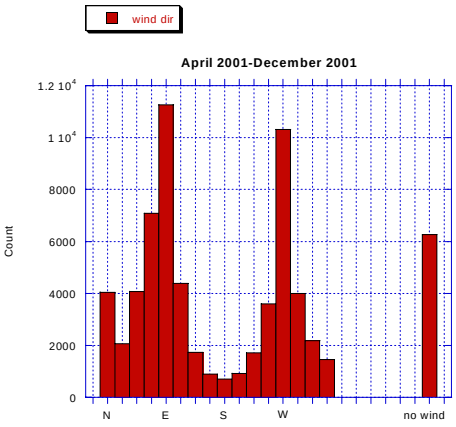

Figure 10. Wind direction for SPL in 2001.

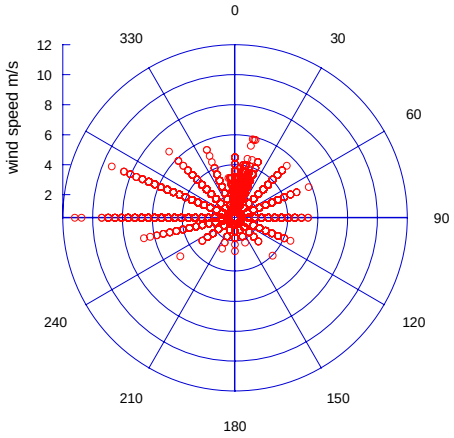

Figure 11. Wind speed for SPL in 2001.

impacted the lake from the east-west direction. Highest wind speeds came from the west and west-north-west directions and exceeded 7 m/s.

Figures 12 and 13 show wind direction and speed data for SPL from January 2002 through June 2002 (5-minute interval average data). Winds during this time period were

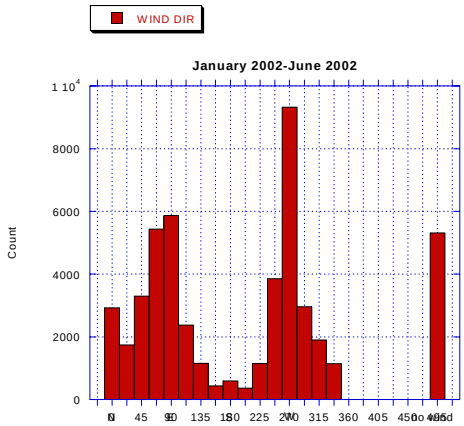

Figure 12. Wind direction for SPL in 2002.

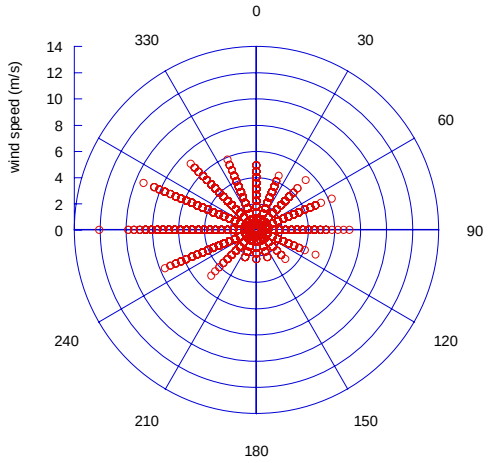

Figures 13. Wind speed for SPL in 2002.

also predominantly along the east-west direction with the highest winds from the west, west-north-west, and west-south-west directions. Winds were slightly higher during this time period, at 9 m/s from the dominant directions.

Figure 14 shows wind gusts for SPL from January 2002 through June 2002. Gusts during this time period were strongest from the west, west-north-west, west-south-west, and north-west. Many gusts exceeded 13 m/s from the dominant directions and the highest gusts were recorded from the west at nearly 25 m/s.

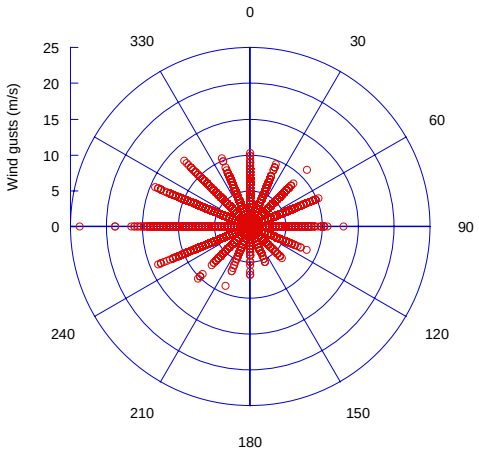

Figure 14. Wind gusts for SPL in 2002.

Figures 15 through 18 show histograms of wind direction for each project year. As a result of lake filling, SPL weatherstation was moved subsequent to the initial deployment on January 28, 2003 and May 9, 2003. The January 2003 move was from the original location on the solar plate, westward, to a more central lake location on a berm on the solar plate. The May 2003 move was westward and the weatherstation was assembled on a buoy. The changes in location are evident in the wind frequency diagrams. Even though there is still an east-west trending wind pattern, the wind

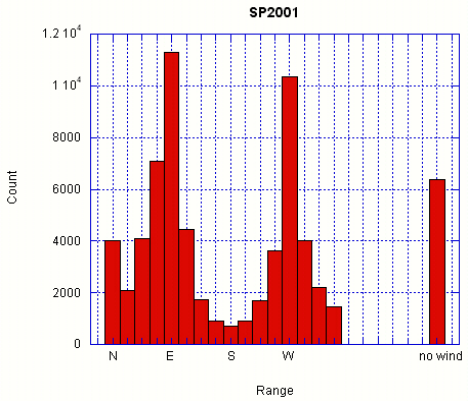

Figure 15. Wind direction for SPL from April 2001 through December 2001.

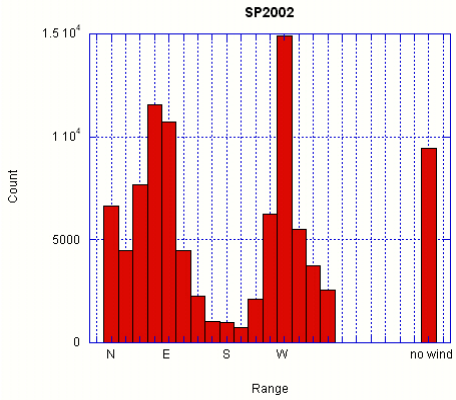

Figure 16. Wind direction for SPL from January 2002 through December 2002.

Figure 17. Wind direction for SPL from January 2003 through December 2003.

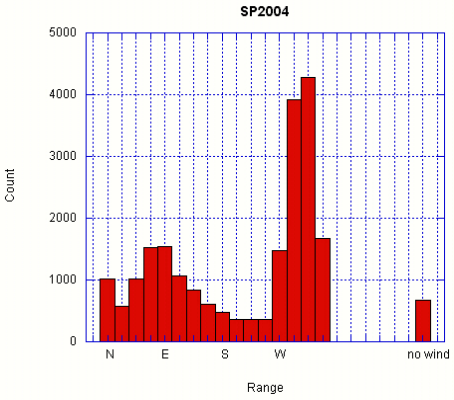

Figure 18. Wind direction for SPL from January 2004 through June 2004.

distribution is more centered around the east-west trend rather than dominantly from the west and east. In addition, wind from the north was more frequent than easterly winds in 2003. As Stevens and Lawrence (1998) pointed out, wind data should be taken near lake surface, but these data suggest that pit wall forcing impacts wind direction on relatively small scales (tens to hundreds of meters) as well.

Sonde Data Results

Temperature Trend

Temperature trends throughout the study period are shown as isotherms in depth-time diagram format (Figure 19). The winter of 2000 was the only time temperature was the same from surface to bottom indicating holomixis. Each subsequent year at least the bottom 5 m of water remained unmixed throughout the winter (meromictic). Mixed layer depth ranged from 3-6 m in early spring to 13-15 m in winter.

Maximum surface temperature increased slightly over the study period from 30.35° C to 31.39° C. Minimum surface temperature decreased over the study period from 8.85° C to 6.85° C. Maximum temperature at the lowest strata within the lake has decreased slightly over time while the minimum temperature has increased slightly over time.

The coldest water of each yearly cycle was always observed during winter, as short duration, cold-water intrusions. These intrusions were always related to winter precipitation events and snowmelt runoff. Interestingly, the intrusions showed a decreasing temperature trend over the duration of the study, which may have resulted from increased vegetation (less sediment loading) throughout the watershed.

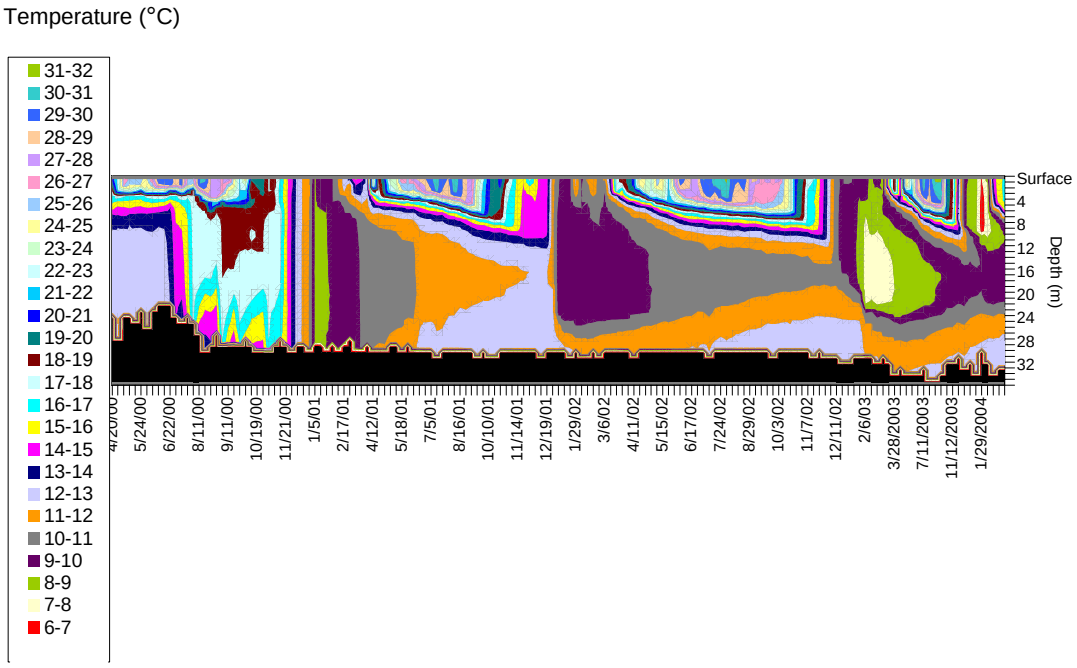

Figure 19. South Pit Lake temperature isopleth depth-time diagram from April 2000 through April 2004.

A trend within the isotherm figure was that the lower monimolimnion (5-10 m of the lake) was always warmer than the mid monimolimnion after holomixis in 2000. This unusual temperature profile (Figure 20), where the coldest water is observed to be at an intermediate depth instead of the lake bottom, is common in meromictic lakes, so common in fact that the term dichothermy was coined to describe this meromictic lake feature (Cole, 1994). Several mechanisms that may have solely or in part contributed to such a trend could have been warm ground water intrusion, direct solar heating of the dense saline layers at the lake's bottom, biogenic metabolism, exothermic chemical reactions, geothermal heating, or a constant flow of heated sediment to the lake bottom along the eastern slope of the lake. Parsing out the contribution of each mechanism to the whole was not pursued.

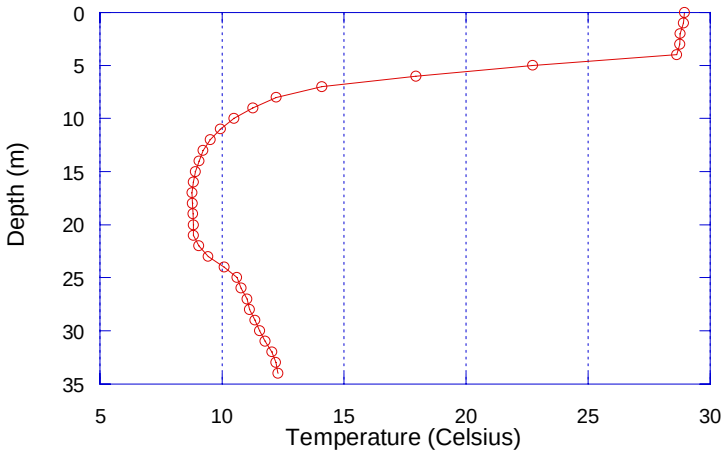

Figure 20. Temperature profile of South Pit Lake on July 24, 2003, showing dichothermy.

Temperature trends for 5 selected depths within the lake are shown in Figure 21. Data for this figure were referenced to the lake bottom and not the lake surface. Overall, temperatures at all strata decreased since 2000. Each stratum was cooler than the lake's bottom except the 21 m stratum during summer heating.

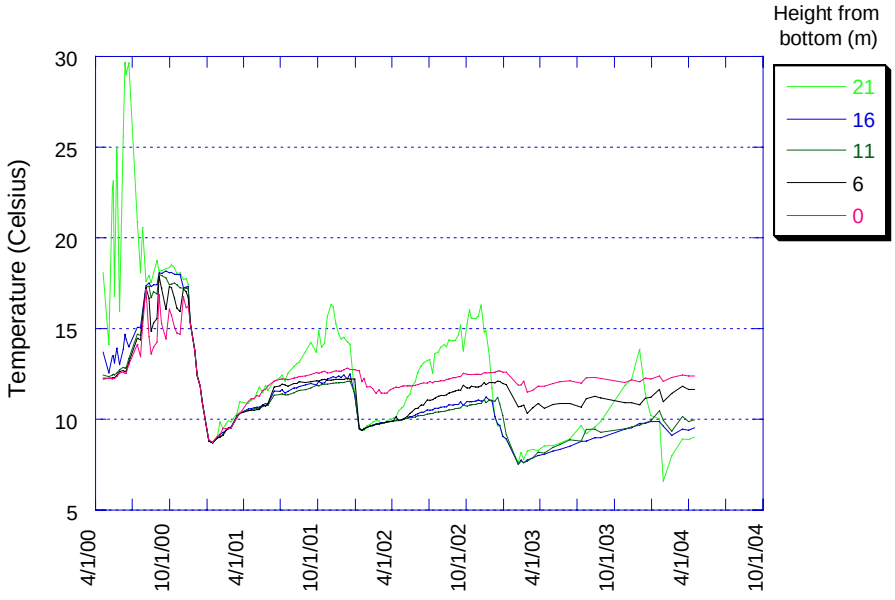

Figure 21. Temperature of individual strata throughout the study period.

From February 2001 until the end of March 2001, the rate of heating for each stratum was the same (0.022° C/d; r^2 =0.94). From the end of March 2001 through June 2001, the 0m and 21 m continued heating at the same rate while the rate of heating at 6 m, 11 m, and 16 m decreased (0.0075° C/d; r^2=0.94). The rate of heating for 6 m, 11 m, and 16 m increased rapidly (0.05° C/d; r^2= 1) from the end of May 2001 to mid June 2001 where the temperatures at each stratum converged at nearly the same temperature. These temperature trends resulted from sediment influx (the sediment trend is more apparent in the turbidity depth-time diagram below). Sediment load as a result of runoff affected the surface and bottom layers from the end of March through June which is why those strata increased at similar rates. None of the middle strata were affected which indicated that the density of the load was rather large. Temperatures at all strata converged in mid June as a result of sediment influx, which affected the entire water column. This event was a result of a sediment load, which must have been slightly higher than the average water column density because it descended the water column slowly and affected each stratum. These trends showed that sediment load and associated nutrients could have rapidly been transported to the lowest portions of the lake.

The cooling period of 2001 showed that the 21 m stratum cooled before the other strata and mixolimnetic deepening rapidly entrained deeper layers. Mixolimnetic entrainment did not include the bottom stratum. Temperature at the bottom decreased nearly 1° C from December 30, 2001, to March 12, 2002, so some heat was released from the lake bottom during that time.

In 2002, heating of the four upper strata began while the bottom stratum was cooling. Rate of temperature increase was the same for the four upper strata until early April when the rate of heating for the 21 m stratum increased by 15x. Rate of temperature increase for the four lower strata was similar despite the temperature difference between the bottom stratum and the three other strata. In early May 2002, temperature of the 6 m stratum increased rapidly and diverged from the rate of the

bottom, 11 m and 16 m strata. In this case, both the bottom and 21 m strata were warmer than the 6 m stratum. Since the rate of temperature increase at the 11 m and 16 m strata were not affected, this isolated temperature increase must have resulted from bottom heating because a transfer of heat can only occur from an area of higher temperature to lower temperature despite total heat content of the two environments. It was during this time that the highest pH was observed in the lake, which indicated that the temperature increase may have resulted from biogenic sources and/or chemical exothermy.

As the lake cooled in the winter of 2002 the mixolimnion deepened and entrained the 16 m and 11 m strata by early December and all three upper strata reached the lowest temperature by late February 2003. The bottom and 6 m strata reached their minimum temperatures slightly after the upper strata but remained warmer by 4° C and 3° C, respectively. This trend indicated that mixing in 2002 did not include the lowest 6 m of water.

The heating period of 2003 began in early February. Rates of temperature increase for the bottom and 6 m strata were similar, but during this time temperatures of the three upper strata were cooler than the two lower strata. In addition, the rate of temperature increase was much higher for the three upper strata (>0.007° C/d for 21 m, 0.007° C/d; r^2 = 0.96 for 16 m and 11 m) than the two lower strata (0.002° C/d; r^2=0.65). This trend indicated that at least the lower 6 meters of South Pit Lake (and up to 10 m) could have heated from the bottom up in 2003. Direct solar heating of the two lowest strata was not believed to contribute to this heating trend because the depth of 1% PAR was only ~4 m.

This analysis showed that the 0 m and 6 m strata were relatively isolated from the annual heating and cooling cycles of the upper three strata. The mechanism, which allowed the isolation, could not be elucidated from temperature trends alone. Temperature trends may not be able to tell the entire story of heating within this system because of the influence of the solute contribution to density. In monomictic natural

systems, water density is mostly a function of temperature so heat flux is less complicated by solute density. Heating rates with consideration of the solute contribution are discussed further below.

Specific Conductance Trend

Trends in specific conductance of the pit lake water throughout the study period are shown as isopleths in depth-time diagram format (Fig. 22). Specific conductance ranged from 0.855 mS/cm in the mixolimnion in 2003 to 3.165 mS/cm in the monimolimnion during the summer of 2002.

Conductivity in the upper water during 2000 was controlled by a relatively dilute $2.84E^{5}$ m^{3} water release from the netted pond. Conductivity in the lower water during 2000 was controlled by backfill activity and runoff sediment deposition.

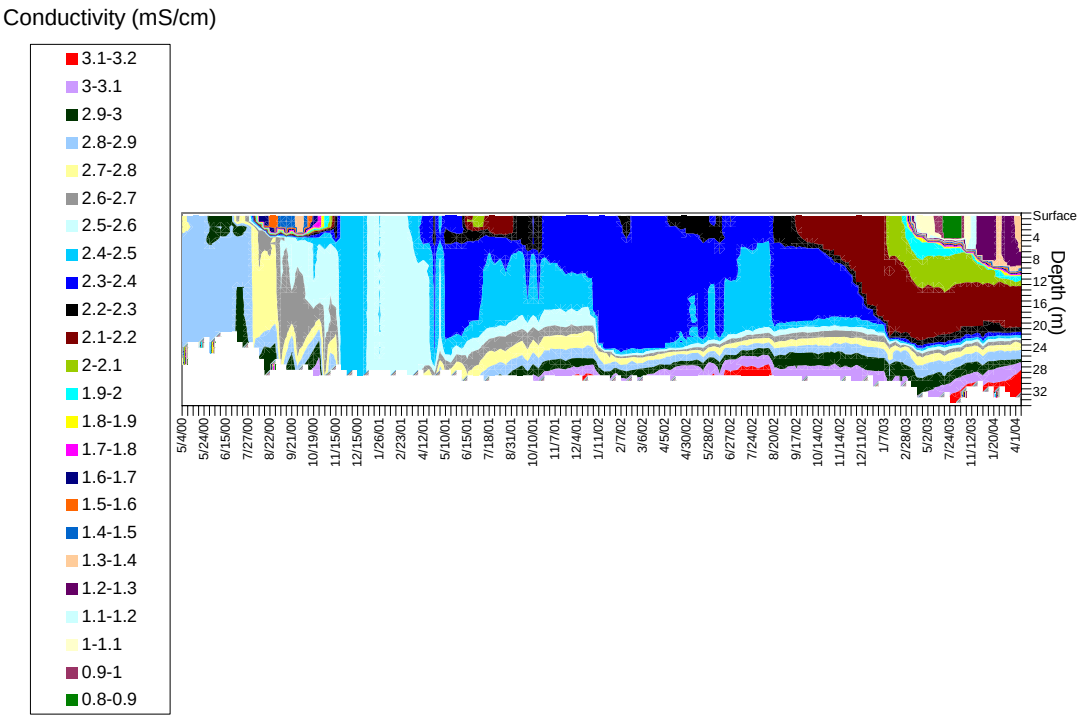

Figure 22. South Pit Lake specific conductance isopleth depth-time diagram from April 2000 through April 2004.

Stratification, phytoplankton, and benthic bacteria controlled the conductivity trend for 2001. Stratification effectively decreased the lake's mixing zone and sealed the lower portion of the lake from the atmosphere, thereby decreasing oxygen transport and diffusion. Photosynthetic processes induced precipitation reactions of carbonate, iron and manganese oxyhydroxides, and possibly gypsum in the upper water, which resulted in a slight dilution. Bacterial respiration in the lower water may have induced anaerobic conditions, which helped to create an optimum environment for resolubilization of material precipitated from the upper water. This assumption was strengthened by the pH trend in the lower water during that time which decreased 1pH unit during the significant DO decrease. Since respiration processes generate CO_2, the addition of CO_2 in a carbonate buffered system tends to decrease pH. This material displacement scenario, precipitation of material from the upper water, which was then resolubilized in the lower water, resulted in an increase in conductivity in the lower water in 2001 and may have lead to the observed meromictic stability.

Established vegetation within the watershed during 2002-2004 helped to reduce significant amounts of sediment that would have been carried to SPL via runoff as in previous years. Most of the unintended runoff channels that were previously adding sediment to the lake were now capturing sediment. Dilute influents were then limited to wetland overflows on the east and west sides of the lake. In addition, submergence of the large backfill area (solar plate) within SPL in early 2003, as a result of rising water level, also helped to decrease sediment transport by transforming a large area of dried soils into lake sediments. These changes contributed to a significant dilution of the mixolimnion throughout the study period. Conductance in the monimolimnion increased steadily throughout the same period. Monimolimnetic increase may have resulted from sediment flux, mixolimnetic precipitate resolubilization, and iron rich groundwater intrusion. Mechanisms that contribute to a divergence in the amount of solutes in the upper water

and lower water (assessed here as conductivity) by either mixolimnetic dilution or monimolimnetic concentration increase meromictic stability.

Figure 23 shows the conductivity trends for several selected strata. All data for this figure were referenced to the lake bottom except the "surface" stratum, which was the true lake surface stratum. Since holomixis in 2000, all strata above 11 meters showed declining conductivity, the 11m stratum remained relatively constant, and the 0 m and 6 m strata showed increasing conductivity throughout the study period. Large dilutions of the upper strata coincided with large watershed events (precipitation, pumping, and netted pond releases and establishment of watershed vegetation).

A large divergence of conductivity between the surface and bottom strata occurred after holomixis in 2000. Conductivity in the bottom stratum in 2001 increased at a rate of 0.0019 mS/cm/d (r^2=0.903) from mid March through early December. Conductivity in the surface stratum in 2001 decreased at a rate of 0.003 mS/cm/d (r^2=0.896) from early March through early July with the highest rate of decrease (0.007 mS/cm/d; r^2=0.900) coinciding with the largest phytoplankton bloom of the study. These trends indicated that phytoplankton induced a large-scale dilution within the upper water

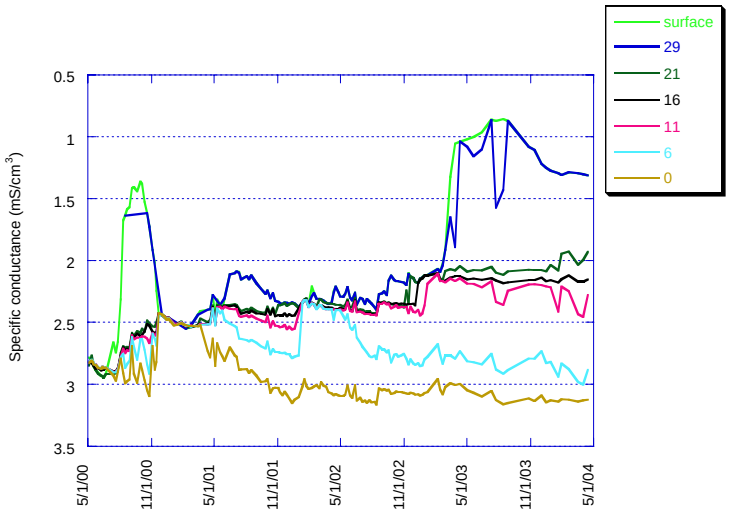

Figure 23. Specific conductance trends of individual strata throughout the study period.

but the displacement of material in the lower water was not proportional. This indicated that not all displaced material was resolubilized within the monimolimnion but may have been removed from the water column as newly formed sediment material.

Figure 24 shows the relationship between phytoplankton counts and conductivity in the lowest stratum from February 2001 through December 2001.

Regression of a subset of these data (April 2001 through December 2001 only) showed a good correlation between plankton counts and conductivity in the bottom of South Pit Lake (R^2=0.80) (Figure 25).

Figure 26 shows the effect of phytoplankton on conductance at the 16 m stratum (approximate location of phytoplankton during spring bloom) in 2001.

The figure below showed a loss of ~0.125 mS/cm during the 2001 spring bloom at the 16 m depth. The loss of 0.125 mS/cm was approximately equal to 1.25 meq of charge/L (method described further below). Maximum concentrations of Ca^{2+}, SO_4^{2-}, or

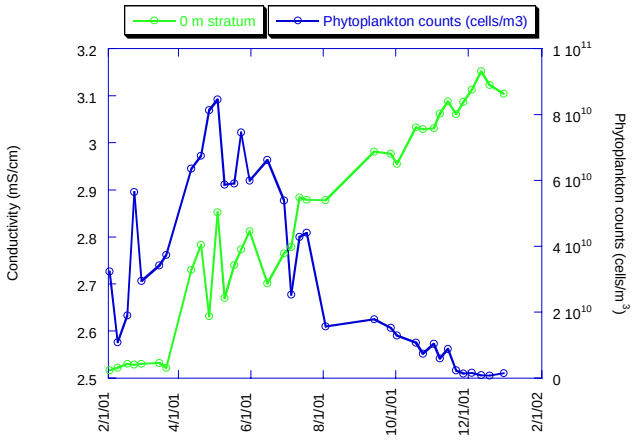

Figure 24. Phytoplankton and conductivity trends from February 2001 through December 2001.

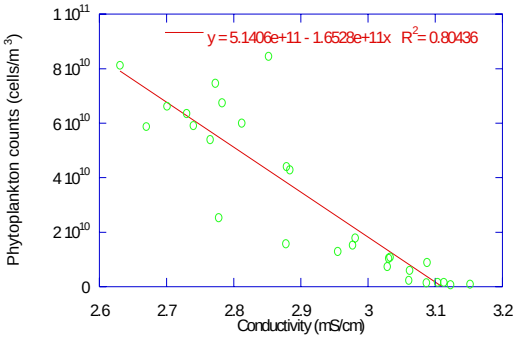

Figure 25. Correlation between plankton counts and conductivity in the lowest strata.

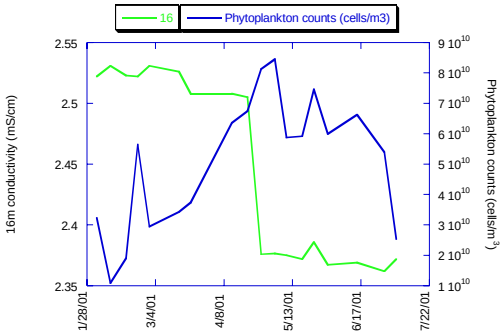

Figure 26. Phytoplankton and 16 meter conductivity trends from January 2001 through July 2001.

HCO_3^- that would have accounted for such a difference in conductivity were 25 mg/L, 60 mg/L, or 76 mg/L, respectively.

The correlations between plankton and chemistry (via specific conductance) showed that the plankton played a significant role in material displacement. This role most likely induced direct and indirect material displacement. Using a simple and well know scenario of a direct phytoplankton mechanism on chemistry, the phytoplankton used dissolved CO_2 from the pit lake water which likely induced calcite ($CaCO_3$) precipitation. The density of the precipitated calcite overcame the density of surrounding water and began its descent to the lake's bottom. Once at the bottom, the calcite redissolved because the bottom water equilibrium condition was such that carbonate species only existed in their dissolved form.

An indirect mechanism of the role of phytoplankton on material displacement would have been the scavenging of zinc from the monimolimnion. Through photosynthesis, the phytoplankton generates O_2. The dissolved O_2 induced MnO_2 formation and precipitation. As the MnO_2 descended to the lake's bottom it encountered dissolved Zn. Through coprecipitation, the dissolved Zn loosely attached to the MnO_2 precipitate and the complex descended to the lake's bottom. The equilibrium condition in the monimolimnion also favored the dissolved Mn form so the complex resolubilized thereby freeing the Zn ion and slightly increasing the conductivity in the monimolimnion.

These are two relatively simple and known mechanisms of phytoplankton induced material displacements to explain the observed correlations between specific conductance and phytoplankton counts. More detailed analysis is described in later sections.

pH Trend

pH trends throughout the study period are shown as isopleths in depth-time diagram format (Figure 27). pH ranged from 5.83 in the monimolimnion during the winter of 2003 to 9.68 in the monimolimnion during the summer of 2002. Seasonally, pH in the mixolimnion increased to 7.50-8.00 and coincided with an increase in phytoplankton. Other than the summer of 2003, the monimolimnion remained nearly circumneutral.

The developing monimolimnion was completely oxic from mid November 2000 through mid March 2001. From late March 2001 through early July 2001 the developing monimolimnion was hypoxic and was anoxic thereafter. The DO trend during this period elucidated a potential mechanism for the pH trend in the lower monimolimnion because pH decreased from 7-7.5 to 6-6.5 over the range from being oxic to anoxic. This may have indicated that a portion of the organic load resulting from the phytoplankton bloom was respired to CO_2 which then affected the carbonate buffered system by decreasing the

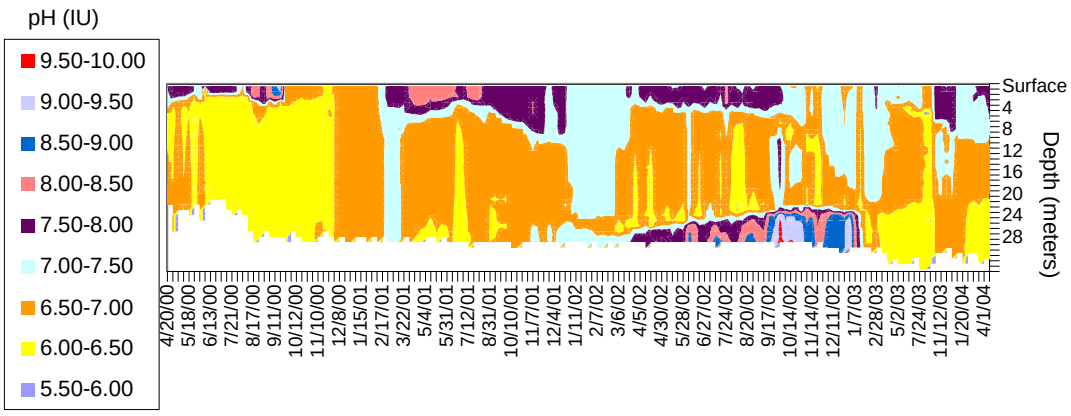

Figure 27. South Pit Lake pH isopleth depth-time diagram from April 2000 through April 2004.

pH. It was clear from this trend that all of the organic material was not utilized in 2001 because the pH decreased by 1 unit only.

Figure 28 shows pH trends of six selected depths within the lake along with the phytoplankton trend. In 2001, the 24 m strata increased from a pH of 7.1 during holomixis to 7.8 during the peak of the phytoplankton bloom. This was a direct effect of photosynthesis on the lake's carbonate buffer system, the removal of CO_2 and the concomitant consumption of H^+ through the formation of HCO_3^- and $H_2CO_3^*$. The same scenario occurred in late 2001 as well.

In late 2001 and early 2002, the lake did not mix fully to the bottom but the pH was relatively homogenous throughout the water column. The most important consequence of incomplete mixing on the pH trend was that the lowest water column strata and sediments were not aerated (the DO condition remained anoxic). This allowed the redox within the sediment and lower water strata to maintain a lower level than if aeration had occurred. In early March 2002, the 0 m stratum pH began increasing from 7.0 and continued to increase steadily through October 2002 to the highest pH of 9.7. This high pH most likely resulted from the anaerobic reduction of sulfate to sulfide within the sediment. Through dissimilatory sulfate reduction by bacteria (e.g.

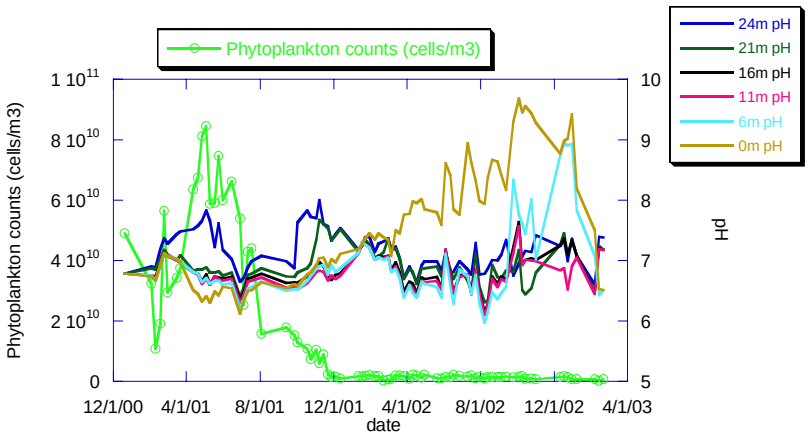

Figure 28. Phytoplankton counts versus pH trends of six selected depths in South Pit Lake from 2000 through 2002.

Desulfovibrio sp.), 2 moles of HCO_3^- and one mole of H_2S are generated as 2 moles of organic carbon and 1 mole of SO_4^{2-} are consumed. Through this process, 2 moles of H^+ are potentially neutralized. Further analysis of this scenario is discussed in the Discussion section.

Dissolved Oxygen Trend

Dissolved oxygen for SPL ranged from <0.5 mg/L to >10.0 mg/L (Figure 29). Highest DO coincided with the spring phytoplankton bloom in 2001 at a depth of 5 meters. Lowest DO was observed in the monimolimnion during all three years. Backfilling in 2000 kept the lake DO relatively homogenous until July when sediment load from the netted pond coincided with complete oxygen removal from most of the water column. Holomixis in 2000/2001 oxygenated the monimolimnion but meromixis in 2001 and 2002 resulted in continuous DO concentrations <0.5 mg/L. In January 2003 a pulse of oxygenated water mixed to lake bottom, but anoxic conditions returned at those depths shortly thereafter.

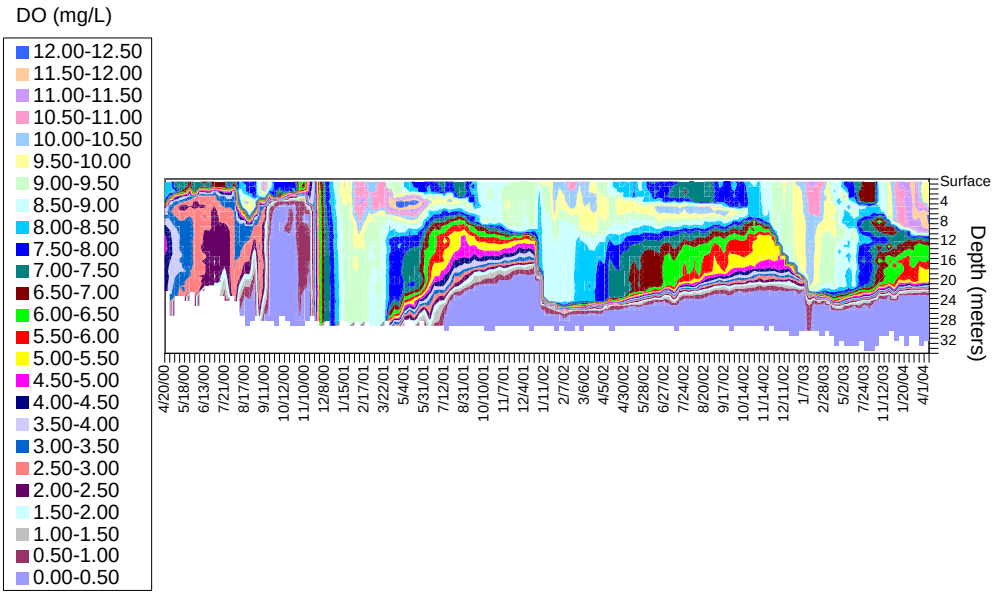

Figure 29. South Pit Lake dissolved oxygen isopleth depth-time diagram from April 2000 through April 2004.

Total water column oxygen content was calculated for each stratum as follows:

$$Oxygen\ \ content\ \ (mg\ O_2) = \sum_{all\ strata} ([DO]_i \times Volume_i)$$

where,

$[DO]_i$ = concentration of dissolved oxygen in stratum *i* (mg/L)
$Volume_i$ = volume of stratum *i* (L)

Theoretical dissolved oxygen concentration was assumed to be dominated by temperature only while the salinity effect was not considered because of the relatively low salinity of this system compared to the oceanographic literature where salinity has significant influence. According to Sherwood et al. (1992), DO saturation due to a salinity difference of 0 g/L to 2 g/L (NaCl) would only depress DO saturation by 0.2 mg/L to 0.07 mg/L over a temperature range of 0° C to 30° C. Theoretical dissolved oxygen concentration was calculated by using the following polynomial developed from dissolved oxygen concentration versus temperature data from Benson and Krause (1980):

$$DO_{theoretical} = 14.592 - 0.39557(x) + 0.0072334(x)^2 - 6.1764E^{-5}(x)^3$$

where,

x = temperature of stratum (°C)

Theoretical oxygen content for each stratum was calculated as follows:

$$Theoretical\ oxygen\ content\ (mg\ O_2) = \sum_{all\ strata} ([DO_{theoretical}]_i \times Volu$$

where,

$[DO_{theoretical}]_i$ = theoretical DO concentration at stratum *i* calculated from above (mg O_2/L)

$Volume_i$ = volume at stratum *i* (L)

Water column dissolved oxygen throughout the study was always well below the temperature regulated saturation for oxygen in water (Figure 30). However, some individual strata were supersaturated during spring as a result of photosynthesis (Figure 31).

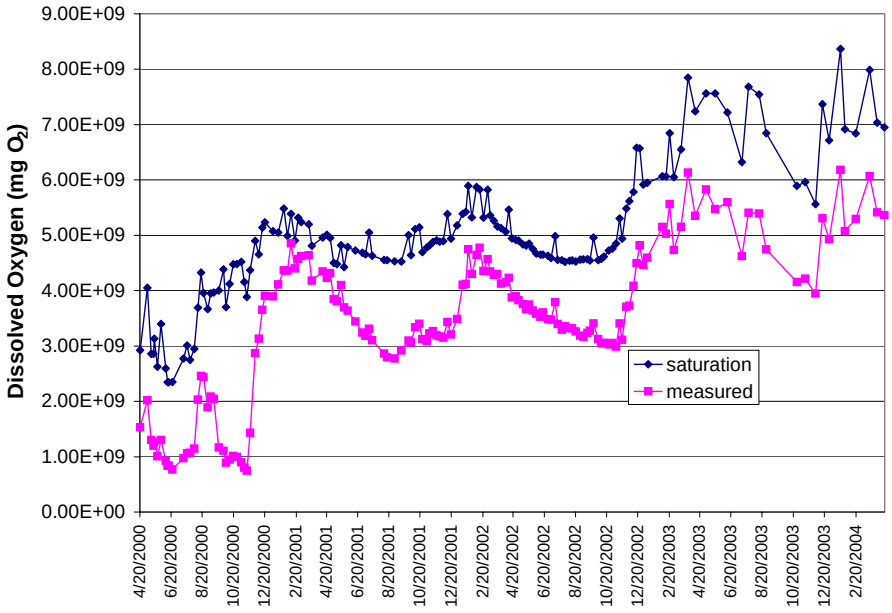

Figure 30. Theoretical versus measured water column DO content.

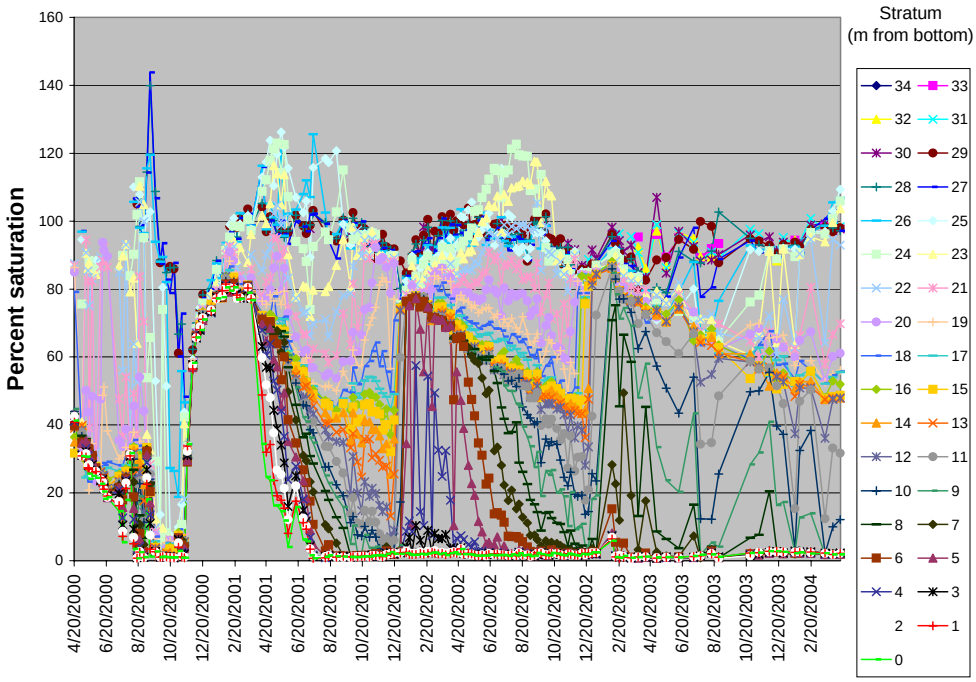

Figure 31. Stratum saturation throughout the study period with lake bottom as the 0 reference.

Meromixis development occurred during 2001. One of the important events that took place in 2001 that helped to develop the meromixis was the steady loss of oxygen from the lower water. The absence of dissolved oxygen from the bottom water allowed for sediment flux and resolubilization of upper water precipitates. These material fluxes added solute density to the lower water and helped to establish meromixis. Several mechanisms that could have contributed to the DO loss from the newly forming monimolimnion were decrease in DO saturation due to temperature, biological respiration, and chemical oxygen demand from the newly formed mine sediments. Rates of DO loss from the monimolimnion were assessed with these mechanisms in mind.

Total $DO_{theoretical}$ loss in the hypolimnion (0-12 m) from February through December 2001 was $7.489E^{8}$ mg O_2. Total $DO_{measured}$ loss in the hypolimnion during the same period was $6.9E^{7}$ mg O_2. Therefore, total estimated loss of DO due to temperature was 9.2%. The same approach for 2002 resulted in an estimate of 8.0% loss due to temperature alone. Isolating the 0 m and 12 m strata, loss within the 0 m stratum resulted in an estimate of 10.41% loss due to temperature and a 9.1% loss due to temperature in 2001.

Figure 32 shows the oxygen content of each stratum in the lower 12 meters of South Pit Lake from 2000 through 2004. A focus on the trends from the peak oxygen content of each stratum as a result of holomixis (~2-2-01) through December 2001 shows that loss of oxygen for the 12 m stratum was nearly linear while the loss for the 0 m stratum showed a slow linear decrease phase followed by a large, exponential loss from 3-22-01 through 7-18-01. Strata between the 12m and 0m extremes showed a steady gradient from the linear to exponential trends.

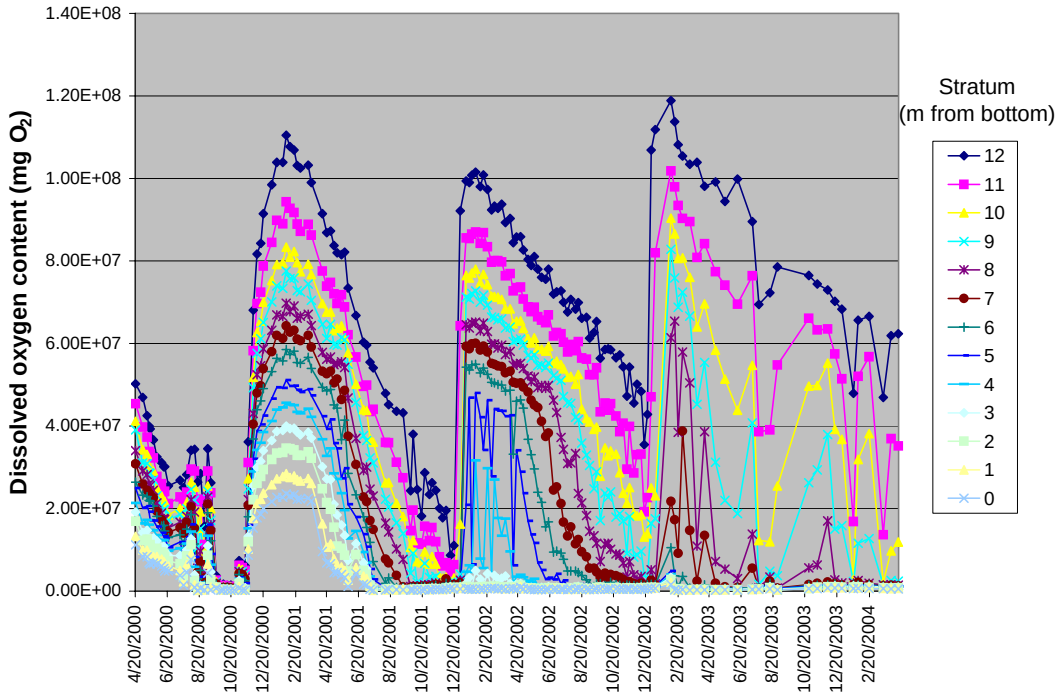

Figure 32. Oxygen content of the lower 12 meters, by stratum, of South Pit Lake from 2000-2004.

Figure 33 shows oxygen loss trends for the 12 m and 0 m strata from 2-2-01 through 12-12-01. Although rates of oxygen loss from 2-2-01 through 3-22-01 (day 1 through day 48 in Figure 33) were quite different between the 12 m ($2.022E^5$ mg O_2/d) and 0m ($3.100E^4$ mg O_2/d) strata, fluctuations in oxygen content between both trends during that time showed a strong correlation (r^r =0.945) (Figure 34).

DO loss between the two strata from 3-22-01 (day 48) through 12-12-01 (day 313) showed that loss remained linear for the 12 m stratum but loss was more appropriately fitted with a power function for the 0 m stratum (Figure 35).

Oxidation Reduction Potential (ORP) Trend

ORP ranged from -23mV in the monimolimnion in January 2004 to +563 mV in the monimolimnion in the spring of 2001 (Figure 36). A strong redoxcline separated the

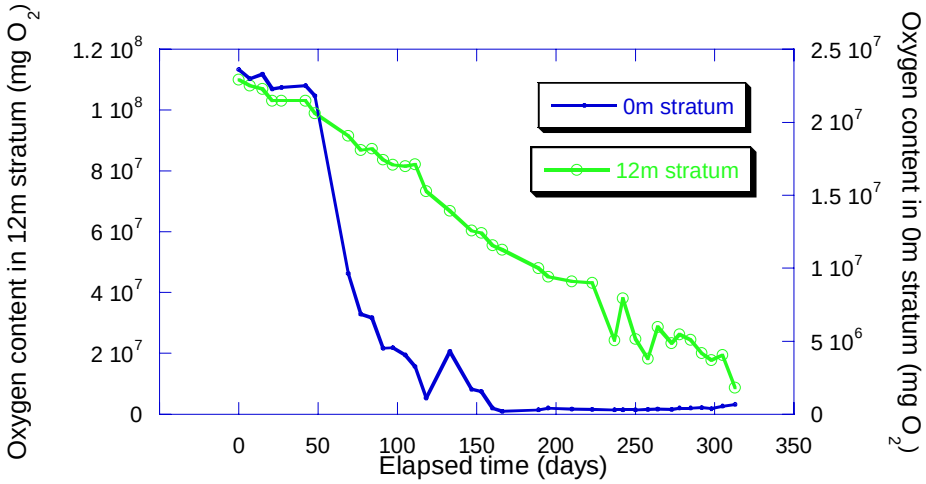

Figure 33. Dissolved oxygen content of 12m and 0m strata from 2-2-01 through 12-12-01. Note y-axis differences.

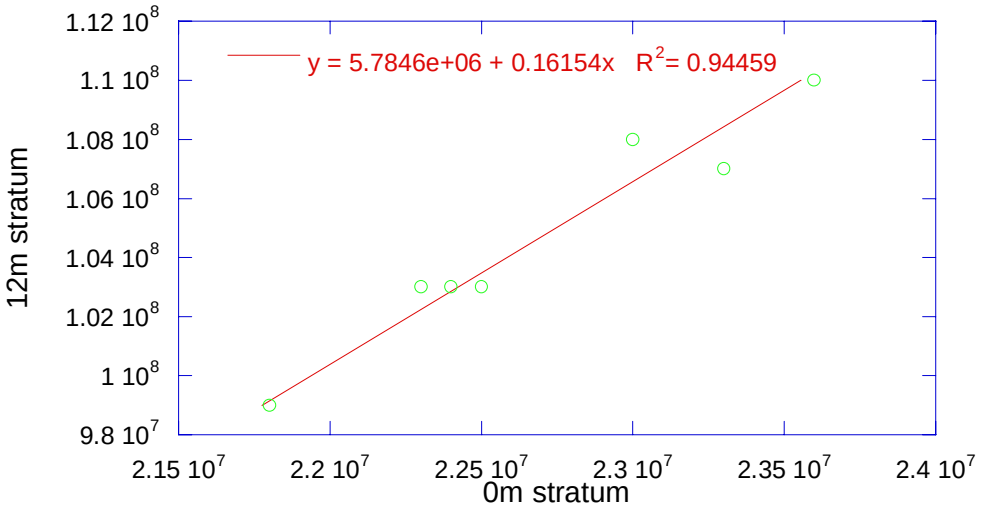

Figure 34. Correlation between 0m and 12m DO loss trends from 2-2-01 through 3-22-01.

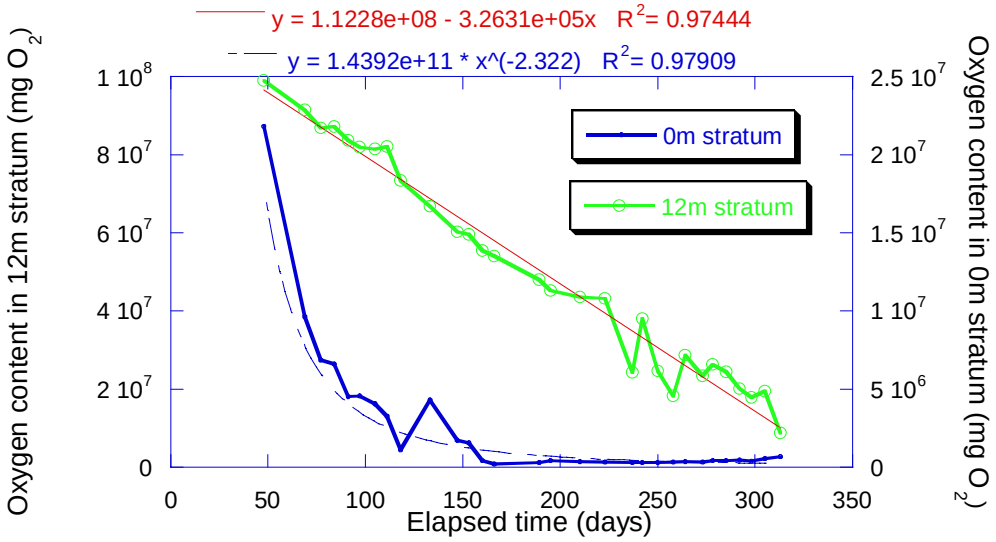

Figure 35. Dissolved oxygen content of the 0 m and 12 m strata within South Pit Lake from March 2001 through December 2001.

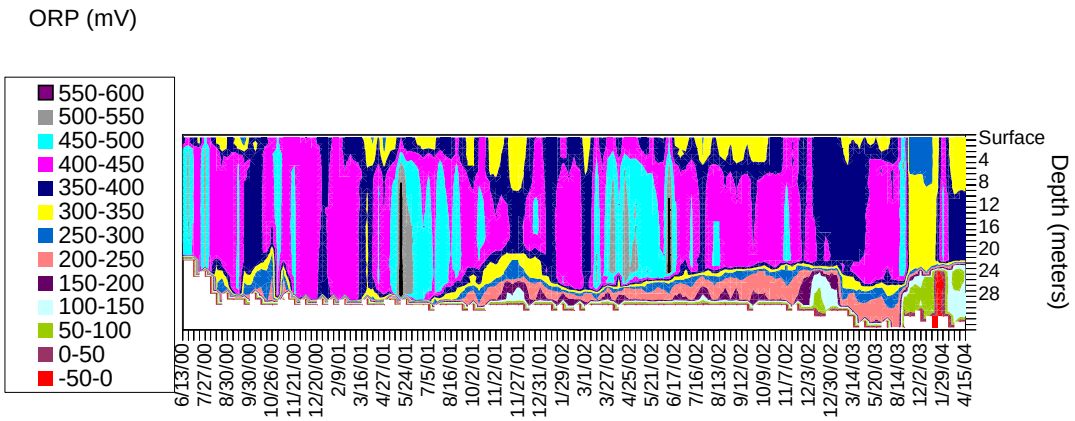

Figure 36. South Pit Lake oxidation reduction potential isopleth depth-time diagram from April 2000 through April 2004.

monimolimnion into upper and lower portions. This division indicated there was sufficient time throughout the year to allow for mostly uninterrupted and consistently lower redox values within the lower portion of the monimolimnion. It was also evident that the depth of the interface between the upper and lower monimolimnion changed throughout the year. Location of the interface was deeper in the winter and gradually rose throughout the year until the following winter. Such a trend may have indicated that the lower monimolimnion was well insulated from wind generated mixing throughout most of the year. However, as the mixolimnion/monimolimnion interface deepened as a result of winter cooling and wind generated mixing, the mixolimnion gradually eroded and may have entrained material from the lower monimolimnion.

Throughout the study period, lake level fluctuated as a result of inflows (precipitation, runoff, groundwater) and outflows (pumping and evaporation) in this filling lake. As a result of using the lake surface as the reference level elevation instead of the lake bottom, the depth time diagrams show the lake level fluctuation at the lake bottom instead of the surface elevation. This can be confusing in a filling lake because some processes are a result of lake surface-atmospheric interactions (i.e. depth of light penetration and lake oxygenation) and other processes result from lake bottom-sediment interactions (i.e. redox processes and oxygen depletion). In order to decrease slight interpolation errors in constructing the depth-time diagrams and to minimize confusion in terms of the redox parameter, redox is plotted with the lake bottom as reference point in Figure 37. It is clear from this figure that despite all stochastic events throughout the study period and the variations in lake depth, the strong redoxcline within the monimolimnion never rose above 10 m from the lake bottom. Figure 38 shows the South Pit Lake bathymetry with the 10 m depth (10 m above the lake bottom at the location of the sampling buoy) highlighted in light blue. These results show that the redox processes in the lower monimolimnion remained relatively isolated from lake

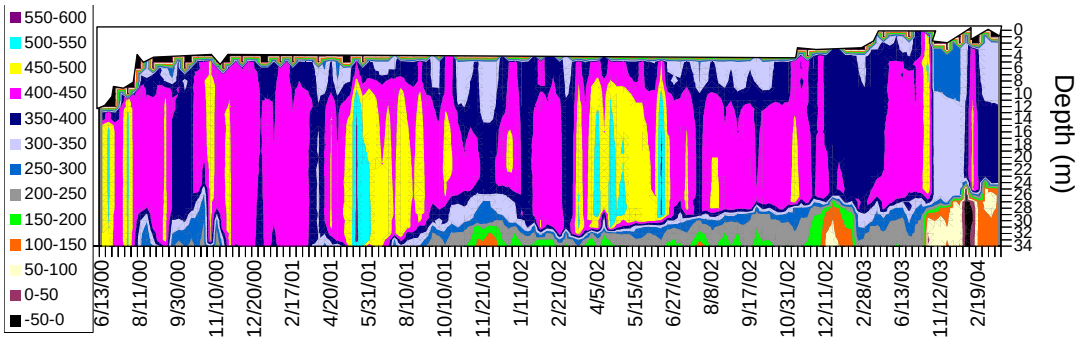

Figure 37. South Pit Lake oxidation reduction potential isopleth depth-time diagram from April 2000 through April 2004 (bottom reference).

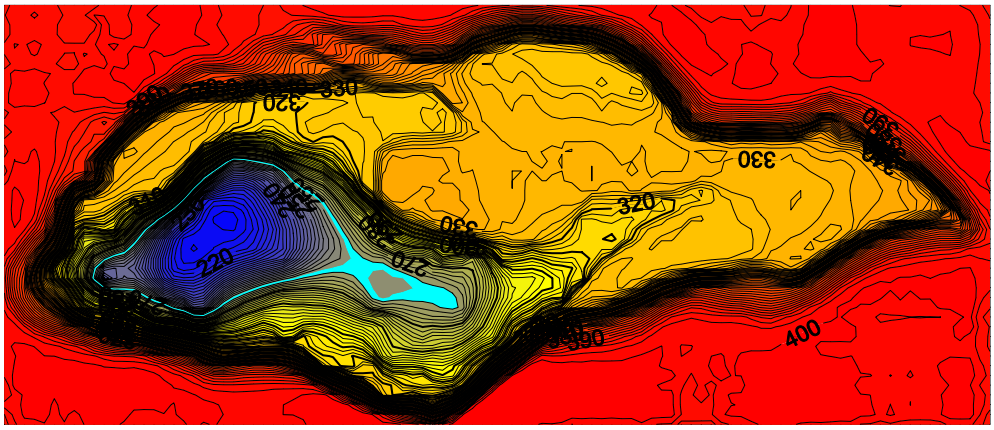

Figure 38. South Pit Lake bathymetry showing possible feature responsible for observed redox profiles.

surface processes (i.e. wind driven mixing and aeration) as a result of lake morphometry. The lake shape may have dissipated the wind energy within the upper monimolimnion or mixolimnion and prevented the energy from penetrating into the deep portions of the lake. An alternative hypothesis would be that there was insufficient wind energy to penetrate to the lower monimolimnion. This argument is discussed in further detail below.

Turbidity Trend

Turbidity ranged from 0 to over 300 NTU throughout the study (Fig. 39). Highest turbidity was observed at lake bottom during the period of backfilling throughout 2000. High turbidity was often associated with rain events especially in the early part of the study when the watershed was mostly void of vegetation. During large rain events (>12 cm/week), the entire water column showed increased turbidity. This trend indicated that material was transported directly to the monimolimnion via the sediment load.

Throughout 2002 and 2003 spikes in turbidity were often observed at the upper monimolimnion/lower monimolimnion interface. Hongve (1997) observed a similar phenomenon at the oxic/anoxic interface in a meromictic lake and suggested that these turbidity spikes were a special feature of meromictic lakes dominated by high iron and manganese concentrations. These spikes are believed to be the result of continual oxidation of reduced iron and manganese, which ascends from the reducing environment below (Davison et al. 1980; Yagi 1986; Kawashima et al. 1988; Balistrieri et al. 1992; Hongve 1994).

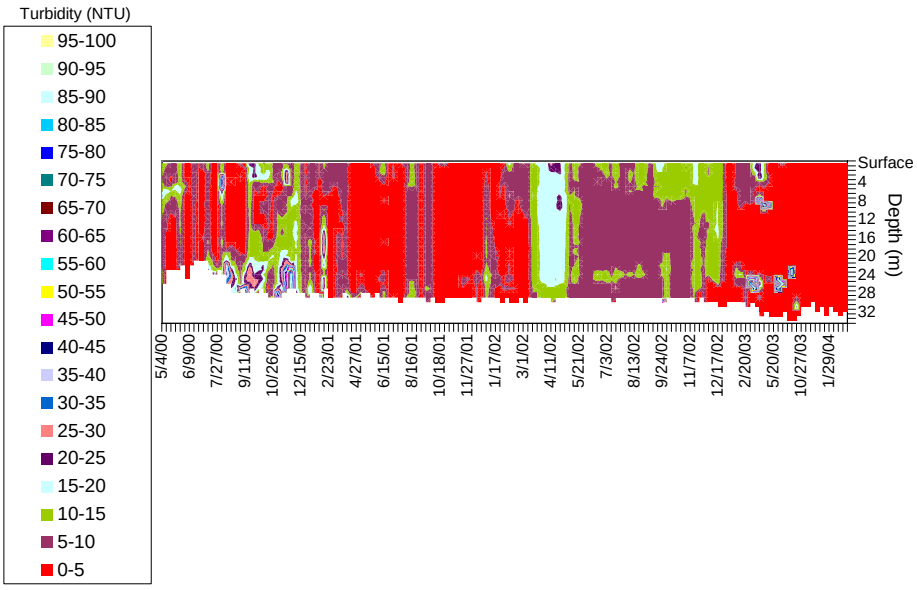

Figure 39. South Pit Lake turbidity isopleth depth-time diagram from April 2000 through April 2004.

Light Field

Figure 40 shows the intensity of Photosynthetically Available Radiation (PAR) at each depth as a function of the surface light intensity. Maximum depth of light penetration in South Pit Lake varied as a result of runoff events and seasonality. Maximum depth of light penetration in the fall of each year was deep enough to heat the dissolved salts within the lower monimolimnion directly. Although the energy reaching that depth was small (1-5 µE), direct radiation to that layer would have been more pronounced than in the lower salinity upper water (Cole, 1994).

Figure 41 shows the rate of light absorption (K_d) of the downwelling light for South Pit Lake from May 2000 through April 2004. K_d was calculated from the following formula:

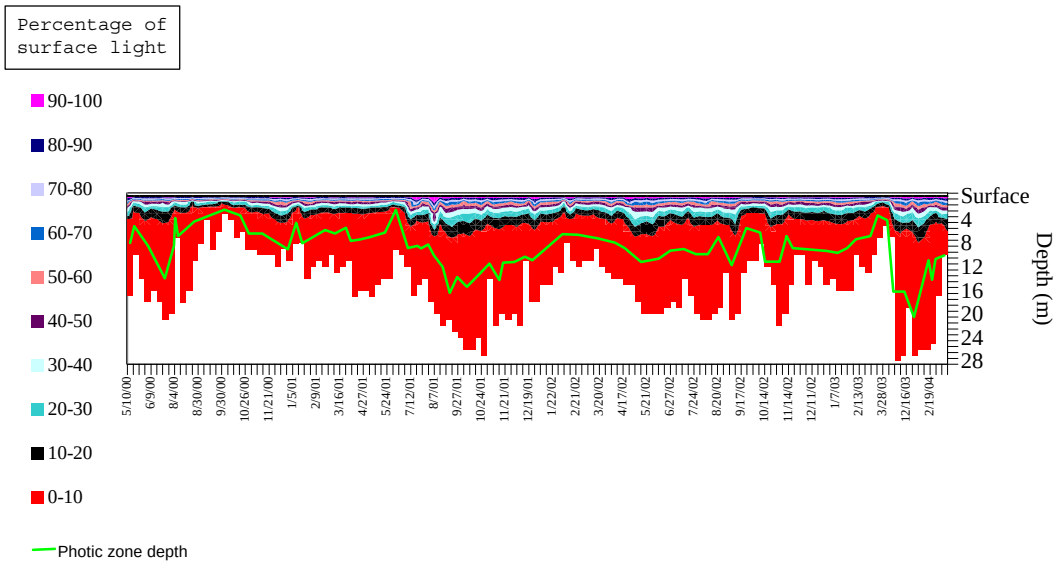

Figure 40. South Pit Lake PAR isopleth depth-time diagram from April 2000 through April 2004.

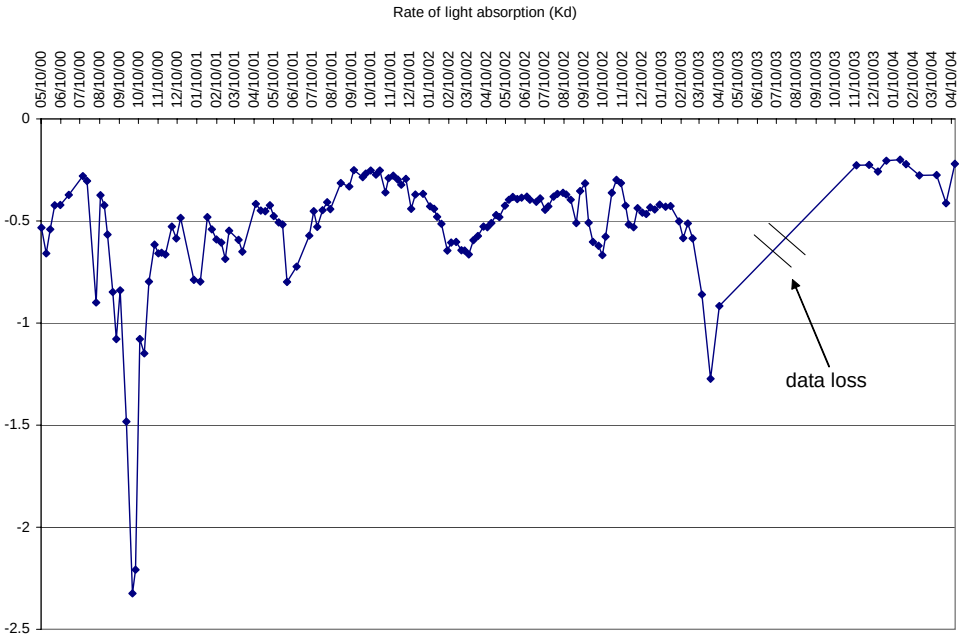

Figure 41. Rate of light absorption for each profile date for South Pit Lake from April 2000 through April 2004.

$$K_d = \frac{\ln I_o - \ln I_z}{z}$$

where, I_o = light intensity at surface
I_z = light intensity at depth z

Seasonality trends were evident with high K_d values (lower slope values, higher water clarity) in the summer and low values (higher slope values, lower water clarity) in spring. Decreased water clarity in 2000 coincided with massive sedimentation as a result of the netted pond release and in 2003 coincided with submergence of the solar plate. Sediment rapidly extinguished the downwelling light and ultimately depth of light penetration by scattering the photons within the first few meters.

Figure 42 shows the amount of precipitation that fell between light profile dates and K_d values for SPL from May 2000 through February 2003. This figure shows that

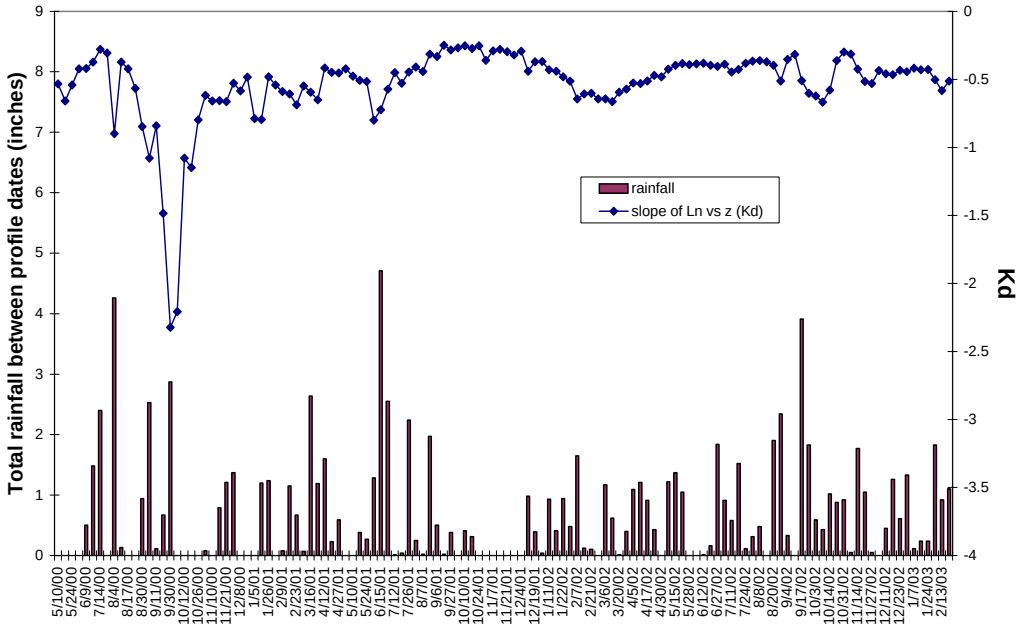

Figure 42. Rate of light absorption and total rainfall for South Pit Lake from April 2000 through March 2003.

sporadic decreases in K_d were associated with rain events. This figure also points to the importance of vegetation within the watershed. During the unvegetated period (2000 through early 2001), rain events and concomitant runoff decreased light penetration more so than during the vegetated period (after mid 2001).

Phytoplankton biomass may have decreased K_d slightly. Figure 43 shows total phytoplankton counts and K_d for SPL from May 2000 through October 2002. Highest phytoplankton counts may have decreased K_d by no more than 0.25.

Chemistry Results

In general, sulfur was the highest elemental concentration in South Pit Lake with sulfate as the dominant species. Tables 3 and 4 show average lake water concentrations resulting from all chemistries throughout the study. For most constituents, higher concentrations were observed in the lower 10 m, so results are shown as mixolimnetic and monimolimnetic concentrations throughout this section.

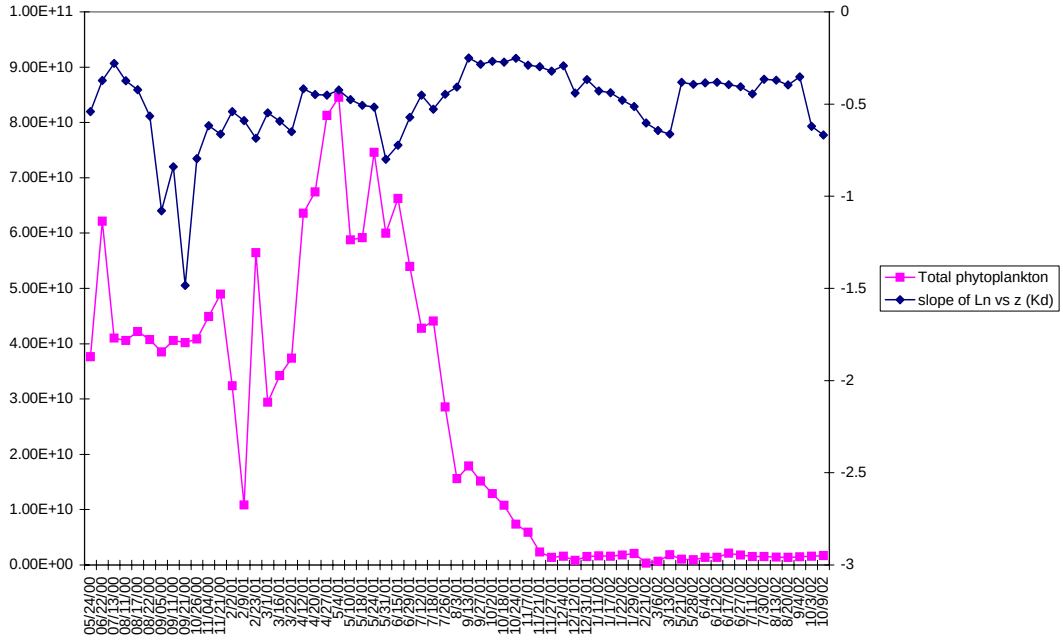

Figure 43. Rate of light absorption and total phytoplankton counts for South Pit Lake from April 2000 through October 2002.

Table 3. Average concentrations of pit lake water (mg/L).

	mixolimnion	monimolimnion
SO_4	1291.32	1677.78
Ca	374.29	477.33
Mg	67.60	93.80
Na	63.14	78.07
K	18.02	25.87
Silica	3.54	10.61
Mn	2.48	16.52
DOC	1.85	1.53
Fe	0.63	11.43
Ba	0.01	0.01
Co	0.00	0.15

Table 4. Average concentrations of nutrients in pit lake water (mg/L).

	mixolimnion	monimolimnion
TKN	1.64	2.50
Org-N	1.45	1.59
NO_3-N	0.21	0.10
NH_3-N	0.19	0.92
Orthophos	0.01	0.04

Depth time diagrams of volume weighted concentrations of components present throughout most of the sampling events within South Pit Lake from June 2001 through January 2004 are shown in Figures 44 through 55. Overall, all components showed a decrease in the mixolimnion over time especially in July 2003 and January 2004. This trend resulted from an increased vegetative cover within the watershed (decreased runoff) and a large flush of water from the netted pond through the wetlands. For some components, highest concentrations decreased from the mixolimnion and concomitantly increased in the monimolimnion, showing that material was displaced from the mixolimnion to the monimolimnion. Nearly all components showed the highest volume-weighted concentrations in the monimolimnion.

Constituent Trends

Sulfate concentrations were higher in the monimolimnion than in the mixolimnion (Figure 44). Since sulfate concentrations were the highest of all constituents, sulfur affected pit lake density more than any other component. MINTEQ results showed that sulfur would have partitioned as SO_4^{2-} (68%), $CaSO_4^{2-}$ (aq) (23%), and $MgSO_4$ (aq) (7%) as the top three sulfur species. The results also showed the lake water was undersaturated with respect to gypsum ($CaSO_4^{2-}$). These results did not help explain why sulfate was partitioned between the mixolimnion and monimolimnion, especially when calcite

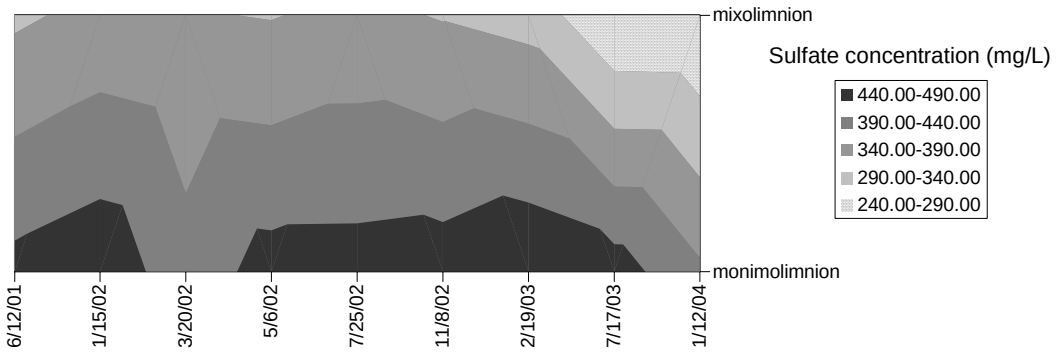

Figure 44. Depth-time diagram of isopleths of volume weighted sulfate concentration.

solubility is lower than gypsum solubility and calcium and carbonate concentrations were high (Ca^{2+} as the common ion). Two mechanisms may have helped to explain the discrepancy. Firstly, one of the drawbacks to using equilibrium modeling programs is that they do not lend insight into chemical equilibrium rates, they are designed to model results to a final theoretical equilibrium. This means that the trend in sulfate may have been a result of sulfide flux from the lake bottom sediment and concomitant oxidation to sulfate. This explanation may also help explain one mechanism for persistent anoxia in the monimolimnion (constant cycling of reduced and oxidized sulfur).

A second explanation was that gypsum was selectively precipitated through a biological mechanism. A meromictic lake in upstate New York (Green Lake, Fayetteville, NY) is believed to be chemically stratified as a result of calcite precipitation on the cells of a small coccoid cyanobacteria, *Synechococcus* spp (Thompson et al., 1990). This cyanobacteria was also found to have the capacity to precipitate gypsum and magnesite ($MgCO_3$) in addition to calcite (Thompson and Ferris, 1990). This species was found in both on-site pit lakes and may have helped to explain the sulfate partitioning observed in the lake.

Calcium concentrations were sporadic with mixolimnetic increases in January 2002 and May 2002 and decreases in September 2001, March 2002, and February 2003 (Figure 45). Monimolimnetic concentrations were always higher than in the mixolimnion

Figure 45. Depth-time diagram of isopleths of volume weighted calcium concentration.

and usually increased at the 20 m oxycline on all dates except in March 2002. This trend indicated that dissolution of calcium carbonate and possibly calcium sulfate precipitates (generated in the mixolimnion) in the anoxic monimolimnion took place. Decreases in calcium concentrations in the mixolimnion, specifically at the location of high phytoplankton density (as indicated by fluorometer readings), were evident on September 2001 (5 meters), March 2002 (10 meters), and July 2002 (15 meters) (data not shown). This trend was consistent with phytoplankton photosynthetic control of calcium. January 2002 increase in the mixolimnion was mostly due to entrainment of monimolimnetic calcium accumulations and runoff. Significant rain events in February 2002 and March 2002 decreased concentrations at all depths for the March 2002 date, but phytoplankton photosynthesis resulted in lower concentrations at the 10-meter depth during that time. Rapid increase of calcium in the monimolimnion on the November 2002 date resulted from sediment flux diffusion. Hamilton-Taylor and Davison (1995) stated how difficult it was to distinguish between sediment flux and dissolution of settling particles, but pointed to earlier work by Sholkovitz (1985) on redox related flux of Ca, Mg, Ba, Fe, Mn, P, Si, and NH_3 from sediments. In addition, Stauffer and Armstrong (1986) showed that lake sediments were net sources of Ca, K, and P during summer stratification and that these elements are potentially exported from lakes. Each of the aforementioned elements except Ba showed increases on the November 2002 date. All depths decreased on the February 2003 date due to dilution. Calcium carbonate solubility is extremely low

in aquatic systems (~$10^{-8.36}$; Benjamin, 2002), so the geochemical control for calcium in pit lakes is either calcite (Eary, 1999) or aragonite (Ehrlich, 1996). Significant decreases in mixolimnetic calcium in 2003 and 2004 mostly resulted from dilution due to netted pond/wetland influent and rainfall.

Alkalinity (as mg $CaCO_3$/L), measured here as Acid Neutralizing Capacity (ANC) by acidifying to an endpoint of pH = 4.5, increased significantly at the bottom of the lake late in November 2003 (Figure 46). The method used for this analysis accounted for all compounds that contributed to acid neutralization (e.g. Fe, NH_3) and was not a direct measurement of carbonate species. The observed trend may have resulted from a large organic amendment from the wetlands in July 2003 and concomitant microbial degradation of that material in the monimolimnion. Although carbonate species would have increased as bacteria utilized the carbon source and generated CO_2, a concomitant decrease in sediment redox would have resulted in an increase in the flux of reduced iron, manganese, and sulfur from the sediment. Each of these reduced species would have contributed to acid neutralizing capacity.

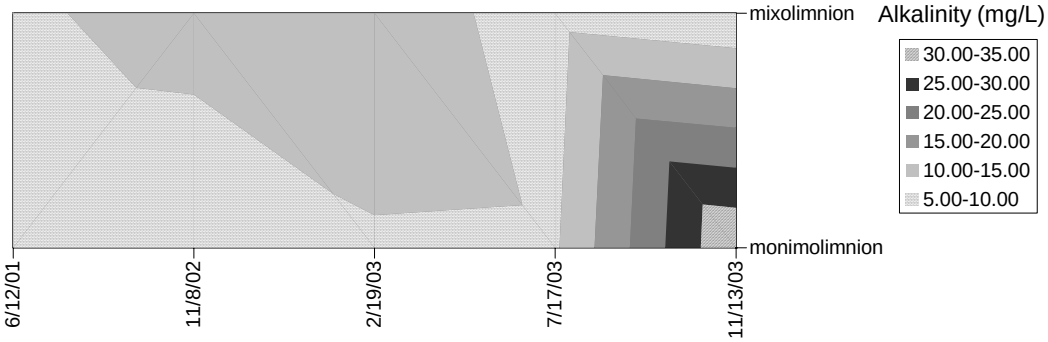

Figure 46. Depth-time diagram of isopleths of volume weighted alkalinity (as mg $CaCO_3$/L).

Magnesium is the second most abundant cation in inland waters and is present in most silicate minerals (Cole, 1994). As a result, magnesium increases were most likely due to surface water inputs (Figure 47). Mixolimnetic dilution in July 2003 resulted from significant rainfall and netted pond influent through the wetlands. This decrease in magnesium during high influent rates also pointed to the important role of increased watershed vegetation in ameliorating sediment runoff. Highest concentrations were observed in the monimolimnion.

Potassium concentrations were highest in the monimolimnion and slightly lower in the mixolimnion (Figure 48). This relatively conservative ion undergoes minor fluctuations between mixolimnion and monimolimnion and the fluctuation may be due to phytoplankton productivity (Wetzel, 2001). However, Stauffer and Armstrong (1986) found that sediments in anoxic hypolimnia could be a source of potassium. Potassium steadily increased from June 2001 through July 2002 and the trends showed some increase due to runoff (feldspar originated backfill piles and unvegetated landscape) and some increase due to sediment flux. Potassium decrease in November 2002 and February 2003 was due to rainwater and netted pond dilution. The potassium trend also pointed to the importance of increased vegetation of the pit lake watershed.

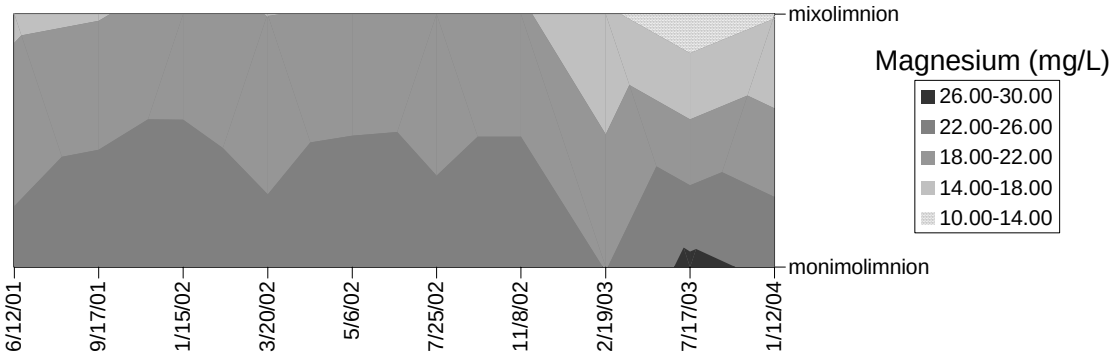

Figure 47. Depth-time diagram of isopleths of volume weighted magnesium concentration.

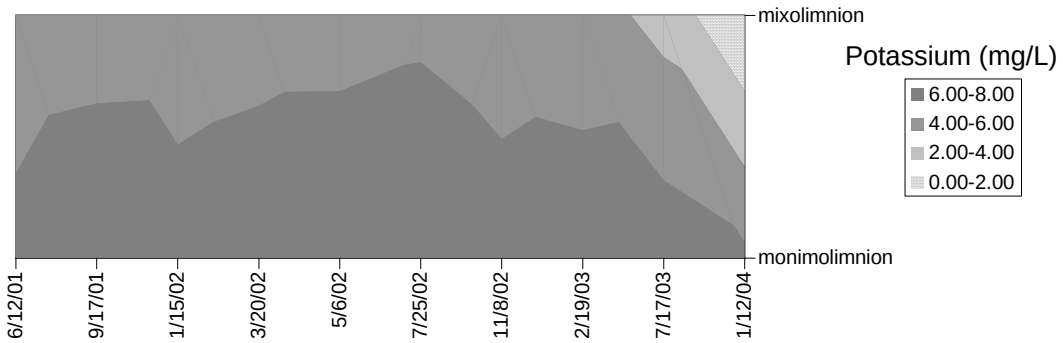

Figure 48. Depth-time diagram of isopleths of volume weighted potassium concentration.

Sodium trends showed a consistent decrease throughout the study period, which was mostly due to mixolimnetic decreases (Figure 49). Sodium is essential for phytoplankton and macrophyte growth, so the phytoplankton induced trends seen with calcium and magnesium can be seen with sodium as well. Furthermore, massive growth of the macrophyte *Potamogeton* spp. may have been important for mixolimnetic decreases as well. Periodic increases were due to influent and backfill pile sloughing, especially in May 2002. Slight increases in the monimolimnion were most likely due to descending particle dissolution and some sediment flux as well. Significant dilution at the end of the study period was due to major rainwater and netted pond dilutions.

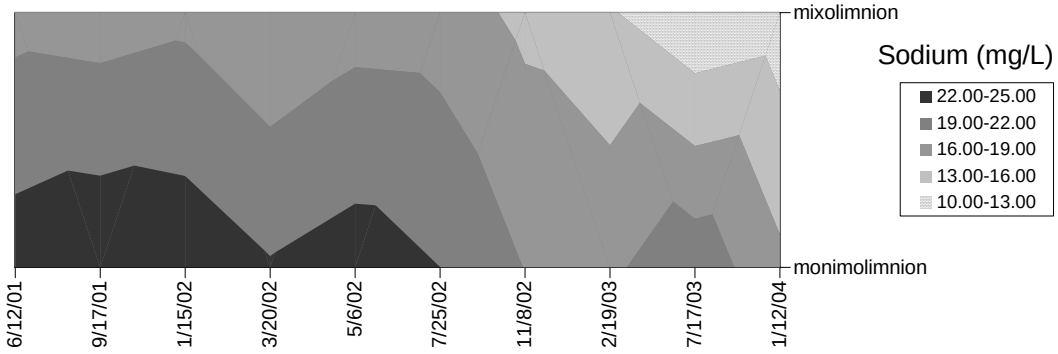

Figure 49. Depth-time diagram of isopleths of volume weighted sodium concentration.

Silica trends also showed a partitioning between the mixolimnion and monimolimnion (Figure 50). In addition, silica over time decreased significantly over the study period but showed some periodicity within the temporal trend. Two mechanisms that most likely dominated the silica trend were diatom biomineralization, deep but incomplete mixing, and increased watershed vegetation. The trend from June 2001 to November 2002 was consistent with the presence and dominance of diatoms. Diatoms utilize silica during biomineralization of frustule formation. A decrease in mixolimnetic silica with a concomitant increase in monimolimnetic silica was consistent with diatom seasonality with mixolimnetic biomineralization, seasonal dieoff, and monimolimnetic resolubilization as the controlling phases. Interestingly, silica dilution over time may limit diatom abundance.

Increases in February 2003 were consistent with reentrainment of silica from the monimolimnion to the mixolimnion. In late 2002, the seasonal thermocline descended to ~25 meters. This depth coincided with the upper zone of the chemocline and may have entrained silica into the mixolimnion. This trend was not consistent with runoff events because calcium, aluminum, and carbonate (as alkalinity) all decreased in February 2003. These components would have increased along with silica during runoff.

Increased vegetation within the watershed did however help to decrease silica mass over the entire study period. This was evident especially in November 2003 when volume weighted silica concentrations decreased to nearly nondetectable limits in response to nearly 46 cm of rain from July 2003 to November 2003.

Manganese mass steadily decreased over the study period, but the concentration trends showed steady decrease in the mixolimnion and steady increase in the monimolimnion (Figure 51). This trend was similar to iron, which is typical for carbonate dominated systems with seasonal anoxia. Manganese precipitates from well oxygenated waters as completely hydrolyzed Mn(III/IV) oxide colloids and particulates

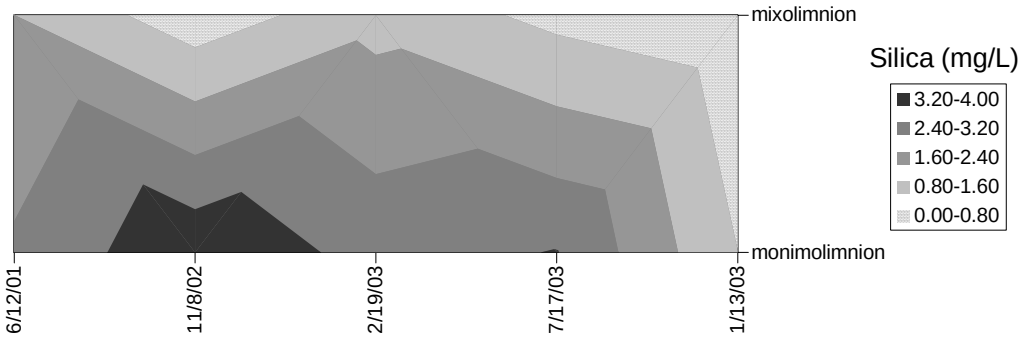

Figure 50. Depth-time diagram of isopleths of volume weighted silica concentration.

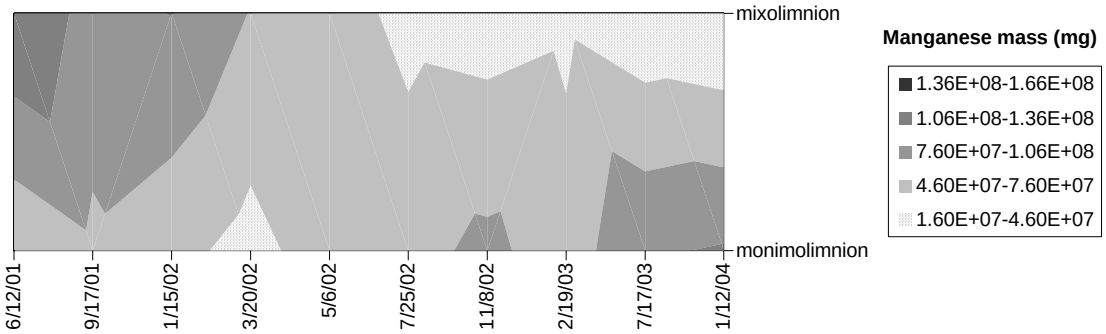

Figure 51. Depth-time diagram of isopleths of volume weighted manganese concentration.

(Hamilton-Taylor and Davison, 1995). Eary (1999) suggested that rhodochrosite ($MnCO_3$) was a reasonable upper bound for manganese concentrations in circumneutral pit lakes. Stauffer and Armstrong (1986) found that rhodochrosite solubility did not influence Mn^{2+} profile development in a Minnesota lake and that sediment flux of Mn^{2+} in one area of the lake reached the oxic region and settled back down in another area of the lake. *Leptothrix* spp. and *Metallogenium* spp., two bacteria known to oxidize manganese, have been observed growing on slides in SPL. Manganese showed a depositional trend in SPL and was most likely a result of biotic and abiotic mechanisms.

The dissolved organic carbon trend showed that the lake had a relatively homogenous distribution early on in the study (Figure 52). Significant increase in DOC

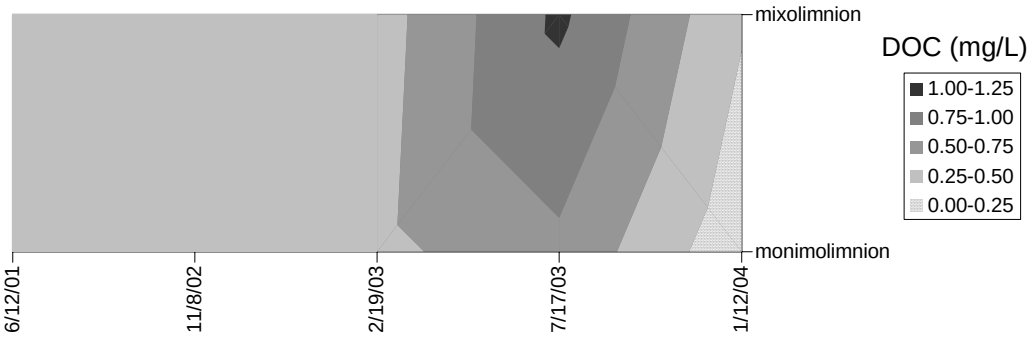

Figure 52. Depth-time diagram of isopleths of volume weighted dissolved organic carbon concentration.

resulted when netted pond influent was used to flush organic material out of the east wetland complex. DOC concentrations decreased significantly in the monimolimnion after the pulse. It was clear that the organic matter was utilized by benthic bacteria resulting in a decrease in redox in the monimolimnion and an increase in material flux from the sediment (e.g. Fe and Mn).

Iron was often present at low concentrations in the mixolimnion for most of the study period, most likely as particulate and colloidal hydrolyzed Fe(III) oxides (Figure 53). Iron concentrations were highest in the anoxic monimolimnion, most likely as Fe(II), which descended from the mixolimnion and redissolved or diffused from the sediment. Iron was the only constituent that had steadily increased over time. Such a trend would have been consistent with inputs originating from the aforementioned ectogenic sources but also a constant input from iron rich groundwater, sediment flux, and pit wall leaching. Iron oxidizing bacteria may also have played a key role in epilimnetic iron oxidation and concomitant resolubilization in the monimolimnion. Glass slides placed just under the surface in the center of SPL showed large populations of *Gallionella* spp. and *Leptothrix* spp., two species known to form iron concretions at the cell surface. Some researchers have found iron deposition rates of up to 6.7 mg/cm^2/d (Ehrlich, 1996). Furthermore, a groundwater discharge pipe located just west of SPL had high concentrations of *Gallionella* spp. as well.

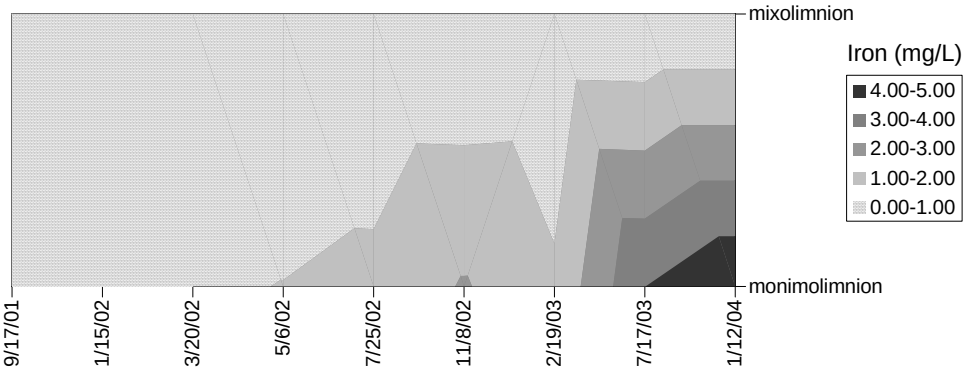

Figure 53. Depth-time diagram of isopleths of volume weighted iron concentration.

Barium was present throughout the water column on the first two sampling dates, but showed a declining and descending trend in the water column (Figure 54). After January 2002 all detected barium was in the monimolimnion. Hamilton-Taylor and Davidson (1995) suggested that the main carrier phase for barium in lakes is manganese oxides and to a lesser extent iron oxides, barite, and possibly organic matter. However, much of the epilimnetic barium decreased in conjunction with a high sulfate spike at 5 meters in January 2002, which may have indicated barite-controlled solubility. Eary (1999) stated that most pit lakes are oversaturated with respect to barite ($BaSO_4$). Regardless of the main geochemical control for barium, excessive concentrations of sulfate and iron and manganese oxides indicated that the presence of barium in the mixolimnion most likely resulted from ectogenic events like runoff and backfill slope

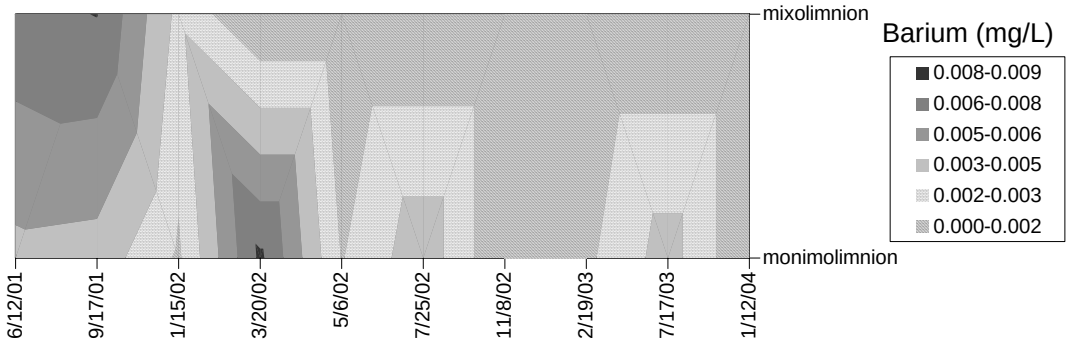

Figure 54. Depth-time diagram of isopleths of volume weighted barium concentration.

entrainment and failure. Barium in the anoxic monimolimnion points toward resolubilization of carrier phase solids. Accumulation of barium in seasonally anoxic hypolimnia has been reported (Hamilton-Taylor and Davidson, 1995) and in one instance was the result of desorption on synthetic hydrous manganese oxides (Sugiyama et al., 1992).

Cobalt was initially present in the entire water column (Figure 55). By September 2001, cobalt was not present in the mixolimnion, but was present in the monimolimnion only. After September 2001, cobalt was only present in the monimolimnion. This trend was consistent with coprecipitation from the mixolimnion and dissolution in the monimolimnion. From May 2002 through January 2004 cobalt concentrations increased in the monimolimnion. This trend most likely resulted from sediment flux into the monimolimnion. The main carrier phase for cobalt is manganese oxide and secondary carriers are iron oxide and sulfide (Hamilton-Taylor and Davison, 1995). In SPL cobalt coprecipitated with the oxides of manganese and iron and redissolved along with the iron and manganese oxides in the monimolimnion.

Geochemical Equilibrium Results

Speciation and saturation indices for each date were determined using PHREEQC Interactive. Measured temperature, pH, redox, and DO were considered to be the master

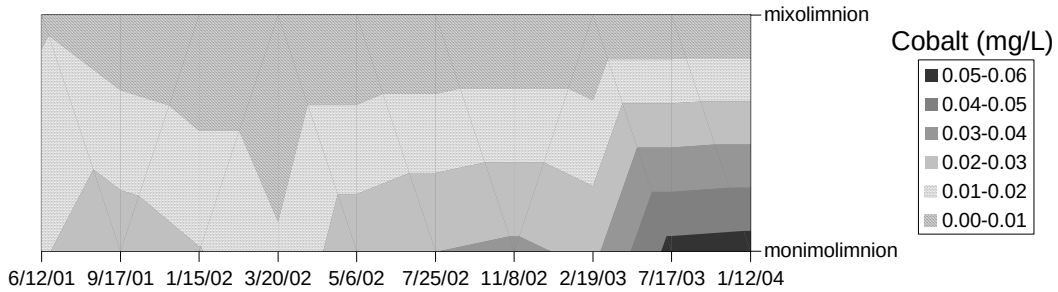

Figure 55. Depth-time diagram of isopleths of volume weighted cobalt concentration.

input variables and were considered to poise the system during the time of sampling. Each depth was assessed separately for each date. The modeling program allowed the input of most elements but some were not available for input (e.g. Co). Speciation results for surface and bottom samples for the 7-24-02 sampling date are shown in Tables 5 and 6, respectively.

Saturation index results for 1-15-02, 3-20-02, and 5-9-02 are shown in Tables 7, 8, and 9, respectively.

Although this study focused on the water column, since mixing occurred in 2000 only, it was assumed that the sediments were completely anoxic and highly reduced. Results showed that redox sensitive elements could have readily cycled from the sediment into the water column and back again through precipitation/dissolution reactions. Iron and manganese species could have fluxed from the sediment in their reduced states and had many species in which they could have precipitated back to the sediment. It was also clear from this analysis that on few occasions sulfate would have precipitated from the mixolimnion to the monimolimnion. Since mixolimnetic concentrations of iron and barium were small, jarosite and barite precipitation could not have accounted for such a large difference in mixolimnetic/monimolimnetic sulfate partitioning. Furthermore, precipitation as gypsum was only thermodynamically possible in the lowest strata in January 2002.

Monimolimnetic Density Dynamics

Total dissolved solids, a function of electrical conductance with the sonde, was used to assess density. Density in the lower monimolimnion was a key component in the establishment and continuation of meromixis. Therefore it was important to find a link between the lower monimolimnion density and the change in one or more chemical constituents within the monimolimnion. This approach was not only an attempt to understand the constituents that may have contributed most to the monimolimnetic

Table 5. Speciation results of the South Pit lake chemistry mixolimnion (7-24-02).

Element	Total (Molal)	Species	Concentration (Molal)	Percent of total
Al	9.28E-06			
		Al(OH)4-	9.25E-06	9.97E+01
		Al(OH)3	2.90E-08	3.12E-01
		Al(OH)2+	1.25E-09	1.34E-02
		AlOH+2	1.33E-12	1.43E-05
		AlSO4+	7.01E-15	7.55E-08
		Al+3	1.32E-15	1.43E-08
		Al(SO4)2-	1.11E-15	1.20E-08
		AlHSO4+2	8.75E-24	9.43E-17
C(4)	6.19E-04			
		HCO3-	5.50E-04	8.88E+01
		CaHCO3+	2.50E-05	4.04E+00
		CaCO3	1.93E-05	3.12E+00
		CO2	7.54E-06	1.22E+00
		CO3-2	6.19E-06	9.99E-01
		MgHCO3+	6.13E-06	9.90E-01
		MgCO3	2.94E-06	4.74E-01
		MnCO3	7.76E-07	1.25E-01
		NaHCO3	6.14E-07	9.92E-02
		NaCO3-	2.17E-07	3.51E-02
		MnHCO3+	1.57E-07	2.54E-02
Ca	1.00E-02			
		Ca+2	6.59E-03	6.59E+01
		CaSO4	3.37E-03	3.37E+01
		CaHCO3+	2.50E-05	2.50E-01
		CaCO3	1.93E-05	1.93E-01
		CaOH+	8.47E-08	8.47E-04
		CaHSO4+	1.99E-10	1.99E-06
H(0)	1.46E-36			
		H2	7.29E-37	5.00E+01
K	5.64E-04			
		K+	5.43E-04	9.63E+01
		KSO4-	2.04E-05	3.62E+00
		KOH	1.99E-10	3.53E-05

Element	Total (Molal)	Species	Concentration (Molal)	Percent of total
Mg	3.01E-03			
		Mg+2	1.80E-03	5.96E+01
		MgSO4	1.20E-03	4.00E+01
		MgHCO3+	6.13E-06	2.04E-01
		MgCO3	2.94E-06	9.76E-02
		MgOH+	8.44E-07	2.80E-02
Mn(2)	1.02E-05			
		Mn+2	6.22E-06	6.10E+01
		MnSO4	3.04E-06	2.98E+01
		MnCO3	7.76E-07	7.61E+00
		MnHCO3+	1.57E-07	1.54E+00
		MnOH+	1.97E-08	1.93E-01
Mn(3)	2.61E-22			
		Mn+3	2.61E-22	1.00E+02
Na	2.92E-03			
		Na+	2.85E-03	9.75E+01
		NaSO4-	7.25E-05	2.48E+00
		NaHCO3	6.14E-07	2.10E-02
		NaCO3-	2.17E-07	7.44E-03
		NaOH	2.01E-09	6.88E-05
O(0)	4.47E-04			
		O2	2.24E-04	5.00E+01
S(6)	1.46E-02			
		SO4-2	9.93E-03	6.80E+01
		CaSO4	3.37E-03	2.31E+01
		MgSO4	1.20E-03	8.25E+00
		NaSO4-	7.25E-05	4.97E-01
		KSO4-	2.04E-05	1.40E-01
		MnSO4	3.04E-06	2.08E-02
		HSO4-	5.01E-09	3.43E-05
		CaHSO4+	1.99E-10	1.37E-06
		AlSO4+	7.01E-15	4.80E-11
		Al(SO4)2-	1.11E-15	7.62E-12
		AlHSO4+2	8.75E-24	5.99E-20

Table 6. Speciation results of the South Pit lake chemistry monimolimnion (7-24-02).

Element	Total (Molal)	Species	Concentration (Molal)	Percent of total
Ba	2.63E-07			
		BaSO4	1.51E-07	5.73E+01
		Ba+2	1.11E-07	4.21E+01
		BaHCO3+	8.56E-10	3.26E-01
		BaCO3	3.13E-10	1.19E-01
		BaOH+	4.42E-13	1.68E-04
C(4)	3.07E-03			
		HCO3-	2.60E-03	8.46E+01
		MnCO3	1.33E-04	4.33E+00
		CaHCO3+	1.04E-04	3.38E+00
		CaCO3	8.64E-05	2.81E+00
		MgHCO3+	4.34E-05	1.41E+00
		CO3-2	3.30E-05	1.07E+00
		CO2	2.83E-05	9.20E-01
		MnHCO3+	2.55E-05	8.32E-01
		MgCO3	1.76E-05	5.74E-01
		NaHCO3	3.79E-06	1.23E-01
		NaCO3-	5.65E-07	1.84E-02
		ZnCO3	1.33E-07	4.34E-03
		Zn(CO3)2-2	9.85E-08	3.21E-03
		FeCO3	4.12E-08	1.34E-03
		FeHCO3+	2.94E-08	9.56E-04
		ZnHCO3+	1.44E-08	4.69E-04
		BaHCO3+	8.56E-10	2.79E-05
		BaCO3	3.13E-10	1.02E-05
Ca	1.30E-02			
		Ca+2	8.62E-03	6.63E+01
		CaSO4	4.20E-03	3.23E+01
		CaHCO3+	1.04E-04	7.98E-01
		CaCO3	8.64E-05	6.64E-01
		CaOH+	1.72E-07	1.32E-03
		CaHSO4+	1.26E-10	9.72E-07
Fe(2)	3.98E-07			
		Fe+2	2.33E-07	5.85E+01
		FeSO4	9.15E-08	2.30E+01
		FeCO3	4.12E-08	1.03E+01
		FeHCO3+	2.94E-08	7.37E+00
		FeOH+	3.29E-09	8.26E-01
		FeHSO4+	3.48E-15	8.75E-07
Fe(3)	4.13E-04			
		Fe(OH)3	3.38E-04	8.19E+01
		Fe(OH)4-	4.62E-05	1.12E+01
		Fe(OH)2+	2.80E-05	6.77E+00
		FeOH+2	1.22E-09	2.95E-04
		FeSO4+	5.36E-14	1.30E-08
		Fe(SO4)2-	6.61E-15	1.60E-09
		Fe+3	3.78E-15	9.15E-10
		Fe2(OH)2+4	3.39E-16	8.21E-11
		Fe3(OH)4+5	3.34E-17	8.08E-12
		FeHSO4+2	1.28E-21	3.11E-16
H(0)	1.16E-30			
		H2	5.79E-31	5.00E+01

Element	Total (Molal)	Species	Concentration (Molal)	Percent of total
K	8.21E-04			
		K+	7.95E-04	9.68E+01
		KSO4-	2.60E-05	3.16E+00
		KOH	4.61E-10	5.62E-05
Mg	4.54E-03			
		Mg+2	3.04E-03	6.70E+01
		MgSO4	1.43E-03	3.15E+01
		MgHCO3+	4.34E-05	9.55E-01
		MgCO3	1.76E-05	3.88E-01
		MgOH+	4.02E-07	8.85E-03
Mn(2)	4.75E-04			
		Mn+2	2.28E-04	4.79E+01
		MnCO3	1.33E-04	2.80E+01
		MnSO4	8.84E-05	1.86E+01
		MnHCO3+	2.55E-05	5.37E+00
		MnOH+	2.38E-07	5.01E-02
Mn(3)	4.95E-25			
		Mn+3	4.95E-25	1.00E+02
Na	3.97E-03			
		Na+	3.86E-03	9.72E+01
		NaSO4-	1.06E-04	2.67E+00
		NaHCO3	3.79E-06	9.55E-02
		NaCO3-	5.65E-07	1.42E-02
		NaOH	4.33E-09	1.09E-04
O(0)	9.40E-06			
		O2	4.70E-06	5.00E+01
S(6)	1.88E-02			
		SO4-2	1.29E-02	6.88E+01
		CaSO4	4.20E-03	2.23E+01
		MgSO4	1.43E-03	7.62E+00
		NaSO4-	1.06E-04	5.63E-01
		MnSO4	8.84E-05	4.70E-01
		KSO4-	2.60E-05	1.38E-01
		BaSO4	1.51E-07	8.02E-04
		FeSO4	9.15E-08	4.87E-04
		ZnSO4	5.42E-08	2.88E-04
		Zn(SO4)2-2	6.49E-09	3.45E-05
		HSO4-	2.59E-09	1.38E-05
		CaHSO4+	1.26E-10	6.72E-07
		FeSO4+	5.36E-14	2.85E-10
		Fe(SO4)2-	6.61E-15	3.52E-11
		FeHSO4+	3.48E-15	1.85E-11
		FeHSO4+2	1.28E-21	6.82E-18
Zn	4.30E-07			
		ZnCO3	1.33E-07	3.10E+01
		Zn(CO3)2-2	9.85E-08	2.29E+01
		Zn+2	9.45E-08	2.20E+01
		ZnSO4	5.42E-08	1.26E+01
		Zn(OH)2	2.37E-08	5.50E+00
		ZnHCO3+	1.44E-08	3.35E+00
		Zn(SO4)2-2	6.49E-09	1.51E+00
		ZnOH+	4.38E-09	1.02E+00
		Zn(OH)3-	1.93E-11	4.48E-03
		Zn(OH)4-2	1.15E-15	2.68E-07

Table 7. Discrete meter PHREEQC results for South Pit Lake (1-15-02). Red = oversaturation; Green = saturation; Blue = undersaturation

		surface	5m	10m	15m	20m	25m	30m
Al $(OH)_3$ (a)	Al $(OH)_3$					-0.03		
Alunite	$KAl_3(SO_4)_2(OH)_6$					5.00		
Anhydrite	$CaSO_4$	-0.39	-0.37	-0.38	-0.39	-0.39	-0.31	-0.25
Aragonite	$CaCO_3$	-0.52	-0.45	-0.39	-0.15	-0.37	-0.61	0.05
Barite	$BaSO_4$	0.58						0.58
Calcite	CaCO3	-0.37	-0.29	-0.24	0.00	-0.22	-0.45	0.20
CO2 (g)	CO_2	-2.43	-2.54	-2.53	-2.46	-2.58	-2.00	-2.16
Dolomite	$CaMg(CO_3)_2$	-1.34	-1.19	-1.09	-0.42	-1.05	-1.49	-0.12
Fe(OH)3 (a)	$Fe(OH)_3$	2.92	3.00	3.02	2.09	3.06	2.90	4.68
Gibbsite	$Al(OH)_3$					2.81		
Goethite	FeOOH	8.24	8.31	8.32	7.98	8.36	8.26	10.09
Gypsum	$CaSO_4:2H_2O$	-0.13	-0.11	-0.13	-0.17	-0.14	-0.05	0.01
H2 (g)	H_2	-34.16	-34.46	-34.54	-34.60	-34.18	-33.02	-28.04
H2O (g)	H_2O	-1.93	-1.93	-1.94	-1.51	-1.94	-1.90	-1.86
Hausmannite	Mn_3O_4	-1.68	-0.90	-0.68	3.41	-0.84	-2.63	-4.46
Hematite	Fe_2O_3	18.40	18.56	18.58	17.97	18.65	18.45	22.12
Jarosite-K	$KFe_3(SO_4)_2(OH)_6$	1.99	1.99	1.91	0.30	1.89	3.01	7.40
Manganite	MnOOH	1.46	1.80	1.89	1.91	1.78	0.86	-0.70
Melanterite	$FeSO_4:7H_2O$	-10.05	-10.27	-10.37	-11.97	-10.22	-8.94	-5.46
O2 (g)	O_2	-0.63	-0.65	-0.67	-0.60	-0.68	-1.50	-2.30
Pyrochroite	$Mn(OH)_2$	-5.48	-5.29	-5.24	-5.25	-5.17	-5.51	-4.58
Pyrolusite	MnO_2	-0.07	0.36	0.49	3.17	0.19	-1.06	-4.88
Rhodochrosite	$MnCO_3$	0.15	0.22	0.27	0.47	0.29	0.55	1.35
Siderite	$FeCO_3$	-5.73	-5.89	-5.92	-7.02	-5.75	-4.76	-0.66
Smithsonite	$ZnCO_3$					-3.36	-3.25	-2.81
Witherite	$BaCO_3$	-5.10						-4.64
$Zn(OH)_2$ (e)	$Zn(OH)_2$					-3.87	-4.37	-3.81

Table 8. Discrete meter PHREEQC results for South Pit Lake (3-20-02). Red = oversaturation; Green = saturation; Blue = undersaturation.

		surface	5m	10m	15m	20m	25m	30m
Al $(OH)_3$ (a)	Al $(OH)_3$							
Alunite	$KAl_3(SO_4)_2(OH)_6$							
Anhydrite	$CaSO_4$	-0.45	-0.42	-0.42	-0.41	-0.39	-0.40	-0.29
Aragonite	$CaCO_3$	0.00	-0.69	-0.70	-0.92	-0.92	-1.00	0.14
Barite	$BaSO_4$					0.61	0.56	0.64
Calcite	CaCO3	0.15	-0.53	-0.55	-0.76	-0.76	-0.85	0.29
CO2 (g)	CO_2	-2.85	-2.34	-2.25	-2.01	-1.99	-1.38	-2.41
Dolomite	$CaMg(CO_3)_2$	-0.19	-1.66	-1.69	-2.13	-2.11	-2.27	0.09
Fe(OH)3 (a)	$Fe(OH)_3$	2.83	2.95	2.97	2.68	2.78	2.43	4.80
Gibbsite	$Al(OH)_3$							
Goethite	FeOOH	8.45	8.30	8.29	8.01	8.11	7.78	10.19
Gypsum	$CaSO_4:2H_2O$	-0.21	-0.16	-0.17	-0.15	-0.14	-0.14	-0.04
H2 (g)	H_2	-33.82	-34.22	-34.72	-34.54	-34.56	-34.38	-27.92
H2O (g)	H_2O	-1.71	-1.91	-1.92	-1.92	-1.92	-1.90	-1.88
Hausmannite	Mn_3O_4	2.32	-2.55	-2.30	-3.82	-3.85	-5.99	-3.59
Hematite	Fe_2O_3	18.87	18.53	18.52	17.95	18.15	17.50	22.31
Jarosite-K	$KFe_3(SO_4)_2(OH)_6$	1.04	2.48	2.64	2.50	2.90	2.94	7.18
Manganite	MnOOH	2.05	1.12	1.34	0.80	0.80	-0.01	-0.37
Melanterite	$FeSO_4:7H_2O$	-11.20	-9.84	-9.96	-9.69	-9.57	-9.16	-5.64
O2 (g)	O_2	-0.59	-0.60	-0.62	-0.69	-0.71	-1.17	-2.22
Pyrochroite	$Mn(OH)_2$	-4.72	-5.85	-5.88	-6.33	-6.34	-7.06	-4.19
Pyrolusite	MnO_2	1.69	-0.26	0.10	-0.52	-0.52	-1.29	-4.72
Rhodochrosite	$MnCO_3$	0.56	-0.13	-0.07	-0.29	-0.28	-0.38	1.47
Siderite	$FeCO_3$	-6.16	-5.64	-5.77	-5.73	-5.63	-5.29	-0.72
Smithsonite	$ZnCO_3$							
Witherite	$BaCO_3$					-5.45	-5.57	-4.45
$Zn(OH)_2$ (e)	$Zn(OH)_2$							

Table 9. Discrete meter PHREEQC results for South Pit Lake (5-9-02). Red = oversaturation; Green = saturation; Blue = undersaturation.

		surface	5m	10m	15m	20m	25m	30m
Al $(OH)_3$ (a)	Al $(OH)_3$	-0.97						
Alunite	$KAl_3(SO_4)_2(OH)_6$	-0.04						
Anhydrite	$CaSO_4$	-0.44	-0.40	-0.39	-0.38	-0.40	-0.32	-0.27
Aragonite	$CaCO_3$	0.08	-0.82	-0.99	-1.15	-1.19	-0.78	0.78
Barite	$BaSO_4$							0.62
Calcite	CaCO3	0.22	-0.67	-0.84	-0.99	-1.04	-0.63	0.93
CO2 (g)	CO_2	-2.91	-2.08	-1.95	-1.79	-1.78	1.20	-2.89
Dolomite	$CaMg(CO_3)_2$	0.03	-1.87	-2.29	-2.61	-2.67	-1.83	1.36
Fe(OH)3 (a)	$Fe(OH)_3$	1.85	2.27	2.69	2.49	2.43	2.34	5.00
Gibbsite	$Al(OH)_3$	1.72						
Goethite	FeOOH	7.75	7.79	8.03	7.82	7.76	7.71	10.40
Gypsum	$CaSO_4:2H_2O$	-0.22	-0.16	-0.13	-0.12	-0.15	-0.06	-0.02
H2 (g)	H_2	-35.06	-35.76	-36.36	-36.38	-36.46	-35.84	-29.84
H2O (g)	H_2O	-1.50	-1.78	-1.91	-1.92	-1.92	-1.89	-1.87
Hausmannite	Mn_3O_4	5.08	-1.58	-2.55	-3.62	-3.61	-2.45	1.71
Hematite	Fe_2O_3	17.51	17.55	18.00	17.57	17.45	17.35	22.74
Jarosite-K	$KFe_3(SO_4)_2(OH)_6$	-1.47	1.54	2.84	2.66	2.54	2.82	6.11
Manganite	MnOOH	2.52	1.29	1.48	1.16	1.18	1.37	1.68
Melanterite	$FeSO_4:7H_2O$	-13.17	-11.02	-10.45	-10.33	-10.40	-9.95	-7.53
O2 (g)	O_2	-0.61	-0.60	-0.68	-0.76	-0.77	-1.89	-2.28
Pyrochroite	$Mn(OH)_2$	-4.87	-6.45	-6.56	-6.89	-6.91	-6.41	-3.10
Pyrolusite	MnO_2	4.05	1.47	1.16	0.79	44.75	0.90	-1.64
Rhodochrosite	$MnCO_3$	0.40	-0.42	-0.45	-0.63	-0.64	0.45	2.08
Siderite	$FeCO_3$	-7.94	-6.89	-6.58	-6.63	-6.72	-5.94	-1.98
Smithsonite	$ZnCO_3$						-2.83	-2.29
Witherite	$BaCO_3$							-3.84
$Zn(OH)_2$ (e)	$Zn(OH)_2$						-4.76	-2.54

stability but also to understand the chemical flux trends and to speculate on the persistence of the meromixis under different scenarios that may drastically change the pathway toward theoretical chemical equilibrium. According to Appelo and Postma (1996), a simplified correlation between electrical conductance and ion concentration can be achieved through the following:

$$\sum anions = \sum cations\ (meq/L) = EC/100\ (\mu S/cm)$$

It should be noted that this relationship assumes electroneutrality and that it correlates with the sum of cations *or* anions. This relationship was used to compare the trend in specific conductance at the bottom stratum of South Pit Lake on 3-20-02 and 5-9-02 to the trend in chemical analysis results from the same strata on the same dates.

Results showed an increase of 2.25 meq/L and a measured conductivity difference of 0.076 mS/cm from 3-20-02 to 5-9-02 (Table 10). Since the calculated electroneutrality was fairly accurate, it was assumed the change in equivalents was electroneutral, so

Table 10. Assessment of chemical species responsible for conductivity increase in monimolimnion from 2-20-02 through 5-9-02.

	5/9/2002		3/20/2002		Equivalents change	Species contribution	Species equivalents	Species equivalents
species	mg/L	meq/L	mg/L	meq/L	(meq/L)	to change (%)	contribution on 5-9-02 (%)	contribution on 3-20-02 (%)
SO_4^{2-}	1800	37.5	1800	37.5	0.00	0.00	45.60	46.88
Ca^{2+}	530	26.4	500	25.0	1.50	66.41	32.18	31.21
HCO_3^-	181	3.0	142	2.3	0.64	28.36	3.61	2.91
Mg^{2+}	110	9.0	110	9.0	0.00	0.00	11.01	11.32
Na^+	88	3.8	90	3.9	-0.09	-3.86	4.66	4.90
K^+	28	0.7	30	0.8	-0.05	-2.27	0.87	0.96
Mn^{2+}	26	0.9	23	0.8	0.11	4.84	1.15	1.05
Fe^{2+}	21	0.8	17	0.6	0.14	6.35	0.91	0.76
Co^{2+}	0.32	0.0	0.25	0.0	0.00	0.11	0.01	0.01
Zn^{2+}	0.037	0.0	0	0.0	0.00	0.05	0.00	0.00
Sum		82.2		79.9	2.25			

sum cations	41.750	40.135
sum anions	-40.443	-39.803
electroneutrality	1.59%	0.42%

	5/9/2002	3/20/2002	SpC change (mS/cm)	SpC change (meq/L)
Specific conductance (mS/cm)	3.019	3.095	0.076	0.76

dividing the equivalents change by two (since the sum of cations *or* anions is approximately equal to conductivity/100) resulted in an increase of 1.125 meq/L. This result was 34% higher than the measured conductivity difference. However, the chemical analyses represented total concentrations. Chemical speciation in the bottom layer of the lake would have resulted in a fraction of the total concentration that contributed to the measured conductivity. For example, the total concentration of Ca^{2+} on 5-9-02 was 530 mg/L but MINTEQ results showed that only 65.2% of that value would have contributed to the conductivity measurement as the ionic Ca^{2+} species, while the predominance of the remainder (34% as $CaSO_4$ (aq)) would not have contributed to measured conductivity (MINTEQ results not shown). After accounting for speciation of the elements that contributed most to the change in equivalents from 3-20-02 to 5-9-02, the corrected value was 1.614 meq/L. Using the above assumption of electroneutrality and after dividing the new result by two, the calculated result (0.807 meq/L) was within 5.8% of the measured conductivity difference (0.76 meq/L). This analysis showed that, for the dates chosen, Ca^{2+} (66%) and HCO_3^- (28%) contributed to over 94% of the conductivity increase in the bottom layer of South Pit lake. Such an increase would most likely have been a result of spring bloom algal photosynthesis and concomitant displacement of calcite from the mixolimnion to the monimolimnion. An additional mechanism may have resulted from

the activity of sulfate reducing bacteria, the reduction of $CaSO_4$ to CaS through the following sequence of reactions (Ehrlich, 1996):

$$CaSO_4 + 2CH_2O \xrightarrow{SRB} CaS + 2CO_2 + 2H_2O$$
$$CaS + H_2O \rightarrow Ca(OH)_2 + H_2S$$
$$CO_2 + H_2O \rightarrow H_2CO_3$$
$$Ca(OH)_2 + H_2CO_3 \rightarrow CaCO_3 + 2H_2O.$$

Such a reaction would have accounted for the observed pH increase as well (generation of $Ca(OH)_2$).

Table 10 also shows that sulfate, although it did not contribute to the change in conductivity from 3-20-02 to 5-9-02, contributed to over 45% of the total equivalents on both dates. Furthermore, sulfate trends for each date showed an increase with depth and an overall water column decrease over time. Since sulfate concentrations comprised nearly 70% of all pit lake chemistry analyses and sulfate concentrations were higher in the monimolimnion, sulfate contributed the most to the density difference between the mixolimnion and monimolimnion.

As an additional analysis, conductance values coinciding with each chemistry sampling date were plotted against each chemical constituent. The most significant correlations were found for iron, manganese, and cobalt only. Figure 56 shows iron and manganese concentrations against conductivity and Figure 57 shows cobalt concentration against conductivity. Regressions between manganese and conductivity (R^2=0.94) and cobalt and conductivity (R^2=0.87) were strong while regression between iron and conductivity was not as strong (R^2=0.40). However, a portion of the iron data was linear (R^2=0.97). Within the portion of iron data that was linear, all concentrations were below 30 mg Fe/L. This may have indicated that iron concentrations above 30 mg Fe/L precipitated out of solution within the monimolimnion, and did not contribute to

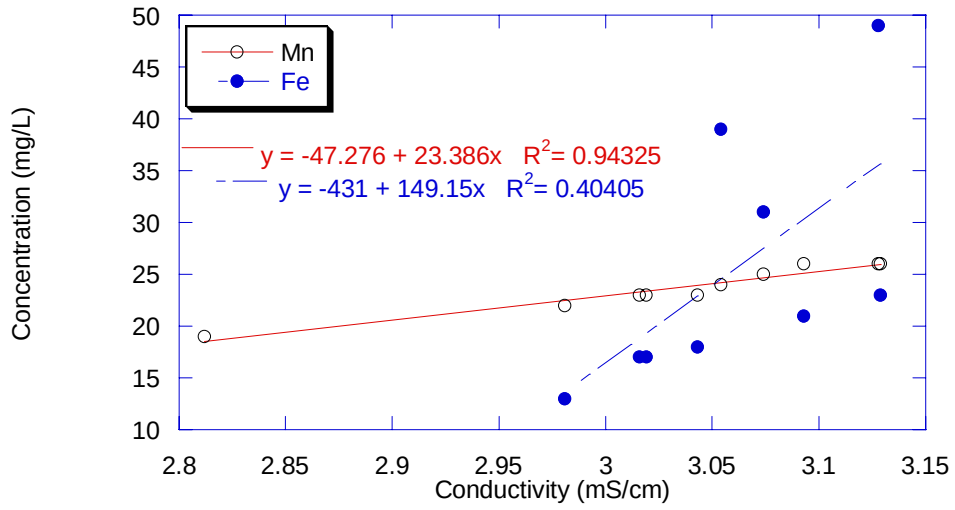

Figure 56. Correlation between iron and manganese concentrations and conductivity.

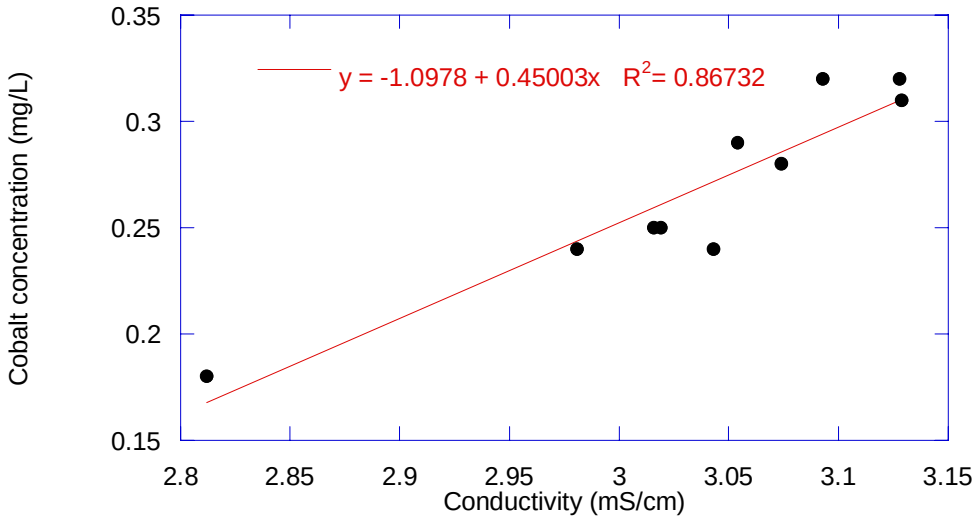

Figure 57. Correlation between cobalt concentration and conductivity.

conductivity at that depth. This precipitated iron would have been accounted for when the monimolimnetic samples were acidified in the lab for metals analysis.

An analysis of the three incidences where iron concentrations exceeded 30 mg/L in the monimolimnion indicated that two mechanisms may have been responsible for iron precipitation; FeS formation and $Fe(OH)_3$ formation. Iron concentrations exceeded 30 mg/L in the bottom lake samples on 11-8-02, 7-17-03, and 1-12-04. Conditions at the bottom of the lake were different for each date. On the 11-8-02 sampling date, pH at lake bottom was 8.73 and the measured redox was ~225 mV. These conditions would have favored goethite, hematite, and $Fe(OH)_3$ formation and precipitation (Table 11).

As for the other two dates, pH was not optimal for $Fe(OH)_3$ formation (pH < 7 on both dates). Preceding these dates, redox values were some of the lowest measured throughout the study period as a result of allochthonous organic loads to the lake. This situation would have led to increased sulfide and iron flux from the sediment and would have increased the potential for FeS(s) generation in the monimolimnion. A simplified Visual MINTEQ assessment of the monimolimnion showed that FeS precipitation would have occurred on those dates (Table 12). Input for the simplified chemistry included 30 mg Fe^{2+}/L, 1800 mg SO_4^{2-}/L, and an estimated H_2S (aq) concentration of $1.47E^{-5}$ M (a conservative estimate of $[H_2S]$ based upon the faint odor of sulfide in bottom stratum samples).

In addition to the equilibrium model results, on several occasions the discoloration of a white rope (used for suspending thermistors) with a black precipitate on the lowest 10 meters was consistent with the assumption of FeS precipitation in the monimolimnion.

Table 11. Discrete meter PHREEQC ion activity product results for South Pit Lake (11-7-02) (Note: empty cells indicate absence of one or more species at specified depth).

		surface	5m	10m	15m	20m	25m	30m
Al (OH)$_3$ (a)	Al (OH)$_3$							
Alunite	$KAl_3(SO_4)_2(OH)_6$							
Anhydrite	$CaSO_4$	-0.44	-0.42	-0.38	-0.38	-0.37	-0.25	-0.26
Aragonite	$CaCO_3$	-1.27	-0.96	-1.21	-1.13	-1.24	1.22	1.36
Barite	$BaSO_4$							
Calcite	CaCO3	-1.12	-0.81	-1.06	-0.98	-1.09	1.37	1.52
CO2 (g)	CO_2	-2.19	-2.43	-1.74	-1.86	-1.77	-3.37	-3.77
Dolomite	$CaMg(CO_3)_2$	-2.76	-2.13	-2.70	-2.57	-2.77	2.20	2.53
Fe(OH)3 (a)	$Fe(OH)_3$						4.54	5.07
Gibbsite	$Al(OH)_3$							
Goethite	FeOOH						9.95	10.50
Gypsum	$CaSO_4{:}2H_2O$	-0.19	-0.17	-0.13	-0.12	-0.11	0.00	-0.01
H2 (g)	H_2	-35.26	-35.24	-35.08	-35.50	-35.46	-32.88	-32.00
H2O (g)	H_2O	-1.72	-1.73	-1.84	-1.89	-1.88	-1.86	-1.85
Hausmannite	Mn_3O_4	-4.06	-2.53	-4.83	-4.24	-3.45	7.21	7.85
Hematite	Fe_2O_3						21.84	22.95
Jarosite-K	$KFe_3(SO_4)_2(OH)_6$						3.42	4.24
Manganite	MnOOH	0.19	0.73	0.28	0.73	0.96	4.00	4.03
Melanterite	$FeSO_4{:}7H_2O$						-10.41	-9.99
O2 (g)	O_2	-0.65	-0.66	-0.82	-0.90	-1.29	-2.34	-2.37
Pyrochroite	$Mn(OH)_2$	-7.30	-6.75	-7.12	-6.88	-6.63	-2.30	-1.83
Pyrolusite	MnO_2	0.49	0.95	-0.24	0.06	0.33	2.24	1.90
Rhodochrosite	$MnCO_3$	-1.36	-1.05	-0.77	-0.68	-0.34	2.41	2.49
Siderite	$FeCO_3$						-4.44	-3.86
Smithsonite	$ZnCO_3$							
Witherite	$BaCO_3$							
Zn(OH)$_2$ (e)	$Zn(OH)_2$							

Table 12. Visual MINTEQ results of simulated monimolimnetic sulfur and iron species.

Mineral	log IAP	Sat. Index	Stoichiometry					
Fe(OH)2 (am)	9.349	-4.698	1	Fe+2	2	H2O	-2	H+1
Fe(OH)2 (c)	9.349	-3.541	1	Fe+2	-2	H+1	2	H2O
FeS (ppt)	-2.515	0.368	1	Fe+2	1	HS-1	-1	H+1
Mackinawite	-2.515	1.085	1	Fe+2	1	HS-1	-1	H+1
Melanterite	-6.188	-3.855	1	Fe+2	1	SO4-2	7	H2O
Siderite	-10.827	-0.281	1	Fe+2	1	CO3-2		

Component	% of total component concentration	Species name
CO3-2	0.026	CO3-2
	27.924	H2CO3* (aq)
	0.051	FeHCO3+
	72	HCO3-
SO4-2	99.245	SO4-2
	0.754	FeSO4 (aq)
Fe+2	25.722	Fe+2
	0.153	FeHCO3+
	0.016	FeOH+
	48.652	FeHS+
	25.457	FeSO4 (aq)
HS-1	3.068	HS-1
	6.602	H2S (aq)
	90.33	FeHS+

Physical Results

Seiche Dynamics

Thermistor data was used to assess the impact of wind and wind direction on lake dynamics. Seiche activity was most evident near the thermocline at 4 m, 6 m, and 10 m depths during August 2001 (Figure 58). Winds exceeding 4.5 m/s impacted seiche activity to a depth of at least 10 m on August 14, 2001.

Raw temperature data were transformed to isotherm displacement data by linear interpolation of data from two adjacent thermistors. Figure 59 shows displacement data for the east and west 18° C isotherm (within the thermocline) from August 9, 2001 through August 14, 2001 during different wind events. It is clear from this figure that the 18° C isotherm was displaced up to 0.5 m when winds were from the east and up to 0.7 m when winds were from the west. It was also clear that the location of the thermistors was near a seiche node because the displacement cycles of both ends were out of synch by nearly 1/2 phase.

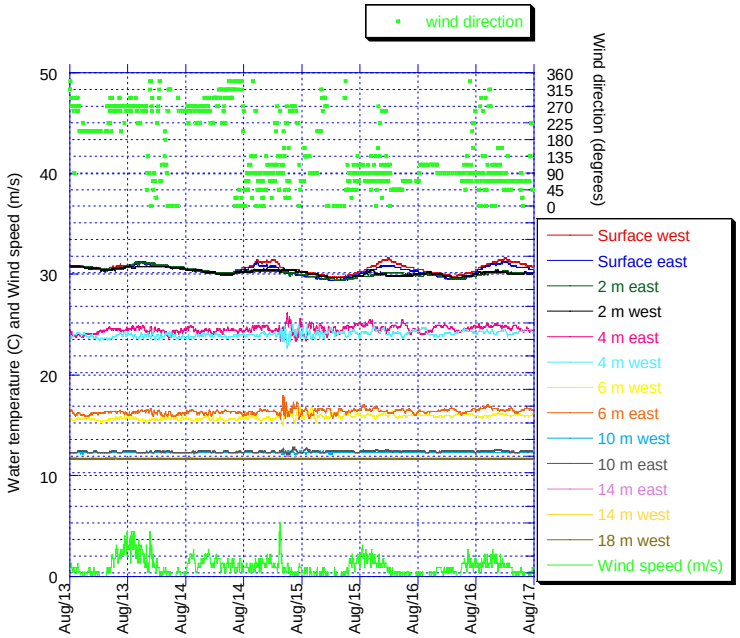

Figure 58. Thermistor data, wind speed, wind direction for South Pit Lake from August 13, 2001 through August 17, 2001.

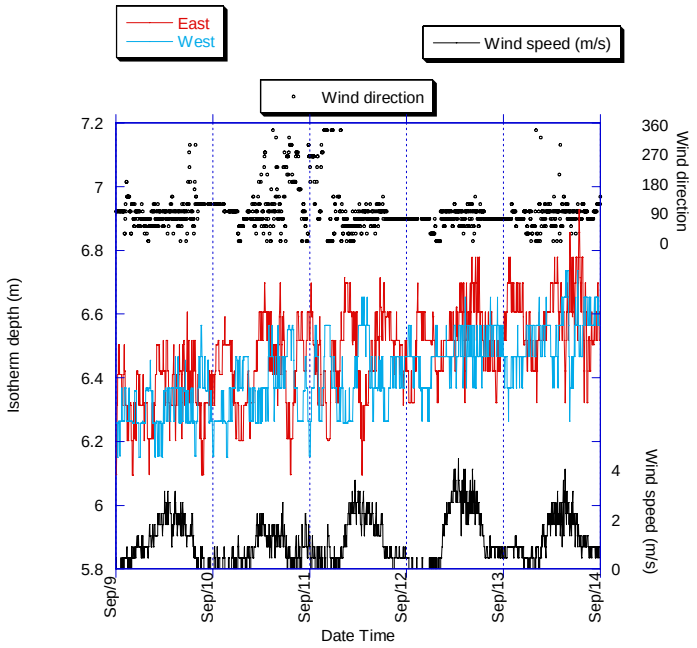

Figure 59. 18° C isotherm displacement, wind direction, and wind speed for South Pit Lake from 9-9-01 through 9-14-01.

One important question that needed to be answered was, did the lake shape help to decrease the amount of wind energy that was transported to the lower depths of the lake, thereby aiding in establishment and persistence of meromixis? One method for making this determination was through power spectral density analysis (PSD). This analysis allowed for parsing of dominant signals from a "noisy" signal such as the displacement data in the figure above and also helped to determine the kinetic energy within the lake. Spectral density of the displacement data was assessed with the MATLAB Signal processing toolbox (Figure 60).

Results for the September 2001 data showed that most of the significant frequencies observed occurred in both east and west ends of the lake but in almost all cases the energy of the paired frequencies was not matched. Significant peaks occurred at $10^{-2.81}$ cpm (640 min), $10^{-2.33}$ cpm (213 min), $10^{-2.15}$ cpm (142 min), $10^{-1.93}$ cpm (85.3 min), $10^{-1.66}$ cpm (45.7 min), $10^{-1.43}$ cpm (26.7 min), and $10^{-1.36}$ cpm (22.9 min).

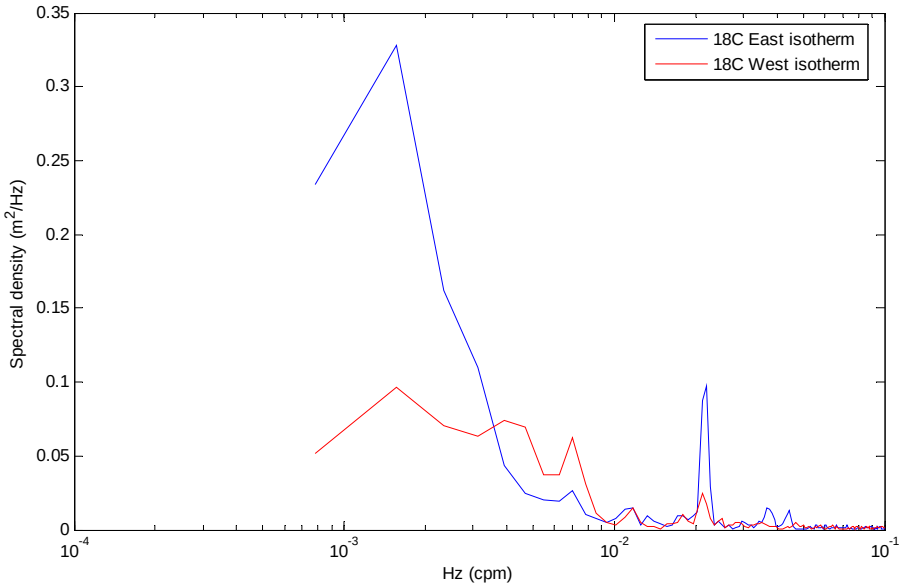

Figure 60. Spectral density analysis results of the 18° C isotherm displacement data.

Use of the internal seiche period function (shown below) allowed for estimation of seiche frequencies as a function of lake bathymetry and water density at the depth of the 18° C isotherm. Comparison of the results for the internal seiche period function and PSD analysis allowed for verification of bathymetry on seiche frequencies and potential bathymetric feature effects on seiche energy.

$$t = \frac{2l}{\sqrt{\frac{g(\rho_h - \rho_e)}{\frac{\rho_h}{z_h} + \frac{\rho_e}{z_e}}}}$$

where,

l = length (cm)
g = force of gravity (980 cm/s^2)
ρ_h = density of hypolimnion (g/cm^3)
ρ_e = density of epilimnion (g/cm^3)
z_h = thickness of hypolimnion (cm)
z_h = thickness of epilimnion (cm)

Results of the internal seiche period function resulted in estimated seiche period frequencies at the depth of the 18° C isotherm of 33 minutes, 45 minutes, and 64 minutes in the NE-SW, NW-SE, and E-W directions, respectively. Comparison of these results with PSD suggested that origin of the 45.7-minute frequency resulted from resonance of the basin in the NW-SE direction at the depth of the 18° C isotherm. In addition, power at this frequency was 4x higher in the east end than the west end.

The 26.7 and 22.9-minute frequencies, which occurred almost exclusively at the east end, may have resulted from fragmentation of the 45.7-minute frequency. Such fragmentation could have resulted from internal wave breaking at the east end boundary layer. As shown in Figure 61, a plateau feature and steep sloping sides at the east end 85 m msl (shown as blue line in figure) could have been responsible for fragmenting the lower frequency spectrum into higher frequencies. However, it was not clear if both higher frequencies could have resulted from such a fragmentation mechanism since summation of the two higher frequencies resulted in an 8% higher energy spectrum than the observed 45.7-minute frequency. An alternative scenario may have been that the 22.9 minute frequency was generated from fragmentation since 22.9 was nearly half of the original 45.7-minute frequency and the 26.7 minute frequency could have resulted from another basin scale resonance or another portion of the fragmentation spectrum of the 45.7 minute spectrum. This second scenario would also explain the energy difference associated with each frequency. The 45.7-minute frequency had approximately 0.1 m^2/cpm while the 22.9-minute frequency had 0.01 m^2/cpm. This difference may have resulted from the dissipation of the seiche energy on the sloping bathymetry.

Dominant peaks at 640 minutes most likely resulted from the periodicity of the barometric pressure. Figure 62 shows the barometric pressure trend for the time period of the analysis. Imboden and Wüest (1995) suggested that small lakes instantaneously react to passing low-pressure zones, where larger lakes respond by giving rise to specific waves and frontal motions. Periods were estimated visually from the figure and were

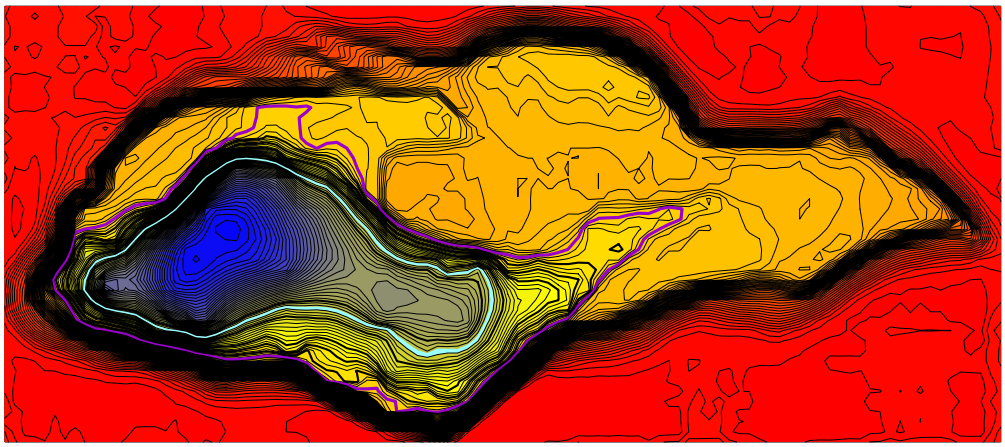

Figure 61. Approximate location of 18° C isotherm during September 2001 (blue line).

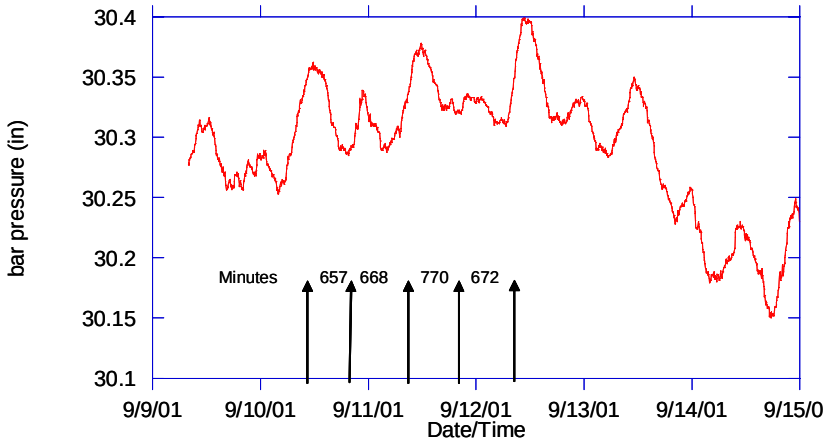

Figure 62. Bathymetric pressure trend for South Pit Lake from 9-9-01 through 9-15-01.

found to be similar to the 640-minute peak resulting from the PSD analysis. It was also apparent from the PSD analysis that barometric pressure generated more energy in the east end than in the west end of the lake. This may have resulted from the volume differences between the two ends. If an equation of continuity can be applied, the kinetic energy resulting from applying the same force to both ends of the lake, where the west end has a larger volume than the east end, more energy would be observed at the east end of the lake.

Heat Content Analysis

Temperature is a measure of the average kinetic energy of individual molecules, thermal or internal energy is the total energy of all molecules within an object, and heat is the transfer of energy from one object to another as a result of a difference in temperature (Giancoli, 1991). These definitions helped to clarify the processes that took place within the monimolimnion regarding monimolimnetic heating and lake stability. Heat content was calculated for each depth from April 2000 through April 2004 according to Cole (1994) as follows:

$$Heat\,content\,(calories) = C \times \rho_i \times V_i \times t_i$$

where,

C = thermal heat capacity of water (1 calorie/ g per °C)
(assumed equal to 1 for simplicity)
ρ_i = density of i_{th} stratum (g/cm^3)
V_i = volume of i_{th} stratum (cm^3)
t_i = temperature of i_{th} stratum (°C)

When the temperature analysis was compared to the heat content analysis, the lake did not undergo hypolimnetic heating. In fact, the least amount of heat was in the lowest stratum and heat content increased steadily from lake bottom to the surface (Figure 63).

Interestingly, during the cooling periods 50% of the heat was approximately retained within 33/66% of the volume and 50% of the volume approximately resided within 33/66% of the depth. Furthermore when lake depth throughout the study period changed, the depth of 50% heat retention changed concomitantly. When the lake was 28 m in the cooling period of 2000-2001 (ex. 1-5-01) the 50% heat retention volume was at 20 meters. In the cooling period of 2001-2002 (ex. 12-31-02) when lake depth was 29 m the 50% heat retention volume was 21 m and when the lake depth was 30 m in the cooling period of 2002-2003 (ex. 12-30-02) the 50% heat retention volume was 21 m.

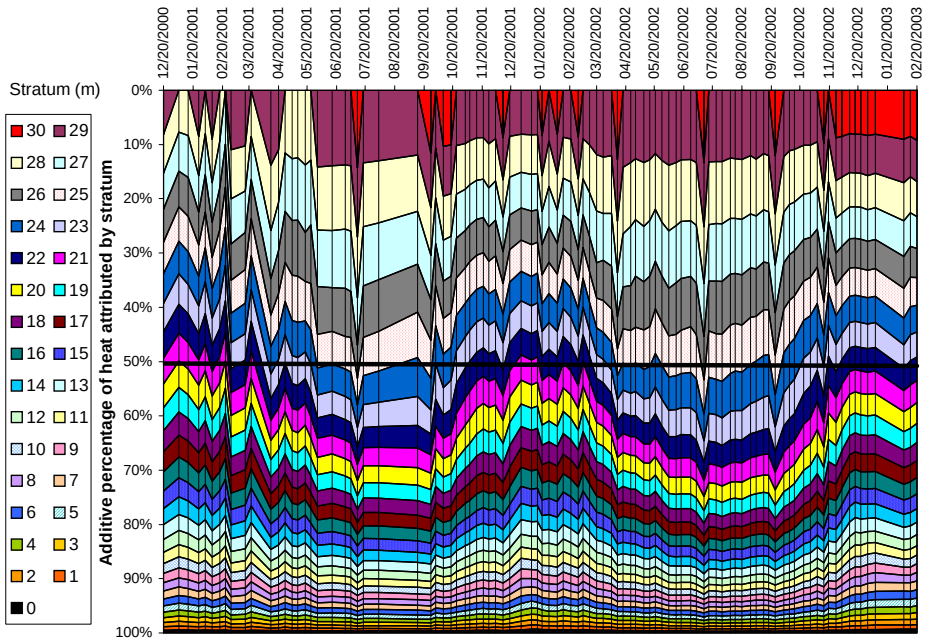

Figure 63. Percent contribution of each strata to the total water column heat content for South Pit lake from December 2000 through February 2003.

This trend suggested that a bathymetric and/or chemical feature of the lake could have been responsible for slowing or impeding lake heat dissipation.

An important factor that contributed to lake stability and ultimately meromixis was that the lake retained nearly half of the total (over 3,800 cal/cm^3) of heat throughout the winters of 2001 through 2003 (Figure 64).

Heat contribution of the lowest stratum to the entire water column was small but was highest during the cooling period (Figure 65). This trend indicated that the lake sediments retained heat throughout the winter.

The rate of heating was highest for upper strata and declined with depth, which indicated a surface to bottom heating trend (Figure 66).

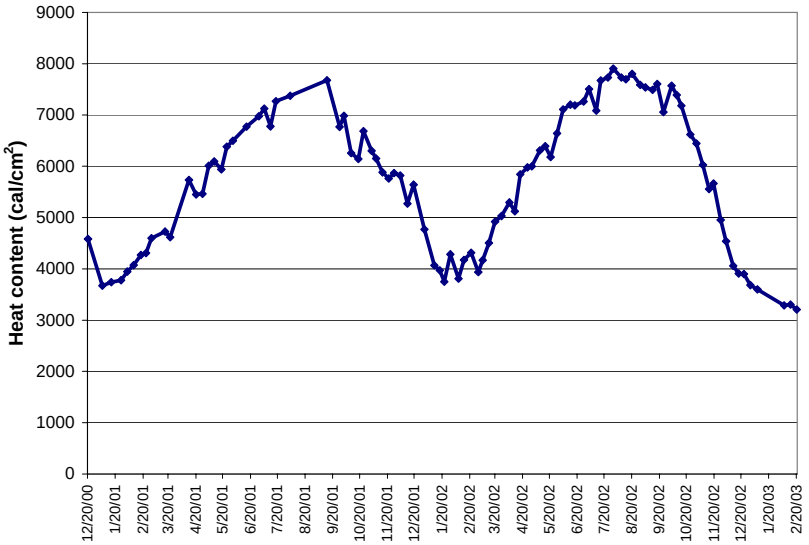

Figure 64. Total heat content for South Pit Lake from December 2000 through February 2003.

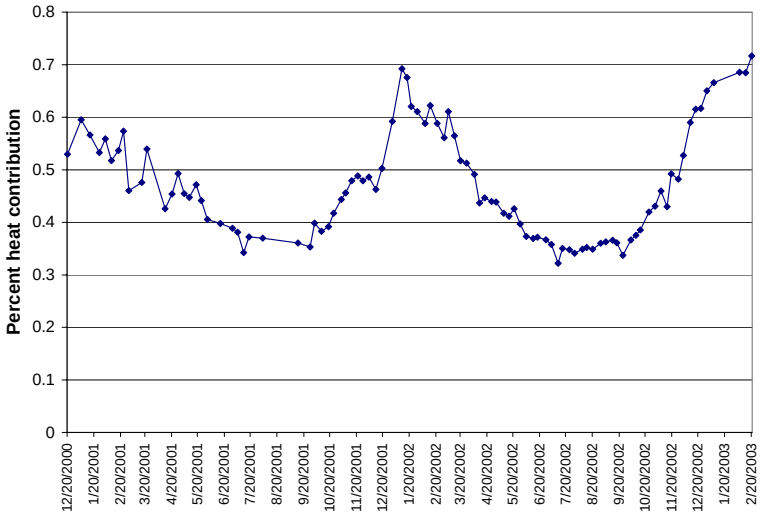

Figure 65. Percent heat contribution to the water column by the 0m stratum from December 2000 through February 2003.

Figure 66. Rates of heating for 5 selected strata in South Pit Lake from December 2000 through April 2003.

Modified Schmidt Stability (Idso, 1973)

Schmidt stability is an index that describes the resistance of a lake to wind mixing. It is the amount of work by the wind required to bring a lake to a uniform temperature without addition or subtraction of heat (Hutchinson, 1957). An alternative definition of stability is the amount of work necessary to lift the entire lake from the calculated center of gravity to the lake's center of mass (Cole, 1994). Idso (1973) modified the Schmidt calculation to allow for analysis of the contribution of each lake layer to overall lake stability:

$$S = \frac{1}{A_o}\int_{Z_o}^{Z_m}(p_z - p_m)(z - z_g)A_z\,dz$$

where:
S = modified Schmidt stability (g-cm/cm^2)
A_o = area at surface (cm)
Z_m = maximum depth (cm)
Z_o = surface
P_z = density at depth z (g/cm^3)
P_m = mean density at complete mixing (g/cm^3)
Z_g = depth of center of gravity (cm)
A_z = area at depth z (cm^2).

The summation is taken over all depths (z) at a specified interval (d_z) (cm).

Density was calculated according to the following (James Schindler, personal communication):

$$Density\ (kg/m^3) = \{[((((6.5343321E^{-9} * T - 1.120083E^{-6}) * T + 1.001685E^{-4}) * T - 9.09529E^{-3}) * T + 6.793952E^{-2}) * T + 0.842594] + 999.0\} + TDS * ((4.99E^{-8} * T - 3.87E^{-6}) * T + 8.221E^{-4})$$

where,

T = temperature of stratum (°C)
TDS = total dissolved solids of stratum (g/m^3)

Lake Number (L_N)

L_N is a dimensionless lake index that compares a lake's stabilizing forces to its destabilizing forces. It is defined as the ratio of the moments about the water body's center of volume (stabilizing forces due to gravity and density stratification) to the wind (destabilizing force) (Robertson and Imberger, 1994). It is assumed that wind is the predominant destabilizing force encountered by a lake and does not include other destabilizing forces such as cooling, inflow, and outflow (Robertson and Imberger, 1994). L_N>1 indicates strong stratification and the effect of wind forcing is minimal. L_N=1 indicates that wind forcing is strong enough to force the seasonal thermocline to the surface at the upwind end of the lake, but is not strong enough for deep mixing. L_N<1 indicates wind forcing is strong enough for severe seiching at the thermocline and turbulent mixing is likely in the hypolimnion (Robertson and Imberger, 1994).

$$L_N = gS_t \frac{\left(1 - \left(\frac{z_t}{Z_m}\right)\right)}{\left(\rho_o u_*^2 A^{1.5} \left(1 - \frac{z_g}{Z_m}\right)\right)}$$

where: g = acceleration due to gravity (cm/s)

S_t = Schmidt stability (g-cm/cm^2)
Z_t = thermocline height (cm above bottom)
Z_m = maximum depth (cm)
P_o = water density at surface (g/cm^3)
A = surface area (cm^2)
Z_g = center of volume (cm above bottom)

$$u_*^{\ 2} = \left(\frac{P_a}{P_o}\right) C_D U_W^2$$

where: P_a/P_o = density of air divided by the density of water (1.23×10^{-3})
C_D = shear coefficient of wind over water for small lakes (1.0×10^{-3})
U_W = wind speed (m/s).

Figure 67 shows a depth time diagram of discreet meter stability for SPL from April 2000 through March 2003. This figure illustrates the contribution of each meter to the overall stability of the lake. Figure 68 shows a summation of stability for each profile date for SPL from April 2000 through March 2003. Generally, stability was highest in the epilimnion during the summer and near zero in the metalimnion during summer and

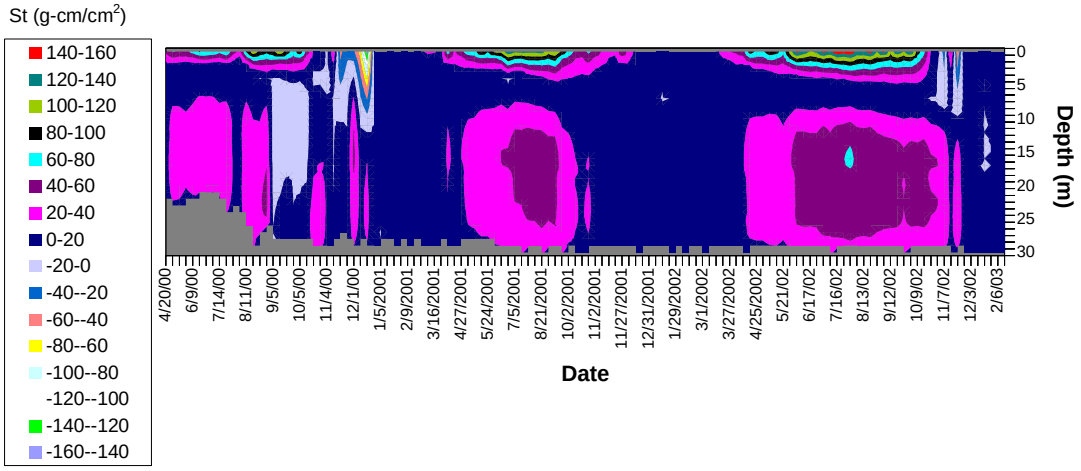

Figure 67. Depth-time diagram of revised Schmidt stability for South Pit Lake from April 2000 through March 2003.

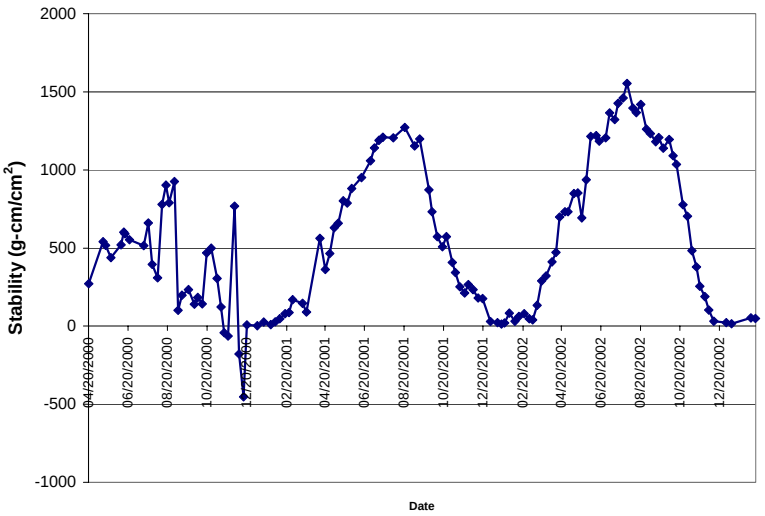

Figure 68. Total water column stability for South Pit Lake from April 2000 through March 2003.

throughout the entire water column in the winter. Stability was highest on the surface in the summer of 2002 (158.0 g-cm/cm^2) and lowest in the epilimnion in the winter of 2000 (-155.0 g-cm/cm^2). For all three years the hypolimnion showed a relatively strong stability during summer stratification. Stability increased from the upper hypolimnion, peaking toward the center hypolimnion and decreased toward lake bottom. Calculated stability was below zero for a prolonged period on two occasions; during the netted pond release in 2000 and during a winter storm in November 2002, which had over 10 cm of snow within a 24 hr period. Negative stability indicated that buoyancy was less than the buoyancy at the lake's center of gravity, so water during those periods would have eventually descended to a suitable level of buoyancy.

Total water column stability increased from 2000 to 2002. Perturbations in 2000 did not allow the lake to fully stratify, so stability was lowest during that year. Stability increased slightly from 2001 to 2002 and was likely due to prolonged epilimnetic temperatures of >29°C. As more water is added to the lake and the lake maintains a distinct chemical stratification, total stability will increase until the lake reaches full capacity. One interesting point to note was that during each winter, lake stability was

near zero and holomixis did not occur. This may have indicated that Schmidt stability did not completely account for all mechanisms that determine lake stability against mixing (e.g. bathymetric effects on wind dissipation).

Wedderburn Number

A dimensionless lake index which compares a lake's stabilizing forces to the destabilizing forces and is a ratio of the epilimnetic buoyancy:length-based wind mixing (Imberger and Patterson, 2003; Robertson and Imberger, 1994; Kalff, 2002). Hence, this index calculates the extent of mixing to the thermocline (Robertson, personal communication, 2003). When W>1.0, epilimnetic buoyancy overcomes the mixing potential and mixing does not reach the thermocline. When W<1.0, wind forcing is stronger than the epilimnetic buoyancy and mixing reaches the thermocline. This index only accounts for mixing to the seasonal thermocline and is not an indicator of deep mixing. The calculation was performed according to Robertson and Imberger (1994):

$$W = \frac{g' H^2}{\mu^{*2} L}$$

where: g' = reduced gravitational acceleration due to the density jump across the thermocline
H^2 = thickness of the mixed layer
L = length of lake at thermocline (m)
μ^{*2} = wind shear velocity

$$\mu^{*2} = \left(\frac{P_a}{P_o}\right) C_D U_W^2$$

where: P_a/P_o = density of air divided by the density of water (1.23×10^{-3})
C_D = shear coefficient of wind over water for small lakes (1.0×10^{-3})
U^2_W = wind speed (m/s).

Lake Number (L_N) and Wedderburn Number (W) Dynamics

Figure 69 shows the monthly calculation results for L_N, W, and Stability for May 2001 through June 2002. Both indices are sensitive to wind speed, so the seasonal trends are similar; each was highest in the summer and lowest in the winter. Only on one date (2-21-02) a value of <1 was calculated for W (0.11). L_N never fell below 1 for the calculated dates. The lowest value was 2.25 on 2-21-02.

Lake stability was lowest on 1-17-02 (12.7 g-cm/cm^2) and L_N was declining. Although lake stability indicated that the lake may have been prone to mixing, L_N and W indicated that the wind was not strong enough to overpower the low stabilizing force. In fact, W increased on 1-17-02, indicating the wind at that time was not strong enough to push the surface water to the thermocline. W and L_N were lowest on 2-21-02 (0.109 and 2.25, respectively). W below 1 on that date indicated the wind was strong enough to push the surface to the thermocline (2 meters on that date) but L_N indicated the wind was not strong enough to cause deep mixing. An increase in stability on 2-21-02 most likely

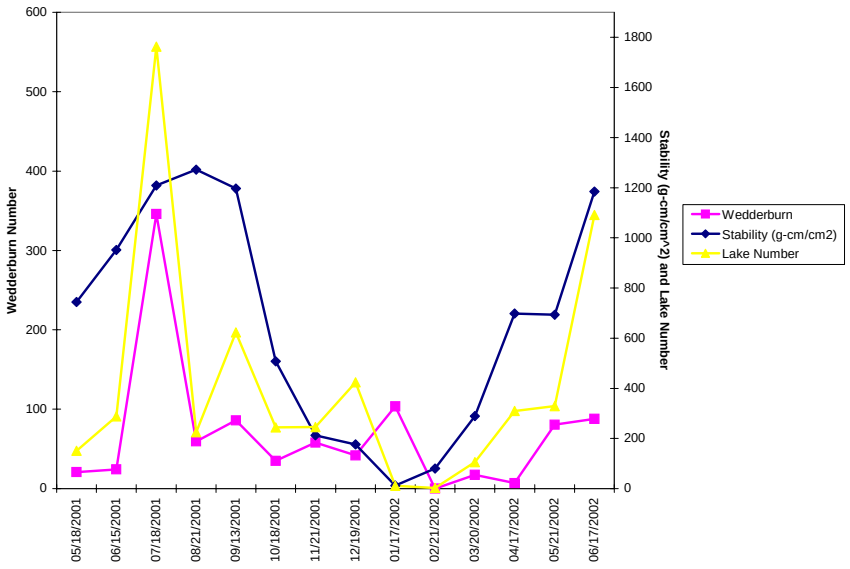

Figure 69. Wedderburn Number, Lake Number, and modified Schmidt stability for South Pit Lake from 5-18-01 through 6-17-02.

decreased the chance of holomixis on that date (stability increase most likely resulted from solar heating of suspended sediments in the metalimnion as a result of runoff due to a rainfall event (data not shown)).

In February 2002 winds were strong enough to force the surface water to the winter thermocline (W < 1) but did not sustain a daily wind speed in excess of 5.4 m/s. Therefore, for the dates calculated in this discussion, it appears that meromixis remained intact for the winter of 2001 because the lowest values for W, L_N, and S_t did not coincide on the same date and wind speeds did not exceed the critical wind speed to force deep mixing.

Critical Wind Speed Modeling

To assess even further the impact of wind mixing on SPL, an array of wind speeds was entered into the W and L_N equations in an effort to model the critical wind speed. Critical wind speed was considered to be the average wind speed over a 24-hour period that will cause mixing of the surface to the thermocline (W) or deep mixing (L_N) for a specified set of lake conditions. Lake conditions chosen for this exercise were chosen from the original data and included one summer (most stable July 2001) and one winter (least stable February 2002) lake configuration. For each configuration all parameters from the original dataset remained constant and only wind speed was varied.

Figure 70 shows the impact of wind speed on Wedderburn Number for SPL during summer and winter configurations. The y-axis in the figure stops at W=20, but the value for W at a wind speed of 0.22 m/s for the summer configuration exceeded 2500 while W for the winter configuration was 38. SPL responds little to wind during the summer. Sustained wind speeds up to 9 m/s are not enough to force the surface water to the summer thermocline. Daily wind speeds during July 2001 averaged 1.3 m/s with a

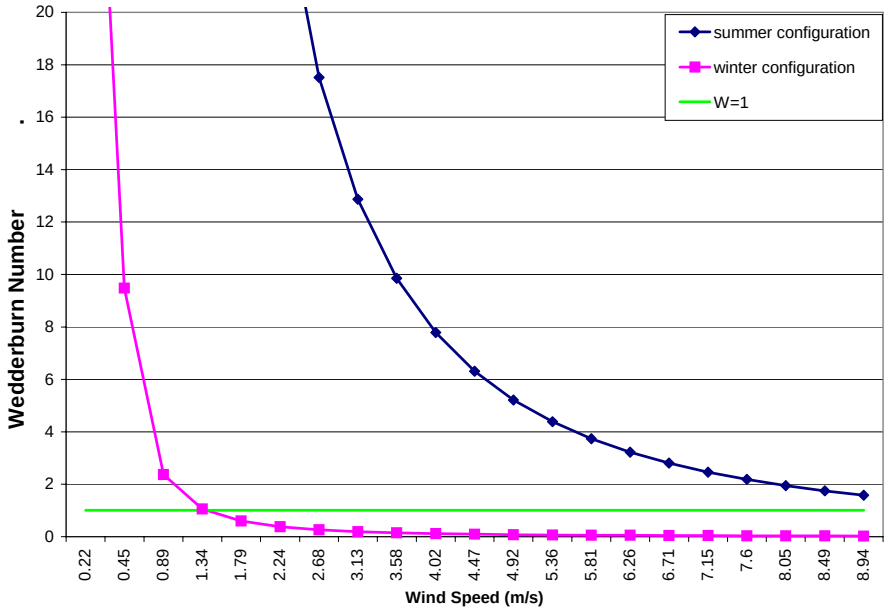

Figure 70. Impact of wind speed on Wedderburn Number for South Pit Lake.

maximum daily average speed of 2.1 m/s and a minimum daily average speed of 0.8 m/s. This indicated that the lake was not disturbed by wind during the entire month and may indicate that SPL will most likely not be disturbed by wind in the summer. During the winter, however, the lake responds greatly to wind and sustained wind speeds >1.34 m/s would force the surface water to the winter thermocline. Daily wind speed during February 2002 averaged 1.74 m/s with a maximum daily average wind speed of 5.4 m/s and a minimum average wind speed of 0.63 m/s. Slightly less than half (46%) of the days during February 2002 had wind speeds, which exceeded 1.34 m/s. Due to higher average wind speeds, thermocline descent, and decreased density difference across the thermocline, this exercise indicated that SPL is highly prone to surface-to-thermocline wind forcing in the winter and is not likely to mix in the summer.

Figure 71 shows the impact of wind speed on Lake Number for SPL during summer and winter configurations. The y-axis stops at L_N=20 but L_N for the summer configuration at a wind speed of 0.22 m/s exceeded 13000 and exceeded 780 for the

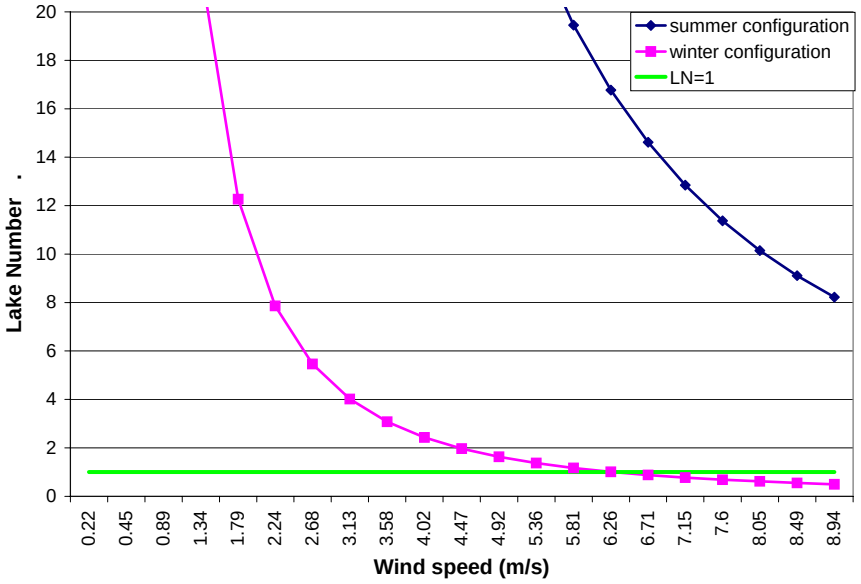

Figure 71. Impact of wind speed on Lake Number for South Pit Lake.

winter configuration. L_N is not significantly responsive to winds up to 9 m/s during the summer and is less responsive to wind during the winter than W. Since L_N <1 at 6.3 m/s, wind speeds greater than 6.3 m/s would induce deep mixing events in SPL.

Figure 72 shows the average daily wind speeds for each month in relation to critical wind speeds calculated from Wedderburn and Lake Number calculations from April 2001 through May 2003. Wind speeds exceeded the critical value, as calculated with the Wedderburn Number, 62% of the assessed time period and never approached the critical value as calculated by the Lake Number. This indicated that it is unlikely for the lake to mix completely as a result of a single event but mixis may result from slow erosion of the mixolimnion/monimolimnion boundary.

Figure 73 shows the trend in specific conductance as a result of winds exceeding 1.34 m/s in late 2002 through early 2003. As predicted by the Wedderburn Number calculation, “surface to thermocline” mixing results when winds exceed 1.34 m/s in the winter. In the case of South Pit Lake, the mixolimnetic/monimolimnetic boundary deepened rapidly as a result of consistent wind speeds above the critical threshold (A and

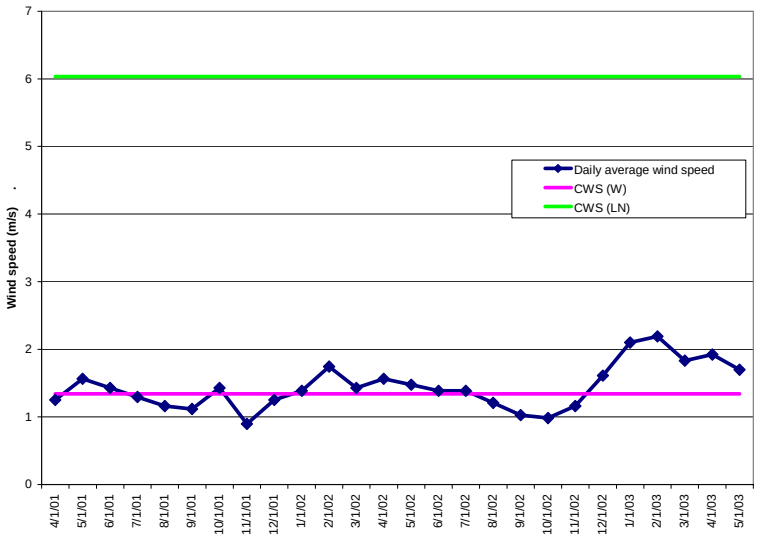

Figure 72. Average daily wind speed for each month from April 2001 through May 2003. CWS (W) = critical wind speed from Wedderburn Number calculation. CWS (LN) = critical wind speed from Lake Number calculation.

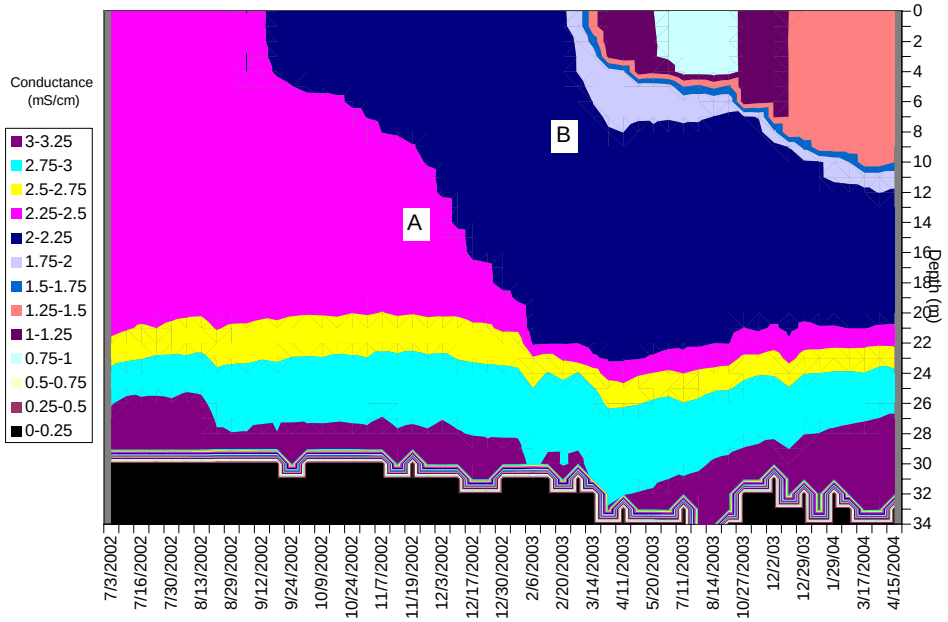

Figure 73. Specific conductance depth time diagram from July 2002 through April 2004. A and B indicate highest rate of wind induced erosion of monimolimnion. B also indicates high surface water influent rates.

B in Figure 73). This event ended in an injection of oxygenated water into the monimolimnion. The most likely barrier to holomixis during this event may have been the rapid release of water to South Pit Lake (B in Figure 73). The added water was warm as a result of increased spring temperature and most likely added stability to the mixolimnion.

Impact of Wind Direction on SPL

All previous W calculations assumed a wind direction blowing in the east-west direction. The Wedderburn calculation can also be used to consider the impact of wind direction on a water body because it has a lake length parameter, which essentially accounts for wind fetch. For SPL at the 98.7 m elevation (depth = 30 m) the north-south axis was approximately half that of the east-west axis. As a result, calculated values for W for a wind blowing in the north-south direction are twice that of the calculated values for the same wind speed in the east-west direction. Calculating W for the same wintertime dataset in the north-south direction results in an increase of the critical wind speed to 4 mph. That is, winds exceeding 1.8 m/s in the north-south direction will mix the surface water to the wintertime thermocline compared to 1.3 m/s in the east-west direction. Unfortunately the dominant wind direction at SPL is along the east-west axis. In February 2002 only ~7% of the wind was along the north-south axis and 70% of the wind was along the east-west axis. These results show that optimal orientation of SPL would have been to have the longest axis in the north-south direction.

Biological Results

South Pit Lake Phytoplankton Trends

Total phytoplankton counts from March 8, 2000, through February 28, 2003, for South Pit Lake are shown in Figure 74. Counts exceeded $4x10^{10}$ cells/L for most of the period from April 2000 through August 2001, but decreased below this mark during late

Figure 74. Total phytoplankton counts for South Pit Lake from March 2000 through February 2003.

winter 2001. Counts never exceeded $2.2x10^6$ cells/L after November 2001. Holomixis in 2000, meromixis in 2001 and 2002, June 2000 netted pond release, and zooplankton grazing were the driving forces for the phytoplankton count trend.

Phytoplankton Family Trends

Figure 75 shows the trends of the dominant phytoplankton families from May 2000 through February 2003. Cyanophyceae dominated the photic zone throughout 2000 with cell counts exceeding $3.5x10^{10}$ cells/m^3 while the second most prevalent class was the Chlorophyceae with counts ~$4.0x10^9$ cells/m^3. All other classes had counts below $1x10^7$ cells/m^3.

In February 2001, Cyanophyceae no longer dominated the photic zone as Chlorophyceae dominance take over. In fact, Cyanophyceae presence was no longer observed to any great extent after holomixis in the winter of 2000. Chlorophyceae dominated the water column throughout 2001 with maximum counts exceeding $8.0x10^{10}$ cells/m^3. Counts of all other classes were below $2x10^8$ cells/m^3 during that time. Plankton dynamics, in terms of biomass and seasonal succession, changed significantly

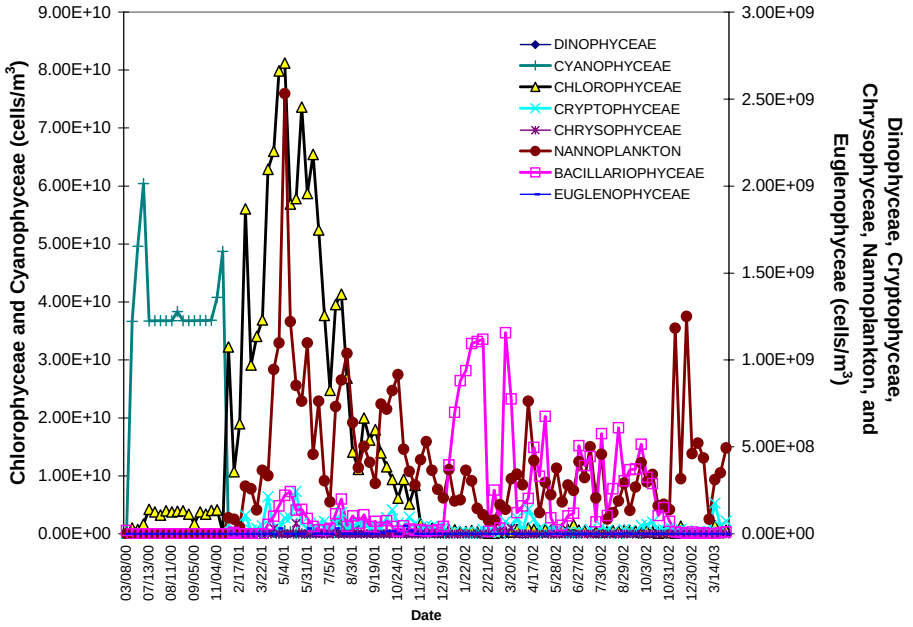

Figure 75. Trends between phytoplankton classes for South Pit Lake from March 2000 through March 2003 (note difference between y-axis scales).

after meromixis was established in 2001 so it was necessary to isolate that portion of the data to clearly view those patterns (Figure 76).

Cyanophyceae

Figure 77 (expanded view shown in Figure 78) shows the Cyanophycean species counts from March 2000 through March 2003. SPL phytoplankton was initially dominated by *Chroococcus* spp. until February 2002, with counts exceeding $3.5x10^7$ cells/L. *Phormidium* spp. was the only other Cyanophyceae of significance for the remainder of the study period, with counts ~$2.3x10^6$ cells/L in the summer of 2001.

These counts do not include blue-greens associated with floating mat communities and littoral observations. The presence of diatom/blue-green mats were extensive in 2000 and early 2001 and steadily decreased toward the end of the study period. Mat communities were mostly composed of *Oscillatoria* spp. in the spring and a mixture of *Oscillatoria* and *Spirulina* spp. in the summer. In the winters of 2000 and

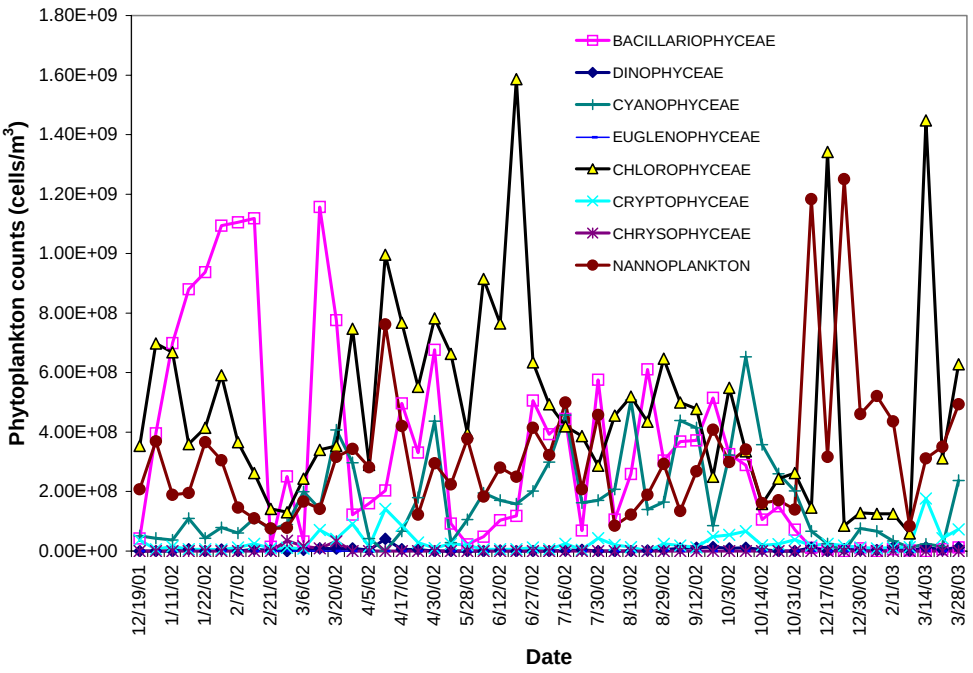

Figure 76. Trends between phytoplankton classes for South Pit Lake from December 2001 through February 2003.

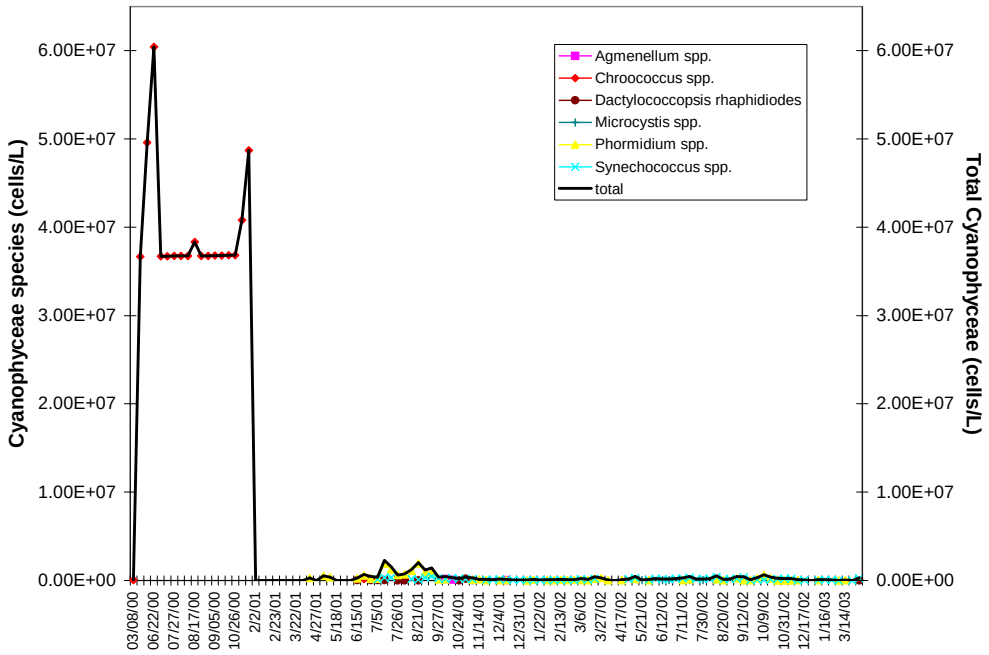

Figure 77. Cyanophyceae species for South Pit Lake from March 2000 through March 2003.

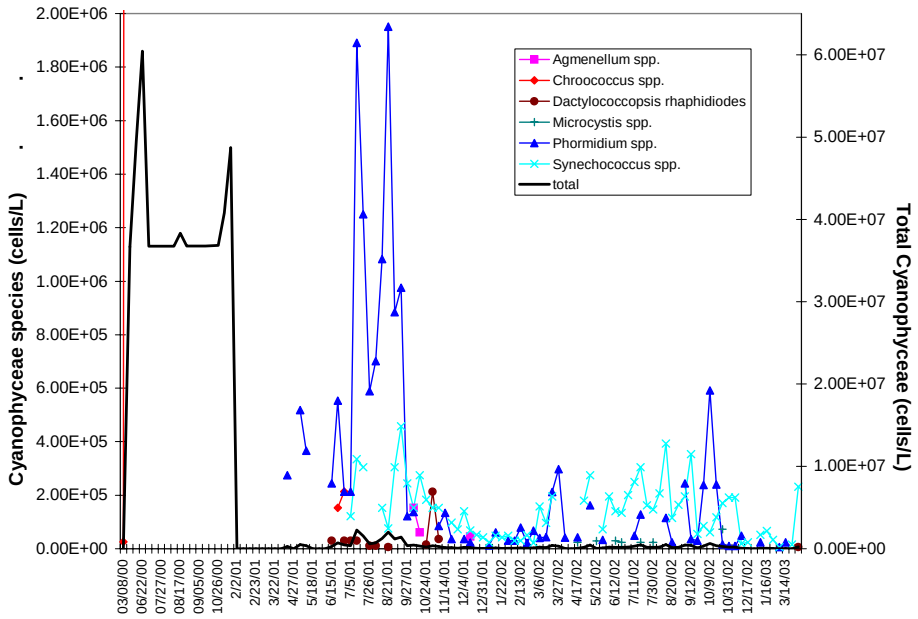

Figure 78. Expanded view of Cyanophyceae species for South Pit Lake from March 2000 through March 2003.

2001, *Oscillatoria* spp. covered most of the littoral zones from the surface to several meters into the water.

Bacillariophyceae

Figure 79 shows the Bacillariophycean species counts from March 2000 through March 2003. Few diatoms were seen in 2000, but diatom species diversity and abundance have increased. The dominant species has changed over the study period with *Nitzschia* spp. initially dominant, giving way to *Cyclotella* spp. and then *Achnanthes* spp.

Although these counts do not directly reflect diatoms within littoral mat communities, breakdown of these mats in the spring and summer could be reflected in the figure below. In addition, periphytometer slides placed in the epilimnion of SPL showed an abundance of diatoms and considerable diatom diversity. These analyses were assessed for qualitative purposes only.

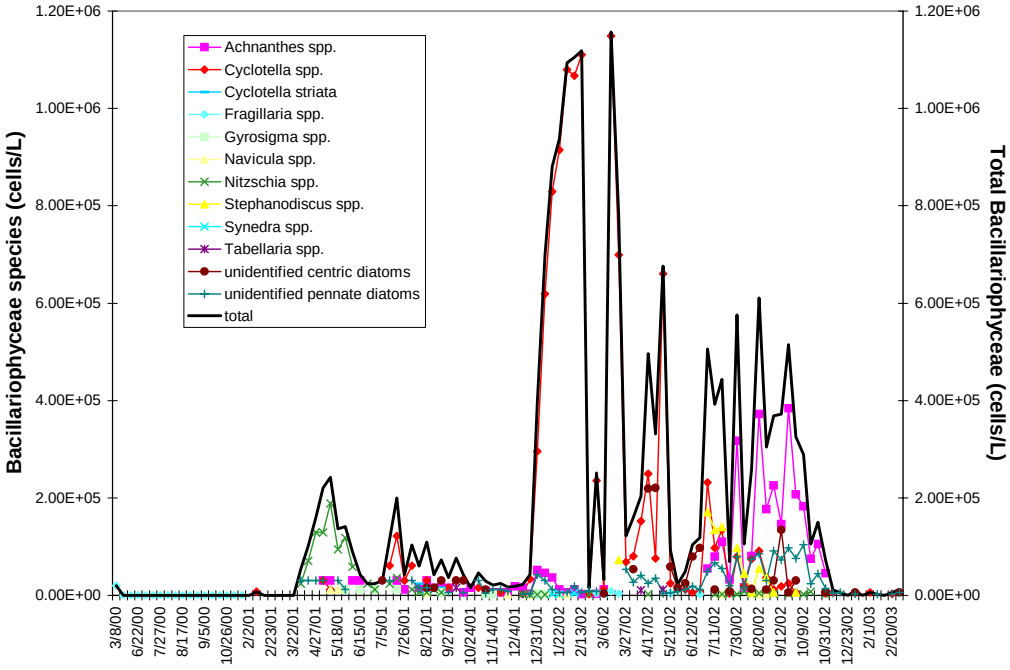

Figure 79. Bacillariophyceae species for South Pit Lake from March 2000 through March 2003.

Euglenophyceae

Figure 80 shows the Euglenophycean species counts from March 2000 through March 2003. Euglenoids were minor species throughout the study period. *Euglena* spp. was present in April 2001 at $3x10^4$ cells/L and was not found in any other sample. *Trachelomonas* spp. was present on several occasions throughout 2001, with counts never exceeding $4.5x10^4$ cells/L.

Sporadic introduction of these species may have been due to wetlands influent since most of the euglenoid spikes coincide with rain events. In the lab, hundreds of euglenoids were observed within the lateral roots of *Typha* plants. In addition, in the springs of 2001 and 2002 massive blooms of euglenoids (reddish in color) were observed in the uppermost section of the west wetland system, so this supposition seems feasible.

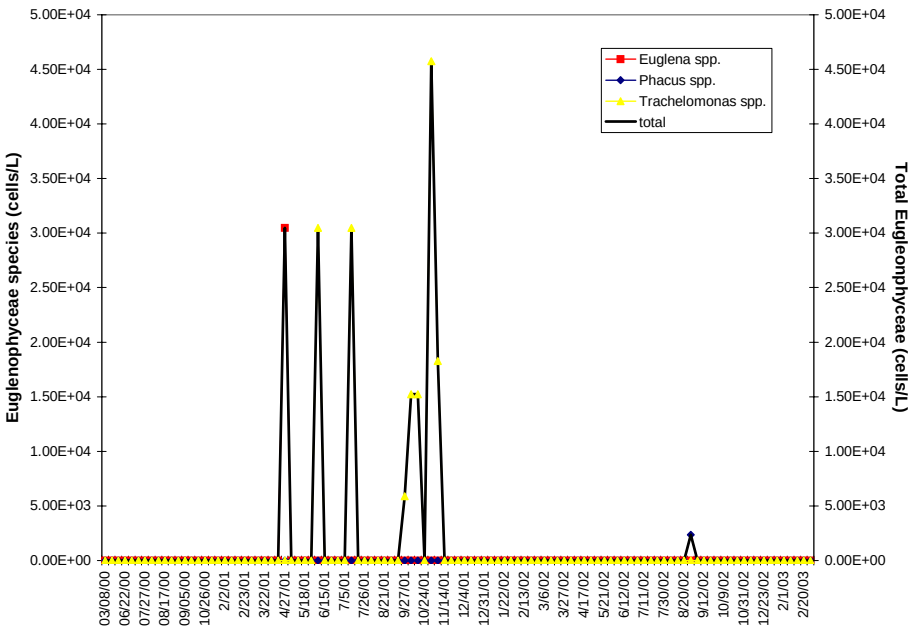

Figure 80. Euglenophyceae species for South Pit Lake from March 2000 through March 2003.

Chlorophyceae

Figure 81 shows the Chlorophycean species counts from March 2000 through March 2003. Figure 82 is the same figure but the y-axis has been enlarged to show the Chlorophycean dynamics for 2001 and 2002. *Ankistrodesmus* spp. dominated the water column for most of 2001, with counts exceeding $7.5x10^7$ cells/L. This species increased slightly as a result of netted pond influent, so it may have been introduced during that time or could have been stimulated as a result of the nutrient laden influent. The highest concentrations of this species coincided with SPL turnover in the winter of 2000-2001. *Chlorella ellipsoidea* and *Chlamydomonas* spp. were also present in significant amounts during 2001 with counts exceeding $2.5x10^6$ cells/L and $1.0x10^6$ cells/L, respectively. In December 2001 *Chlorella ellipsoidea* became the dominant phytoplankton species in SPL. All other species did not exceed counts above $2x10^4$ cells/L throughout the study period.

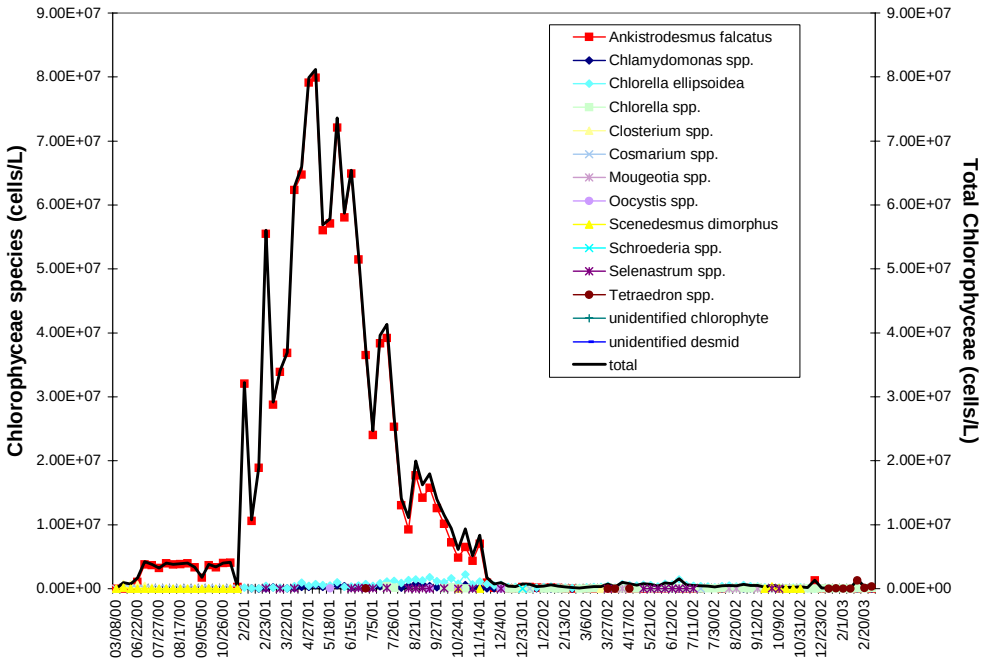

Figure 81. Chlorophyceae species for South Pit Lake from March 2000 through March 2003.

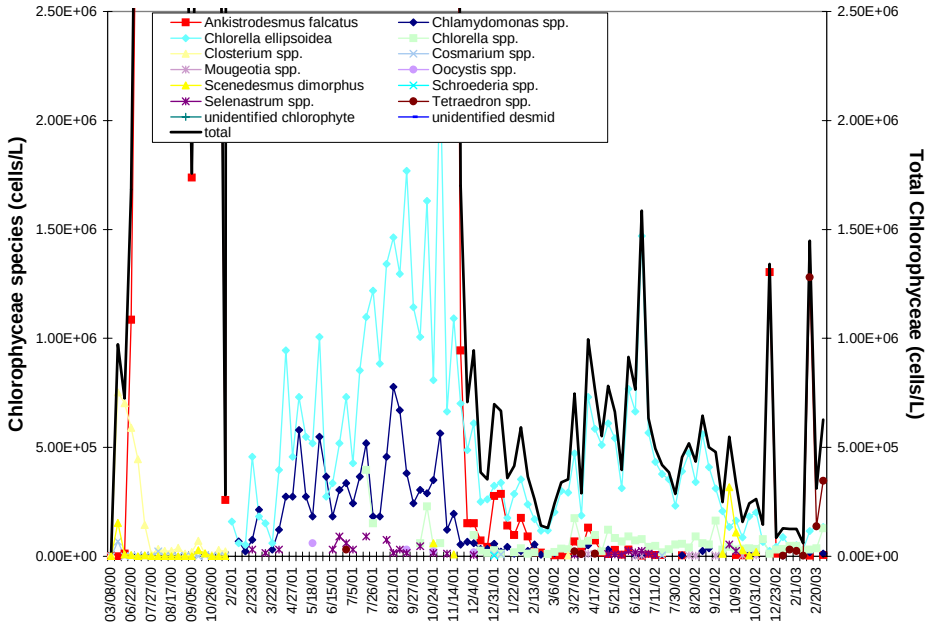

Figure 82. Chlorophyceae species for South Pit Lake from March 2000 through March 2003 emphasizing the 2001-2003 dynamics.

Cryptomonas spp.

Figure 83 shows *Cryptomonas* spp. counts from March 2000 through March 2003. Trends for this species were similar to the trends for Chlorophyceans and most likely resulted from netted pond influent as well. No *Cryptomonas* spp. were observed in 2000, so this species may have come directly from the netted pond influent. *Cryptomonas* spp. decline coincided with high zooplankton biomass. Reynolds (1984) suggested that *Cryptomonas* spp. are sensitive to grazing pressure.

Chrysophyceae

Figure 84 shows the Chrysophycean species counts from March 2000 through March 2003.

Nanoplankton

Figure 85 shows the nanoplankton counts from March 2000 through March 2003.

Phytoplankton Species Richness

Figure 86 shows phytoplankton species richness from March 2000 through March 2003. Phytoplankton species richness increased from a maximum number of 6 species in 2000 to a maximum number of 17 species in the summers of 2001 and 2002.

South Pit Lake Zooplankton Trend

Calanoid Copepods

Figure 87 shows the calanoid copepod counts for all life stages from May 2000 through January 2003. Copepod counts increased in the winter of 2000 and decreased until the summer of 2001. Maximum counts were observed in the winter of 2001 and exceeded 7500 counts/m^3. Another bloom took place in the spring of 2002 and decreased in the summer. A fourth bloom occurred in the winter of 2002. Counts during copepod blooms steadily decreased from the winter 2001 date.

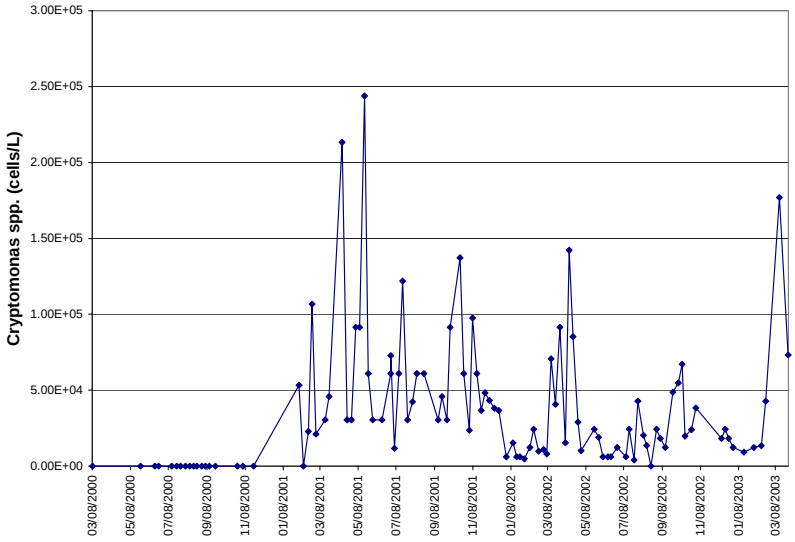

Figure 83. *Cryptomonas* spp. for South Pit Lake from March 2000 through October 2002.

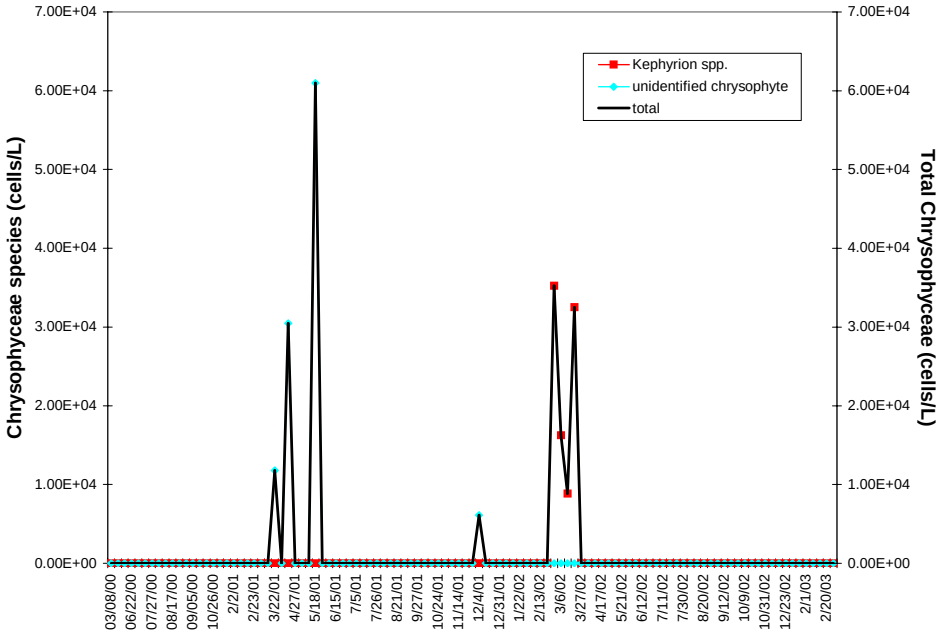

Figure 84. *Chrysophyceae* species for South Pit Lake from March 2000 through March 2003.

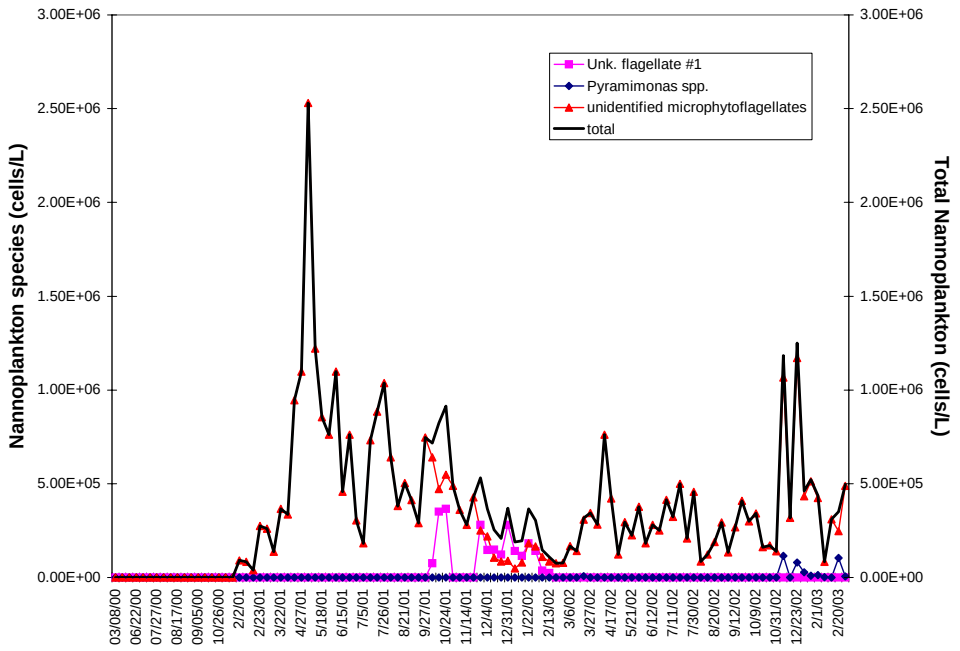

Figure 85. *Nanoplankton* for South Pit Lake from March 2000 through March 2003.

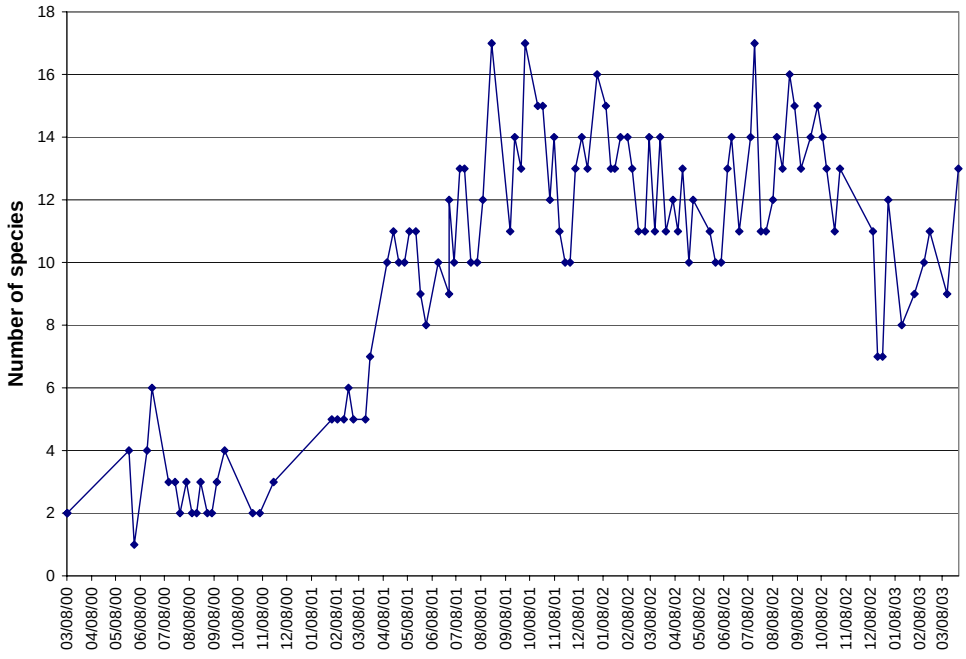

Figure 86. Phytoplankton species richness for South Pit Lake from March 2000 through March 2003.

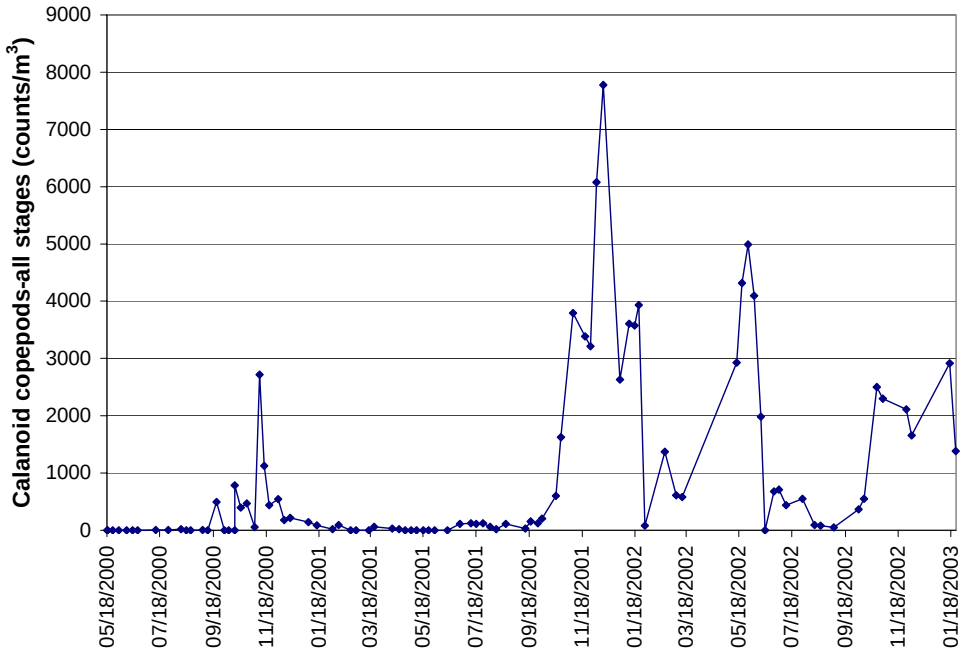

Figure 87. Total calanoid copepod counts (all stages) for South Pit Lake from May 2000 through January 2003.

Figure 88 shows the total calanoid copepod counts broken down by copepodid and naupliar life stages from May 2000 through January 2003. The initial copepodid bloom was preceded by a naupliar stage bloom. All subsequent blooms either had coinciding copepodid-naupliar blooms or just copepodid stage initiation. Both naupliar and copepodid stage bloom counts have decreased since the 2001 winter blooms.

Figure 89 shows the calanoid copepod counts broken down by all life stages from February 2001 through January 2003.

Cyclopoid Copepods

Figure 90 shows the cyclopoid copepod counts for naupliar and copepodid life stages from May 2000 through January 2003. Cyclopoid counts were somewhat sporadic, but showed bloom periods mostly during the summer.

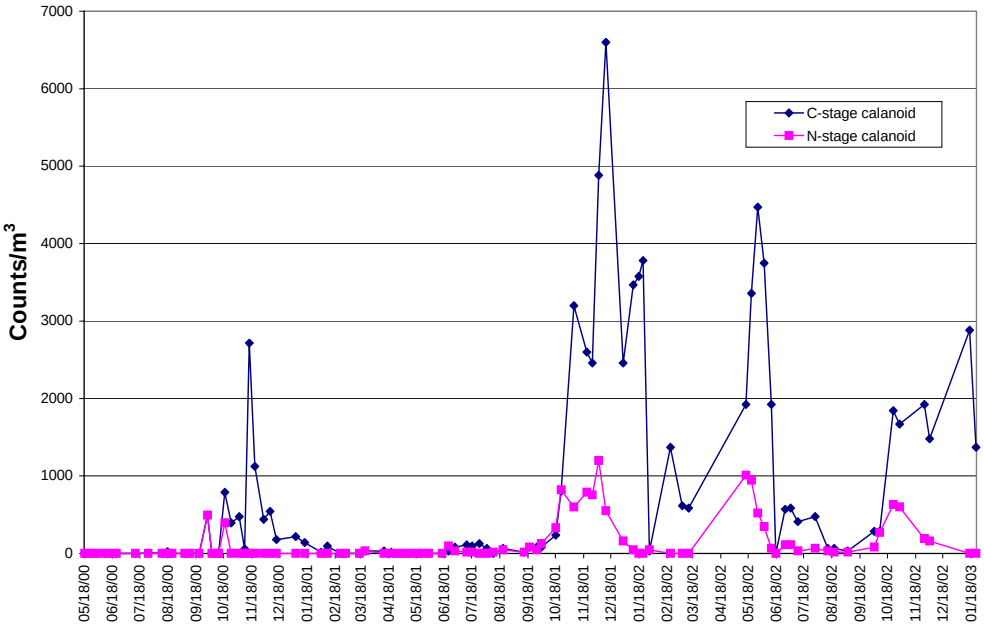

Figure 88. Naupliar and copepodid stage calanoid counts for South Pit Lake from May 2000 through January 2003.

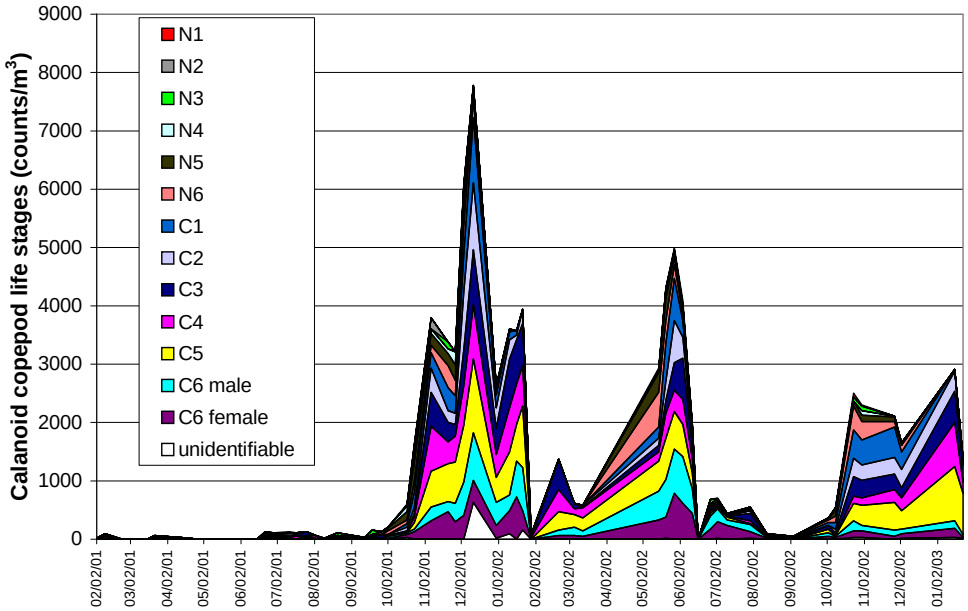

Figure 89. Calanoid copepod counts broken down by life stages for South Pit Lake from February 2001 through January 2003.

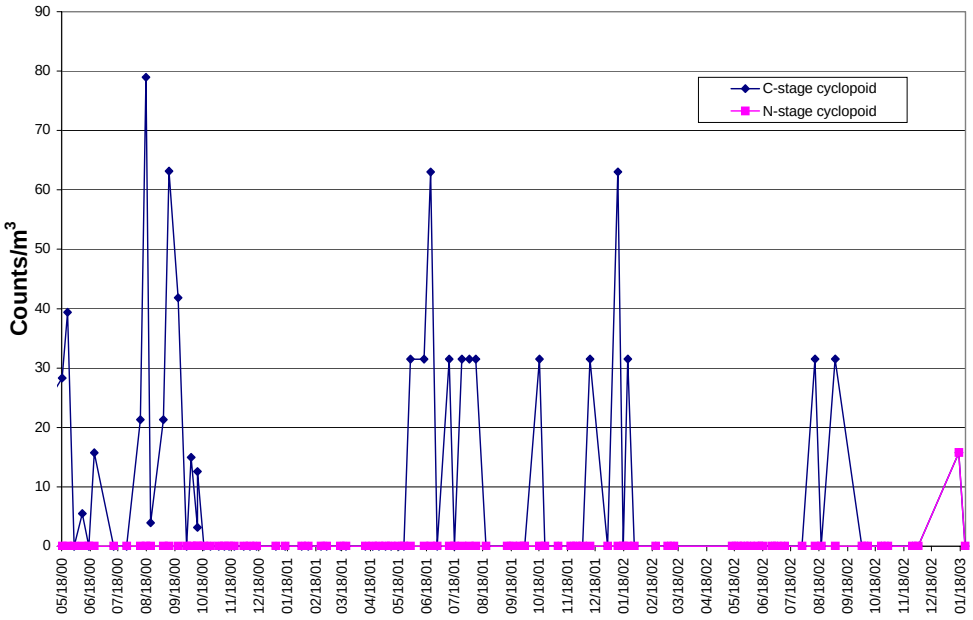

Figure 90. Cyclopoid copepod counts for South Pit Lake from May 2000 through January 2003.

Rotifers

Figure 91 shows the rotifer dynamics from February 2001 through December 2002. Several species of rotifers were observed in SPL during the 2001-2003 study period. *Brachionus* spp. were the dominant species in winter 2001 and 2002 and *Lecane* spp. was dominant in April and May 2001 only. Counts were not conducted in 2000, but the presence of *Brachionus* spp. was noted.

Figure 92 shows the *Branchionus* spp. counts for all life stages from January 2000 through December 2002. *Brachionus* was the dominant rotifer throughout most of the study period.

Phytoplankton-Zooplankton Dynamics

Figure 93 shows the phytoplankton-calanoid copepod dynamics from May 2000 through October 2002.

Figure 94 shows the general biotic dynamics for SPL from May 2000 through October 2002.

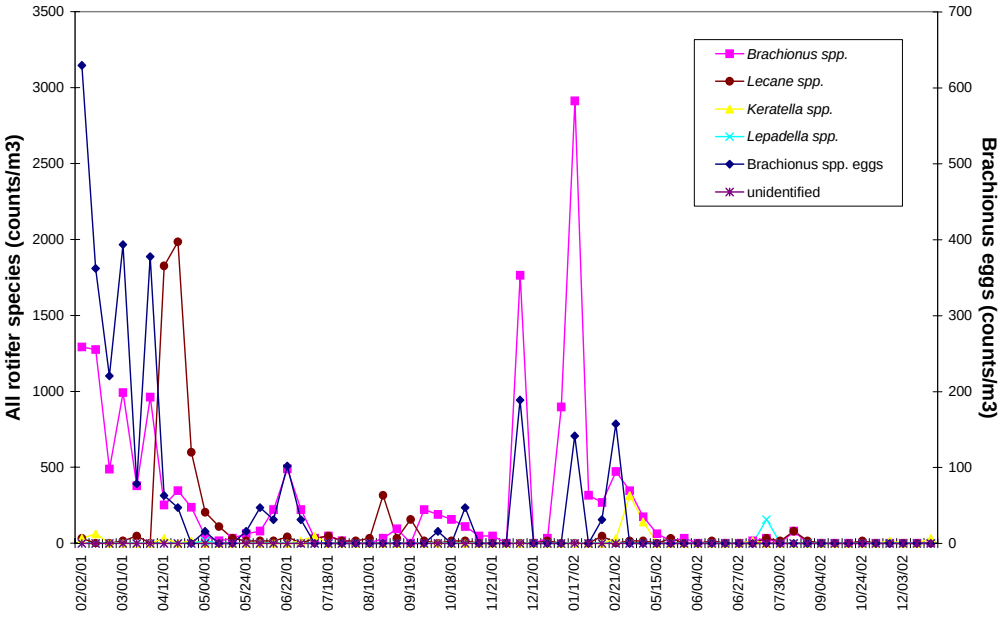

Figure 91. Rotifer counts for South Pit Lake from February 2001 through December 2002.

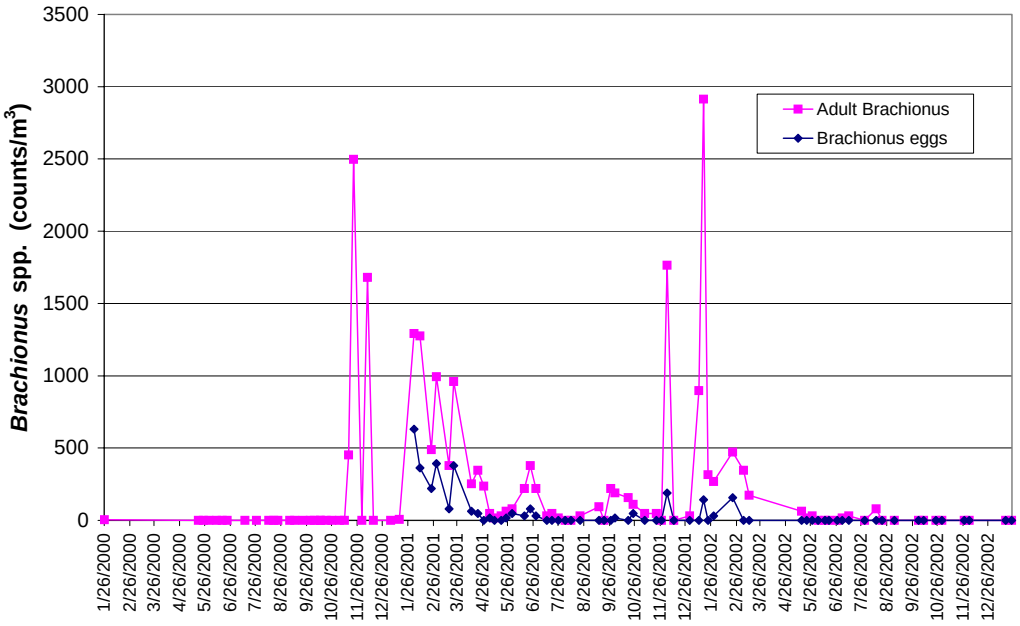

Figure 92. *Brachionus* spp. counts for South Pit Lake from January 2000 through December 2002.

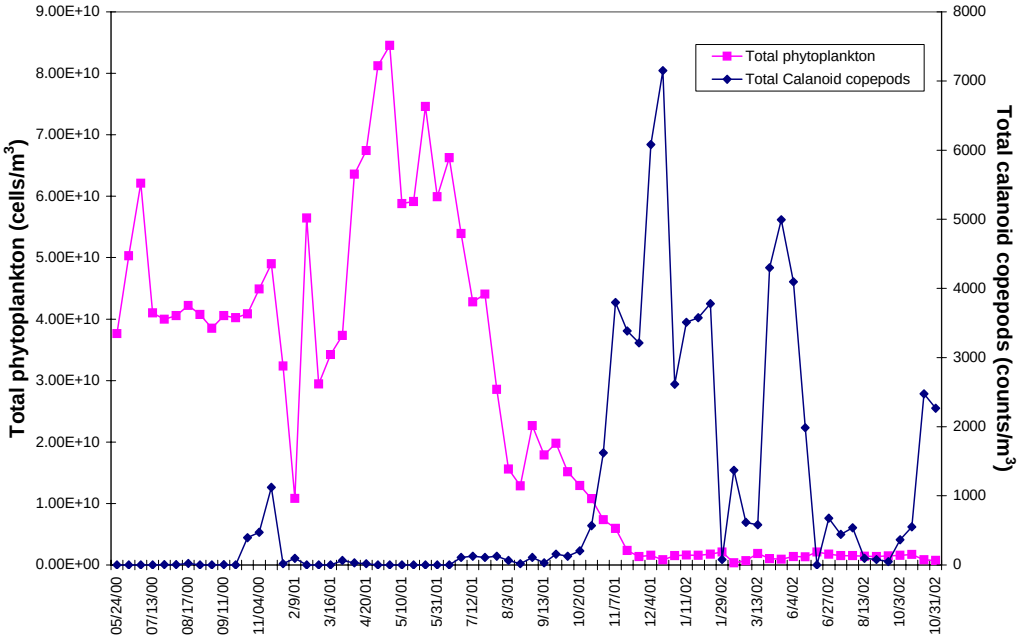

Figure 93. Copepod phytoplankton dynamics for South Pit Lake from May 2000 through October 2002.

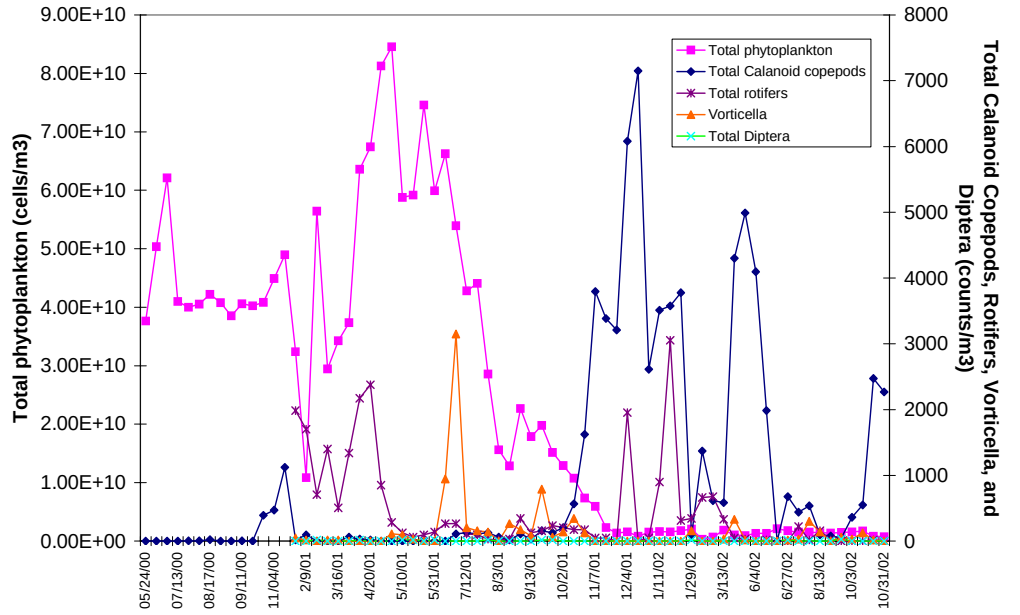

Figure 94. Biotic dynamics for South Pit Lake from May 2000 through October 2002.

CHAPTER IV

CONCLUSIONS

Physical

The physical structure of SPL was resolved with continuous thermistor and meteorological data as well as weekly vertical water column profiles of temperature and conductivity. Heat content, modified Schmidt stability (S), Lake Number (LN), Wedderburn number (W), and seiche dynamics analyses were used to determine the lake's response to physical forcing, bathymetric effects on lake stability, and to determine the role of the physical limnology on chemical stability in light of biological processes. Heat content analysis showed that nearly 50% of the heat was retained within the lake during the characteristic cooling period. S showed that the lake was prone to mixing during the coolest part of the year. LN and W results showed that, although the lake was prone to mixing during the winter of 2001, the wind field was not conducive for mixing. However, in 2002 the wind was conducive for mixing and did result in steady erosion of the monimolimnion as predicted by W but spring heating ceased further mixolimnetic deepening. Modeling results of LN showed that the lake would require a daily average wind speed of 14 mph to mix the lake completely during the winter. Seiche dynamics showed that the lake was prone to basin scale motions despite its small size. Displacement analysis showed that wind events could induce an isotherm tilt of nearly 0.6 m at mid lake depth. Power spectral density analysis of displacement data showed that the basin resonated at several frequencies and that lake bathymetry may have induced differences in basin resonance between the east and west ends of the lake.

To date, pit lake bathymetry and hence the physical structure have been determined by mining economics and not final pit lake stability.

Importance of Bathymetry on Meromixis

Results of the physical structure analyses indicated that the lake orientation toward prevailing winds and the unique bathymetry may have played a significant role in the onset and persistence of meromixis. As pointed out by Walker and Likens (1975) meromictic lakes generally have a similar morphometry, that is they have a small surface area relative to their deep depth. Findenegg (1935), Hutchinson (1937), and Walker (1974) postulated that lakes that did not present a salinity stratification but were meromictic must have been stabilized by an as yet undetermined morphometric or climatic mechanism. A limited review of the literature on meromictic lakes potentially reveals such specific bathymetric lake features. Appendix A is a compilation of all available bathymetric maps of meromictic lakes reported in the journal *Limnology and Oceanography* from volumes 1-43. Most of these studies dealt with subjects other than stability against wind mixing, so the wind fields and climate conditions of each of these lakes was unknown. Generally, the following bathymetric features were observed:

- lake shapes were either exceptionally circular or exceptionally linear
- most of the lakes had one side which had an extended slope compared to the other sides, and/or lengthy and extensive underwater shallow regions or ledges adjacent and connected to deeper bowl shaped regions.

Fluid dynamics within exceptionally linear or circular forms may play a role in facilitation of meromixis. This study showed that, if oriented along a north-south axis, South Pit Lake (a relatively linear form) would have required a daily average wind speed of 1.8 m/s (7% of the total wind field) rather than 1.3 m/s (70% of the wind field). This finding indicated that linear pit lakes, if oriented perpendicular to the prevailing wind field, may allow for exceptional stability and increased meromictic potential by decreasing fetch length.

Fricker and Nepf (2000), using a 2-D numerical model, showed that changes in basin shape (from rectangular to parabolic), mixed layer depth, and pycnocline height

significantly affected seiche structure and velocities at the sediment water interface. They showed that, under a consistent density profile, a transition from a rectangular to a parabolic shape induced changes in bed velocities from a midlake maximum velocity into two dual peaked maxima away from the midlake maxima. This finding showed that basin shape may help dampen internal seiche motions. They also showed that as the pycnocline thickened in a parabolic-shaped basin, bed velocities at midlake dropped to zero and the midlake location was eventually cut off from all seiche motions. Such a mechanism may have contributed to stagnation within the bowl-shaped deep portion of South Pit Lake. In a laboratory study, Wake et al. (2005) showed that in a rotating (Kelvin wave) circular basin ~15% of the wave energy was dissipated as frictional losses along the basin boundary. Energy loss increased to 55% with introduction of a radially protruding bathymetric cape feature[1] and ~60% to ~75% with introduction of bathymetric ridges of increasing heights. It was postulated that energy was converted to the creation an eddy field by the cape feature and offshore flow by the bathymetric ridges. South Pit Lake not only had several radially protruding cape features (a backfill pile in the northeast corner, a solid rock face on the south edge, and along the western edge) but also had two ridge features as well (on the north edge and the largest feature which separated the deep basin from the slowly sloping eastern edge).

Much of the study concerning the bathymetric effects (slopes and ledges) on mixing was initiated in oceanography and began mostly with observational changes in temperatures along slopes (Lee, 1961), theoretical exercises (Wunsch, 1968), and laboratory studies (e.g. Cacchione and Wunsch, 1974). Until recently, few studies in limnology had focused on the effects of those specific bathymetric features on mixing processes in lakes (e.g. Thorpe et al. 1972, Eriksen, 1982, Boegman et. al 2005) and possibly just one example in pit lakes (Boerher and Stevens, 2005). The most salient

[1] Geographical landform surrounded by water on 3 sides which is known to effect currents

point about bathymetric features on mixing in lakes is that, depending upon the bed slope angle and the incident angle of an internal seiche (ray angle), energy within internal waves can either dissipate upon contact of the slope, create secondary waves which break in the field of the primary wave (upslope), or propagate downslope, potentially creating offslope turbulence (Thorpe, 1998). Boegman et al (2005) showed that 10%-75% of the incident wave energy along a sloping boundary was dissipated through wave breaking (spilling, plunging, collapsing, and Kelvin-Helmholtz breakers) with the remaining energy being reflected in a long wave. This is important to manmade pit lakes because if the bathymetry is able to facilitate energy dissipation within the upper water and along the vertical boundary, the lower water remains relatively stagnant and potentially becomes meromictic.

One additional contribution to "natural" meromictic lake stability is the influence of the surrounding topography on lake sheltering or fetch disruption. Fundamentally, anything that decreases the destabilizing potential of wind on lakes increases the potential for permanent stabilization. Regarding pit lakes, steep sided pit walls should serve to protect wind impacts until the lake level reaches a critical point after which wind impacts should be of some significance. The wind field of the other pit lake on the Ridgeway property showed a cyclonic pattern with decreased wind speeds compared to South Pit Lake. That lake had steep walls that extended nearly 30-50 m above the lake surface. MacIntyre and Melack (1982) postulated such a sheltering mechanism in a crater lake that had steep sided walls, which extended 30-115 m above the lake surface. Since pit lakes are manmade, it seems necessary to plan the location of post mining topography and forested buffer zones during active mining so buffer zones will have matured in time to act as wind buffers.

It should be made clear that bathymetry alone is generally not the sole mechanism for meromixis but is often the most overlooked mechanism, especially in pit lakes. This study showed that bathymetric features may play a significant role in pit lake stability and

since these lakes are manmade, much thought should go into designing bathymetries, which facilitate energy dissipation within the upper lake strata.

Chemical

The chemical dynamics within South Pit Lake were determined by weekly profiles of conductivity, redox, dissolved oxygen, pH and phytoplankton, quarterly vertical chemistry profiles, and an understanding of the stochastic events within the watershed (precipitation and lake filling events). Specific conductance and dissolved oxygen trends departed from a completely mixed, homogenous condition in the winter of 2000 to a partitioned, heterogeneous condition in the spring of 2001 through the end of the study. This departure marked the onset of meromixis and coincided with a large phytoplankton bloom. Since phytoplankton biomass never approached the spring 2001 event, chemical fluxes, biological processes, and physical forcing maintained meromixis after the original event. Elemental trends showed that all concentrations decreased in the mixolimnion and concomitantly increased in the monimolimnion. Trends for barium showed that this element most likely cycled between the sediment and water column as a coprecipitate on manganese hydroxides and showed that sediment flux contributed to bottom water density. PHREEQC results showed that iron and manganese cycles were constant and may have kept heavy metals mobilization in check since oxides of these elements are known to readily coprecipitate heavy metals.

One of the most important aspects of this lake was that it was within the carbonate buffer system. Kennecott implemented a liming scheme once the lake started filling with water. Lime was added to maintain pH and alkalinity. Eventually the lake was neutralized to the point where it was in equilibrium with the atmosphere and was maintaining alkalinity and pH by the carbonate system (~1999). Liming was important because it helped facilitate meromixis by allowing elemental displacement events to occur, such as photosynthetic calcite precipitation, and iron and manganese oxidation and

precipitation reactions. In addition, mixolimnetic/monimolimnetic partitioning may have been dependent upon the interplay between iron, manganese, calcium, sulfate, and carbonate cycles within the monimolimnion. Typically these cycles do not occur in pit lakes because these species and cycles do not occur within acidic environments. For example, iron speciation is dependent upon pH not oxygen concentration and the carbonate system does not play a significant role in pH regulation and calcite formation below pH ~6.4. Furthermore oxidation and coprecipitation of heavy metals on iron and manganese (oxy)hydroxides occurs at circumneutral pH. Basic amendments to pit lakes are typically not the preferred method of neutralization due to immediate costs but this study shows that, in the long run, it may be significantly cheaper and more effective.

Meromictic lakes are usually stabilized by dissolved solutes within the monimolimnion. South Pit Lake was meromictic after the spring of 2001 and it seems that meromixis was caused by a biogenic event. During the phytoplankton bloom of 2001, pH decreased by ~1 pH unit. The following exercise is meant to quantify the events of 2001 surrounding the biogenic meromixis and to show the importance of the plankton amendment to monimolimnetic pH trends and ultimately, chemical stability.

Simplifying assumptions for Visual MINTEQ input:

- Carbonate system dominated the chemistry at the bottom of the lake (CO_2 and CO_3^{2-} were used as input variables; initial $[CO_3^{2-}] = 0$mg/L)
- Any CO_2 released as a result of respiration affected the carbonate system in the bottom of the lake
- Through the respiration equation, $CH_2O + O_2 \leftrightarrow CO_2 + H_2O$, one mole of organic carbon generated one mole of gaseous inorganic carbon
- MINTEQ results showed that a decrease in pH from 6.998 to 5.929 required an increase in CO_2 from $3.162E^{-7}$ atm to $7.94E^{-5}$ atm or an increase of 250 mol inorganic carbon.

Assumptions regarding carbon amendment to hypolimnion:

- *Ankistrodesmus* dominated the phytoplankton bloom
- All *Ankistrodesmus* cells died and sedimented to the lake bottom by the end of 2001
- Organic carbon from *Ankistrodesmus* was available to benthic bacteria and was the sole source of carbon to benthic bacteria
- Carbon content (C, pg) was estimated from cell volume (V, um^3) by the following equation:

  $\ln(C) = -1.952 + 0.996 \ln(V)$ (Rocha and Duncan, 1985)

- Estimates of *Ankistrodesmus falcatus* cell volumes range from 26-30um^3/cell (Reynolds, 1984)
- Therefore, organic carbon per *Ankistrodesmus* cell: 3.6439pg C/cell
- Highest cell counts in 2001 (5-4-01): $8.46E^{10}$ cells/m^3
- Sampled volume of lake on 5-4-01: $1.23E^6m^3$
- Carbon amendment to hypolimnion: $3.80E^5$g

Final analysis:

- pH decreased from ~7.00 to 6.00 so ~250 mol inorganic carbon were generated from respiration
- 250 mol inorganic carbon resulted from 250 mol organic carbon respired
- 250 mol organic carbon x 12.011g/mol org C = 3,003g C

Therefore, $3E^3$g C out of a possible pool of $3.8E^5$g C or 0.8% was utilized by the benthic bacteria. Clearly, a large portion of organic carbon was added to the lake bottom sediments, was not respired to inorganic carbon in 2001, and remained as a carbon pool throughout the rest of the study period. One important future study would be to analyze

the bottom sediment for carbon content and to observe the sediments for signs of laminations, especially at the depth of the 2001 sedimentation.

Although sulfate (~45%) and calcium (~32%) dominated the chemical equivalents within this lake, PHREEQC results showed that gypsum precipitation was not likely. However, if gypsum precipitation was unlikely, why was sulfate partitioned between the mixolimnion and monimolimnion and not homogenous within the water column? The answer to this question was important because of the stabilizing contribution of sulfur species to the monimolimnion. Two possible mechanisms could have contributed to the sulfate heterogeneity, oxidation of reduced sulfur species at the oxycline and/or direct precipitation of gypsum by algae. One drawback to this study was the limitation of the general chemistry analyses and lack of sediment chamber studies. By analyzing sulfate as the only sulfur species and by not analyzing water column sedimentation, sulfur dynamics were limited to conjecture based upon periodic discrete meter water column chemistry analyses and weekly conductivity trends. As shown by the MINTEQ results, FeS (s) would have formed within the monimolimnion and such a precipitate was observed on the white thermistor rope. Since this lake has not mixed and since reduced sulfur species could have ascended from the sediment and would have been trapped within the monimolimnion by oxidation and precipitation reactions, a water column sulfur inhomogeneity would have occurred. In addition, dilution of the mixolimnion, with respect to sulfate, and lack of mixis would have also lead to the observed sulfur heterogeneity.

The second possible mechanism for water column sulfur inhomogeneity was the direct precipitation of gypsum by algae. Thompson and Ferris (1990) showed that *Synechococcus* sp., a unicellular coccoid cyanobacteria, was responsible for a major proportion of marl and carbonate bioherm formation in meromictic Green Lake in upstate New York. They showed that this organism was capable of biomineralizing gypsum and calcite epicellularly in a slightly alkaline environment ($7.97 \leq pH \leq 8.57$). Schultze-Lam

et al (1992) and Schultze-Lam and Beveridge (1994) showed that the *Synechococcus* sp. isolated from Green Lake had a hexagonally symmetric S layer protein matrix on the outermost surface. Those studies showed that this layer acted as a template for gypsum, calcite, celestite ($SrSO_4$), and strontianite ($SrCO_3$) formation by providing nucleation sites for mineralization. *Synechococcus* sp. has been identified in South Pit Lake since July 2001 and may have played a role in sulfur partitioning, and ultimately meromictic stability, within this lake.

The controlling mechanisms for persistent meromixis were not completely elucidated within the confines of this study. Future studies should focus solely on the dynamic interplay between the sediments, monimolimnion, and mixolimnion. The key question to be answered is how does the monimolimnion maintain its density? Is it maintained by high rates of sediment flux, precipitation reactions at the oxic/anoxic boundary, or calcite and gypsum displacement from the mixolimnion to the monimolimnion (as a result of algal photosynthesis). Future studies should follow a strict flux based approach to determine the contributions of each of the aforementioned processes to the overall stability of meromixis. Future studies should incorporate acoustic Doppler systems, turbulence meters, thermistor strings, and meteorological data to define the physical structure and physical forcing, sediment analyses, sediment chambers, and discrete meter chemistry sampling to detail the elemental cycling among the three lake compartments (sediment, monimolimnion, mixolimnion), and frequent phytoplankton and zooplankton sampling of the pelagic zone and sediment chambers as well as frequent sonde and PAR profiles to define the seasonal biological cycles and light field.

Biological

Phytoplankton

Initially, SPL was dominated by cyanobacteria. Cyanobacteria are recognized for their ability to inhabit extreme environments, fix atmospheric nitrogen, and bind and enrich soil (Graham and Wilcox, 2000), so it may be fitting that they were the first organisms to dominate SPL. Since cyanobacteria are nitrogen fixers, they may not have needed a source of nitrogen, but could have gotten trace amounts from residual ammonium based blasting material, weathering of the pit wall rock, and fine grained backfill material. Phosphorus supplements could have come from weathering processes and backfill material coupled with microscale anaerobic release at the sediment water interface. In the spring of 2000 the soil cover on the tailings mass was hydroseeded with a mixture of grass seed and nutrients. Approximately 18 cm of rain fell in June and July 2000 and washed a portion of the nutrients into the netted pond (the collection basin for tailings surface runoff). In late July 2000, $2.84E^5$ m^3 of water (3/4 of the total volume of the netted pond) was released to SPL. A slight increase in *Ankistrodesmus* spp coincided with the netted pond release so that water may have carried nutrients and algae to SPL or could have just carried nutrients, which stimulated that species in the lake. Cyanobacteria still dominated the water column through January 2001.

Since much of the material and associated nutrients that entered SPL from the netted pond was in the form of heavy sediment, most of that nutrient laden density current went to the lake bottom. SPL underwent holomixis in the winter of 2000. This process is known to fully mix the water column and redistribute nutrients and settled plankton trapped in the hypolimnion of lakes to the epilimnion. Impact of the netted pond nutrients was not seen until February 2001 when it stimulated *Ankistrodesmus* spp., which quickly became the dominant phytoplankton. The enrichment stimulated the phytoplankton from an oligotrophic condition to a eutrophic condition in the summer of 2001. Measured productivity values exceeded 1800 mg $C/m^3/d$ (results not shown) at the

peak of the bloom. Assuming Redfield's ratio of 106:16:1 (C:N:P), holomixis resulted in peak water column nitrogen and phosphorus concentrations exceeding 272 mg/L and 17 mg/L, respectively. These concentrations, multiplied out over the volume of the photic zone at that time, corresponded to $2.18x10^5$ kg N and $1.36x10^4$ kg P within the top 10 meters of water.

In December 2001 most of the Ankistrodesmus biomass died off and on January 11, 2002, diatoms dominated the phytoplankton. Phytoplankton dominance from that point on was shared between nearly all families and phytoplankton numbers rarely exceeded $1x10^6$ cells/L. *Ankistrodesmus* spp. was replaced as the dominant chlorophycean by *Chlorella ellipsoidea*.

Successional pattern for the phytoplankton was not much different than patterns observed in newly filled reservoirs (Baxter, 1985). The dynamics, however, were slightly different. In newly filled reservoirs much of the area being submerged is usually vegetated and upon degradation of that plant material, nutrients are released into the water column. Massive loads of nutrients from the decaying plant material often results in opportunistic species of phytoplankton taking advantage of the temporary and readily available nutrients. These opportunists are termed r-selected species and can grow exponentially while optimal conditions permit. Die off of r-selected species may be just as rapid when conditions become unfavorable. This phenomenon is called trophic upsurgence. SPL had little vegetation, so it did not undergo typical trophic upsurgence. Instead of decayed vegetation, a significant nutrient load entered the water column as a result of the holomictic reintroduction of lake bottom sediments. Those sediments were placed there by the previous year's density currents. The r-selected species was *Ankistrodesmus* spp. and underwent massive bloom and massive die off. It is doubtful that calanoid copepod grazing was responsible for the decline in *Ankistrodesmus* spp. because the number of individuals and potential clearing rates for the calanoid copepods were too small. *Ankistrodesmus falcatus* had a greatest axial linear dimension (GALD)

of 35µm (Reynolds, 1984) and the range of GALD feeding size for *Diaptomus oregonensis* was 2.5µm to 30µm (Reynolds, 1984). This indicated that *Ankistrodesmus* spp. could have been prey for the SPL *Diaptomus* spp., but the large size of the phytoplankton would have decreased the clearing rate to the lower end of the range (~2.4mL/d) (Reynolds, 1984). At peak calanoid numbers (~7800 calanoids/m^3), with a clearing rate of 2.4mL/d, a total of 0.01872 m^3/d would have been cleared. The die off phase of trophic upsurgence is most likely due to nutrient utilization.

Phytoplankton species richness increased from 2000 and peaked in summer 2001 and 2002. Similar to eutrophic plankton dynamics, SPL species richness was lowest during the chlorophycean bloom in 2000 and higher during lower biomass periods. Average species richness from March 2000 through March 2001 was 3.26, from March 2001 through March 2002 was 12.09, and from March 2002 through October 2002 was 12.69.

Similar findings have been reported for other pit lakes. Nixdorf et al. (1998) observed highest phytoplankton diversity in carbonate buffered lakes (circumneutral) when compared to iron buffered (pH<4) or aluminum buffered (pH 3.6-4.3) pit lakes. Carbonate buffered lakes were dominated by diatoms (*Asteroinella, Cyclotella*) or cryptomonads (*Cryptomonas, Rhodomonas*) and had 8-10 species. Iron buffered lakes were dominated by chrysophyceae (*Ochromonas)* and chlorophyceae (*Chlamydomonas*). No species counts were given for this lake type, but the highest biomass recorded for this study was in an iron buffered lake (>100,000 cells/mL). Aluminum buffered lakes were dominated by dinoflagellates, chrysophytes, chlorophytes, or euglenoids and species counts never exceeded 6.

Kalin et al. (2001) observed a weedy species dominance and die off about one year after filling of a circumneutral pit lake in Canada. *Dictyosphaerium*, a chlorophycean, dominated in 1997, about one year after filling commenced, and was hardly present in samples in 1998. After die off of *Dictyosphaerium* in 1998, species

richness increased and total phytoplankton density decreased. They attributed increased phytoplankton diversity and composition to improved water chemistry.

Banoub (2000) studied phytoplankton succession in a carbonate buffered gravel pit pond in Germany. The first year bloom was dominated by a cyanobacteria, *Chroococcus minimum*. The second year spring bloom was dominated by a chrysophycean (*Chromulina*) and a summer bloom of diatom (*Cyclotella*). In the third and fourth years, diatoms dominated. In the fifth year chrysomonads dominated throughout most of the year and diatoms remained a secondary species. In the sixth and seventh years diatoms dominated except in the spring of the sixth year. Banoub (2000) also found a decrease in phytoplankton counts over time and attributed the phytoplankton changes to agricultural runoff.

Zooplankton

Further evidence of the influent of nutrients and biota to SPL via the netted pond may have been the import of copepodid stage calanoid copepods to SPL. This observation stems from the appearance of the copepodid stage calanoids in August 2000 without a preceding bloom of naupliar stage calanoids. Copepods undergo 12 instars, 6 naupliar stages followed by 6 copepodid stages, the final copepodid stage being the adult, which is the only stage capable of reproduction. However, some species of copepods may aestivate in the summer as copepodid stages and reemerge in the winter. This is also a reasonable explanation but is less plausible because no copepods were counted in the spring of 2000. Copepodid counts in September 2000 exceeded 21 individuals/m^3. The nauplii bloom occurred in late September 2000, with counts exceeding 492 individuals/m^3, and was followed by a large bloom of copepodid stage calanoids in November 2000 with counts exceeding 1100 individuals/m^3. Calanoid copepod trends showed consistent periodicity in 2001 and 2002.

Cyclopoid copepods are also omnivorous, but are mostly raptorial (Thorp and Covich, 2001). These copepods were observed in SPL well before the netted pond release. Since they are raptors and mostly inhabit the littoral zones, counts may not have fully represented the total cyclopoid population. Only the pelagic zone was sampled, so these counts represented organisms found in the water column.

Rotifer species richness increased from 1 in 2000 to 4 in 2001 and 2002. The original species was *Brachionus* and subsequent species were *Keratella*, *Lecane*, and *Lepadella*. Rotifers most likely benefited from complete and incomplete digestion of algae. The largest rotifer counts were associated with copepod blooms in November 2000, December 2001, and February 2002. Observation of gut contents under the microscope showed rotifer diets also consisted of bacteria and small phytoplankton.

Biological Dynamics

In terms of the biological assemblage in South Pit Lake, mechanisms controlling pelagic biomass were the meromictic condition, the lack of a significant littoral zone, and the hydrologically closed condition (lack of influent with a watershed derived nutrient component). In lakes that mix annually, nutrients are redistributed throughout the water column each year. South Pit Lake received internal nutrients through sediment flux and boundary layer turbulence releases only. In addition, those species which required redistribution of spores which settled to the bottom of the lake were not selected for in this lake system and may have limited species richness. Kalff (2002) suggested that littoral biomass associated with rooted plants grew optimally at slopes of <~5% and Duarte and Kalff (1990) suggested rooted plants were unable to grow at slopes >15-20%. For pit lakes, these observations indicate that nutrient sources offered by decaying littoral vegetation would limit pelagic zone biomass because slopes are usually greater than 15%. Finally, South Pit Lake was essentially a closed hydrological system. Except for precipitation and runoff of its immediate watershed, the lake's hydrologic system had

controlled influent and effluent sources. Significant watershed nutrients, which a typical lake receives, were limited to periodic flushing of water through a series of wetland channels. Such controlled flushing events could be managed for timely stimulation of phytoplankton biomass in the future but indicates that this lake will most likely be ultraoligotrophic to oligotrophic for the long term.

The Future of South Pit Lake

The stability of South Pit Lake is maintained by a dynamic interplay between physical, chemical, and biological elements. At its core, the stability of meromixis is fundamentally a *chemical* stability. Therefore, understanding the dynamics of the chemical milieu in terms of the physical and biological domains is of utmost importance.

Potential Mixing Event Resulting from A Biological-Chemical Mechanism

As shown, ~98% of the lake's chemistry was dominated by the following 5 species: SO_4^{2-} (46%), Ca^{2+} (32%), Mg^{2+} (11%), Na^{+} (5%), HCO_3^{-} (4%). Changes within the existing chemical composition of South Pit Lake will ultimately change the density structure, thereby changing the lake's stability against wind mixing. Such a change could either increase or decrease the lake's resistance to mixing depending upon the processes that occur over time. As a biological-chemical example, if a significant organic load is added to the lake either in the form of massive nutrients leading to a large algal bloom and subsequent dieoff or through a large amount of stored carbon released from the constructed wetlands, anaerobic respiration processes will increase within the bottom of the lake. This may lead to sulfate reduction. Since SO_4^{2-} contributes the highest percentage of molar equivalents within this lake and the transformation of the sulfur species from a dissolved salt (SO_4^{2-}) to a gas (H_2S) will remove a portion of the chemical stability, monimolimnetic density will be compromised. At the present time, the lake's

biomass is maintained at a low carrying capacity due to the lack of nutrients that a typical lake would receive through various inputs. This is just one example of a biological-chemical mechanism that may impact meromictic stability. Many scenarios exist in terms of the dominant chemical species responsible for meromictic stability. It is therefore necessary to monitor the interplay between nutrient loads, biomass, and pit lake chemistry.

Potential Mixing Event Resulting from
A Physical-Chemical Mechanism

Stability within South Pit Lake is also threatened by physical-chemical mechanisms as well. The most likely scenario follows. Over time, depth of light penetration increased in SPL. This clearing process may have been a result of increased clarity of the mixolimnion due to increased dilution of the lake influents and chemical precipitation reactions within the mixolimnion. Increased light penetration will result in more solar energy reaching the dense monimolimnion, resulting in increased light scattering and absorption within that layer due to dissolved and particulate material (Kirk, 1994), ultimately leading to a rise in temperature within the monimolimnion. This effect has already been observed during this study (and may have been the mechanism responsible for the observed dichothermy). Since temperature and the chemical milieu (and pressure to a much lesser extent) determine the density of water, changes in either will affect the overall density. Increasing temperatures decrease water density whereas increasing solute concentrations increase water density. Once the salty layer warms to a critical point, local instabilities occur within the parcels of water and small portions of the warm salty layer rise within the water column. The warm salty parcels continue to rise until they lose heat, creating another local instability due to salinity higher up in the water column. That parcel then descends to the location of similar density. This phenomenon is known as double diffusion or salt fingering and can be observed within high-resolution

temperature data (Imboden and Wüest, 1995). If temperatures within the monimolimnion continue to increase and the solute concentrations remain the same, density and meromictic stability will decrease within the South Pit Lake monimolimnion and holomixis will most likely result.

These are two of the most likely scenarios that threaten the meromictic stability within South Pit Lake. If long-term meromixis is the goal for South Pit Lake, then further study within this lake is required.

A Modeled Mixing Event within South Pit Lake

Lake stability indices (LN, St, and W) showed that South Pit Lake is prone to mixing during the cooler months and that given a long enough duration of wind speeds in excess of the modeled critical wind speed, South Pit Lake will likely mix. In the event of a complete mixis, water quality within the lake would decrease slightly but would most likely recover. PHREEQC Interactive was used to model the results of a complete mix of the mixolimnion and monimolimnion. A summary of the results follows but the complete input and output files of the mixing scenario are presented in Appendix B.

Input data included the latest discrete meter chemistry profile results (1-12-04) along with sonde data (pH, ORP, DO, and temperature) taken at the time of the chemistry sampling event. PHREEQC Interactive allows for mixing model scenarios of two or more water sources by using separate input chemistry data and the total water volumes of each source water. Input data for this exercise was the average constituent concentration within each of the two lake layers (mixolimnion and monimolimnion) and the known percent volumes of the two layers (mixolimnion = 89.95%, monimolimnion = 10.05%). Only water column chemistry data were used to model this scenario, therefore this modeling effort does not reflect chemical additions resulting from disturbed South Pit Lake sediments.

Model results showed that pH would decrease from an average water column pH of 6.818 (mixolimnion = 7.087, monimolimnion = 6.548) to 6.773. This decrease would most likely result from monimolimnetic iron oxidation. Minerals that would theoretically precipitate as a result of the mixis (SI>1) would be $Fe(OH)_3$, goethite (FeOOH), hausmannite (MN_3O_4), jarosite-K ($KFe(SO_4)_2(OH)_6$), manganite (MnOOH), and pyrolusite (MnO_2). The significant benefit resulting from precipitation of the oxidized iron and manganese species would be that if heavy metals were mobilized as a result of lake sediment stirring, these supersaturated species would most likely act as nanoparticles and coprecipitate the metals of significant concern back to the lake bottom.

The Biogeochemistry of Pit Lakes

> *"It is well known that in aquatic ecosystems, physics plays a crucial role in controlling the biogeochemical cycles… In contrast, the influence of biogeochemical cycles on the physics of lakes has seldom attracted the attention of limnologists, in spite of the number of situations that demonstrate the importance of this influence."* D.M. Imboden (1998)

> "*In order to understand the chemistry of an aquatic habitat, the causal and reciprocal relationship between organisms and their aquatic environment must be taken into consideration*" Stumm and Morgan (1996).

In assessing mechanisms leading to meromixis, one must take a holistic approach and consider strictly physical, chemical, and biological mechanisms as well as the interactions within each of those domains as indicated by the Venn diagram in Figure 95.

Such a holistic, biogeochemical, approach is more robust and allows less bias toward one domain based upon one's personal formal training. This view is indeed the proper approach for such complex systems as pit lakes. Meromixis, especially of the biogenic type, requires assessment of all domains simultaneously and the ability to synthesize the results within the holistic viewpoint.

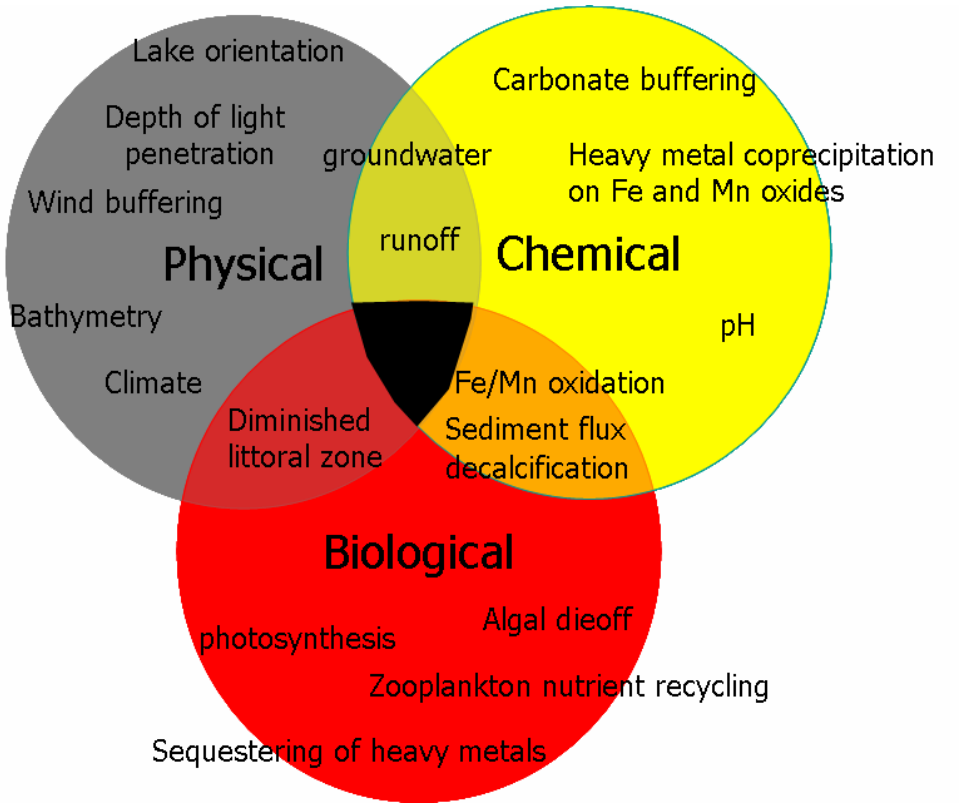

Figure 95. Venn diagram of the holistic, biogeochemical approach to pit lake studies.

Hutchinson (1948) wrote about circular causal systems in ecology: "… groups [of organisms] may be acted upon by their environment, and they may react upon it. If a set of properties in either system changes in such a way that the action of the first system on the second changes, this may cause changes in the properties of the second system which alter the mode of action of the second system on the first." This study showed, for example, that respiration of the phytoplankton biomass generated in 2001 effectively removed oxygen from the lower water and lowered the redox level. This resulted in an increase in sediment flux rates and ultimately caused the redoxcline to rise from, most likely, somewhere at or within the sediment to a point within the water column. This induced stability to the lower water and generated meromixis. Since the lake did not mix in 2001, the organisms that required seasonal mixing (for redistribution of nutrients and propagules) were no longer players within the pit lake ecosystem. So the condition

selected the organism, and the circular causal system was shown. Moreover, the complexity of the system was revealed only through the holistic approach.

This circular causal system is particularly interesting for the case of pit lake "sustainability" in terms of meromixis. At least two pit lake studies (Brugam and Stahl, 2000; Harrington, 2004) have shown that not considering the physical limnology of these lakes during remediation can lead to unintended consequences. One of the favored methods of pit lake remediation has been to add large amounts of readily available carbon sources. These organic sources range from potato peels and molasses to horse manure. The goal in this mode of remediation is to stimulate sulfate reducing bacteria (SRB). The action of the SRB would add biogenic alkalinity and decrease sulfate concentrations through sulfate reduction. It has worked well in lab scale studies but to a much lesser degree when scaled up to pit lakes. The reason for failure at the lake scale is that the physical limnology of the lake is not usually considered, more specifically, the interplay between the biological metabolism of the organic amendment, sediment flux, redoxcline location, and mixing zone depth location. More generally, the point that needs to be considered is the interaction of nutrient inputs (from all sources) and biological processing on meromictic stability. If the system is overwhelmed by nutrients, it runs the risk of chemical destabilization if the nutrient addition stimulates the benthic bacteria, which then induces higher rates of sediment flux, which then causes the chemocline to rise in the water column due to diffusion. If the chemocline elevation rises to a point within the mixed layer and the rate of sediment flux persists, the density difference between the mixolimnion and monimolimnion will decrease and so will the meromictic stability. If the goal is to maximize the density difference between upper and lower layers of the lake, anything that causes the upper water density to increase will go against the stated goal. Therefore, the location of the redoxcline in terms of the mixing zone is of considerable importance for monitoring meromixis in pit lakes.

On the Restoration of Current Pit Lakes and an Outlook on Future Pit Lakes

Pit lakes can be less of an environmental concern. Based upon this study, the following chronology seems to be appropriate for development of new hard rock mining sites.

Chronology of Pit Lake Sustainability

- Pit lake bathymetry
  - Optimally shape pit lake bathymetry to diminish wind driven mixing
    - Consider fetch orientation regarding prevailing winds
    - Keep fetch length along the prevailing wind direction to a minimum
    - Design wave breaking features such as ledges, sloping topography, nd capes
    - Small surface area. Possibly implement a series of small, ydrologically disconnected pit lakes (no underground conduits from one lake to the other) if a large ore body is present
  - Surrounding watershed topography should decrease wind field
    - Create topographic highs to decrease predominant winds
    - Plant vegetated buffers early on in the reclamation phase
- Pit lake watershed should be vegetated to avoid destabilization of the eveloping “orthograde” density gradient
  - May be optimized with wetlands for sediment retention
  - Wetlands may offer some future “water purification” for increased ctogenic meromictic stability
  - Wetlands may be a future source of allochthonous organic material
- Bring water column into carbonate system
  - Use lime during summer
  - Use carbonate during winter (due to solubility differences)
    - Must be dilute concentrations and treat from “top-down”

- Inoculate/stimulate algal community
    - Being careful not to cause permanent eutrophication. A stochiometric approach is necessary
    - Target iron, manganese, calcite, and gypsum oxidizing organisms
- Monitor redoxcline location to maintain mixolimnetic/monimolimnetic boundary
- Monitor and manage freshwater inputs to maintain low mixolimnetic density

This viewpoint can be applied to existing pit lakes as well. In filled lakes, such an approach would require underwater blasting of the optimum bathymetry and/or excavation of new areas in an effort to put cape and sloping features in place. It would also require a different approach in the mode of base element additions. These additions must be added so treatment will occur in a top-down fashion. That is, base additions in mine sites are often added as high density slurries. If the base addition is added such that the amendment has a density that is slightly higher than the lake water density, the lake will have a better chance of equilibrating with the atmosphere sooner than if treated from the bottom-up. In addition, precipitation reactions in the upper water will promote a mechanism for deriving a density difference between the upper and lower water.

A [Brief] Treatise on Limnology

A comprehensive viewpoint is not only lacking for pit lake studies but is mostly absent from limnology as a discipline. Limnology, in general, is the study of lakes and streams. More specifically, limnology is the study of the physics, chemistry, and biology of natural waters. Too often the lines between the three disciplines of limnology are well defined with little overlap among the disciplines. This situation, as pointed out by Hairston (1990) with reference to plankton biologists, leads to specialization within disciplines to the point where communication between the disciplines is difficult, eventually leading to professional isolation. Such isolation specialization in limnology is

tragic because the reality of natural systems is that they are highly complex and understanding of that complexity can only be obtained if the interplay between all three disciplines is elucidated. As is often the case, natural limnological systems are studied by teams of specialized researchers who, as a whole, cover all three disciplines. However, this approach does not always suffice. It is incumbent upon the individual, despite one's formal training and perceived educational shortcomings and/or phobias, to grapple with the interplay between the disciplines to achieve *system* level understanding. Anything short of this grueling task is myopic and will often lead dangerously toward conjecture and speculation or even worse, complacency. If limnologists are to be looked upon to answer important questions about freshwater issues, then it is necessary for limnologists to have the comprehensive understanding required to develop the necessary predictive tools. Such capability is only approached through interdisciplinary understanding.

APPENDICES

Appendix A

Bathymetric Maps Of All Meromictic Lakes in *Limnology and Oceanography* (v. 1-43)

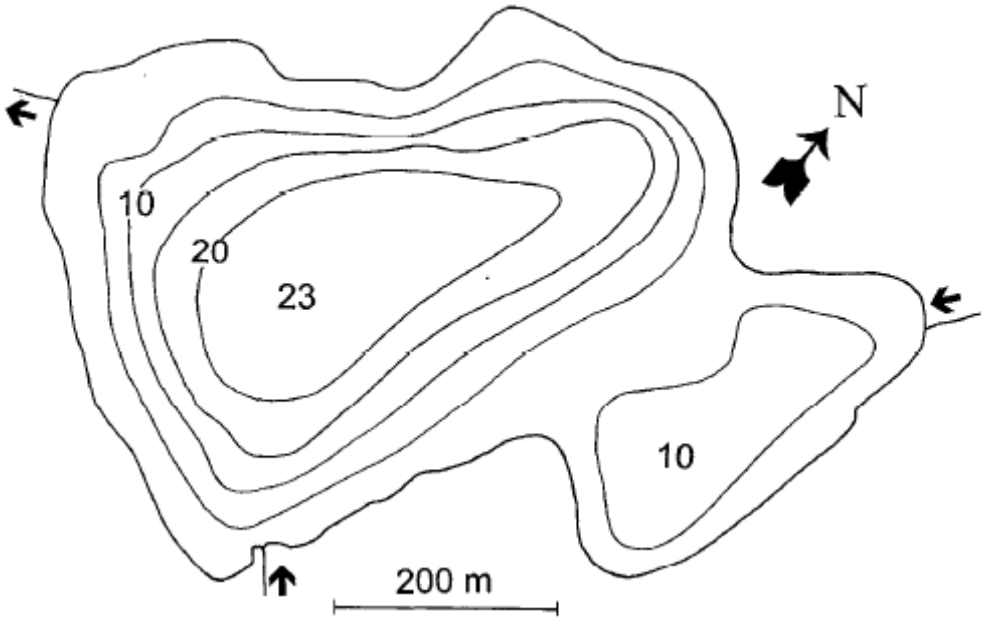

(from Hongve, 1997)

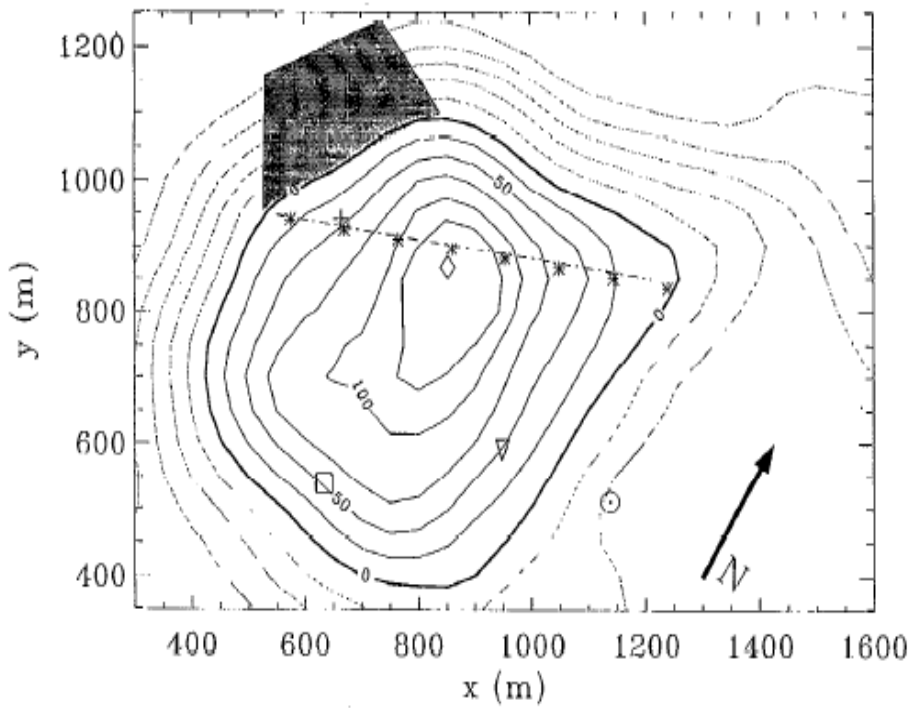

(from Stevens and Lawrence, 1998)

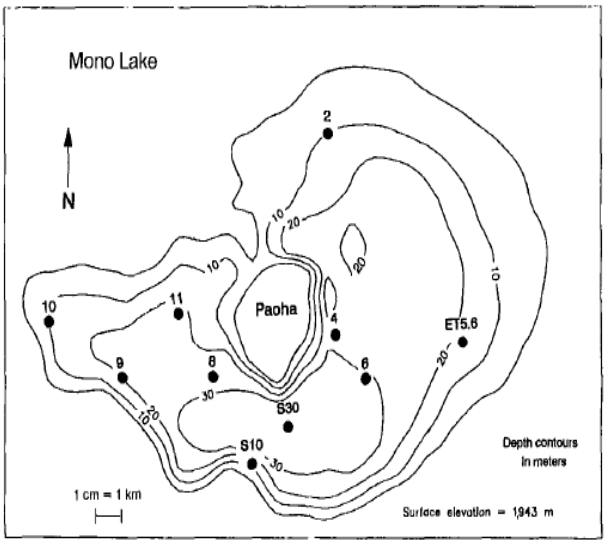

(from Jellison and Melack, 1993)

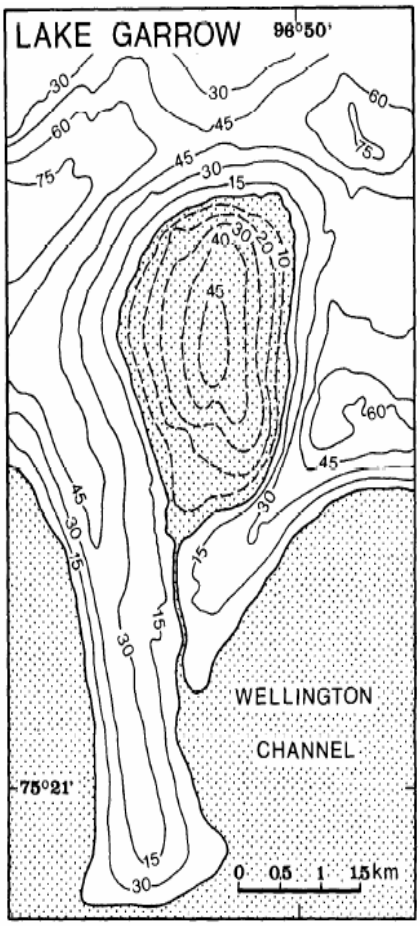

(from Page et al., 1984)

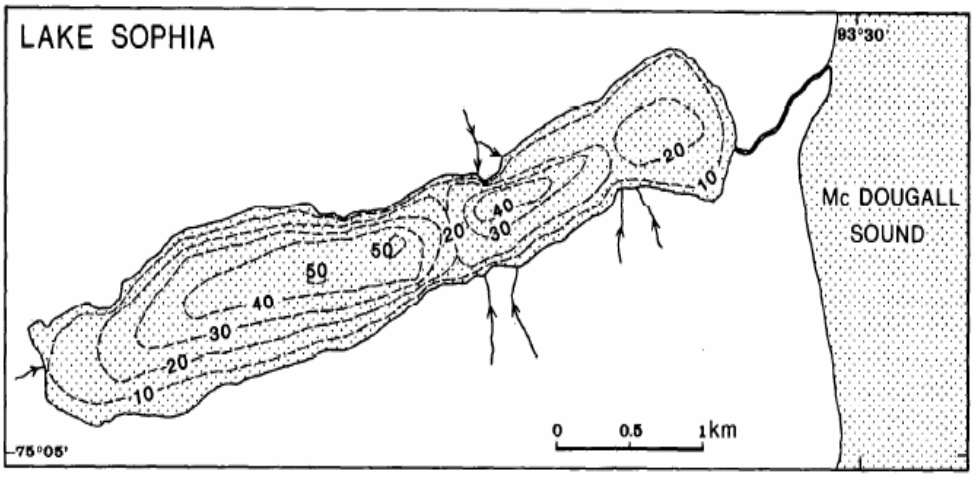

(from Page et al., 1984)

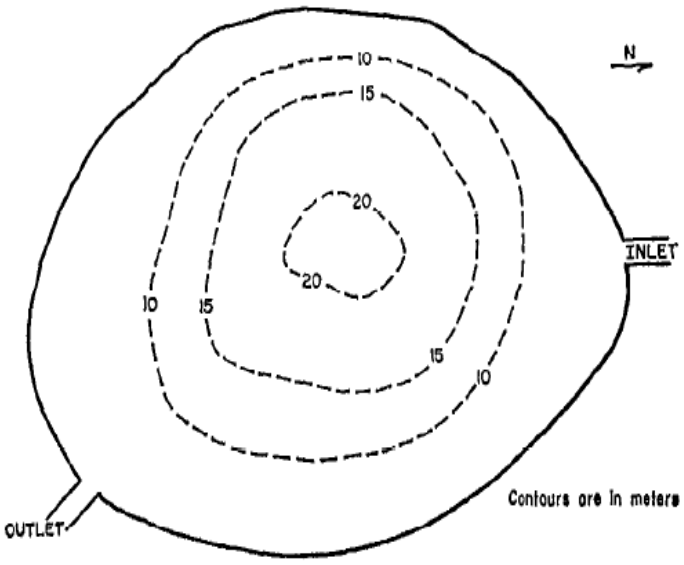

(from Weimer and Lee, 1973)

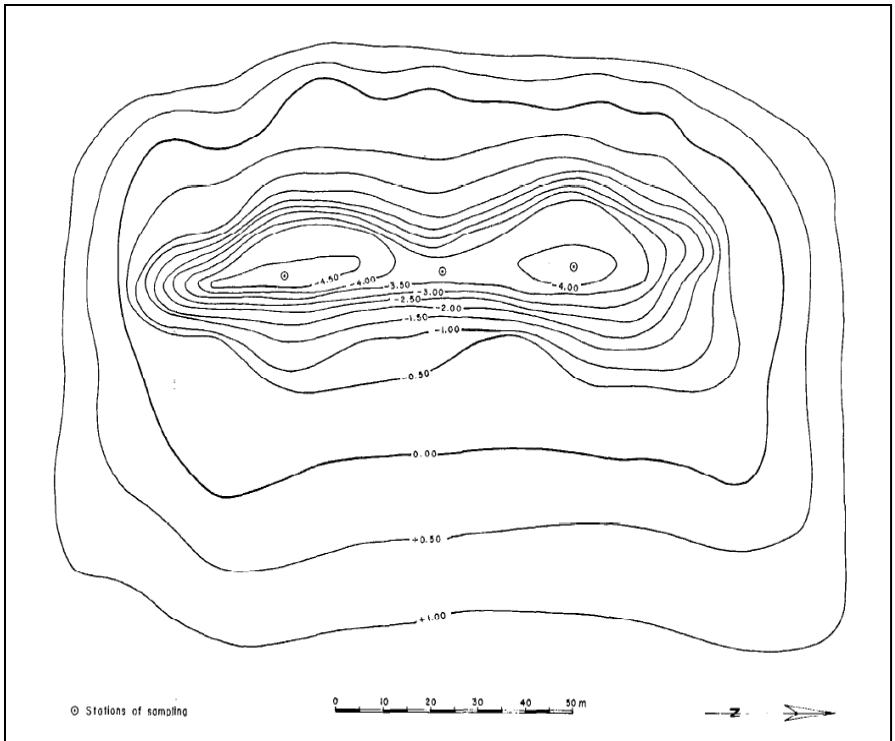

(from Eckstein, 1970)

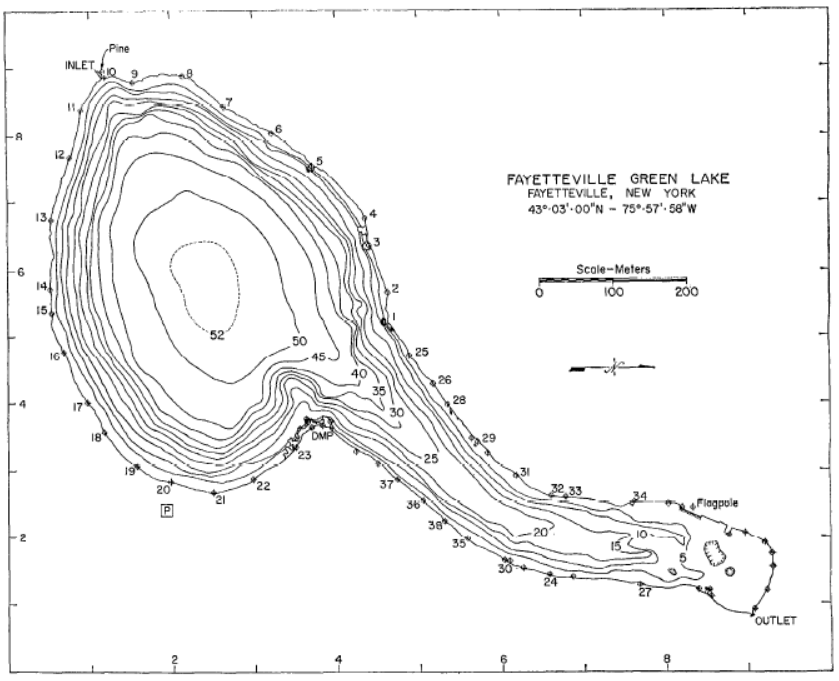

(from Brunskill and Ludlam, 1969)

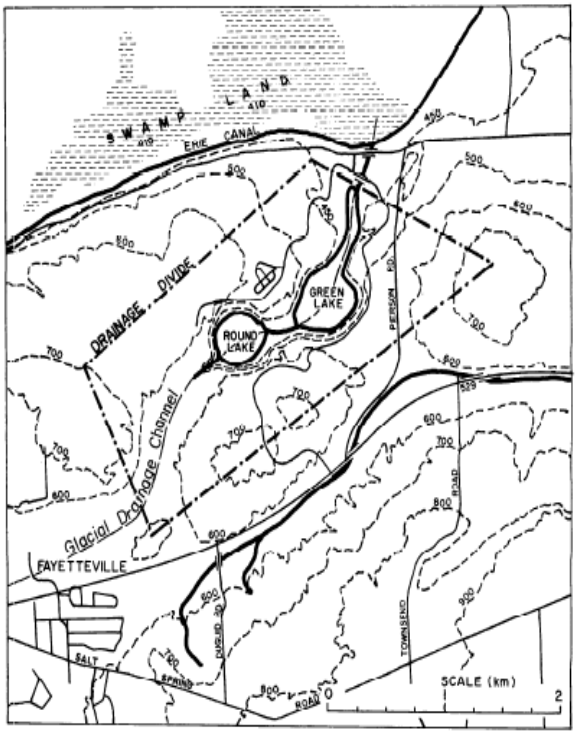

(from Takahashi et al., 1968)

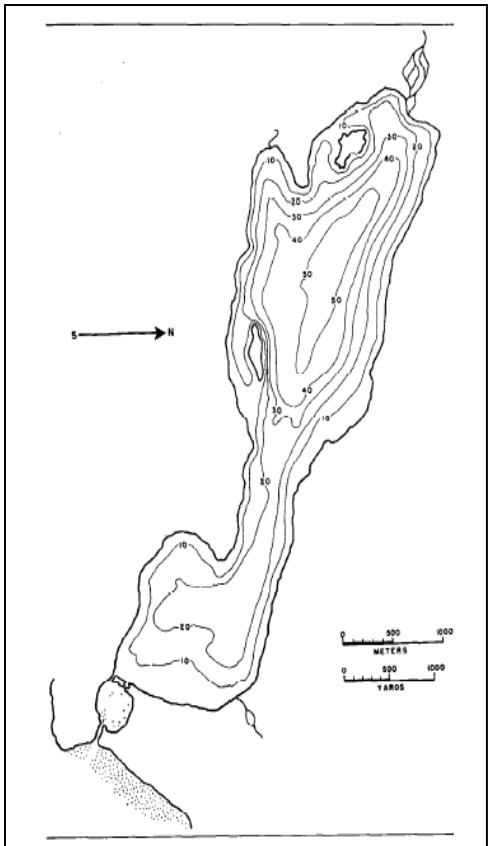

(from Carter, 1965)

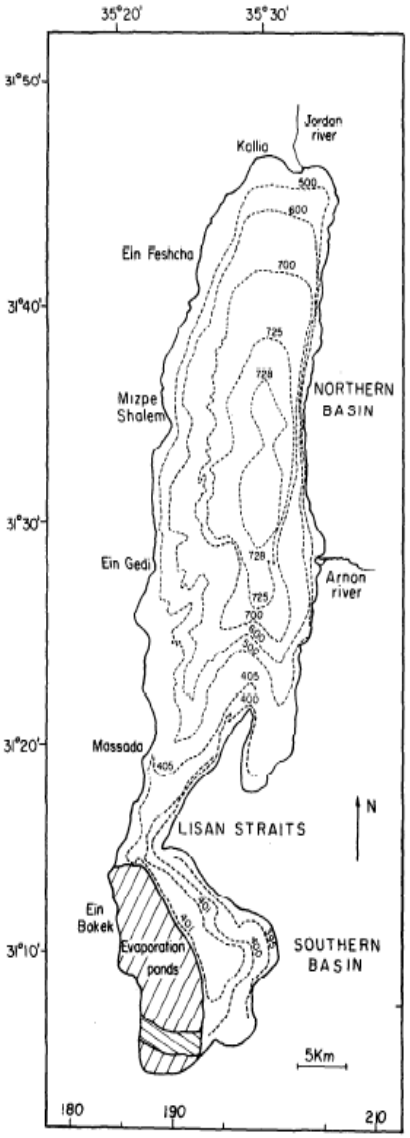

(from Steinhorn, 1985)

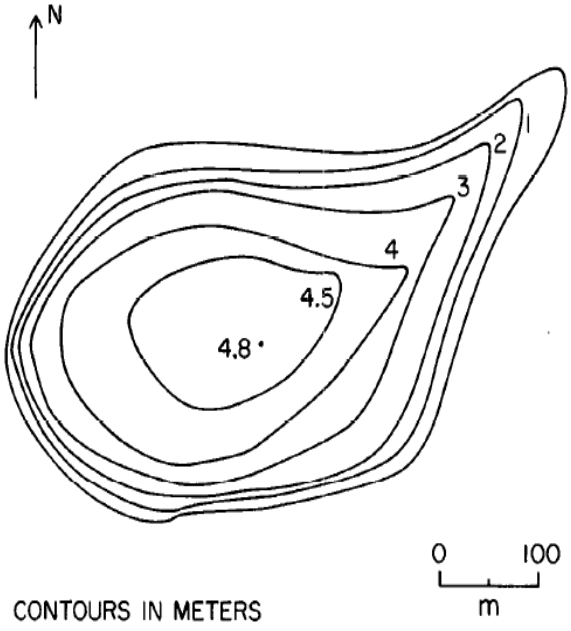

(from MacIntyre and Melack, 1982)

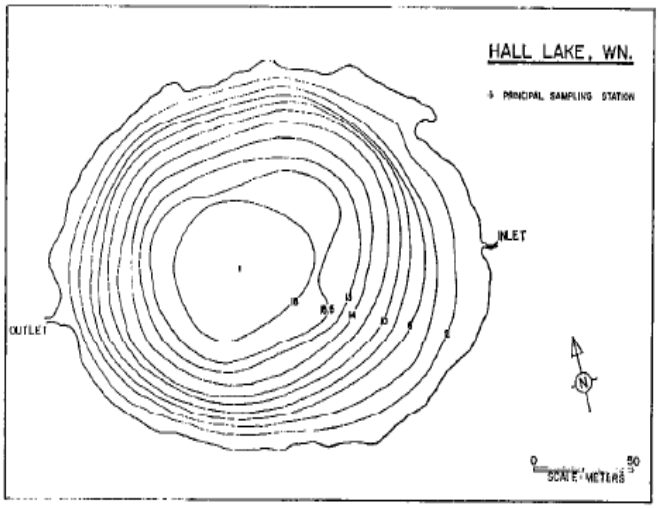

(from Culver, 1977)

Appendix B

Lake mixing event simulation using PHREEQC2

```
           Input file: G:\lake mix exercise (1-12-04 chem).pqi
  Output file: G:\lake mix exercise (1-12-04 chem).pqo
Database file: C:\Program Files\USGS\Phreeqc Interactive
2.8\phreeqc.dat

------------------
Reading data base.
------------------

      SOLUTION_MASTER_SPECIES
      SOLUTION_SPECIES
      PHASES
      EXCHANGE_MASTER_SPECIES
      EXCHANGE_SPECIES
      SURFACE_MASTER_SPECIES
      SURFACE_SPECIES
      RATES
      END
-----------------------------------
Reading input data for simulation 1.
-----------------------------------

      DATABASE C:\Program Files\USGS\Phreeqc Interactive
2.8\phreeqc.dat
      SOLUTION 1 upper water
          temp      9.35
          pH        7.087
          pe        6.104
          redox     pe
          units     mg/l
          density   1
          N(-3)     0.022
          Ca        306
          Cl        6.28
          Pb        0.0032
          Mg        55.6
          Mn        0.858
          N(5)      0.1364
          P         0.013
          Si        0.72
          Na        46.8
          S(6)      994
          O(0)      8.5
          Alkalinity 55.64
          water    1 # kg
      SOLUTION 2 lower water
          temp      11.96
          pH        6.548
          pe        -0.4506
          redox     pe
          units     mg/l
          density   1
          O(0)      0.68
          Alkalinity 230
          N(-3)     1.1933
          Ca        546.67
          Cl        8.033
```

```
          Fe        28.57
          Pb        0.01
          Mg        112.33
          Mn        25
          P         0.104
          K         27.67
          Si        3.63
          Na        72
          S(6)      1733.33
          water    1 # kg
      MIX 1
          1    0.8995
          2    0.1005
-----------------------------------------
Beginning of initial solution calculations.
-----------------------------------------

Initial solution 1.     upper water

-----------------------------Solution composition----------------------

      Elements           Molality       Moles

      Alkalinity       1.113e-003  1.113e-003
      Ca               7.646e-003  7.646e-003
      Cl               1.774e-004  1.774e-004
      Mg               2.290e-003  2.290e-003
      Mn               1.564e-005  1.564e-005
      N(-3)            1.573e-006  1.573e-006
      N(5)             9.753e-006  9.753e-006
      Na               2.039e-003  2.039e-003
      O(0)             5.320e-004  5.320e-004
      P                4.203e-007  4.203e-007
      Pb               1.547e-008  1.547e-008
      S(6)             1.036e-002  1.036e-002
      Si               1.200e-005  1.200e-005

----------------------------Description of solution--------------------

                                     pH  =   7.087
                                     pe  =   6.104
                        Activity of water  =   1.000
                           Ionic strength  =  3.155e-002
                       Mass of water (kg)  =  1.000e+000
                   Total carbon (mol/kg)  =  1.330e-003
                      Total CO2 (mol/kg)  =  1.330e-003
                     Temperature (deg C)  =   9.350
                  Electrical balance (eq)  = -8.188e-005
 Percent error, 100*(Cat-|An|)/(Cat+|An|)  =  -0.25
                                Iterations  =   9
                                   Total H  = 1.110136e+002
                                   Total O  = 5.555205e+001

---------------------------------Redox couples-------------------------

      Redox couple             pe  Eh (volts)
```

```
      N(-3)/N(5)           7.0775      0.3967
      O(-2)/O(0)          14.9084      0.8356

----------------------------Distribution of species-------------------

                                                      Log       Log
Log
      Species            Molality    Activity  Molality  Activity
Gamma

      H+               9.355e-008  8.185e-008    -7.029    -7.087    -
0.058
      OH-              3.993e-008  3.372e-008    -7.399    -7.472    -
0.073
      H2O              5.551e+001  9.996e-001     1.744    -0.000
0.000
C(4)           1.330e-003
      HCO3-            1.066e-003  9.134e-004    -2.972    -3.039    -
0.067
      CO2              2.190e-004  2.206e-004    -3.660    -3.656
0.003
      CaHCO3+          2.907e-005  2.490e-005    -4.537    -4.604    -
0.067
      MgHCO3+          1.122e-005  9.542e-006    -4.950    -5.020    -
0.070
      CaCO3            1.438e-006  1.449e-006    -5.842    -5.839
0.003
      NaHCO3           8.698e-007  8.761e-007    -6.061    -6.057
0.003
      CO3-2            6.616e-007  3.561e-007    -6.179    -6.448    -
0.269
      MnHCO3+          6.040e-007  5.138e-007    -6.219    -6.289    -
0.070
      MgCO3            2.471e-007  2.489e-007    -6.607    -6.604
0.003
      MnCO3            1.772e-007  1.785e-007    -6.751    -6.748
0.003
      PbCO3            8.212e-009  8.272e-009    -8.086    -8.082
0.003
      NaCO3-           5.780e-009  4.916e-009    -8.238    -8.308    -
0.070
      PbHCO3+          1.140e-009  9.698e-010    -8.943    -9.013    -
0.070
      Pb(CO3)2-2       1.413e-011  7.398e-012   -10.850   -11.131    -
0.281
Ca             7.646e-003
      Ca+2             5.548e-003  2.989e-003    -2.256    -2.525    -
0.269
      CaSO4            2.067e-003  2.082e-003    -2.685    -2.681
0.003
      CaHCO3+          2.907e-005  2.490e-005    -4.537    -4.604    -
0.067
      CaCO3            1.438e-006  1.449e-006    -5.842    -5.839
0.003
      CaHPO4           9.112e-008  9.179e-008    -7.040    -7.037
0.003
```

```
      CaH2PO4+         7.214e-009  6.137e-009    -8.142    -8.212    -
0.070
      CaOH+            7.122e-009  6.058e-009    -8.147    -8.218    -
0.070
      CaPO4-           2.285e-009  1.943e-009    -8.641    -8.711    -
0.070
      CaHSO4+          9.965e-010  8.476e-010    -9.002    -9.072    -
0.070
Cl                1.774e-004
      Cl-              1.774e-004  1.500e-004    -3.751    -3.824    -
0.073
      MnCl+            4.533e-009  3.856e-009    -8.344    -8.414    -
0.070
      PbCl+            6.230e-012  5.299e-012   -11.206   -11.276    -
0.070
      MnCl2            2.506e-013  2.524e-013   -12.601   -12.598
0.003
      PbCl2            1.702e-015  1.715e-015   -14.769   -14.766
0.003
      MnCl3-           1.226e-017  1.043e-017   -16.912   -16.982    -
0.070
      PbCl3-           2.169e-019  1.845e-019   -18.664   -18.734    -
0.070
      PbCl4-2          2.227e-023  1.166e-023   -22.652   -22.933    -
0.281
H(0)              6.875e-030
      H2               3.438e-030  3.463e-030   -29.464   -29.461
0.003
Mg                2.290e-003
      Mg+2             1.701e-003  9.317e-004    -2.769    -3.031    -
0.262
      MgSO4            5.774e-004  5.816e-004    -3.239    -3.235
0.003
      MgHCO3+          1.122e-005  9.542e-006    -4.950    -5.020    -
0.070
      MgCO3            2.471e-007  2.489e-007    -6.607    -6.604
0.003
      MgHPO4           3.841e-008  3.869e-008    -7.416    -7.412
0.003
      MgOH+            1.093e-008  9.297e-009    -7.961    -8.032    -
0.070
      MgH2PO4+         2.864e-009  2.436e-009    -8.543    -8.613    -
0.070
      MgPO4-           9.608e-010  8.173e-010    -9.017    -9.088    -
0.070
Mn(2)             1.564e-005
      Mn+2             1.154e-005  6.312e-006    -4.938    -5.200    -
0.262
      MnSO4            3.313e-006  3.337e-006    -5.480    -5.477
0.003
      MnHCO3+          6.040e-007  5.138e-007    -6.219    -6.289    -
0.070
      MnCO3            1.772e-007  1.785e-007    -6.751    -6.748
0.003
      MnCl+            4.533e-009  3.856e-009    -8.344    -8.414    -
0.070
```

```
      MnOH+           6.061e-010  5.155e-010    -9.217    -9.288    -
0.070
      MnCl2           2.506e-013  2.524e-013   -12.601   -12.598
0.003
      Mn(NO3)2        1.741e-015  1.754e-015   -14.759   -14.756
0.003
      MnCl3-          1.226e-017  1.043e-017   -16.912   -16.982    -
0.070
Mn(3)           9.526e-026
      Mn+3            9.526e-026  2.221e-026   -25.021   -25.653    -
0.632
N(-3)           1.573e-006
      NH4+            1.493e-006  1.250e-006    -5.826    -5.903    -
0.077
      NH4SO4-         7.715e-008  6.563e-008    -7.113    -7.183    -
0.070
      NH3             2.685e-009  2.704e-009    -8.571    -8.568
0.003
N(5)            9.753e-006
      NO3-            9.753e-006  8.202e-006    -5.011    -5.086    -
0.075
      PbNO3+          1.906e-013  1.622e-013   -12.720   -12.790    -
0.070
      Mn(NO3)2        1.741e-015  1.754e-015   -14.759   -14.756
0.003
Na              2.039e-003
      Na+             2.001e-003  1.706e-003    -2.699    -2.768    -
0.069
      NaSO4-          3.688e-005  3.137e-005    -4.433    -4.503    -
0.070
      NaHCO3          8.698e-007  8.761e-007    -6.061    -6.057
0.003
      NaCO3-          5.780e-009  4.916e-009    -8.238    -8.308    -
0.070
      NaHPO4-         2.982e-010  2.536e-010    -9.526    -9.596    -
0.070
      NaOH            1.366e-010  1.376e-010    -9.864    -9.861
0.003
O(0)            5.320e-004
      O2              2.660e-004  2.680e-004    -3.575    -3.572
0.003
P               4.203e-007
      HPO4-2          1.476e-007  7.626e-008    -6.831    -7.118    -
0.287
      H2PO4-          1.296e-007  1.103e-007    -6.887    -6.957    -
0.070
      CaHPO4          9.112e-008  9.179e-008    -7.040    -7.037
0.003
      MgHPO4          3.841e-008  3.869e-008    -7.416    -7.412
0.003
      CaH2PO4+        7.214e-009  6.137e-009    -8.142    -8.212    -
0.070
      MgH2PO4+        2.864e-009  2.436e-009    -8.543    -8.613    -
0.070
      CaPO4-          2.285e-009  1.943e-009    -8.641    -8.711    -
0.070
```

```
      MgPO4-           9.608e-010  8.173e-010    -9.017    -9.088    -
0.070
      NaHPO4-          2.982e-010  2.536e-010    -9.526    -9.596    -
0.070
      PO4-3            1.334e-012  3.020e-013   -11.875   -12.520    -
0.645
Pb              1.547e-008
      PbCO3            8.212e-009  8.272e-009    -8.086    -8.082
0.003
      PbSO4            3.041e-009  3.063e-009    -8.517    -8.514
0.003
      Pb+2             2.553e-009  1.337e-009    -8.593    -8.874    -
0.281
      PbHCO3+          1.140e-009  9.698e-010    -8.943    -9.013    -
0.070
      PbOH+            3.743e-010  3.183e-010    -9.427    -9.497    -
0.070
      Pb(SO4)2-2       1.251e-010  6.550e-011    -9.903   -10.184    -
0.281
      Pb(CO3)2-2       1.413e-011  7.398e-012   -10.850   -11.131    -
0.281
      PbCl+            6.230e-012  5.299e-012   -11.206   -11.276    -
0.070
      Pb(OH)2          1.502e-012  1.513e-012   -11.823   -11.820
0.003
      PbNO3+           1.906e-013  1.622e-013   -12.720   -12.790    -
0.070
      PbCl2            1.702e-015  1.715e-015   -14.769   -14.766
0.003
      Pb(OH)3-         2.494e-016  2.121e-016   -15.603   -15.673    -
0.070
      Pb2OH+3          4.087e-017  9.527e-018   -16.389   -17.021    -
0.632
      PbCl3-           2.169e-019  1.845e-019   -18.664   -18.734    -
0.070
      Pb(OH)4-2        1.134e-020  5.935e-021   -19.946   -20.227    -
0.281
      PbCl4-2          2.227e-023  1.166e-023   -22.652   -22.933    -
0.281
S(6)            1.036e-002
      SO4-2            7.678e-003  4.075e-003    -2.115    -2.390    -
0.275
      CaSO4            2.067e-003  2.082e-003    -2.685    -2.681
0.003
      MgSO4            5.774e-004  5.816e-004    -3.239    -3.235
0.003
      NaSO4-           3.688e-005  3.137e-005    -4.433    -4.503    -
0.070
      MnSO4            3.313e-006  3.337e-006    -5.480    -5.477
0.003
      NH4SO4-          7.715e-008  6.563e-008    -7.113    -7.183    -
0.070
      HSO4-            2.773e-008  2.359e-008    -7.557    -7.627    -
0.070
      PbSO4            3.041e-009  3.063e-009    -8.517    -8.514
0.003
```

```
      CaHSO4+          9.965e-010  8.476e-010    -9.002    -9.072    -
0.070
      Pb(SO4)2-2       1.251e-010  6.550e-011    -9.903   -10.184    -
0.281
Si              1.200e-005
      H4SiO4           1.199e-005  1.207e-005    -4.921    -4.918
0.003
      H3SiO4-          1.397e-008  1.188e-008    -7.855    -7.925    -
0.070
      H2SiO4-2         6.160e-015  3.225e-015   -14.210   -14.491    -
0.281

-----------------------------Saturation indices-----------------------

      Phase               SI log IAP  log KT

      Anglesite        -3.39  -11.26   -7.88  PbSO4
      Anhydrite        -0.58   -4.91   -4.34  CaSO4
      Aragonite        -0.72   -8.97   -8.25  CaCO3
      Calcite          -0.56   -8.97   -8.41  CaCO3
      Cerrusite        -2.00  -15.32  -13.33  PbCO3
      Chalcedony       -1.17   -4.92   -3.74  SiO2
      Chrysotile      -10.65   23.59   34.24  Mg3Si2O5(OH)4
      CO2(g)           -2.40  -20.62  -18.23  CO2
      Dolomite         -1.75  -18.45  -16.71  CaMg(CO3)2
      Gypsum           -0.32   -4.91   -4.59  CaSO4:2H2O
      H2(g)           -26.38  -26.38    0.00  H2
      H2O(g)           -1.94   -0.00    1.94  H2O
      Halite           -8.14   -6.59    1.54  NaCl
      Hausmannite     -11.81   53.30   65.12  Mn3O4
      Hydroxyapatite   -3.67  -43.10  -39.42  Ca5(PO4)3OH
      Manganite        -3.18   22.16   25.34  MnOOH
      NH3(g)          -10.67    1.18   11.85  NH3
      O2(g)            -0.69   -3.57   -2.89  O2
      Pb(OH)2          -3.42    5.30    8.72  Pb(OH)2
      Pyrochroite      -6.23    8.97   15.20  Mn(OH)2
      Pyrolusite       -8.67   35.36   44.02  MnO2
      Quartz           -0.69   -4.92   -4.22  SiO2
      Rhodochrosite    -0.58  -11.65  -11.07  MnCO3
      Sepiolite        -8.66    7.53   16.19  Mg2Si3O7.5OH:3H2O
      Sepiolite(d)    -11.13    7.53   18.66  Mg2Si3O7.5OH:3H2O
      SiO2(a)          -2.07   -4.92   -2.85  SiO2
      Talc             -9.52   13.76   23.28  Mg3Si4O10(OH)2

Initial solution 2.     lower water

-----------------------------Solution composition---------------------

      Elements           Molality       Moles

      Alkalinity       4.609e-003  4.609e-003
      Ca               1.368e-002  1.368e-002
      Cl               2.272e-004  2.272e-004
      Fe               5.130e-004  5.130e-004
      K                7.096e-004  7.096e-004
      Mg               4.633e-003  4.633e-003
      Mn               4.563e-004  4.563e-004
```

```
      N(-3)            8.543e-005  8.543e-005
      Na               3.141e-003  3.141e-003
      O(0)             4.262e-005  4.262e-005
      P                3.367e-006  3.367e-006
      Pb               4.840e-008  4.840e-008
      S(6)             1.809e-002  1.809e-002
      Si               6.058e-005  6.058e-005

----------------------------Description of solution----------------------------

                                       pH  =   6.548
                                       pe  =  -0.451
                          Activity of water  =   0.999
                             Ionic strength  =  5.492e-002
                         Mass of water (kg)  =  1.000e+000
                    Total carbon (mol/kg)  =  7.310e-003
                       Total CO2 (mol/kg)  =  7.310e-003
                     Temperature (deg C)  =  11.960
                  Electrical balance (eq)  =  1.469e-003
 Percent error, 100*(Cat-|An|)/(Cat+|An|)  =   2.48
                                Iterations  =  11
                                   Total H  = 1.110176e+002
                                   Total O  = 5.559811e+001

---------------------------------Redox couples---------------------------------

      Redox couple             pe  Eh (volts)

      O(-2)/O(0)          14.9354      0.8449

----------------------------Distribution of species----------------------------

                                                  Log       Log
Log
      Species            Molality    Activity  Molality  Activity
Gamma

      H+               3.321e-007  2.831e-007    -6.479    -6.548    -
0.069
      OH-              1.517e-008  1.227e-008    -7.819    -7.911    -
0.092
      H2O              5.551e+001  9.993e-001     1.744    -0.000
0.000
C(4)           7.310e-003
      HCO3-            4.211e-003  3.480e-003    -2.376    -2.458    -
0.083
      CO2              2.712e-003  2.747e-003    -2.567    -2.561
0.005
      CaHCO3+          1.796e-004  1.485e-004    -3.746    -3.828    -
0.083
      MgHCO3+          7.293e-005  5.976e-005    -4.137    -4.224    -
0.087
      FeHCO3+          6.621e-005  5.426e-005    -4.179    -4.266    -
0.087
      MnHCO3+          5.302e-005  4.345e-005    -4.276    -4.362    -
0.087
```

```
      NaHCO3           4.853e-006  4.915e-006    -5.314    -5.308
0.005
      MnCO3            4.642e-006  4.701e-006    -5.333    -5.328
0.005
      CaCO3            2.519e-006  2.551e-006    -5.599    -5.593
0.005
      FeCO3            1.560e-006  1.580e-006    -5.807    -5.801
0.005
      CO3-2            9.054e-007  4.225e-007    -6.043    -6.374    -
0.331
      MgCO3            4.974e-007  5.038e-007    -6.303    -6.298
0.005
      PbCO3            2.161e-008  2.188e-008    -7.665    -7.660
0.005
      NaCO3-           1.212e-008  9.933e-009    -7.916    -8.003    -
0.087
      PbHCO3+          1.005e-008  8.238e-009    -7.998    -8.084    -
0.087
      Pb(CO3)2-2       5.151e-011  2.322e-011   -10.288   -10.634    -
0.346
Ca            1.368e-002
      Ca+2             9.294e-003  4.355e-003    -2.032    -2.361    -
0.329
      CaSO4            4.201e-003  4.254e-003    -2.377    -2.371
0.005
      CaHCO3+          1.796e-004  1.485e-004    -3.746    -3.828    -
0.083
      CaCO3            2.519e-006  2.551e-006    -5.599    -5.593
0.005
      CaHPO4           4.790e-007  4.851e-007    -6.320    -6.314
0.005
      CaH2PO4+         1.350e-007  1.106e-007    -6.870    -6.956    -
0.087
      CaHSO4+          7.478e-009  6.128e-009    -8.126    -8.213    -
0.087
      CaPO4-           3.826e-009  3.135e-009    -8.417    -8.504    -
0.087
      CaOH+            3.113e-009  2.551e-009    -8.507    -8.593    -
0.087
Cl            2.272e-004
      Cl-              2.270e-004  1.839e-004    -3.644    -3.735    -
0.091
      MnCl+            1.281e-007  1.050e-007    -6.892    -6.979    -
0.087
      FeCl+            4.831e-008  3.959e-008    -7.316    -7.402    -
0.087
      PbCl+            1.899e-011  1.556e-011   -10.721   -10.808    -
0.087
      MnCl2            8.323e-012  8.429e-012   -11.080   -11.074
0.005
      PbCl2            5.780e-015  5.854e-015   -14.238   -14.233
0.005
      MnCl3-           5.211e-016  4.270e-016   -15.283   -15.370    -
0.087
      PbCl3-           9.596e-019  7.863e-019   -18.018   -18.104    -
0.087
```

```
      FeCl+2           1.999e-020  9.010e-021   -19.699   -20.045    -
0.346
      PbCl4-2          1.383e-022  6.233e-023   -21.859   -22.205    -
0.346
      FeCl2+           1.392e-023  1.141e-023   -22.856   -22.943    -
0.087
      FeCl3            2.072e-028  2.098e-028   -27.684   -27.678
0.005
Fe(2)          5.130e-004
      Fe+2             3.262e-004  1.559e-004    -3.487    -3.807    -
0.321
      FeSO4            1.186e-004  1.202e-004    -3.926    -3.920
0.005
      FeHCO3+          6.621e-005  5.426e-005    -4.179    -4.266    -
0.087
      FeCO3            1.560e-006  1.580e-006    -5.807    -5.801
0.005
      FeHPO4           1.607e-007  1.627e-007    -6.794    -6.789
0.005
      FeH2PO4+         1.231e-007  1.008e-007    -6.910    -6.996    -
0.087
      FeOH+            7.665e-008  6.281e-008    -7.115    -7.202    -
0.087
      FeCl+            4.831e-008  3.959e-008    -7.316    -7.402    -
0.087
      FeHSO4+          2.677e-010  2.194e-010    -9.572    -9.659    -
0.087
Fe(3)          2.617e-011
      Fe(OH)2+         2.169e-011  1.778e-011   -10.664   -10.750    -
0.087
      Fe(OH)3          4.405e-012  4.461e-012   -11.356   -11.351
0.005
      FeOH+2           5.660e-014  2.551e-014   -13.247   -13.593    -
0.346
      Fe(OH)4-         1.013e-014  8.300e-015   -13.994   -14.081    -
0.087
      FeSO4+           1.375e-016  1.127e-016   -15.862   -15.948    -
0.087
      Fe(SO4)2-        1.586e-017  1.300e-017   -16.800   -16.886    -
0.087
      Fe+3             1.050e-017  2.499e-018   -16.979   -17.602    -
0.623
      FeH2PO4+2        1.925e-018  8.679e-019   -17.716   -18.062    -
0.346
      FeHPO4+          1.379e-019  1.130e-019   -18.860   -18.947    -
0.087
      FeCl+2           1.999e-020  9.010e-021   -19.699   -20.045    -
0.346
      FeHSO4+2         1.959e-022  8.833e-023   -21.708   -22.054    -
0.346
      FeCl2+           1.392e-023  1.141e-023   -22.856   -22.943    -
0.087
      Fe2(OH)2+4       7.453e-025  3.078e-026   -24.128   -25.512    -
1.384
      FeCl3            2.072e-028  2.098e-028   -27.684   -27.678
0.005
```

```
      Fe3(OH)4+5       5.850e-032  4.023e-034   -31.233   -33.395    -
2.163
H(0)           1.023e-015
      H2               5.113e-016  5.178e-016   -15.291   -15.286
0.005
K              7.096e-004
      K+               6.886e-004  5.579e-004    -3.162    -3.253    -
0.091
      KSO4-            2.097e-005  1.719e-005    -4.678    -4.765    -
0.087
      KHPO4-           3.480e-010  2.852e-010    -9.458    -9.545    -
0.087
      KOH              6.742e-012  6.828e-012   -11.171   -11.166
0.005
Mg             4.633e-003
      Mg+2             3.176e-003  1.527e-003    -2.498    -2.816    -
0.318
      MgSO4            1.383e-003  1.401e-003    -2.859    -2.854
0.005
      MgHCO3+          7.293e-005  5.976e-005    -4.137    -4.224    -
0.087
      MgCO3            4.974e-007  5.038e-007    -6.303    -6.298
0.005
      MgHPO4           2.271e-007  2.299e-007    -6.644    -6.638
0.005
      MgH2PO4+         6.025e-008  4.937e-008    -7.220    -7.307    -
0.087
      MgOH+            6.968e-009  5.710e-009    -8.157    -8.243    -
0.087
      MgPO4-           1.809e-009  1.482e-009    -8.743    -8.829    -
0.087
Mn(2)          4.563e-004
      Mn+2             2.931e-004  1.401e-004    -3.533    -3.854    -
0.321
      MnSO4            1.055e-004  1.068e-004    -3.977    -3.971
0.005
      MnHCO3+          5.302e-005  4.345e-005    -4.276    -4.362    -
0.087
      MnCO3            4.642e-006  4.701e-006    -5.333    -5.328
0.005
      MnCl+            1.281e-007  1.050e-007    -6.892    -6.979    -
0.087
      MnOH+            5.103e-009  4.181e-009    -8.292    -8.379    -
0.087
      MnCl2            8.323e-012  8.429e-012   -11.080   -11.074
0.005
      MnCl3-           5.211e-016  4.270e-016   -15.283   -15.370    -
0.087
Mn(3)          1.257e-030
      Mn+3             1.257e-030  2.093e-031   -29.901   -30.679    -
0.779
N(-3)          8.543e-005
      NH4+             7.982e-005  6.367e-005    -4.098    -4.196    -
0.098
      NH4SO4-          5.567e-006  4.562e-006    -5.254    -5.341    -
0.087
```

```
      NH3               4.822e-008  4.883e-008    -7.317    -7.311
0.005
Na                3.141e-003
      Na+               3.057e-003  2.511e-003    -2.515    -2.600    -
0.085
      NaSO4-            7.835e-005  6.420e-005    -4.106    -4.192    -
0.087
      NaHCO3            4.853e-006  4.915e-006    -5.314    -5.308
0.005
      NaCO3-            1.212e-008  9.933e-009    -7.916    -8.003    -
0.087
      NaHPO4-           1.567e-009  1.284e-009    -8.805    -8.892    -
0.087
      NaOH              5.783e-011  5.856e-011   -10.238   -10.232
0.005
O(0)              4.262e-005
      O2                2.131e-005  2.158e-005    -4.671    -4.666
0.005
P                 3.367e-006
      H2PO4-            1.577e-006  1.290e-006    -5.802    -5.889    -
0.087
      HPO4-2            5.980e-007  2.621e-007    -6.223    -6.581    -
0.358
      CaHPO4            4.790e-007  4.851e-007    -6.320    -6.314
0.005
      MgHPO4            2.271e-007  2.299e-007    -6.644    -6.638
0.005
      FeHPO4            1.607e-007  1.627e-007    -6.794    -6.789
0.005
      CaH2PO4+          1.350e-007  1.106e-007    -6.870    -6.956    -
0.087
      FeH2PO4+          1.231e-007  1.008e-007    -6.910    -6.996    -
0.087
      MgH2PO4+          6.025e-008  4.937e-008    -7.220    -7.307    -
0.087
      CaPO4-            3.826e-009  3.135e-009    -8.417    -8.504    -
0.087
      MgPO4-            1.809e-009  1.482e-009    -8.743    -8.829    -
0.087
      NaHPO4-           1.567e-009  1.284e-009    -8.805    -8.892    -
0.087
      KHPO4-            3.480e-010  2.852e-010    -9.458    -9.545    -
0.087
      PO4-3             2.032e-012  3.178e-013   -11.692   -12.498    -
0.806
      FeH2PO4+2         1.925e-018  8.679e-019   -17.716   -18.062    -
0.346
      FeHPO4+           1.379e-019  1.130e-019   -18.860   -18.947    -
0.087
Pb                4.840e-008
      PbCO3             2.161e-008  2.188e-008    -7.665    -7.660
0.005
      PbHCO3+           1.005e-008  8.238e-009    -7.998    -8.084    -
0.087
      PbSO4             9.203e-009  9.320e-009    -8.036    -8.031
0.005
```

```
      Pb+2            6.611e-009  2.980e-009    -8.180    -8.526    -
0.346
      Pb(SO4)2-2      6.034e-010  2.720e-010    -9.219    -9.565    -
0.346
      PbOH+           2.503e-010  2.051e-010    -9.602    -9.688    -
0.087
      Pb(CO3)2-2      5.151e-011  2.322e-011   -10.288   -10.634    -
0.346
      PbCl+           1.899e-011  1.556e-011   -10.721   -10.808    -
0.087
      Pb(OH)2         2.781e-013  2.816e-013   -12.556   -12.550
0.005
      PbCl2           5.780e-015  5.854e-015   -14.238   -14.233
0.005
      Pb2OH+3         8.217e-017  1.368e-017   -16.085   -16.864    -
0.779
      Pb(OH)3-        1.393e-017  1.141e-017   -16.856   -16.943    -
0.087
      PbCl3-          9.596e-019  7.863e-019   -18.018   -18.104    -
0.087
      Pb(OH)4-2       2.046e-022  9.226e-023   -21.689   -22.035    -
0.346
      PbCl4-2         1.383e-022  6.233e-023   -21.859   -22.205    -
0.346
S(6)          1.809e-002
      SO4-2           1.218e-002  5.561e-003    -1.914    -2.255    -
0.341
      CaSO4           4.201e-003  4.254e-003    -2.377    -2.371
0.005
      MgSO4           1.383e-003  1.401e-003    -2.859    -2.854
0.005
      FeSO4           1.186e-004  1.202e-004    -3.926    -3.920
0.005
      MnSO4           1.055e-004  1.068e-004    -3.977    -3.971
0.005
      NaSO4-          7.835e-005  6.420e-005    -4.106    -4.192    -
0.087
      KSO4-           2.097e-005  1.719e-005    -4.678    -4.765    -
0.087
      NH4SO4-         5.567e-006  4.562e-006    -5.254    -5.341    -
0.087
      HSO4-           1.428e-007  1.170e-007    -6.845    -6.932    -
0.087
      PbSO4           9.203e-009  9.320e-009    -8.036    -8.031
0.005
      CaHSO4+         7.478e-009  6.128e-009    -8.126    -8.213    -
0.087
      Pb(SO4)2-2      6.034e-010  2.720e-010    -9.219    -9.565    -
0.346
      FeHSO4+         2.677e-010  2.194e-010    -9.572    -9.659    -
0.087
      FeSO4+          1.375e-016  1.127e-016   -15.862   -15.948    -
0.087
      Fe(SO4)2-       1.586e-017  1.300e-017   -16.800   -16.886    -
0.087
      FeHSO4+2        1.959e-022  8.833e-023   -21.708   -22.054    -
0.346
```

```
Si              6.058e-005
      H4SiO4            6.056e-005  6.133e-005    -4.218    -4.212
0.005
      H3SiO4-           2.377e-008  1.947e-008    -7.624    -7.711    -
0.087
      H2SiO4-2          4.144e-015  1.868e-015   -14.383   -14.729    -
0.346

-----------------------------Saturation indices----------------------

      Phase               SI log IAP  log KT

      Anglesite        -2.92  -10.78   -7.86  PbSO4
      Anhydrite        -0.28   -4.62   -4.33  CaSO4
      Aragonite        -0.47   -8.74   -8.26  CaCO3
      Calcite          -0.32   -8.74   -8.42  CaCO3
      Cerrusite        -1.61  -14.90  -13.29  PbCO3
      Chalcedony       -0.50   -4.21   -3.71  SiO2
      Chrysotile      -11.47   22.41   33.89  Mg3Si2O5(OH)4
      CO2(g)           -1.26  -19.47  -18.21  CO2
      Dolomite         -1.15  -17.93  -16.77  CaMg(CO3)2
      Fe(OH)3(a)       -2.85   15.39   18.24  Fe(OH)3
      Goethite          2.56   15.39   12.83  FeOOH
      Gypsum           -0.03   -4.62   -4.59  CaSO4:2H2O
      H2(g)           -12.19  -12.19    0.00  H2
      H2O(g)           -1.86   -0.00    1.86  H2O
      Halite           -7.89   -6.34    1.55  NaCl
      Hausmannite     -24.48   39.92   64.40  Mn3O4
      Hematite          7.06   30.77   23.72  Fe2O3
      Hydroxyapatite   -3.15  -42.75  -39.60  Ca5(PO4)3OH
      Jarosite-K      -13.12   18.75   31.87  KFe3(SO4)2(OH)6
      Manganite       -10.00   15.34   25.34  MnOOH
      Melanterite      -3.68   -6.06   -2.38  FeSO4:7H2O
      NH3(g)           -9.36    2.35   11.71  NH3
      O2(g)            -1.77   -4.67   -2.90  O2
      Pb(OH)2          -4.05    4.57    8.62  Pb(OH)2
      Pyrochroite      -5.96    9.24   15.20  Mn(OH)2
      Pyrolusite      -22.13   21.44   43.56  MnO2
      Quartz           -0.03   -4.21   -4.18  SiO2
      Rhodochrosite     0.85  -10.23  -11.08  MnCO3
      Sepiolite        -8.20    7.92   16.12  Mg2Si3O7.5OH:3H2O
      Sepiolite(d)    -10.74    7.92   18.66  Mg2Si3O7.5OH:3H2O
      Siderite          0.63  -10.18  -10.81  FeCO3
      SiO2(a)          -1.39   -4.21   -2.82  SiO2
      Talc             -8.96   13.99   22.95  Mg3Si4O10(OH)2
      Vivianite        -0.42  -36.42  -36.00  Fe3(PO4)2:8H2O

----------------------------------------
Beginning of batch-reaction calculations.
----------------------------------------

Reaction step 1.

Using mix 1.

Mixture 1.
```

```
       8.995e-001 Solution 1  upper water
       1.005e-001 Solution 2  lower water

----------------------------Solution composition----------------------

      Elements           Molality       Moles

      C                1.931e-003  1.931e-003
      Ca               8.252e-003  8.252e-003
      Cl               1.824e-004  1.824e-004
      Fe               5.156e-005  5.156e-005
      K                7.132e-005  7.132e-005
      Mg               2.526e-003  2.526e-003
      Mn               5.993e-005  5.993e-005
      N                1.877e-005  1.877e-005
      Na               2.149e-003  2.149e-003
      P                7.165e-007  7.165e-007
      Pb               1.878e-008  1.878e-008
      S                1.114e-002  1.114e-002
      Si               1.688e-005  1.688e-005

---------------------------Description of solution--------------------

                                       pH  =   6.773      Charge
balance
                                       pe  =  15.171      Adjusted to
redox equilibrium
                         Activity of water  =   1.000
                            Ionic strength  =  3.392e-002
                        Mass of water (kg)  =  1.000e+000
                 Total alkalinity (eq/kg)  =  1.393e-003
                       Total CO2 (mol/kg)  =  1.931e-003
                     Temperature (deg C)  =   9.612
                  Electrical balance (eq)  =  7.398e-005
 Percent error, 100*(Cat-|An|)/(Cat+|An|)  =   0.21
                                Iterations  =  23
                                   Total H  = 1.110140e+002
                                   Total O  = 5.555668e+001

----------------------------Distribution of species--------------------

                                                    Log       Log
Log
      Species            Molality    Activity  Molality  Activity
Gamma

      H+               1.932e-007  1.685e-007    -6.714    -6.773    -
0.059
      OH-              1.996e-008  1.677e-008    -7.700    -7.776    -
0.076
      H2O              5.551e+001  9.996e-001     1.744    -0.000
0.000
C(-4)           0.000e+000
      CH4              0.000e+000  0.000e+000  -152.271  -152.268
0.003
C(4)            1.931e-003
```

```
      HCO3-            1.320e-003  1.126e-003    -2.879    -2.949    -
0.069
      CO2              5.519e-004  5.562e-004    -3.258    -3.255
0.003
      CaHCO3+          3.814e-005  3.252e-005    -4.419    -4.488    -
0.069
      MgHCO3+          1.493e-005  1.264e-005    -4.826    -4.898    -
0.072
      MnHCO3+          2.789e-006  2.362e-006    -5.555    -5.627    -
0.072
      NaHCO3           1.123e-006  1.132e-006    -5.950    -5.946
0.003
      CaCO3            9.136e-007  9.207e-007    -6.039    -6.036
0.003
      CO3-2            4.061e-007  2.148e-007    -6.391    -6.668    -
0.277
      MnCO3            3.985e-007  4.016e-007    -6.400    -6.396
0.003
      MgCO3            1.608e-007  1.620e-007    -6.794    -6.790
0.003
      PbCO3            7.456e-009  7.515e-009    -8.127    -8.124
0.003
      NaCO3-           3.727e-009  3.156e-009    -8.429    -8.501    -
0.072
      PbHCO3+          2.126e-009  1.800e-009    -8.672    -8.745    -
0.072
      Pb(CO3)2-2       7.889e-012  4.054e-012   -11.103   -11.392    -
0.289
      FeHCO3+          4.826e-015  4.086e-015   -14.316   -14.389    -
0.072
      FeCO3            1.856e-016  1.871e-016   -15.731   -15.728
0.003
Ca            8.252e-003
      Ca+2             5.939e-003  3.144e-003    -2.226    -2.502    -
0.276
      CaSO4            2.274e-003  2.292e-003    -2.643    -2.640
0.003
      CaHCO3+          3.814e-005  3.252e-005    -4.419    -4.488    -
0.069
      CaCO3            9.136e-007  9.207e-007    -6.039    -6.036
0.003
      CaHPO4           1.190e-007  1.199e-007    -6.925    -6.921
0.003
      CaH2PO4+         1.946e-008  1.648e-008    -7.711    -7.783    -
0.072
      CaOH+            3.657e-009  3.096e-009    -8.437    -8.509    -
0.072
      CaHSO4+          2.273e-009  1.925e-009    -8.643    -8.716    -
0.072
      CaPO4-           1.465e-009  1.240e-009    -8.834    -8.907    -
0.072
Cl            1.824e-004
      Cl-              1.824e-004  1.534e-004    -3.739    -3.814    -
0.075
      MnCl+            1.738e-008  1.471e-008    -7.760    -7.832    -
0.072
```

```
      PbCl+            9.711e-012  8.223e-012   -11.013   -11.085    -
0.072
      MnCl2            9.774e-013  9.851e-013   -12.010   -12.007
0.003
      FeCl+2           1.140e-014  5.858e-015   -13.943   -14.232    -
0.289
      PbCl2            2.686e-015  2.707e-015   -14.571   -14.568
0.003
      MnCl3-           4.916e-017  4.162e-017   -16.308   -16.381    -
0.072
      FeCl+            9.080e-018  7.688e-018   -17.042   -17.114    -
0.072
      FeCl2+           7.929e-018  6.714e-018   -17.101   -17.173    -
0.072
      PbCl3-           3.524e-019  2.984e-019   -18.453   -18.525    -
0.072
      FeCl3            1.022e-022  1.030e-022   -21.991   -21.987
0.003
      PbCl4-2          3.763e-023  1.934e-023   -22.425   -22.714    -
0.289
Fe(2)          9.280e-014
      Fe+2             6.750e-014  3.631e-014   -13.171   -13.440    -
0.269
      FeSO4            2.024e-014  2.040e-014   -13.694   -13.690
0.003
      FeHCO3+          4.826e-015  4.086e-015   -14.316   -14.389    -
0.072
      FeCO3            1.856e-016  1.871e-016   -15.731   -15.728
0.003
      FeOH+            2.393e-017  2.026e-017   -16.621   -16.693    -
0.072
      FeHPO4           1.351e-017  1.361e-017   -16.869   -16.866
0.003
      FeCl+            9.080e-018  7.688e-018   -17.042   -17.114    -
0.072
      FeH2PO4+         6.016e-018  5.094e-018   -17.221   -17.293    -
0.072
      FeHSO4+          2.625e-020  2.222e-020   -19.581   -19.653    -
0.072
      Fe(HS)2          0.000e+000  0.000e+000  -301.802  -301.799
0.003
      Fe(HS)3-         0.000e+000  0.000e+000  -448.344  -448.416    -
0.072
Fe(3)          5.156e-005
      Fe(OH)2+         3.908e-005  3.309e-005    -4.408    -4.480    -
0.072
      Fe(OH)3          1.237e-005  1.247e-005    -4.908    -4.904
0.003
      FeOH+2           6.065e-008  3.117e-008    -7.217    -7.506    -
0.289
      Fe(OH)4-         4.151e-008  3.514e-008    -7.382    -7.454    -
0.072
      FeSO4+           8.130e-011  6.884e-011   -10.090   -10.162    -
0.072
      Fe+3             7.251e-012  2.115e-012   -11.140   -11.675    -
0.535
```

```
      Fe(SO4)2-        7.097e-012  6.009e-012   -11.149   -11.221    -
0.072
      Fe2(OH)2+4       7.329e-013  5.112e-014   -12.135   -13.291    -
1.156
      FeH2PO4+2        3.101e-013  1.593e-013   -12.509   -12.798    -
0.289
      Fe3(OH)4+5       1.013e-013  1.579e-015   -12.995   -14.801    -
1.807
      FeHPO4+          3.731e-014  3.159e-014   -13.428   -13.500    -
0.072
      FeCl+2           1.140e-014  5.858e-015   -13.943   -14.232    -
0.289
      FeHSO4+2         6.328e-017  3.252e-017   -16.199   -16.488    -
0.289
      FeCl2+           7.929e-018  6.714e-018   -17.101   -17.173    -
0.072
      FeCl3            1.022e-022  1.030e-022   -21.991   -21.987
0.003
H(0)           0.000e+000
      H2               0.000e+000  0.000e+000   -46.973   -46.970
0.003
K              7.132e-005
      K+               6.976e-005  5.867e-005    -4.156    -4.232    -
0.075
      KSO4-            1.559e-006  1.320e-006    -5.807    -5.879    -
0.072
      KHPO4-           1.273e-011  1.077e-011   -10.895   -10.968    -
0.072
      KOH              1.197e-012  1.207e-012   -11.922   -11.918
0.003
Mg             2.526e-003
      Mg+2             1.859e-003  1.001e-003    -2.731    -2.999    -
0.269
      MgSO4            6.519e-004  6.571e-004    -3.186    -3.182
0.003
      MgHCO3+          1.493e-005  1.264e-005    -4.826    -4.898    -
0.072
      MgCO3            1.608e-007  1.620e-007    -6.794    -6.790
0.003
      MgHPO4           5.123e-008  5.163e-008    -7.290    -7.287
0.003
      MgH2PO4+         7.894e-009  6.684e-009    -8.103    -8.175    -
0.072
      MgOH+            5.886e-009  4.984e-009    -8.230    -8.302    -
0.072
      MgPO4-           6.292e-010  5.328e-010    -9.201    -9.273    -
0.072
Mn(2)          5.993e-005
      Mn+2             4.377e-005  2.354e-005    -4.359    -4.628    -
0.269
      MnSO4            1.296e-005  1.306e-005    -4.887    -4.884
0.003
      MnHCO3+          2.789e-006  2.362e-006    -5.555    -5.627    -
0.072
      MnCO3            3.985e-007  4.016e-007    -6.400    -6.396
0.003
```

```
      MnCl+            1.738e-008  1.471e-008    -7.760    -7.832    -
0.072
      MnOH+            1.130e-009  9.565e-010    -8.947    -9.019    -
0.072
      MnCl2            9.774e-013  9.851e-013   -12.010   -12.007
0.003
      Mn(NO3)2         2.377e-014  2.396e-014   -13.624   -13.620
0.003
      MnCl3-           4.916e-017  4.162e-017   -16.308   -16.381    -
0.072
Mn(3)           4.515e-016
      Mn+3             4.515e-016  1.010e-016   -15.345   -15.996    -
0.650
N(-3)           0.000e+000
      NH4+             0.000e+000  0.000e+000   -67.291   -67.371    -
0.080
      NH4SO4-          0.000e+000  0.000e+000   -68.560   -68.633    -
0.072
      NH3              0.000e+000  0.000e+000   -70.344   -70.341
0.003
N(0)            1.680e-023
      N2               8.402e-024  8.468e-024   -23.076   -23.072
0.003
N(3)            5.006e-019
      NO2-             5.006e-019  4.187e-019   -18.301   -18.378    -
0.078
N(5)            1.877e-005
      NO3-             1.877e-005  1.570e-005    -4.726    -4.804    -
0.078
      PbNO3+           5.522e-013  4.676e-013   -12.258   -12.330    -
0.072
      Mn(NO3)2         2.377e-014  2.396e-014   -13.624   -13.620
0.003
Na              2.149e-003
      Na+              2.108e-003  1.789e-003    -2.676    -2.747    -
0.071
      NaSO4-           4.061e-005  3.438e-005    -4.391    -4.464    -
0.072
      NaHCO3           1.123e-006  1.132e-006    -5.950    -5.946
0.003
      NaCO3-           3.727e-009  3.156e-009    -8.429    -8.501    -
0.072
      NaHPO4-          3.879e-010  3.285e-010    -9.411    -9.484    -
0.072
      NaOH             6.956e-011  7.011e-011   -10.158   -10.154
0.003
O(0)            4.171e-004
      O2               2.085e-004  2.102e-004    -3.681    -3.677
0.003
P               7.165e-007
      H2PO4-           3.305e-007  2.799e-007    -6.481    -6.553    -
0.072
      HPO4-2           1.859e-007  9.418e-008    -6.731    -7.026    -
0.295
      CaHPO4           1.190e-007  1.199e-007    -6.925    -6.921
0.003
```

```
      MgHPO4           5.123e-008  5.163e-008    -7.290    -7.287
0.003
      CaH2PO4+         1.946e-008  1.648e-008    -7.711    -7.783    -
0.072
      MgH2PO4+         7.894e-009  6.684e-009    -8.103    -8.175    -
0.072
      CaPO4-           1.465e-009  1.240e-009    -8.834    -8.907    -
0.072
      MgPO4-           6.292e-010  5.328e-010    -9.201    -9.273    -
0.072
      NaHPO4-          3.879e-010  3.285e-010    -9.411    -9.484    -
0.072
      KHPO4-           1.273e-011  1.077e-011   -10.895   -10.968    -
0.072
      PO4-3            8.418e-013  1.822e-013   -12.075   -12.739    -
0.665
      FeH2PO4+2        3.101e-013  1.593e-013   -12.509   -12.798    -
0.289
      FeHPO4+          3.731e-014  3.159e-014   -13.428   -13.500    -
0.072
      FeHPO4           1.351e-017  1.361e-017   -16.869   -16.866
0.003
      FeH2PO4+         6.016e-018  5.094e-018   -17.221   -17.293    -
0.072
Pb             1.878e-008
      PbCO3            7.456e-009  7.515e-009    -8.127    -8.124
0.003
      PbSO4            4.775e-009  4.813e-009    -8.321    -8.318
0.003
      Pb+2             3.917e-009  2.013e-009    -8.407    -8.696    -
0.289
      PbHCO3+          2.126e-009  1.800e-009    -8.672    -8.745    -
0.072
      PbOH+            2.751e-010  2.329e-010    -9.561    -9.633    -
0.072
      Pb(SO4)2-2       2.089e-010  1.074e-010    -9.680    -9.969    -
0.289
      PbCl+            9.711e-012  8.223e-012   -11.013   -11.085    -
0.072
      Pb(CO3)2-2       7.889e-012  4.054e-012   -11.103   -11.392    -
0.289
      PbNO3+           5.522e-013  4.676e-013   -12.258   -12.330    -
0.072
      Pb(OH)2          5.333e-013  5.375e-013   -12.273   -12.270
0.003
      PbCl2            2.686e-015  2.707e-015   -14.571   -14.568
0.003
      Pb2OH+3          4.694e-017  1.050e-017   -16.328   -16.979    -
0.650
      Pb(OH)3-         4.324e-017  3.661e-017   -16.364   -16.436    -
0.072
      PbCl3-           3.524e-019  2.984e-019   -18.453   -18.525    -
0.072
      Pb(OH)4-2        9.683e-022  4.976e-022   -21.014   -21.303    -
0.289
      PbCl4-2          3.763e-023  1.934e-023   -22.425   -22.714    -
0.289
```

```
S(-2)           0.000e+000
      H2S               0.000e+000  0.000e+000  -148.258  -148.255
0.003
      HS-               0.000e+000  0.000e+000  -148.579  -148.654    -
0.076
      S-2               0.000e+000  0.000e+000  -155.000  -155.282    -
0.282
      Fe(HS)2           0.000e+000  0.000e+000  -301.802  -301.799
0.003
      Fe(HS)3-          0.000e+000  0.000e+000  -448.344  -448.416    -
0.072
S(6)            1.114e-002
      SO4-2             8.158e-003  4.251e-003    -2.088    -2.372    -
0.283
      CaSO4             2.274e-003  2.292e-003    -2.643    -2.640
0.003
      MgSO4             6.519e-004  6.571e-004    -3.186    -3.182
0.003
      NaSO4-            4.061e-005  3.438e-005    -4.391    -4.464    -
0.072
      MnSO4             1.296e-005  1.306e-005    -4.887    -4.884
0.003
      KSO4-             1.559e-006  1.320e-006    -5.807    -5.879    -
0.072
      HSO4-             6.013e-008  5.092e-008    -7.221    -7.293    -
0.072
      PbSO4             4.775e-009  4.813e-009    -8.321    -8.318
0.003
      CaHSO4+           2.273e-009  1.925e-009    -8.643    -8.716    -
0.072
      Pb(SO4)2-2        2.089e-010  1.074e-010    -9.680    -9.969    -
0.289
      FeSO4+            8.130e-011  6.884e-011   -10.090   -10.162    -
0.072
      Fe(SO4)2-         7.097e-012  6.009e-012   -11.149   -11.221    -
0.072
      FeSO4             2.024e-014  2.040e-014   -13.694   -13.690
0.003
      FeHSO4+2          6.328e-017  3.252e-017   -16.199   -16.488    -
0.289
      FeHSO4+           2.625e-020  2.222e-020   -19.581   -19.653    -
0.072
      NH4SO4-           0.000e+000  0.000e+000   -68.560   -68.633    -
0.072
Si              1.688e-005
      H4SiO4            1.687e-005  1.701e-005    -4.773    -4.769
0.003
      H3SiO4-           9.711e-009  8.222e-009    -8.013    -8.085    -
0.072
      H2SiO4-2          2.153e-015  1.106e-015   -14.667   -14.956    -
0.289

-----------------------------Saturation indices----------------------

      Phase               SI log IAP  log KT

      Anglesite        -3.19  -11.07   -7.88  PbSO4
```

Anhydrite	-0.54	-4.87	-4.34	CaSO4
Aragonite	-0.92	-9.17	-8.25	CaCO3
Calcite	-0.76	-9.17	-8.41	CaCO3
Cerrusite	-2.04	-15.36	-13.32	PbCO3
CH4(g)	-149.54	-195.77	-46.23	CH4
Chalcedony	-1.03	-4.77	-3.74	SiO2
Chrysotile	-12.10	22.10	34.21	Mg3Si2O5(OH)4
CO2(g)	-1.99	-20.21	-18.22	CO2
Dolomite	-2.12	-18.84	-16.71	CaMg(CO3)2
Fe(OH)3(a)	3.75	22.05	18.30	Fe(OH)3
FeS(ppt)	-151.41	-191.37	-39.96	FeS
Goethite	9.07	22.05	12.98	FeOOH
Gypsum	-0.28	-4.87	-4.59	CaSO4:2H2O
H2(g)	-43.89	-43.89	0.00	H2
H2O(g)	-1.93	-0.00	1.93	H2O
H2S(g)	-147.44	-191.48	-44.04	H2S
Halite	-8.11	-6.56	1.55	NaCl
Hausmannite	5.60	70.65	65.04	Mn3O4
Hematite	20.07	44.10	24.03	Fe2O3
Hydroxyapatite	-4.52	-43.96	-39.44	Ca5(PO4)3OH
Jarosite-K	4.60	36.86	32.26	KFe3(SO4)2(OH)6
Mackinawite	-150.67	-191.37	-40.70	FeS
Manganite	5.52	30.86	25.34	MnOOH
Melanterite	-13.40	-15.81	-2.42	FeSO4:7H2O
N2(g)	-19.87	-242.60	-222.74	N2
NH3(g)	-72.44	-187.14	-114.70	NH3
O2(g)	-0.79	87.78	88.57	O2
Pb(OH)2	-3.86	4.85	8.71	Pb(OH)2
Pyrite	-247.93	-338.96	-91.03	FeS2
Pyrochroite	-6.28	8.92	15.20	Mn(OH)2
Pyrolusite	8.83	52.81	43.98	MnO2
Quartz	-0.55	-4.77	-4.22	SiO2
Rhodochrosite	-0.22	-11.30	-11.07	MnCO3
Sepiolite	-9.40	6.79	16.19	Mg2Si3O7.5OH:3H2O
Sepiolite(d)	-11.87	6.79	18.66	Mg2Si3O7.5OH:3H2O
Siderite	-9.32	-20.11	-10.79	FeCO3
SiO2(a)	-1.92	-4.77	-2.85	SiO2
Sulfur	-109.63	-147.59	-37.96	S
Talc	-10.68	12.57	23.25	Mg3Si4O10(OH)2
Vivianite	-29.80	-65.80	-36.00	Fe3(PO4)2:8H2O

```
------------------
End of simulation.
------------------
-----------------------------------
Reading input data for simulation 2.
-----------------------------------
End of run.
```

REFERENCES

Appelo, C. A. J., and D. Postma. 1993. *Geochemistry, Groundwater, and Pollution*. A.A. Balkema.

Atkins, D., J. H. Kempton, T. Martin, and P. Maley. 1997. *Limnologic Conditions in ThreeExisting Nevada Pit Lakes: Observations and Modeling using CE-QUAL-W2*, p. 697-713. Proceedings of the Fourth International Conference on Acid Rock Drainage, May 30-June 6, 1997.

Balistrieri, L. S., J. W. Murray, and B. Paul. 1992. The cycling of iron and manganese in the water column of Lake Sammamish, Washington. *Limnol. Oceanogr* **37:** 510-528.

Banoub, M. W. 2000. The Testsee - a gravel-pit pond (1974-1980): a site for experimental lake and groundwater studies in the Upper Rhine valley in Bad/Wurtt, Germany. *Verhandlungen Internationale Vereinigung für Theoretische und Angewandte Limnologie* **27:** 1366-1370.

Baxter, R. M. 1985. Environmental effects of reservoirs, p. 1-26. In: D. Gunnison [ed.], *Microbial Processes in Reservoirs*. Dr W. Junk Publishers.

Benjamin, M. M. 2002. *Water Chemistry*. McGraw-Hill.

Benson, B. B., and D. Krause. 1980. The Concentration and Isotopic Fractionation of Gases Dissolved in Freshwater in Equilibrium with the Atmosphere. 1. Oxygen. *Limnology and Oceanography* **25:** 662-671.

Bird, D. A. 1993. *Geochemical modeling of mine pit water: An overview and application of computer codes.* Masters thesis. University of Nevada, Reno.

Bird, D. A., W. B. Lyons, and G. C. Miller. 1994. An Assessment of Hydrogeochemical Computer Codes Applied to Modeling Post-Mining Pit Water Geochemistry. *Tailings and Mine Waste* 1994**:** 31-40.

Boegman, L., G. N. Ivey, and J. Imberger. 2005. The degeneration of internal waves in lakes with sloping topography. *Limnol. Oceanogr* **50:** 1620-1637.

Boerher, B., and C. Stevens. 2005. Ray waves in a pit lake. *Geophys. Res. Lett.* **32:** L24608.

Boerher, B., and C. L. Stevens. 2005. Ray waves in a pit lake. *Geophys. Res. Lett* **32**.

Brugam, R. B., and J. B. Stahl. 2000. The potential of organic matter addition for neutralizing surface mine lakes. *Transactions of the Illinois State Academy of Science* **93:** 127-144.

Brunskill, G. J., and S. D. Ludlam. 1969. Fayetteville Green Lake, New York. I. Physical and chemical limnology. *Limnology and Oceanography* **14:** 817-829

Cacchione, D., and C. Wunsch. 1974. Experimental study of internal waves over a slope. *Journal of Fluid Mechanics* **66:** 223-239.

Carter, J. C. H. 1965. The ecology of the calanoid copepod *Pseudocalanus minutus* Kroyer in Tessiarsuk, a coastal meromictic lake of Northern Labrador. *Limnology and Oceanography* **10:** 345-353.

Castro, J. M., and J. N. Moore. 2000. Pit lakes: their characteristics and the potential for their remediation. *Environmental Geology* **39:** 1254-1260.

Cole, G. A. 1994. *Textbook of Limnology, 4 ed.* Waveland Press Inc.

Culver, D. A. 1977. Biogenic meromixis and stability in a soft-water lake. *Limnology and Oceanography* **22:** 667-686.

Davison, W., S. I. Hraney, J. E. Talling, and E. Rigg. 1980. Seasonal tranformations and movements of iron in a productive English lake with deep water anoxia. *Schweiz. Z. Hydrol*. **42:** 196-224.

Doyle, G. A., and D. D. Runnels. 1997. Physical limnology of existing mine pit lakes. *Mining Engineering* **49:** 76-80.

Duarte, C. M., and J. Kalff. 1990. Patterns in submerged macrophyte biomass of lakes and the importance of the scale of analysis in the interpretation. *Can. J. Fish. Aquat. Sci.* **47:** 357-363.

Eary, L. E. 1999. Geochemical and equilibrium trends in mine pit lakes. *Applied Geochemistry* **14:** 963-987.

Eckstein, Y. 1970. Physicochemical limnology and geology of a meromictic pond on the Red Sea shore. *Limnology and Oceanography* **15:** 363-372.

Ehrlich, H. L. 1996. *Geomicrobiology*. Marcel Dekker.

Eriksen, C. C. 1982. Observations of internal wave reflection off sloping bottoms. *J. Geophys. Res*. **87:** 525-538.

Findenegg, I. 1935. Limnologische Untersuchungen im Kärtner Seengebiete. *Int. Revue ges. Hydrobiol* **32:** 369-423.

Fisher, T. S. R. 2002. *Limnology of the meromictic Island Copper Mine pit lake*. PhD-thesis. University of British Columbia, Vancouver, Canada.

Fricker, P., and H. Nepf. 2000. Bathymetry, stratification, and internal seiche structure. *J. Geophys. Res.* **105:** 14237 - 14251.

Giancoli, D. C. 1991. *Physics: Principles with applications, 3rd ed.* Prentice Hall.

Gillon, K. A., W. H. Spence, R. P. Duckett, and C. J. Benson. 1995. Geology of the Ridgeway gold deposits, Ridgeway, South Carolina, p. 53-87. In: D. E. Crowe [ed.], *Selected Mineral Deposits of the Gulf coast and southeastern United States: Part II. - Gold deposits of the Carolina slate belt*: Society of Economic Geologists Guidebook Series.

Graham, L. D., and L. W. Wilcox. 2000. *Algae*. Prentice-Hall.

Hairston, N. G., Jr. 1990. Problems with the perception of zooplankton research by colleagues outside aquatic sciences. *Limnol. Oceanogr*. **35:** 1214-1216.

Hamblin, P. F., C. L. Stevens, and G. A. Lawrence. 1999. Simulation of vertical transport in a mining pit lake. *Journal of Hydraulic Engineering* **125:** 1029-1038.

Hamilton-Taylor, J., and W. Davison. 1995. Redox-Driven Cycling of Trace Elements in Lakes, p. 217-258. In: A. Lerman, D. M. Imboden and J. Gat [eds.], *Physics and Chemistry of Lakes*. Springer-Verlag.

Hanna Murphy, C. 1995. *Carolina rocks!: The geology of South Carolina.* Sandlapper Publishing.

Harrington, J., N. Lewis, and S. Fundingsland. 2004. *Ecosystem Restoration within the Anchor Hill Pit Lake, Gilt Edge Mine Superfund Site, South Dakota.* U.S. EPA Pit Lakes 2004.

Hongve, D. 1994. Nutrient metabolism (C, N, P, and Si) in the trophogenic zone of a meromictic lake. *Hydrobiologia* **277:** 17-39.

---. 1997. Cycling of iron, manganese, and phosphate in a meromictic lake. *Limnology and Oceanography* **42:** 635-647.

Hutchinson, G. E. 1937. A contribution to the limnology of arid regions, primarily founded on observations made in the Lahontan Basin. *Transactions of the Connecticut Academy of Arts and Sciences* **33:** 47-132.

---. 1948. Circular Causal Systems in Ecology. *Annals of the New York Academy of Sciences* **50:** 221-246.

---. 1957. *A treatise on limnology: Geography, Physics and Chemistry*. Wiley.

Idso, S. B. 1973. On the concept of lake stability. *Limnol. Oceanogr* **18:** 681-683.

Imberger, J., and J. C. Patterson. 1990. Physical Limnology, p. 303-475. In: T. Wu [ed.], *Advances in Applied Mechanics*. Academic Press.

Imboden, D. M. 1998. The influence of biogeochemical processes on the physics pf lakes. In: J. Imberger [ed.], *Physical Processes in Lakes and Oceans. Coastal and estuarine studies.* American Geophysical Union.

Imboden, D. M., and A. Wüest. 1995. Mixing Mechanisms in Lakes, p. 83-138. In: A. Lerman, D. M. Imboden and J. R. Gat [eds.], *Physics and Chemistry of Lakes*. Springer Verlag.

Jellison, R., and J. M. Melack. 1993. Meromixis in hypersaline Mono Lake, California. Part 1: Stratification and vertical mixing during the onset, persistence, and breakdown of meromixis. *Limnol. Oceanogr* **38:** 1008-1019.

Kalff, J. 2002. *Limnology*. Prentice Hall.

Kalin, M., Y. Cao, M. Smith, and M. M. Olaveson. 2001. Development of the phytoplankton community in a pit-lake in relation to water quality changes. *Water Res* **35:** 3215-3225.

Kawashima, M., T. Takamatsy, and M. Koyama. 1988. Mechanisms of precipitation of manganese (II) in Lake Biwa, a freshwater lake. *Water Res.* **22:** 613-618.

Kirk, J. T. O. 1994. *Light and Photosynthesis in Aquatic Ecosystems*. Cambridge University Press.

Lee, O. 1961. Observations of internal waves in shallow water. *Limnol. Oceanogr* **6:** 312-321.

Levy, D. B., K. H. Custis, W. H. Casey, and P. A. Rock. 1997. The aqueous geochemistry of the abandoned Spenceville copper Pit, Nevada County, California. *Journal of Environmental Quality* **26:** 233-243.

Macintyre, S., and J. M. Melack. 1982. Meromixis in an equatorial African soda lake. *Limnol. Oceanogr* **27:** 595-609.

Miller, G. C., W. B. Lyons, and A. Davis. 1996. Understanding the Water Quality of Pit Lakes. *Environmental Science and Technology* **30:** 118A-123A.

Newbrough, P., and C. H. Gammons. 2002. An experimental study of water-rock interaction and acid rock drainage in the Butte mining district, Montana. *Environmental Geology* **41:** 705-719.

Nixdorf, F. B., U. Mischke, and D. Lessmann. 1998. Chrysophytes and chlamydomonads: pioneer colonists extremely acidic minig lakes (pH < 3) in Lusatia (Germany). *Hydrobiologia* **369-370:** 315-327.

Page, P., M. Ouellet, C. Hillaire-Marcel, and M. Dickman. 1984. Isotopic Analyses (^{18}O, ^{13}C, ^{14}C) of Two Meromictic Lakes in the Canadian Arctic Archipelago. *Limnology and Oceanography* **29:** 564-573.

Parkhurst, D. L. 1995. User's guide to PHREEQC-A computer program for speciation, reaction-path, advective-transport, and inverse geochemical calculations. *Water-Resources Investigation Report* 95-4227, U.S. Geological Survey, Lakewood CO**:** 143.

Podda, F., P. Zuddas, A. Minacci, M. Pepi, and F. Baldi. 2000. Heavy metal coprecipitation with hydrozincite [Zn-5(CO3)(2)(OH)(6)] from mine waters caused by photosynthetic microorganisms. *Applied and Environmental Microbiology* **66:** 5092-5098.

Reynolds, C. S. 1984. *The Ecology of Freshwater Phytoplankton.* Cambridge University Press.

Robertson, D. M., and J. Imberger. 1994. Lake Number, a quantitative indicator of mixing used to estimate changes in dissolved oxygen. *International Review of Hydrobiology* **79:** 159-176.

Rocha, O., and A. Duncan. 1985. The relationship between cell carbon and cell volume in freshwater algal species used in zooplankton studies. *Journal of Plankton Research* **7:** 279-294.

Schultze-Lam, S., and T. J. Berveridge. 1994. Nucleation of celestite and Strontianite on a Cyanobacterial S-layer. *Applied and Environmental Microbiology* **60:** 447-453.

Schultze-Lam, S., G. Harauz, and T. J. Beveridge. 1992. Participation of a cyanobacterial S layer in fine-grain mineral formation. *Journal of Bacteriology* **174:** 7971-7981.

Sherwood, J., F. Stagnitti, M. J. Kokkinn, and W. D. Williams. 1992. A standard table for predicting equilibrium dissolved oxygen concentrations in salt lakes dominated by sodium chloride. *International Journal of Salt Lake Research* **1:** 1-61.

Shevenell, L., K. A. Connors, and C. D. Henry. 1999. Controls on pit lake water quality at sixteen open-pit mines in Nevada. *Applied Geochemistry* **14:** 669-687.

Sholkovitz, E. R. 1985. Redox-related geochemistry in lakes: Alkali metals, alkaline-earth elements, and ^{137}Cs, p. 119-142. In: W. Stumm [ed.], *Chemical processes in lakes.* John Wiley and Sons.

Sigg, L., M. Sturm, and D. Kistler. 1987. Vertical Transport of Heavy-Metals by Settling Particles in Lake Zurich. *Limnology and Oceanography* **32:** 112-130.

Stauffer, R. E., and D. E. Armstrong. 1986. Cycling of iron, manganese, silica, phosphorus, calcium, and potassium in two stratified basins of Shagawa Lake, Minnesota. *Geochim. Cosmochim. Acta* **50:** 215-229.

Steinhorn, I. 1985. The disappearance of the long term meromictic stratification of the Dead Sea. *Limnology and Oceanography* **30:** 451-472.

Stevens, C. L., and G. A. Lawrence. 1998. Stability and meromixis in a water filled mine pit. Limnology and Oceanography **43:** 946-954.

Stumm, W., and J. J. Morgan. 1996. *Aquatic Chemistry: Chemical Equilibria and Rates in Natural Waters, 3rd ed*. John Wiley & Sons, Inc.

Sugiyama, M., T. Hori, S. Kihara, and M. Matsui. 1992. A geochemical study of the specific distribution of barium in Lake Biwa, Japan. *Geochim. Cosmochim. Acta* **56:** 597-605.

Sunda, W. G., and S. A. Huntsman. 1990. Diel Cycles in Microbial Manganese Oxidation and Manganese Redox Speciation in Coastal Waters of the Bahama-Islands. *Limnology and Oceanography* **35:** 325-338.

Takahashi, T., W. Broecker, Y. Hui Li, and D. Thurber. 1968. Chemical and isotopic balances for a meromictic lake. *Limnol. Oceanogr*. **13:** 272-292.

Thompson, J. B., and F. G. Ferris. 1990. Cyanobacterial precipitation of gypsum, calcite,and magnesite from natural alkaline lake water. *Geology* **18:** 995-998.

Thompson, J. B., F. G. Ferris, and D. A. Smith. 1990. Geomicrobiology and sedimentology ofthe mixolimnion and chemocline in FayettevilleGreen Lake, New York. *Palaois* **5:** 52-75.

Thorp, J. H., and A. P. Covich. 2001. *Ecology and classification of North American freshwater invertebrates, 2nd ed*. Academic Press.

Thorpe, S. A. 1998. Some dynamical effects of the sloping sides of lakes. In: J. Imberger [ed.], *Physical Processes in Lakes and Oceans. Coastal and estuarine studies*. American Geophysical Union.

Thorpe, S. A., A. Hall, and I. Crofts. 1972. The internal surge in Loch Ness. *Nature* **237:** 96-98.

Wake, G. W., G. N. Ivey, and J. Imberger. 2005. The temporal evolution of baroclinic basin-scale waves in a rotating circular basin. *Journal of Fluid Mechanics* **523:** 367-392.

Walker, K. F. 1974. The stability of meromictic lakes in central Washington. *Limnol. Oceanogr* **19:** 209-222.

Walker, K. F., and G. E. Likens. 1975. Meromixis and a reconsidered typology of lake circulation patterns. *Verhandlungen Internationale Vereinigung für Theoretische und Angewandte Limnologie* **19:** 442-458.

Wetzel, R. G. 2001. Limnology. *Lake and River Ecosystems, Third ed.* Academic Press.

Wetzel, R. G., and G. E. Likens. 2000. *Limnological analyses, Third edition ed.* Springer-Verlag Inc.

Wunsch, C. H. 1968. On the propagation of internal waves up a slope. *Deep-Sea Research* **15:** 251-258.

Yagi, A. 1986. Seasonal change of iron and manganese in Lake Fukami-ike-occurrence of turbid manganese layer. *Jpn. J. Limnol.***:** 279-289.